2006

JAEA R&D Review

-The First Issue-

MONJU

J-PARC

Message from the President

戸塚 雄一

President Yuichi Tonozuka

Welcome to this first issue of "JAEA R&D Review", aimed at informing you about the current R&D of the Japan Atomic Energy Agency (JAEA).

Since the integration of the Japan Atomic Energy Research Institute (JAERI) and the Japan Nuclear Cycle Development Institute (JNC) in October 2005, I have greatly appreciated your support and advice for the wide range of JAEA activities, from fundamental and basic research to projects for practical applications.

JAEA is the R&D institute in Japan dedicated to comprehensive nuclear R&D in such areas as Advanced Nuclear Systems, Geological Isolation, Fusion, Photon and Ion-Beam Applications, and Nuclear Safety, drawing upon its tradition and R&D activities over 50 years since the establishment both of JAERI and JNC.

I would like to share with you my vision for JAEA. The mission of JAEA is to "Improve the quality of human life by innovative advancements in nuclear energy". I strongly believe that JAEA will achieve this goal for which it is striving, and become one of the world's most authoritative and comprehensive institutes, "a Center of Excellence(COE)," for creative and reliable nuclear energy R&D.

As one of the ways to share with you my vision, JAEA has disseminated its R&D achievements by providing a number of meetings, seminars, JAEA Technical Reports etc. In addition, this annual publication will be released from now on.

This first issue of this annual publication constitutes a review of the achievements in the year 2005. It provides you with a flavour of some of the work that has been carried out and invites you to contact with the researchers, or check the references, if there is more that you wish to learn about these topics.

I wish to share some of JAEA activities in this publication, with those of you interested in nuclear energy development and applications. I hope that you will take a few minutes to read further. I would be most pleased if I hear from you with any comments on this publication.

I hope that you enjoy this publication and subsequent issues. Thank you.

JAEA R&D Review 2006

2 Research and Development on Geological Disposal of High-Level Radioactive Waste

3 Nuclear Fusion Research and Development

R&D Centers of JAEA

Japan Atomic Energy Agency – Outline of Organaization –

Colophon

1 Research and Development of Advanced Nuclear System

1-1 Toward the Commercialization of Fast Reactor Fuel Cycle Systems

The number of neutrons born from a nuclear fission in the fast reactor (FR) is more than that in the light water reactor (LWR). Uranium-238 in concentration of 70% or more in the nuclear fuel of the fast reactor core captures these neutrons and thus is transmuted to plutonium 239. Therefore, the rate of plutonium 239 generation in the FR is more than in the LWR. The production of plutonium 239 in the FR is more than the consumption of nuclear fuel (breeding of nuclear fuel). So, as shown in Fig.1-1, there is a possibility that there will be no need for import of natural uranium from foreign countries in the 22nd century, if the introduction of FRs replacing LWRs starts in 2050.

At the same time, minor actinides (collective term of three elements: americium, curium and neptunium), which are difficult to transmute in the LWR core, are more fissionable in the FR core which has higher neutron energy. Accordingly, the radioactivity in the high-level radioactive waste after disposal is much less, so we have a possibility of decreasing the environmental burden per unit of generated energy significantly.

Based on the experience of R&D results, such as the developing the prototype fast breeder reactor (FBR), "MONJU," and related fuel cycle, JAEA is conducting the joint study "Feasibility Study on Commercialized Fast Reactor Cycle Systems" (hereinafter, "FS") with electric utilities, the Central Research Institute of Electric Power Industry (CRIEPI) and manufacturers. This study has two objectives, presenting "an appropriate concept of the commercial FBR cycle system" and "the R&D programs for commercialization", toward 2015. As shown in Fig.1-2, the FS phase Ⅱ final report was compiled in March 2006, and now is being evaluated by the Government. The evaluation results will be finalized by October 2006. We give an outline of FS phase Ⅱ final report below.

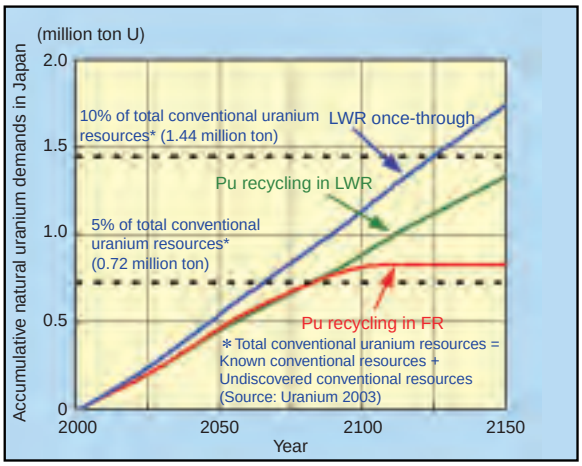

Fig.1-1 Estimated cumulative natural uranium demand in Japan with the introduction of FRs replacing LWRs starting in 2050

We created various concepts for FR and nuclear fuel cycle, exploiting innovative technologies, and developed the elemental technologies necessary for these systems. Total FR cycle systems were set up with design concepts that can realize the best possible performance of each of the FR and nuclear fuel cycle system design concepts, also considering their technical consistency. Further, they were evaluated for prospective conformity to five development requirements (safety, economic competitiveness, low environmental burden, efficient utilization of nuclear fuel resources and nuclear non-proliferation) and for overall technical feasibility. Then we will select the design concepts on which the main R&D investment will be focused.

We selected the "Combined system of sodium-cooled reactor, advanced aqueous reprocessing and simplified

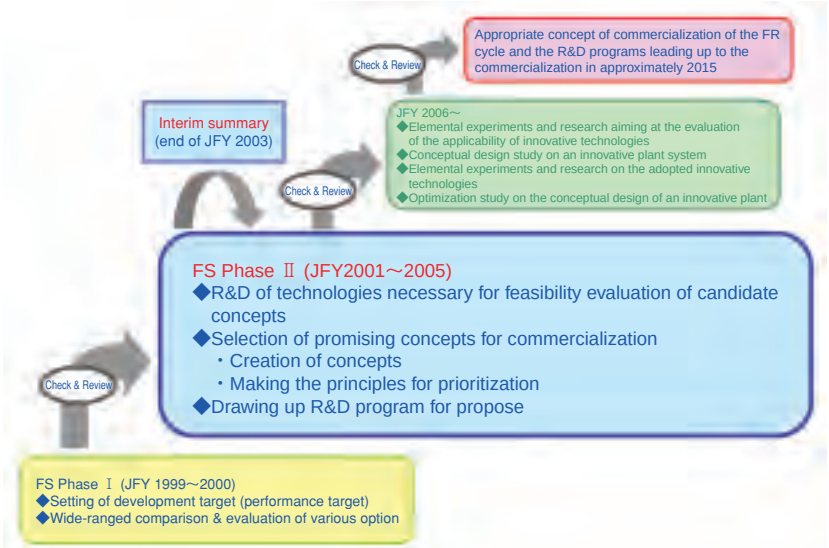

Fig.1-2 Progress & Prospect of the Feasibility Study on Commercialized Fast Reactor Cycle Systems (FS)

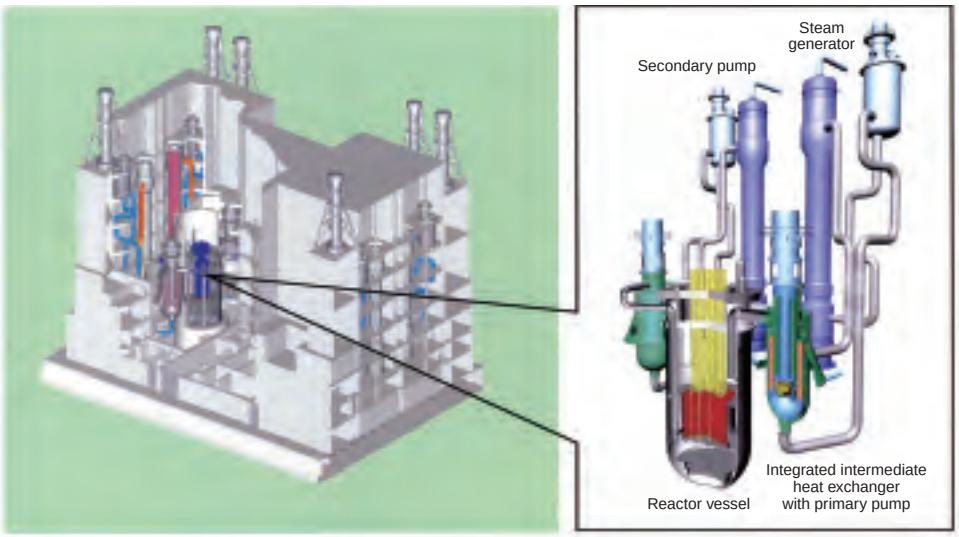

Fig.1-3 Sodium-cooled reactor concept image to be developed with a focus on from now

pelletizing fuel fabrication (MOX fuel)" (Fig.1-3 and refer to Chap.1 Sec.5) as the concept to be developed mainly from now, because it is judged to have the greatest potential conformity to the development requirements and have the high technical feasibility because it uses the accumulated results of past R&D, and international cooperation in this is possible. "Combined system of sodium-cooled reactor, metal electrorefining reprocessing and injection casting fuel fabrication" (metallic fuel) and "Combined system of helium gas-cooled reactor, advanced aqueous reprocessing and coated particle fuel fabrication (nitride fuel) " are selected as the complementary concepts. We think that their R&D should be conducted with a focus on concerns that are judged as essential for technical feasibility.

Fig.1-4 shows the image of the stages of R&D until ~2050. In ~2015, We will present both an appropriate plan for commercialization of the FR cycle and for the R&D programs leading up to commercialization achieved by R&D of elemental technologies based on current innovative technologies, making decisions on the innovative technologies to be adopted for commercial plants and carrying out a conceptual design study of the entire commercial plant and its optimization.

As it is risky and difficult in introduction of a FR cycle on a commercial basis to immediately aim at the construction and operation of middle or large-scale commercial plants employing many innovative technologies, we think that it is necessary to increase the scale of facilities and components step by step, verifying conformity to the development requirements as well as the feasibility and reliability of the innovative technologies.

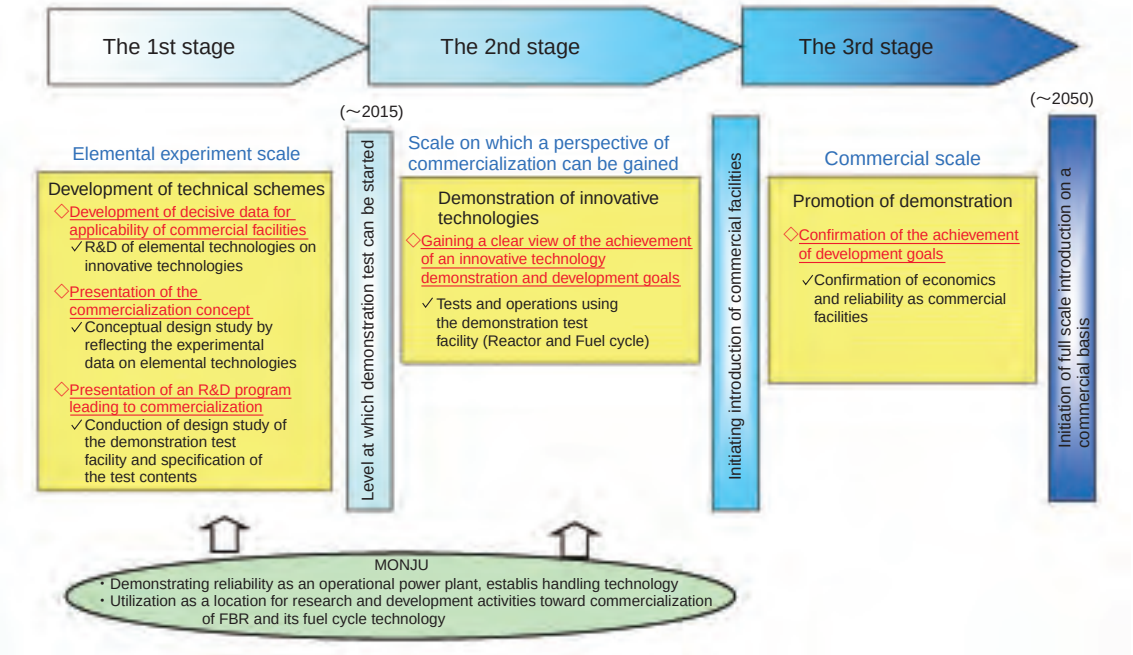

Fig.1-4 Image of the stepwise R&D until approximately 2050

1-2 Fast Reactor System with Promise as Major Energy Source
－Design Study of JAEA Sodium-Cooled Fast Reactor (JSFR)－

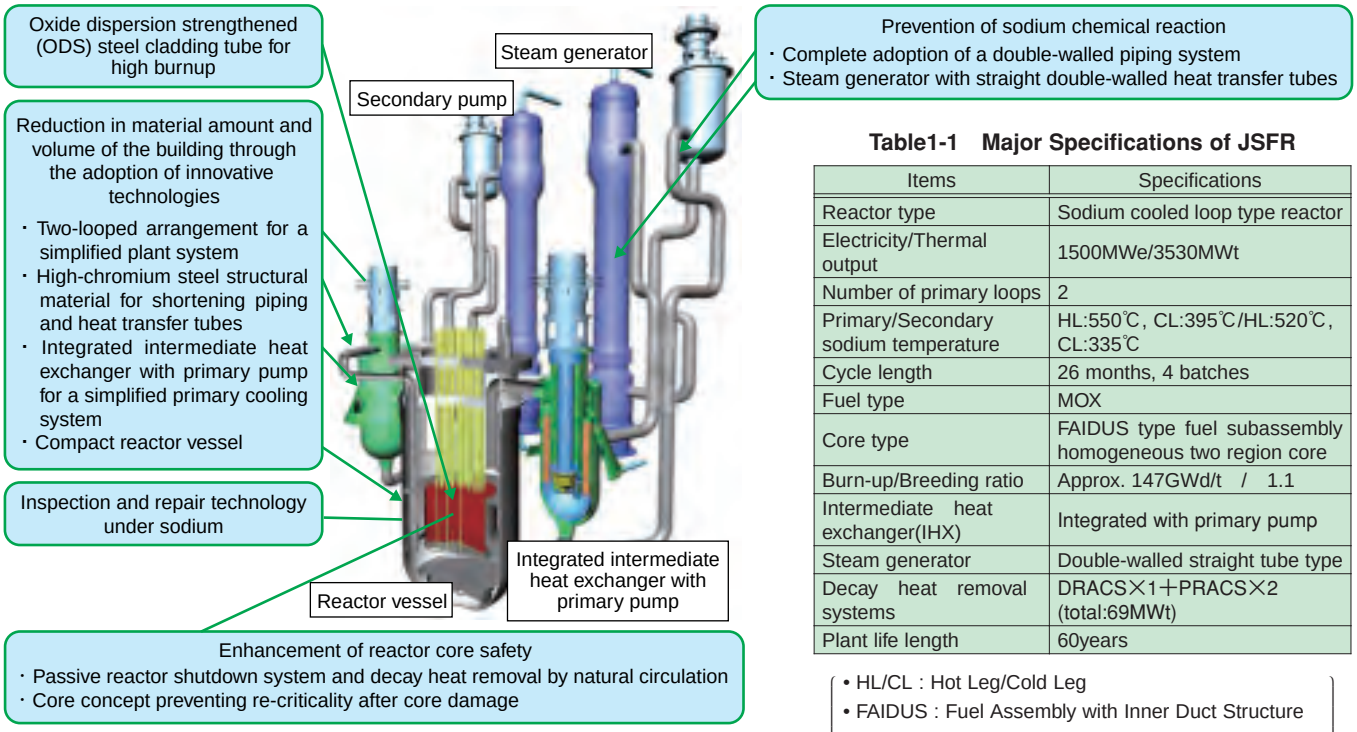

Fig.1-5 Concept of JSFR and the innovative technologies

Table1-1 Major Specifications of JSFR

Items	Specifications
Reactor type	Sodium cooled loop type reactor
Electricity/Thermal output	1500MWe/3530MWt
Number of primary loops	2
Primary/Secondary sodium temperature	HL:550℃, CL:395℃/HL:520℃, CL:335℃
Cycle length	26 months, 4 batches
Fuel type	MOX
Core type	FAIDUS type fuel subassembly homogeneous two region core
Burn-up/Breeding ratio	Approx. 147GWd/t / 1.1
Intermediate heat exchanger(IHX)	Integrated with primary pump
Steam generator	Double-walled straight tube type
Decay heat removal systems	DRACS×1＋PRACS×2 (total:69MWt)
Plant life length	60years

- HL/CL : Hot Leg/Cold Leg
- FAIDUS : Fuel Assembly with Inner Duct Structure
- DRACS : Direct Reactor Auxiliary Cooling System
- PRACS : Primary Reactor Auxiliary Cooling System

The plant concept of the JAEA sodium-cooled fast reactor (JSFR), one promising candidate for the fast reactor (FR) system that will be a future major energy source, has been established (Fig.1-5). There is a high possibility that this reactor will meet development requirements (safety, economic competitiveness, reduction of environmental burden, efficient utilization of nuclear fuel resources and enhancement of nuclear non-proliferation) and the design requirements of the feasibility study on commercialized fast reactor cycle systems (Phase-Ⅱ). The major specifications of this plant are shown in Table1-1.

To improve economy, following innovative technologies are adopted in the reactor design: compact reactor vessel, two-looped heat transport system, integrated intermediate heat exchangers with primary pumps, high-chromium steel, and ODS (Oxide Dispersion Strengthened) steel cladding. Consequently, the amount of plant materials and volume of the building can be greatly reduced, and therefore it is anticipated that the construction cost can be lowered below the design requirement cost (200,000yen/kWe) which is equal to that of future light water reactors (LWRs).

This design adopts a re-criticality free core concept using an innovative fuel assembly with an inner duct to enhance early discharge of molten fuel during core disruptive accidents, and decay heat removal systems depending on natural circulation are adopted for enhancing safety and reliability. Furthermore, to prevent sodium leakage, the whole sodium boundaries are covered with the guard vessels or guard pipings, and double-walled heat transfer tubes for the steam generator are adopted to prevent or minimize a sodium-water reaction. As a result of the above measures, the core damage frequency is estimated to be less than the design requirement (10^{-6} per reactor year).

In the fuel and core design, a mixed oxide (MOX) fueled core was adopted. In this core concept, higher burn-up can be achieved by using large diameter fuel pins which could increase internal conversion ratio. Further, from the viewpoints of the efficient utilization of nuclear fuel resources and the reduction of environmental burden, trans-uranium fuels including minor actinide (up to 5%) recovered from LWR spent fuels can be loaded, and long-lived fission products can be transmuted into shorter nuclides by installing the target assemblies in the radial blanket zone. As a result, the fuel cycle costs can be reduced greatly by increasing the average burn-up of the whole core including blanket fuels (90-110GWd/t). Accordingly, the power generating costs can be reduced due to improvement of utilization rate by extending the operation period (26 months).

The JSFR concept was selected as one of the representative candidate concepts in the Generation Ⅳ international forum. In the future, it is possible that this plant will be developed as the international standard breeding FR concept. Japan shall continue to take the lead in developing sodium-cooled fast reactors.

Reference

Japan Atomic Energy Agency and The Japan Atomic Power Company, Feasibility Study on Commercialized Fast Reactor Cycle Systems－Phase Ⅱ Final Report－, 2006, JAEA-Evaluation 2006-002, 12p. (in Japanese).

1-3 Smooth and Calm Flow in a Compact Reactor Vessel
—Flow Optimization in a Compact Sodium Cooled Reactor—

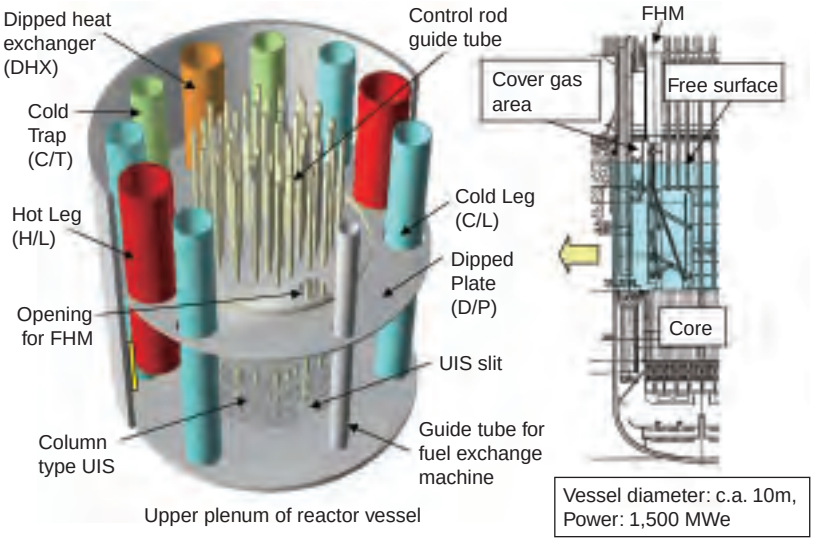

Fig.1-6 Schematic of reactor vessel of sodium cooled reactor

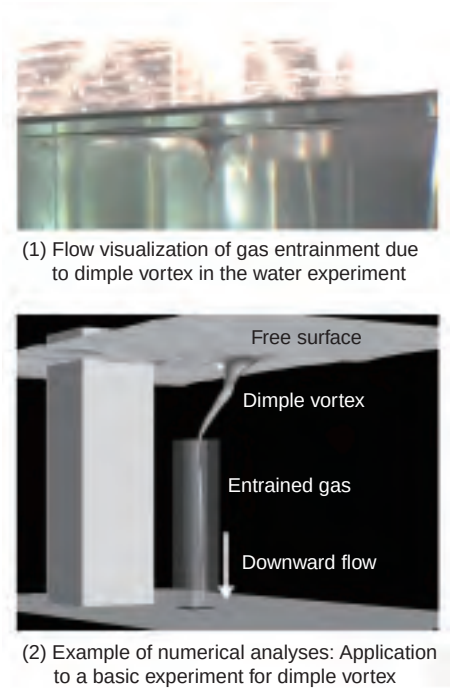

(1) Flow visualization of gas entrainment due to dimple vortex in the water experiment

(2) Example of numerical analyses: Application to a basic experiment for dimple vortex

Fig.1-8 Visualization of gas entrainment and example of numerical analyses

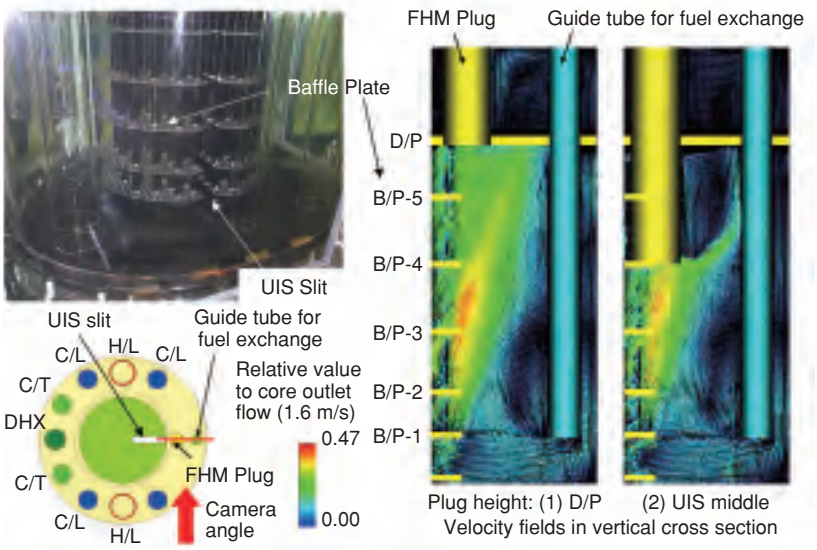

Fig.1-7 Velocity measurement and effect of FHM Plug in 1/10 scaled model
Flow velocity field was measured in the 1/10 scaled water test model of the reactor vessel. The FHM plug at middle height could change the flow direction and reduce the velocity near the free surface. Particle Image velocimetry was applied to get the detailed flow velocity fields.

Development of advanced technology for a sodium cooled reactor has been carried out as a part of the fast breeder reactor (FBR) feasibility study. A compact, high power system as shown in Fig.1-6 is planned to reduce construction cost. The Upper Inner Structure (UIS) has a slit where an arm of Fuel Handling Machine (FHM) can go inside so as to reduce the diameter of the reactor vessel (RV). Further, sodium can flow through the UIS.

Because of these design features, the sodium exiting from the core flowed upward with high velocity through the UIS slit. As a result, flow velocity near the free surface in the RV was increased. This may results in gas entrainment (GE) at the free surface. Dipped plates were set below the free surface to reduce the flow velocity near the surface. However, prevention of the GE is still a significant issue in the design.

A flow optimization study based on experiments and numerical analyses has been performed. An FHM plug was invented to shut the high velocity flow toward the free surface based on the velocity calculation shown in Fig.1-7. Velocity near the free surface was reduced by half.[1] Further, numerical analyses as shown in Fig.1-8 were applied to the GE phenomena and an estimation method of the GE was developed.[2] The prospect of preventing GE in the reactor was obtained by these studies.

References

1) Kimura, N., Hayashi, K., Kamide, H. et al., Experimental Study on Flow Optimization in Upper Plenum of Reactor Vessel for a Compact Sodium-Cooled Fast Reactor, Nuclear Technology, vol.152, 2005, p.210-222.

2) Sakai, T. et al., Study on the Gas Entrainment Design Method by CFD Data on Steady Cylindrical Systems for a Sodium-Cooled Reactor, Proceedings of 2006 International Congress on Advances in Nuclear Power Plants (ICAPP '06), Reno, USA, 2006, Paper 6409, 7p. in CD-ROM.

1-4 Vibration Characteristics of Piping Excited by Turbulent Flows

—Flow-Induced Vibration of Large Diameter Piping System under High Flow Velocity Condition—

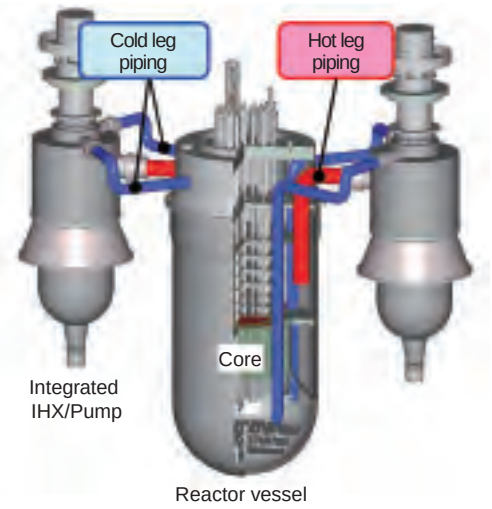

Fig.1-9 Schematic view of primary cooling system of JAEA sodium-cooled fast reactor (JSFR)

The primary cooling system consists of the reactor vessel, integrated intermediate heat exchangers (IHXs) with pumps, and large diameter piping (one hot leg piping and two cold leg pipings in each loop). The primary piping penetrates the roof deck of the reactor vessel ("top-entry system"), and is made with high chromium steel which has high strength and low thermal expansion, so that it can be shortened. As a result, a compact plant layout has been achieved.

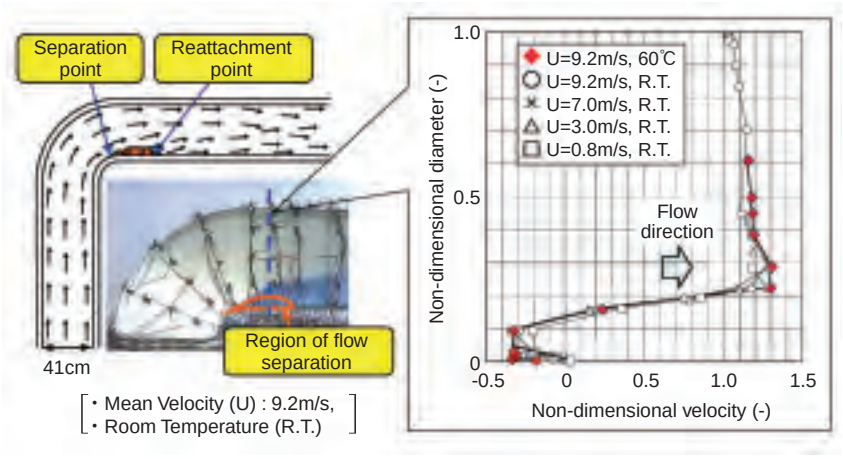

Fig.1-10 Flow pattern and velocity distributions in acrylic pipe

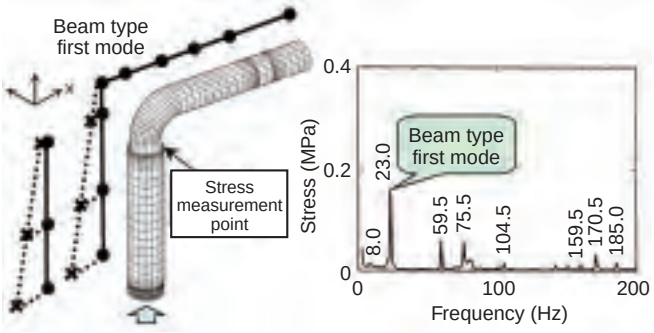

Fig.1-11 Natural vibration mode and stress of steel pipe

A JAEA sodium-cooled fast reactor (JSFR) is characterized by the use of a simplified two-looped large-scaled heat transport system as shown in Fig.1-9. As the results, the diameter of the piping system and the sodium flow velocity reach up to 1.3m and the order of 9.0m/s, respectively.

Generally, sodium-cooled fast reactors (FRs) use thin piping walls because of higher temperature and lower pressure operation conditions than light water reactors. JSFR operates with thin and larger diameter piping and higher flow velocity than conventional FR concepts. Therefore, maintaining structural integrity of the piping system is an important issue for the realization of the two-looped heat transport system, and vibration characteristics of the piping system, which is excited by turbulent flows generated at a 90° elbow, must be elucidated.

Addressing the above problems, water experiments on flow and vibration behavior of the piping system were carried out using a 1/3 scale model which simulates the hot leg piping of the primary cooling system. In this experiment, an acrylic pipe is used to visualize the flow pattern and a stainless steel pipe is used to simulate vibration response. As test parameters, mean velocity and water temperature, which are dominant factors affecting the flow condition, were selected; the dependencies of the flow conditions and vibration behavior were examined.

Firstly, flow pattern and the velocity distributions in the pipe were examined using the acrylic pipe (Fig.1-10). The region of flow separation, which becomes main source of the turbulent flows, was observed at the corner of the elbow. The sizes and locations of the region of flow separation and non-dimensional velocity distributions normalized by mean velocity almost coincided even in different velocity and water temperature conditions. Therefore, it was confirmed that flow pattern and velocity distributions in the piping were independent of flow conditions.

Next, the natural modes of vibration of the piping were identified using the steel pipe. Further, it was found that vibration stresses caused by turbulent flow were excited at the natural frequencies of the steel pipe (Fig.1-11).

From the test results, it was clarified that the turbulent flow and the vibration stress depended on the mean velocity. Then, the exciting force on the hot leg piping was characterized by converting the characteristics of the turbulent flow which were obtained in the acrylic pipe under the same velocity, based on the scale ratio, and the vibration response of the hot leg piping was evaluated. The maximum stress of the hot leg piping was below the design fatigue limit of the piping material, and therefore it is expected that the integrity of the large diameter piping will be maintained under high flow velocity condition.

Reference

Japan Atomic Energy Agency, Feasibility Study on Commercialized Fast Reactor Cycle Systems Technical Study on Report of Phase Ⅱ－(1) Fast Reactor Plant Systems－, 2006, JAEA-Research 2006-042, p.486 in CD-ROM attached (in Japanese).

1-5 Research and Development of Advanced Aqueous Reprocessing and Simplified Pelletizing Fuel Fabrication

—Fuel Recycling System (Reprocessing and Fuel Fabrication) for the Next Generation—

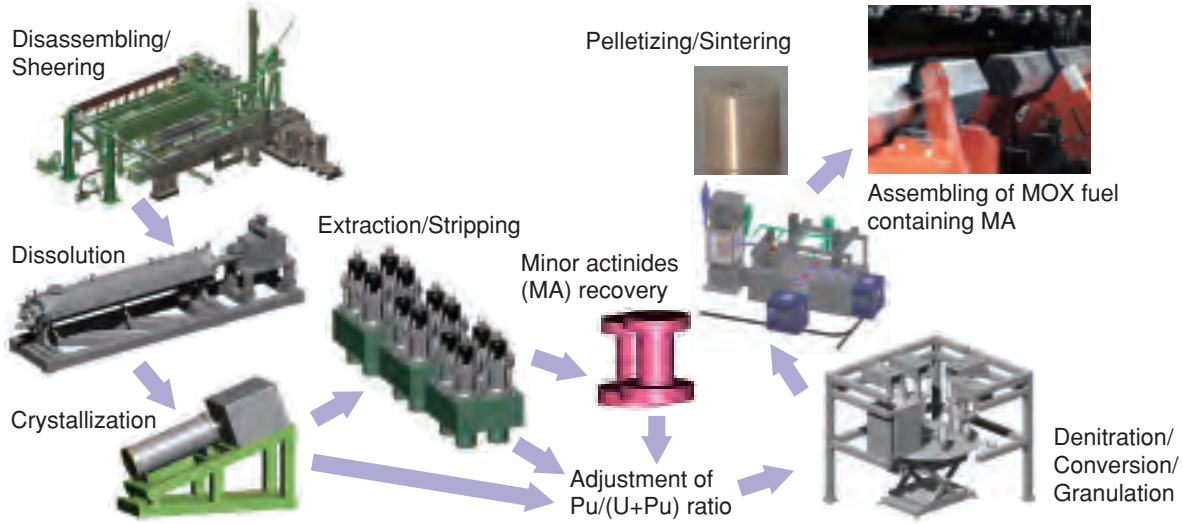

Fig.1-12 The combination of the advanced aqueous reprocessing process and the simplified pelletizing process
The advanced aqueous reprocessing process reduces the amount of aqueous and organic solutions processed in the following extraction/stripping process by the partial separation of uranium (U). Co-extraction and co-stripping of U, neptunium (Np) and plutonium (Pu) eliminate the need for separate partitioning of Pu and purification of U and Pu. Moreover, these fuel products with low decontamination will aid in proliferation resistance.
For adjustment of Pu/(U+PU) ratio, a simplified pelletizing process replaces powder mixing with mixing of solutions: U, U/Pu and minor actinides (MA) solutions. Lubricant-free pelletization and remote fuel fabrication in a cell for producing low-decontamination fuel assemblies and for recycling MA are adopted.

The fast reactor fuel cycle makes possible fuel products with lower decontamination factor (DF) than that of the conventional fuel cycle system. Fig.1-12 shows the key components of a plant based on the advanced aqueous reprocessing process and the simplified pelletizing fuel fabrication process to be used in the fuel recycling system of the next generation. In the advanced aqueous reprocessing process, U, Np and Pu are co-extracted and co-stripped by a single-cycle extraction process. Therefore, partitioning and purification can be eliminated from the conventional PUREX process. In addition, the integration of the reprocessing facility and fuel fabrication facility can contribute to reduction of capital cost.

On the other hand, some modifications of the conventional fuel cycle system may cause increase of capital cost:

-adding the MA recovery process to the reprocessing process,

-adopting remote processing in a hot cell for the fuel fabrication, for extensive-decontamination of fuel products.

It is evaluated that the capital cost of the plant can be reduced to about 50% from that of the conventional fuel recycling plant by optimization of the equipment and application of the above-mentioned new technologies. One concrete example of technology developed for the conceptual design study is minimization of solvent extraction by crystallization. U comprises about 80% of the heavy metal elements contained in the dissolver solution of the spent fuel, and most of the U can be crystallized and separated in the crystallization process. Partial separation of U in the crystallization process greatly reduces the following extraction/stripping of the aqueous and organic solutions. Application of the extraction chromatography leads to the downsizing of the equipment of the MA recovery process. In the simplified pelletizing process, in order to minimize the fuel fabrication processing required in a hot cell, Pu/(U+Pu) ratio is adjusted by mixing a U solution which has been crystallized, a U/Pu solution which has been subjected to extraction/stripping, and a MA solution obtained from the MA recovery, instead of a U and Pu powder mixing process that is a major part of the conventional fuel fabrication process. By these modifications, the fuel cycle system considered in this design study met the requirements for economic competitiveness, efficient utilization of resources, low environmental impact, and proliferation resistance.

The advanced aqueous reprocessing process is considered to be feasible based on the technical information gained at existing plants (Tokai Reprocessing Plant and Rokkasho Reprocessing Plant) although the system and the components for the crystallization and MA recovery should be investigated. Also, feasibility may be attained faster by cooperating with countries that also are developing an aqueous reprocessing process for the next generation. The above fuel fabrication process is also considered to be feasible because the simplified pelletizing is a modified process based on the conventional pelletizing process, although the remote-controlled components have yet to be investigated.

Reference

Japan Atomic Energy Agency and The Japan Atomic Power Company, Feasibility Study on Commercialized Fast Reactor Cycle Systems—Phase Ⅱ Final Report—, 2006, JAEA-Evaluation 2006-002, 191p. (in Japanese).

1-6 Solvent Extraction of Actinide Elements in New Extraction System for TRU Recovery (NEXT) —Development of Advanced Reactor Fuel Reprocessing—

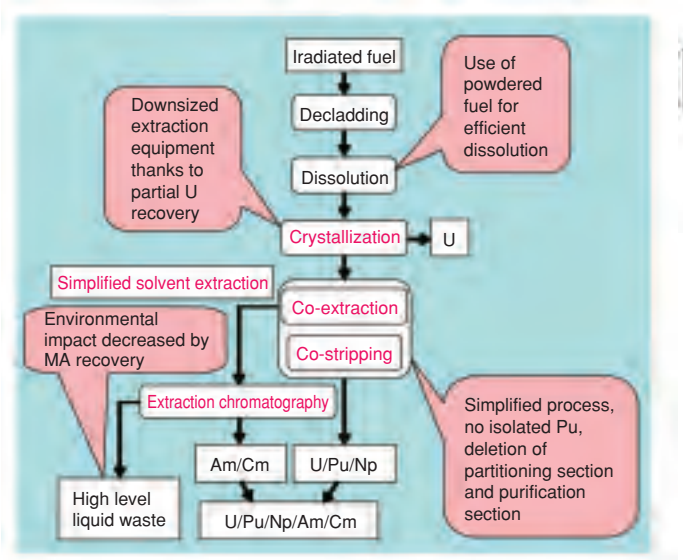

Fig.1-13 Outline of the NEXT Process
The NEXT process is a simplified conventional PUREX process aiming for economic competitiveness. MAs are recovered and loaded as MOX fuel of the advanced reactor for efficient utilization of resources and low environmental impact.

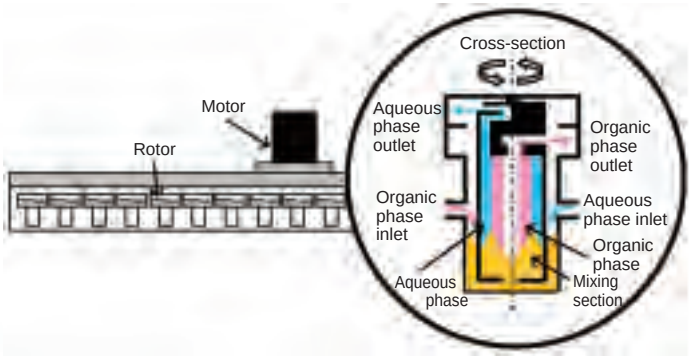

Fig.1-14 Type CPF centrifugal contactor
Centrifugal contactors separate organic phase from aqueous phase by centrifugal force. These have large throughput and low degradation of solvent in comparison with mixer-settlers because residence time is very short.

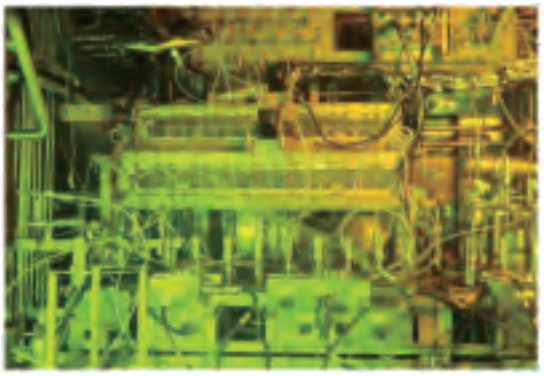

Fig.1-15 Centrifugal contactors in hot cell

We have been studied an advanced aqueous reprocessing process, named New Extraction System for TRU Recovery (NEXT) (Fig.1-13). The NEXT process basically consists of Uranium (U) crystallization, simplified solvent extraction of U by the extractant tri-n-butylphosphate (TBP), Plutonium (Pu) and Neptunium (Np) co-recovery, and Americium (Am) and Curium (Cm) recovery with extraction chromatography technology.

In the NEXT process, it is desirable to recover not only U and Pu but also minor actinides (MAs) for loading them in MOX fuel of the advanced reactor. This will be effective in decreasing environmental impact because it brings about the reduction of long-lived radioactive elements in the wastes.

Among the MAs, Am and Cm are poorly extracted by TBP. Therefore, these elements need to be separated from high level waste using a new extractant which has stronger affinity to MAs than TBP. On the contrary, by proper control of Np valence, it is possible to recover Np with U and Pu by TBP. Assuming that a rather low decontamination factor of the reprocessing product is made possible by the fast reactor fuel cycle, partitioning section and purification section are deleted, and U, Pu and Np co-recovery flow sheet is designed by single cycle.

Experimental studies using irradiated fuel have been carried out at the Chemical Processing Facility (CPF) with centrifugal contactors, whose residence time is considerably smaller than that of mixer-settler (Fig.1-14, Fig.1-15). The feed solution is adjusted to have high nitric acid concentration ([HNO_3]). This condition adjusts the Np valence so that it is extractible by TBP. As expected, about 99% of Np was recovered with U and Pu in this process. Through this series of studies, a U, Pu and Np co-recovery process using high [HNO_3] feed solution was successfully demonstrated.

Reference

Nakahara, M. et al., U, Pu and Np Co-recovery in Simplified Solvent Extraction Process—The Extraction Behavior of Np at the Condition of High HNO_3 Concentration Feed Solution and Scrubbing Solution—, 2006, JAEA-Research 2006-030, 43p. (in Japanese).

1-7 Establishment of a Remote Fabrication Technique Making Fast Reactor Fuel from Excess Minor Actinide
—Development of Fabrication Technique for MOX Fuels Containing Americium—

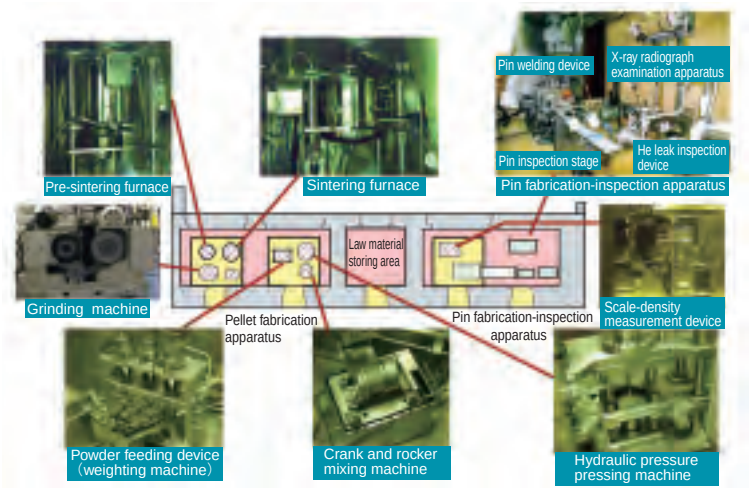

Fig.1-16 (upper left) The aspects of remote fuel fabrication system in AGF
All apparatuses for fuel pin fabrication are placed in hot cells, and can be operated by remote control.

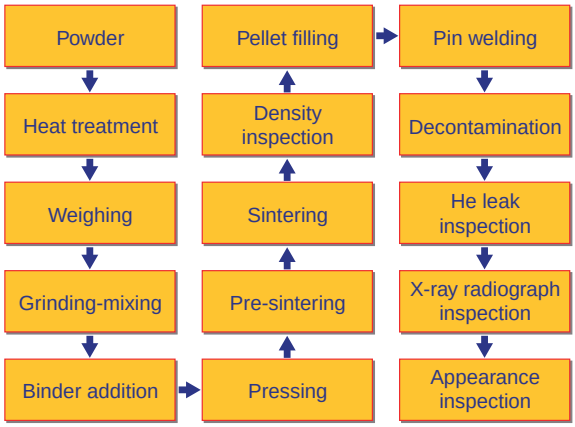

Fig.1-17 The fuel fabrication process in hot cells
Schematic flow of main process was illustrated on fuel pin fabrication.

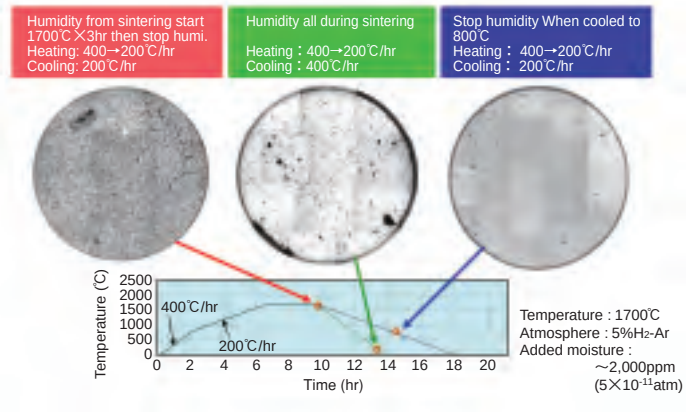

Fig.1-18 (lower left) Optimization of the sintering condition for Am-MOX fuels
Homogeneous and dense pellet could be fabricated by optimizing the moisturized condition.

In the Alpha-Gamma Facility (AGF), a fabrication technique incorporating americium (Am) in mixed oxide fuel (Am-MOX fuel) has been developed for a low decontamination TRU fuel system, required in plans for a commercial Fast Breeder Reactor (FBR) fuel cycle with low environmental burden. This remote fabrication technique was demonstrated through fabrication of Am-MOX fuel into pins for irradiation tests performed in the experimental fast reactor "JOYO" in order to elucidate the irradiation behavior of Am-MOX fuel.

The outlines of the apparatuses and the fabrication tests are mentioned below.

The pellet fabrication system was composed by some equipments, such as a powder feeder, a grinding-mixing machine, a hydraulic pressure pressing machine, sintering furnaces, and a pellet measurement-inspection devices. These equipments were installed in three inner-boxes surrounded with concrete shield walls of 1 meter thickness. Moreover, pin fabrication and inspection apparatuses such as a pellet filling device, a welding device, and a non-invasive inspection system were installed. In this process, after fuel pellets are inserted in fuel cladding tubes, they are welded to keep them air-tight. An outline of the facility and the fabrication process are shown in Fig.1-16 and Fig.1-17, respectively. The whole facility is operated remotely using manipulators, and therefore, new features were introduced for operability. Consequently, highly radioactive MA and/or fission products (FP) can be treated safely.

Firstly, a fabrication test of 200 UO_2 pellets confirmed that there were no technical issues in the remote-operability of the designed fabrication system even though it is a small scale facility.

Next, in the Am-MOX fabrication tests, decrease of pellet density occurred due to micro cracks and pores formed as the content of Am increased. In addition, it was found that the sintering time should be longer than for normal MOX fuel. Based on other information and a lot of trial tests as well as these experiences, the optimum fabrication conditions (Fig.1-18) achieving high density and stable structure were developed.

Up to now, five Am-MOX fuel pins (maximum Am content 5 wt.%) have been fabricated, for short-term (3 pins) and for long-term (2 pins) irradiation tests in "JOYO". This technique should be of use in other kinds of low decontamination factor fuels planned in the future.

Reference

Yoshimochi, H. et al., Fabrication Technology for MOX Fuel Containing AmO_2 by an In-cell Remote Process, Journal of Nuclear and Technology, vol.41, no.8, 2004, p.850-856.

1-8 Search for the Way to Nuclear Power Sustainability
－Fast Reactor Cycle Deployment Scenario Analysis－

Table1-2 Candidate in the phase Ⅱ of Feasibility Study on commercialized FR cycle systems

	FR systems	Fuel cycle systems	Upper box: Breeding ratio Lower box: Average burn-up (GWd/t)	
			High breeding type	Low breeding type
(a)	Sodium-cooled reactor (MOX Fuel)	・Advanced aqueous method ・Simplified pelletizing method	1.10 90	1.03 115
(b)	Sodium-cooled reactor (Metal Fuel)	・Metal electrorefining method ・Injection casting method	1.11 134	1.03 153
(c)	Lead-bismuth-cooled reactor (Nitride Fuel)	・Advanced aqueous method ・Simplified pelletizing method	1.10 105	1.04 128
(d)	Helium gas-cooled reactor (Nitride coated-particle fuel)	・Advanced aqueous method ・Vibro-packing method	1.11 69	1.03 89
(e)	Water-cooled reactor (MOX Fuel)	・Advanced aqueous method ・Simplified pelletizing method	1.05 45	

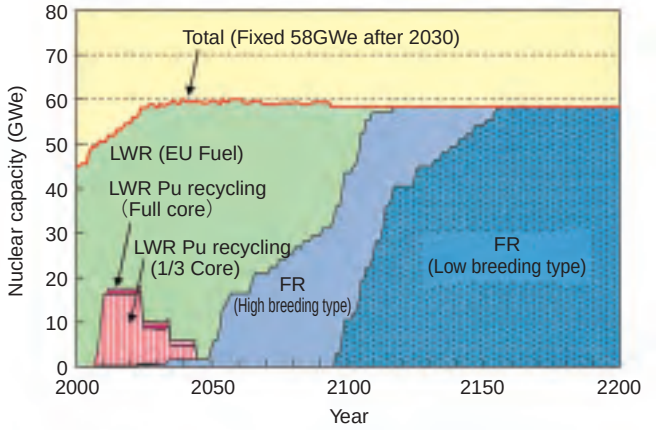

Fig.1-19 The shift from phase Ⅱ candidate (a) LWR to FR

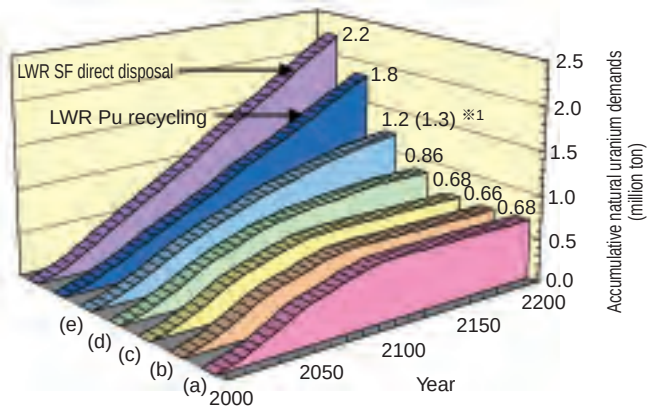

Fig.1-20 Accumulative natural uranium demands of the phase Ⅱ candidates

※1 Accumulative demands up to 2300 when the shift to Water-cooled reactor from LWR will be complete

Regarding the Fast Reactor (FR) cycle which is expected to provide efficient use of uranium resources and the reduction of high-level radioactive wastes, the Japan Cabinet Council decided on October 14th 2005 that the government shall respect the Framework for Nuclear Energy Policy which will aim at a commercial base for the FR cycle by 2050. JAEA is carrying out a "Feasibility Study on commercialized FR cycle systems" (FS) to present a scenario for FR cycle actualization and an R&D plan for commercialization to the government by 2015. In the phase Ⅱ research finished in fiscal 2005, scenario analysis of deployment from a LWR cycle to FR cycle was performed for a typical candidate (Table1-2) among several that combine the FR and Fuel cycle system.

The FR cycle deployment scenario analysis and the cycle material flow analysis estimated parameters for future nuclear capacity, planned fuel cycle facilities, start time of FR cycle system installation to be completed by 2050, the recycling method of MA contained in LWR spent fuel reprocessing waste fluid, etc. This scenario analysis estimated each candidate FR cycle system regarding deployment period from LWR to FR, the accumulative natural uranium demands, LWR spent fuel quantity to be stored, amount of high-level-waste to be stored, etc. The FR cycle deployment scenario analysis assumes that high breeding FRs are introduced replacing LWRs which finish their life and low breeding FRs are gradually introduced keeping plutonium demand/supply balance. In concept (a), the shift from LWR to FR 2100 will be complete under the conditions of the New Nuclear Policy-Planning Council (i.e. future nuclear capacity is fixed at 58 GWe in 2030 and FR introduction starts in 2050) (Fig.1-19). Fig.1-20 shows the accumulative natural uranium demand of several nuclear scenarios. In LWR SF direct disposal and LWR plutonium recycling, the accumulative natural uranium demand continues to increase. On the other hand, the demand of the candidates (a) ~ (d) reaches saturation at the beginning or middle of the next century and then does not require importation of natural uranium. This result shows that nuclear power can be sustainable.

One scenario analysis result is that in shortening the deployment period from LWR to FR as much as possible and lowering natural uranium use, small in-core plutonium inventory and a FR system with a high breeding ratio is desirable, and especially in the transition term the plutonium recovered from the spent fuel of LWR and breeding FR must be used effectively.

Reference

Japan Atomic Energy Agency and The Japan Atomic Power Company, Feasibility Study on Commercialized Fast Reactor Cycle Systems－Phase Ⅱ Final Report－, 2006, JAEA-Evaluation 2006-002, p.59-60 (in Japanese).

1-9 Finding Promising Fast Reactor Cycle Concepts from Multiple Viewpoints
—Multidimensional Evaluation of Fast Reactor Cycle Systems—

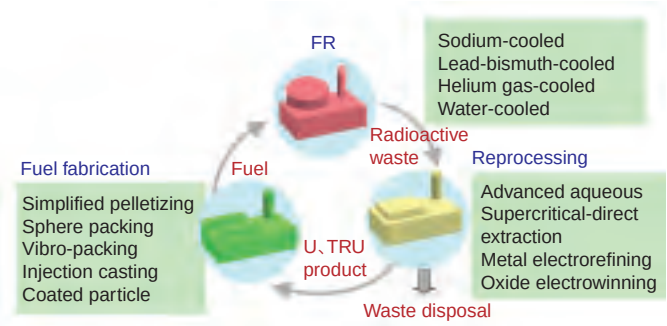

Fig.1-21 FR cycle candidate concepts
Promising technologies are developing for the nuclear power plant, reprocessing, and fuel fabrication of the FR cycle. FR candidate concepts consisting of a combination of these technologies are proposed.

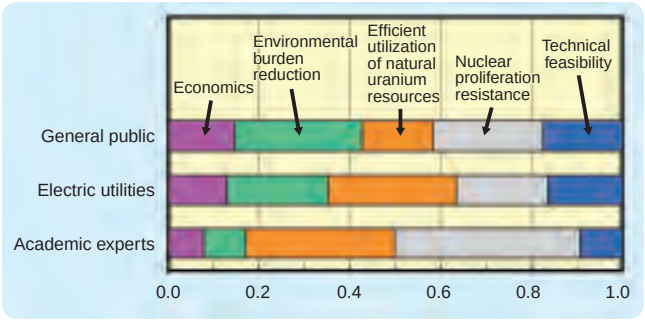

Fig.1-22 The weight given to five evaluation viewpoints
The weight given to these five evaluation viewpoints by the general public, the electric utilities, and the academic experts was determined from questionnaire.

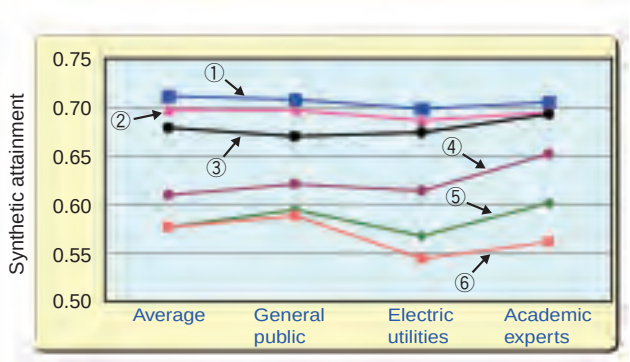

Six FR cycle candidate concepts which have combined the FR cycle fields of reactor and fuel cycles.

①Sodium-cooled + Advanced aqueous + Simplified pelletizing (MOX Fuel)
②Sodium-cooled + Advanced aqueous + Vibro-packing (MOX Fuel)
③Sodium--cooled + Metal electrorefining+ Injection casting (Metal Fuel)
④Pb-Bi-cooled + Advanced aqueous + Simplified pelletizing (Nitride Fuel)
⑤He gas-cooled + Advanced aqueous + Coated particle (Nitride Fuel)
⑥Water-cooled + Advanced aqueous + Simplified pelletizing (MOX Fuel)

Fig.1-23 Multidimensional evaluation of FR cycle candidate concepts by five evaluation viewpoints
A higher value on the vertical axis indicates concepts with higher attainment of the five evaluation viewpoints: Economics, Environmental Burden Reduction, Efficient Utilization of Natural Uranium Resources, Nuclear Proliferation Resistance, and Technical Feasibility.

Phase Ⅱ of the Feasibility Study on Commercialized fast reactor (FR) Cycle Systems (FS) was launched in 2001 as a five-year project. As part of the FS, the objective evaluation of multiple aspects of some FR cycle concepts (Fig.1-21) was performed, thus identifying promising FR cycle candidate concepts.

This multidimensional evaluation resulted in the determination of the degree to which the development objectives of the FR cycle system are attained.

We selected 8 evaluation viewpoints for this multidimensional evaluation. With regard to safety, we made pass or fail evaluations since this is considered to be a necessary precondition for the FR cycle. The economics, the environmental burden reduction and the efficient utilization of natural uranium resources were quantitatively evaluated. The nuclear proliferation resistance, the technical feasibility, the business applicability and the public acceptance were evaluated by the combination of the judgment of the academic experts and a quantitative evaluation.

These evaluation viewpoints each have a maximum of four ranks down to a low rating (the hierarchical structure). In the quantitative evaluation, the physical quantity of the lowest rank is converted into a utility value from 0 to 1 using the utility function. All indicators are given appropriate weighting.

We determined the weighting of the evaluation viewpoints based on a questionnaire asking the importance of various considerations for energy in future society, given to the stakeholders, that is, the general public, the electric utilities (the electric power company employees) and the academic experts in the energy field. 5 viewpoints pertinent to energy development were chosen out of 8 possible viewpoints based on these questionnaires. The general public tended to give importance to the environmental burden reduction and the nuclear proliferation resistance, the utility people tended to give importance to the efficient utilization of natural uranium resources, and the academic experts tended to give importance to the efficient utilization of natural uranium resources and the nuclear proliferation resistance (Fig.1-22).

For 5 viewpoints, we calculated the weighting from the results of the questionnaire and calculated the degree to which these viewpoints were satisfied (the sum of all utility values) (Fig.1-23). As a result, it was found that the combination of Sodium cooled FR with MOX fuels, advanced aqueous reprocessing and simplified pelletizing fuel fabrication seems to be satisfy all viewpoints to the highest degree, and is the most promising FR cycle candidate concept.

Reference

Japan Atomic Energy Agency, The Japan Atomic Power Company, Feasibility Study on Commercialized Fast Reactor Cycle Systems—Phase Ⅱ Final Report—, 2006, JAEA-Evaluation 2006-002, p.43-45 (in Japanese).

1-10 Probabilistic Safety Assessment Study of Fast Reactor Cycle

—Development of World's First Safety Evaluation Method for the Entire Fuel Cycle—

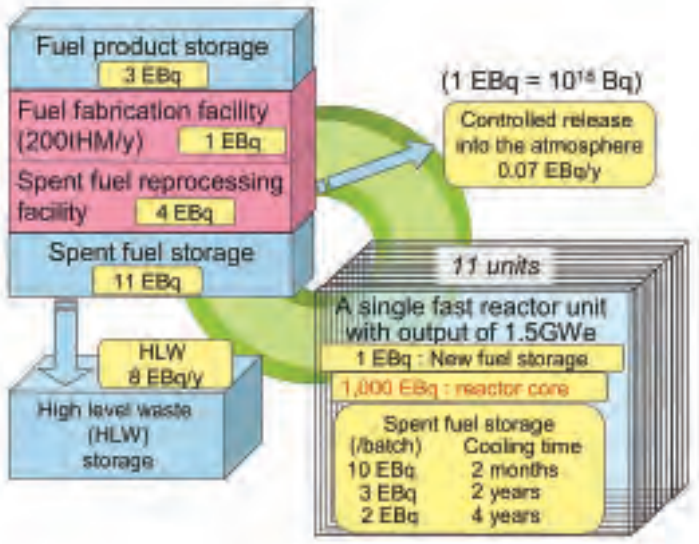

Fig.1-24 Radioactivity inventory in the fast reactor cycle

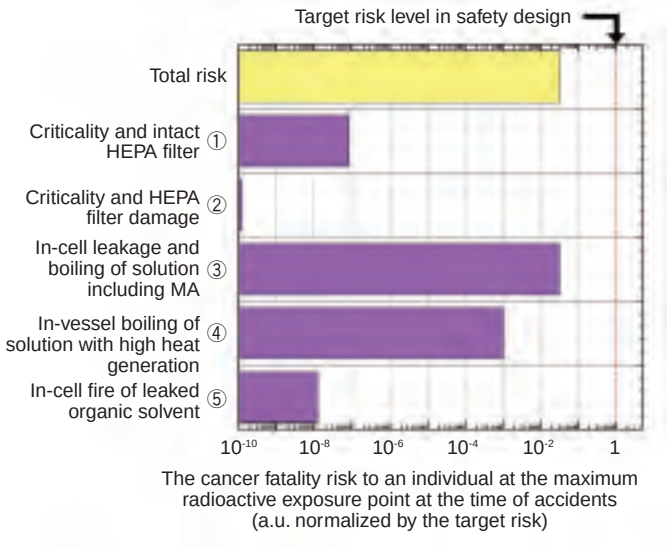

Fig.1-25 Breakdown of the public cancer fatality risk in the aqueous reprocessing facility upon various accidents

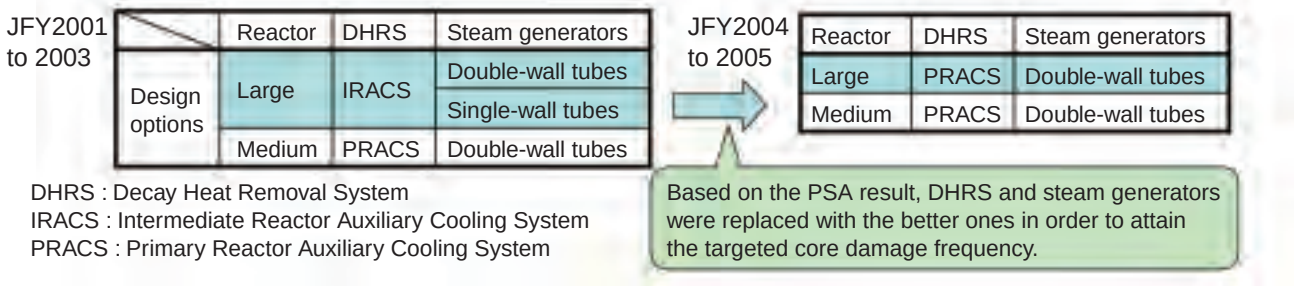

Fig.1-26 Effect of the probabilistic safety assessment on the conceptual design of fast reactor cooling systems

Systematic risk analyses were conducted on design concepts of fast reactors (FR), spent fuel reprocessing facilities and fuel fabrication facilities formulated in phase Ⅱ of the feasibility study on commercialized FR cycle systems, aiming at restraining adequately the entire risk of the FR cycle and assuring safety.

First, envisioning an FR cycle that consists of 11 FR units with the output of 1.5GWe and a pair of fuel cycle facilities that can treat 200tHM of reactor fuel per year, corresponding to operation of the 11 units, the radioactivity inventory of each facility was calculated. Fig.1-24 shows the result that radioactivity in the fuel cycle facilities (total about 5×10^{18}Bq) is about 1/200 of that in the single FR unit (about 1000×10^{18}Bq). Then, a probabilistic safety assessment (PSA) of the solution system in the aqueous reprocessing facility was made in order to obtain comprehensive and simple analysis and estimation of the public risk due to abnormal radioactive material release outside the facility. Fig. 1-25 shows that the risk is lower than the target risk level in the safety design and that criticality and fire make a small contribution to the risk. Our risk analysis of FR fuel cycle is the first such trial in the world and it is necessary to develop further our analytic model and data in the future.

Since the severe core damage can be regarded as a dominant factor in the risk of the sodium-cooled FR, the core damage frequency of some design concepts was calculated through PSA based on the component operating time and failure instances that were accumulated in the sodium-cooled FR. In the conceptual design stage, adequate safety must be verified in selecting the basic design concept to be refined in future design and development work. From the safety point of view, it is important to select a design concept that will certainly attain the targeted core damage frequency based on all the current available information. As shown in Fig.1-26, the present study served to selection of the suitable concept from among the design options of the reactor cooling system.

References

Japan Atomic Energy Agency, Feasibility Study on Commercialized Fast Reactor Cycle Systems Technical Study Report of Phase Ⅱ, JAEA-Research 2006-042, 1807p. in CD-ROM attached and JAEA-Research 2006-043, 1327p. in CD-ROM attached (in Japanese).

1-11 System Start Up Test of the Prototype Fast Breeder Reactor MONJU

—From the Achieved Test Results (Criticality Test to Power Up Test(40% Power))—

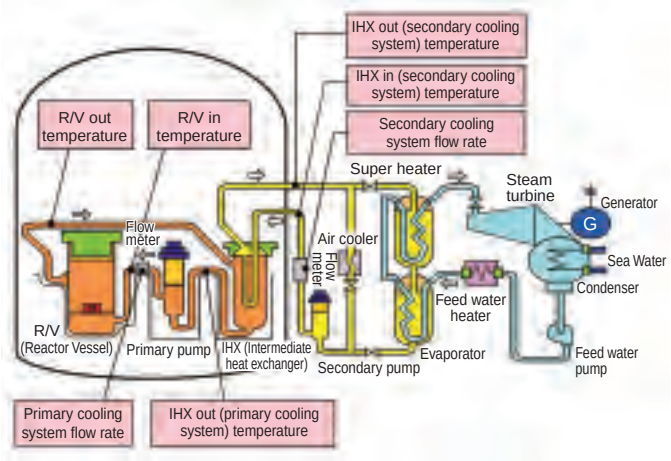

Fig.1-27 "MONJU" components and test points

The heat from the reactor is transferred through the primary and secondary cooling system to the evaporator and super heater which generates steam to drive the turbine generator. In this plant, liquid metal sodium is used as the coolant of the primary and secondary cooling system.

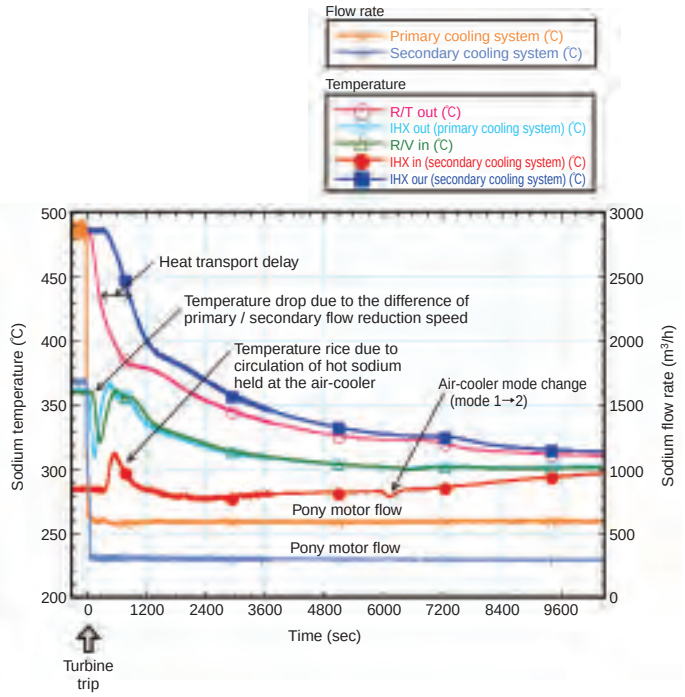

Fig.1-28 Changes in major process parameters (Plant trip evaluation test)

In the nuclear power plant design, changes of plant condition (such as coolant temperature and flow rate) during supposed accidents or events are estimated by numerical analysis (Plant dynamic response analysis) for design validation. These test data from the actual plant should also contribute to future plant design because they will help to improve analyzing methods.

The system startup test (SST) of "MONJU" has been suspended since the secondary cooling system sodium leak accident on December 8, 1995. However, specific test results have been disclosed to academic organizations (e.g. Atomic Energy Society of Japan), and all results have recently been summarized and disclosed in preparation for the upcoming restart.

Among the test results, this paper will focus on the "Plant trip evaluation test (triggered by turbine trip)" which is one of the typical tests conducted in the power up test phase.

In this test, vacuum failure in the condenser was simulated during 40% rated power operation to induce turbine and reactor trip. The behavior of the plant has been observed during the transient and it has been confirmed that the interlock system can shut down the plant safely . Also the status of each component and the process parameter data were obtained to check details of the plant behavior comprehensively.

In the results of this test, the equipment status, annunciator indications, and plant process parameter values indicate that the safety interlock worked successfully and the plant shut down automatically and safely.

Moreover, detailed data on the plant during the transient was obtained.

The "MONJU" components and test points are shown in Fig.1-27, and the transient data of the major process parameters (temperature & flowrate of the primary and secondary cooling system) in Fig.1-28.

Since the motor of the main circulation pump changes from the main motor to auxiliary motor with the plant trip, the flow rate of primary and secondary cooling system decreases. The primary sodium temperature at the inlet of the reactor vessel decreases temporarily due to the difference in the reduction speed of flow rate between the primary and secondary system, but then it recovers as the primary and secondary system flow rates stabilize at respective levels.

On the other hand, the secondary sodium temperature at the inlet of Intermediate Heat Exchanger (IHX) rises shortly after the event since the high temperature sodium held at the air cooler flows to the IHX when the main flow path is switched from steam generator to air cooler.

Such data from actual plant operation is necessary to confirm performance and complete R&D of "MONJU" itself, and furthermore contributes to future reactor design through the advancement of plant dynamics analysis technique etc.

"MONJU" is currently under modification to add mitigation measures against sodium leak etc, in preparation for restarting the SST. The program will be conducted carefully step by step, reflecting past experience so that we could obtain valuable data.

Reference

1) Miyakawa, A. et al., The Prototype Fast Breeder Reactor Monju System Startup Tests Report Summary Report of the System Startup Tests < Criticality Test ~ Power Up Test(40% Power)>, Japan Nuclear Cycle Development Institute, 2005, JNC-TN 2410 2005-002, p.267-269 (in Japanese).

1-12 Prediction of Unplanned MONJU Shutdown Frequency
—Reactor Trip Frequency Prediction Using Fault Tree Analysis Method—

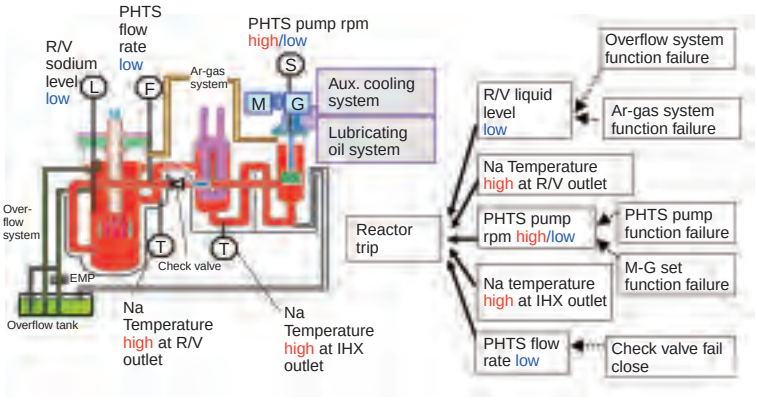

Fig.1-29 Reactor trip on primary system
Fault Tree development through clarification of causes of system component failures leading to reactor trip

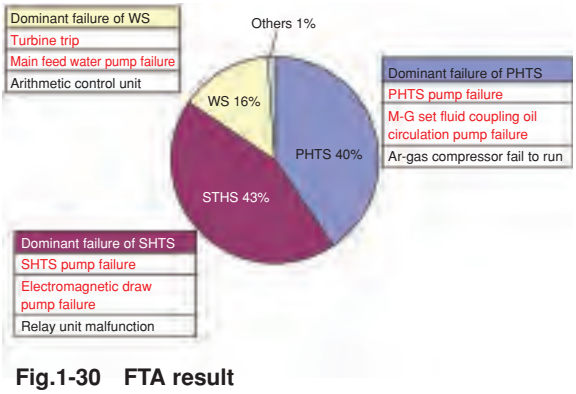

Fig.1-30 FTA result
Failures contributing to reactor trip, broken down by component

Table1-3 Actual case of mechanical sodium pump failure (19 cases)

Parts	Shaft	Motor	Lub. Oil	Others
Cause	Deformation or Sodium oxide accumulation	Brush failure, dust penetration	Seal failure	Unknown
Number of failure	9	6	3	1

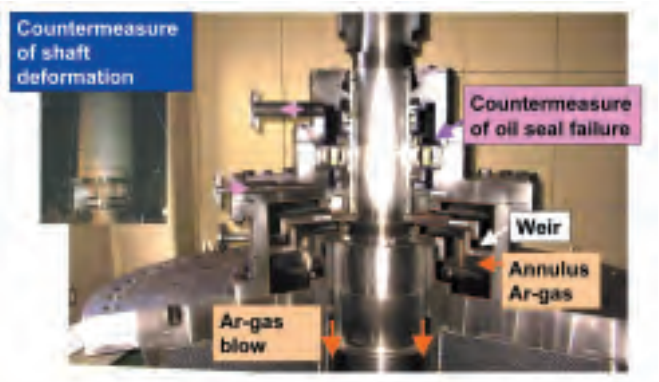

Fig.1-31 Countermeasures of mechanical sodium pump
Countermeasures against the pump failures shown in Table1-3: Thermal convection restrainer prevents thermal deformation of the shaft. Argon gas blower prevents sodium oxide accumulation.

Since safe and stable operation is required for nuclear power plants, including the fast breeder prototype reactor "MONJU", it is important to reduce occurrence of unplanned shutdowns of power operation as much as possible.

To improve operational reliability, we have performed fault tree analysis (FTA) to identify the important component failures leading to reactor trip, and to estimate the reactor trip frequency.

The fast breeder reactor component reliability database "CORDS" and Japanese LWR component failure database were used in the FTA of "MONJU". As the result of FTA, the reactor trip frequency was estimated as 1.2/reactor year, and the primary and secondary main circulation pumps were identified as the important components.

The failure cases of sodium circulation pumps recorded in "CORDS" database were refereed to in designing countermeasures in similar mechanical sodium pumps of "MONJU". Therefore high operational reliability has been kept and the actual reactor trip frequency is expected to be smaller than the FTA prediction.

Through this study,

(1) The components crucial to "MONJU" operational reliability have been identified.

(2) Frequency of unplanned reactor shutdown based on the current component failure rate has been estimated to be slightly higher than domestic LWRs, but the actual value is seen to be significantly smaller, due to the countermeasures against pump failures.

(3) If there are modifications to "MONJU" new prediction of unplanned reactor shutdown frequency has been enabled, through appropriate amendment of the fault tree.

Reference

Sotsu, M. et al., Unplanned Shutdown Frequency Prediction of FBR MONJU using Fault Tree Analysis Method, Proceedings of 13th International Conference on Nuclear Engineering (ICONE 13), 2005.

1-13 An Advanced Transport Cross-Section Collapsing Method for Three Dimensional Transport Code Was Developed
—MONJU Core Neutronics Analysis Method Upgrading Research—

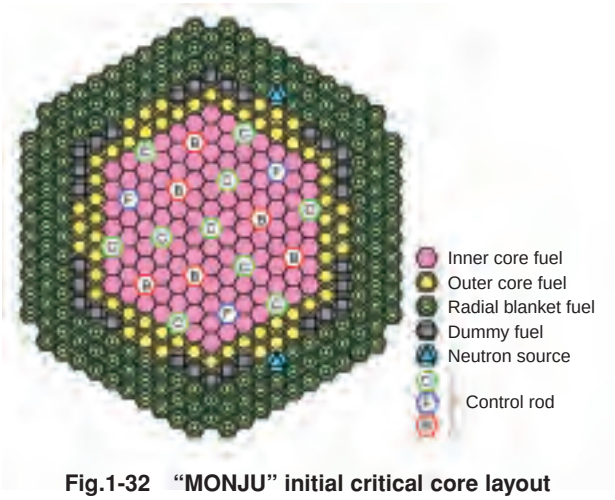

Fig.1-32 "MONJU" initial critical core layout

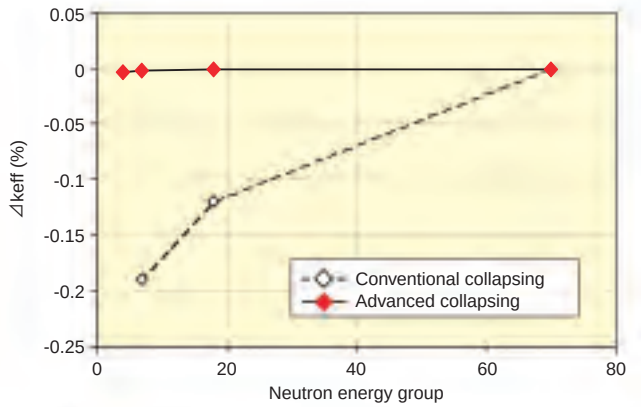

Fig.1-33 Neutron energy collapsing effect by whole core calculation

This figure shows the difference of the effective multiplication factor (collapsing error), calculated by the conventional and advanced collapsing method, based on the 70 energy-group calculation as the reference. The newly developed advanced method gives drastically negligible collapsing error, independent to the number of neutron energy groups (horizontal axis).

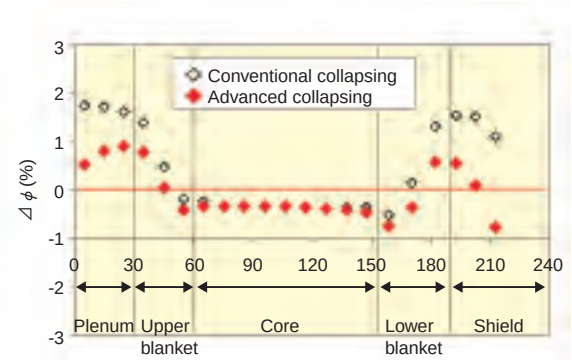

Fig.1-34 Neutron energy collapsing effect on neutron flux distribution

This figure shows the difference of the neutron flux spatial distribution (collapsing error), calculated by the conventional and advanced collapsing method in 18 neutron energy groups, based on the 70 energy-group calculation as the reference. The newly developed advanced method gives improved coincidence with the reference calculation, especially in the core peripheral region (axial blanket).

It is of great significance, from the viewpoint of the future fast breeder reactor (FBR) commercialization, to evaluate and to validate the current design analysis method and to rationalize the design margin, by effectively using the "MONJU" core physics test data. A series of analysis has been carried out on the "MONJU" core criticality (effective multiplication factor) from this viewpoint.

It is general to analyze the core criticality by a diffusion approximation calculation (isotropic scattering approximation) to save the computer resources, while this requires the correction for the approximation based on the comparison with the more detailed and exact transport theory analysis. A criticality analysis of the "MONJU" initial critical core (Fig.1-32) by the three-dimensional nodal Sn transport code; NSHEX has been conducted for this purpose and it became clear that coarse neutron energy group approximation (discrimination of continuous neutron energy into a coarse group structure, which allows for computer resource saving) gives non-negligible neutron energy collapsing effect (approximation error).

An investigation into the calculational algorithm of transport cross-section in NSHEX was conducted and it was found out that the neutron leakage between the nodes would not be preserved by the conventional neutron energy collapsing method because of the intra-nodal polynomial approximation of the neutron flux spatial distribution in NSHEX. An advanced neutron energy collapsing method, which preserves the inter-nodal neutron leakage, has been developed instead of the conventional neutron-current-weighted collapsing method and incorporated into the code NSHEX. The effectiveness of the newly developed advanced method has been confirmed by validation calculations. As a result, not only the energy-group dependency of the effective multiplication factor (Fig.1-33) but also the spatial neutron flux distribution (Fig.1-34) ware found out to be improved and it was concluded that this newly developed method can be recommended as the transport cross-section collapsing method for NSHEX.

The results mentioned above are newly obtained knowledge based on the detailed analysis of the "MONJU" whole core by this study. To improve the accuracy of the conventional analytical calculation method is still of great importance, while the most recent method can exclude the energy-group collapsing approximation by introducing exact continuous neutron energy algorithm, which requires huge amount of computer resources and then not practical especially in case of large core analysis, like "MONJU" whole core. This study expanded the possibility to improve the calculational accuracy of the conventional transport calculation method.

Reference

Todorova, G., Nishi, H., Ishibashi, J., Monju Core Neutronics Analysis Method Upgrading Research—New Collapsing Algorithm for Condensation of the 3-D Transport Code NSHEX—, 2005, JNC Technical Review (27), JNC TN1340 2005-001, p.1-16.

1-14 Personal Computer Plant Simulation in 1/1000 Real Time
—Validation of Versatile Plant Simulation Code—

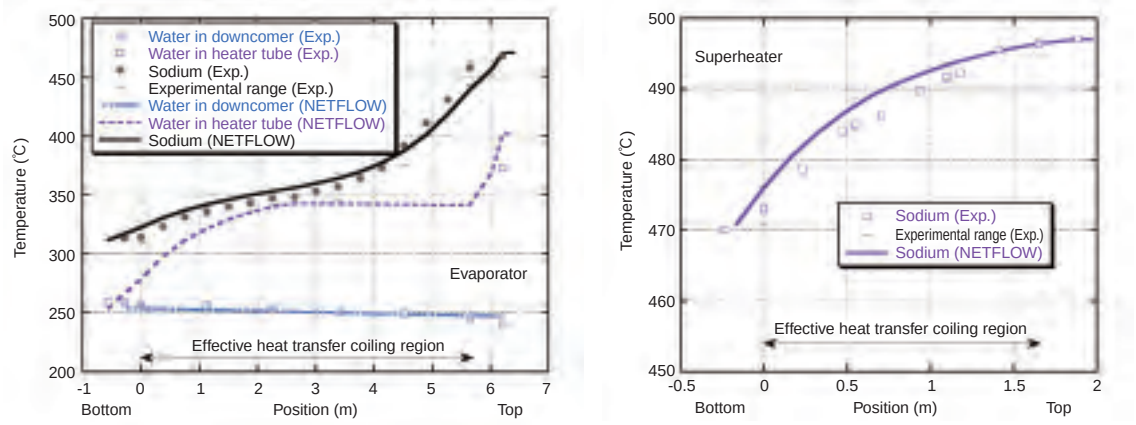

Fig.1-35 (upper) Temperature distribution in the 50MW steam generators
Simulation of sodium temperature by the shell and water / vapor temperature in tubes of steam generators at rated output using the NETFLOW code. Agrees well with actual boiling behavior in the evaporator.

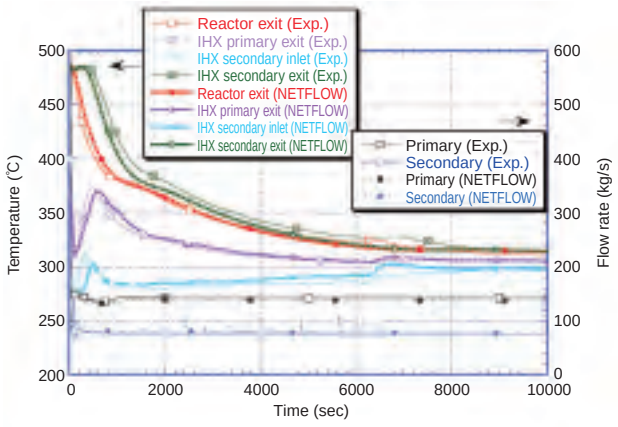

Fig.1-36 (left) Turbine trip test of "MONJU" at 45% thermal power
A turbine trip test was simulated by the NETFLOW code, modeling the first through the third loop of Monju. Important plant parameters are shown. Good agreement was obtained between test and calculation results over 10000 seconds.

The NETFLOW code was developed in order to simulate complex flow systems like an auxiliary cooling system of a nuclear power plant. Good applicability of the code was confirmed through validation using data obtained from experimental facilities regarding pump, heat exchanger, piping, flow control valve and so on, and plant data obtained at a nuclear power plant.

In order to increase the versatility of the code, modifications make it applicable to a liquid metal cooled reactor have also been conducted, and validation analyses have been done using data obtained at sodium facilities. The data at the 50 MW steam generator (SG) facility and the fast breeder reactor (FBR) "MONJU" are introduced here. Since the SG of an FBR has different configuration and characteristics than that of an LWR, SG validation was necessary, as this is an important component. When a model of SG was incorporated into the code and applied, the calculated temperature distributions in the evaporator and super-heater of the 50MW SG agreed well with actual values. Plant transients were calculated for the loops of the 1/3 Monju model: the core, primary coolant system, secondary coolant system, and SG/third coolant system. The calculated events were a natural circulation test of the secondary loop for 24 hours under primary pump heating, and a turbine trip test at 45% thermal output. In the natural circulation test, heat removed by a finned tube air cooler in the secondary system was evaluated under forced and natural circulation conditions. Applicability of the code to a sodium flow system is confirmed by the fact that the code reproduced the test results.

Fast running of the code was realized in the calculation. In flow system modeling of one of three loops in operating state, a plant transient lasting 1000 seconds was calculated within 1 second using a personal computer (PC) with a 2GHz clock. Therefore, plant transient for a couple of days can be analyzed simply, e.g., the natural circulation test of the second system for 24 hours was calculated within two minutes.

At present, there are plans for this code can calculate flow systems for light water, heavy water, and various liquid metals, to be used for research and education in graduate schools in order to improve the skills of nuclear engineers. Furthermore, this code can be applied to chemical plants etc., adjusting the physical properties of the liquid used.

Reference

Mochizuki, H., Verification of NETFLOW Code using Plant Data of Sodium Cooled Reactor and Facility, Nuclear Engineering and Design, vol.237, Issue 1, 2007, P87-93.

1-15 Study of Fast Breeder Reactor Safety with Laser

—Fuel Failure Detection System by means of Laser Resonance Ionization Mass Spectrometry—

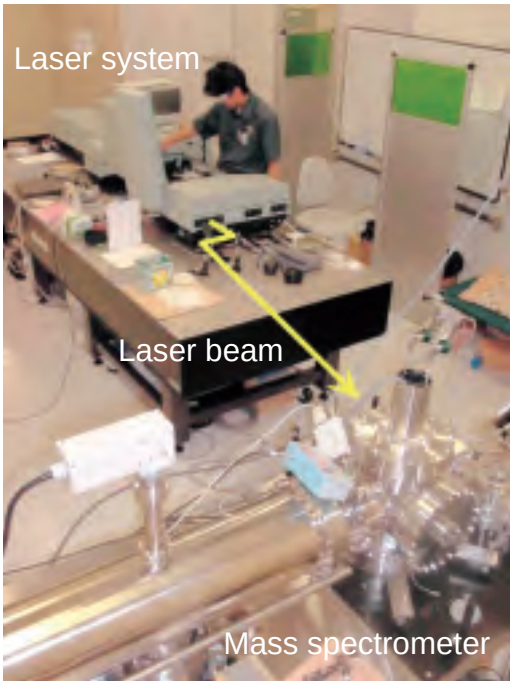

Photo1-1 RIMS System
The laser system radiates ultraviolet rays of 256 nm for Xe analysis and 217 nm for Kr analysis. The mass spectrometer ionizes and analyses Xe or Kr gas.

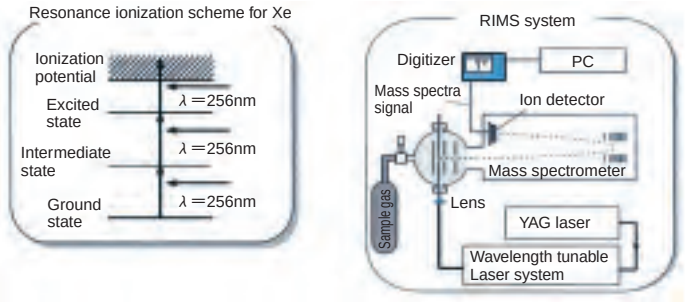

Fig.1-37 Principle of Resonance Ionization and RIMS System
The wavelength tunable YAG laser system ionizes the sample (Xe. here) by resonance excitation. The intensity of ions is analyzed by mass spectrometry.

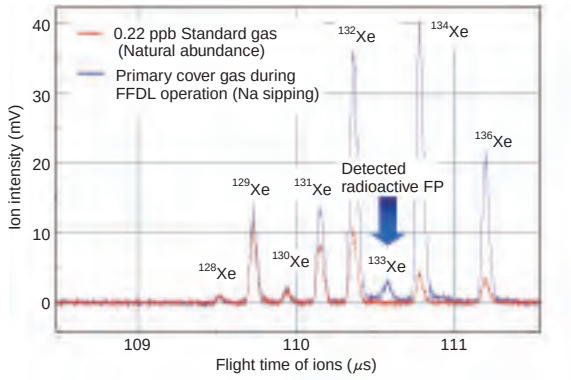

Fig.1-38 Mass Spectra of Xe FP released from Test Subassembly
The RIMS system simultaneously detected both stable xenon nuclides and the radioactive nuclide (^{133}Xe).

We have developed a rapid isotopic analysis system for fission products (FPs) released from a failed fuel cladding tube to the sodium (Na) coolant in a fast reactor.

Development of the wavelength tunable laser resonance ionization mass spectrometry (RIMS) system has significantly improved detection sensitivity by utilizing the latest nonlinear optics for effective ionization of the sample without increasing interfering ions (Photo1-1 and Fig.1-37). As a result, the RIMS system successfully analyzes isotopic ratios of ultratrace xenon (Xe) and krypton (Kr) at ppt levels without enrichment in the cover gas.

An in-pile fuel failure simulation test was performed in the experimental fast reactor "JOYO" in November 2004 to confirm the plant operation procedures in the event of fuel failure, such as the detection of fuel failure, and identification and unloading of failed fuel.

The test fuel subassembly contained two test fuel pins, each of which had an artificial slit through their cladding tubes 0.1 mm wide and 1 mm long, which was sealed with a lead alloy. The slit opened to simulate the fuel failure when the test fuel pin temperature exceeded 300°C. FPs were released through the slit and transported to the reactor vessel cover gas. The reactor was shut down manually when the reactor power reached 120 MWt because the fuel failure detection signal was quickly transmitted.

During the Na sipping operation for failed fuel detection and location (FFDL), a sample of cover gas was collected in a small container and Xe nuclides were analyzed by the RIMS system.

As a result, the RIMS system successfully identified stable Xe nuclides (^{132}Xe, ^{134}Xe, etc.) and ultratrace ^{133}Xe at a concentration of 8 ppt (Fig.1-38). Pre-identification by means of the cover gas analysis can shorten the time required for FFDL because the fuel burnup can be estimated from the isotopic ratios of stable and radioactive Xe nuclides.

We are also currently developing Na leak detection technology for the primary cooling system by means of the RIMS system.

In addition to the atomic energy field, the RIMS system may have possible applications in atmospheric and environmental analysis, impurity control for semiconductor manufacturing environment, etc.

Reference

Ito, C. et al., Fuel Failure Simulation Test in JOYO—FFDL In-Pile Test (Ⅲ)—, Japan Nuclear Cycle Development Institute, 2005, JNC TN9410 2005-003, p.53 (in Japanese).

1-16 Development of Multi-Functional Reprocessing and Utilization of Separated Elements
－Establishment of Advanced Separation Process Using Pyridine Resin－

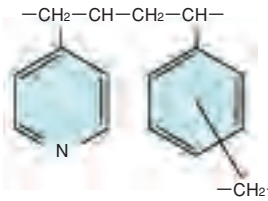

Fig.1-39 Basic structure of tertiary pyridine resin
Two types of resins, gelated-type by suspension polymerization and porous-type supported by silica beads (60 μm), were used in this study.

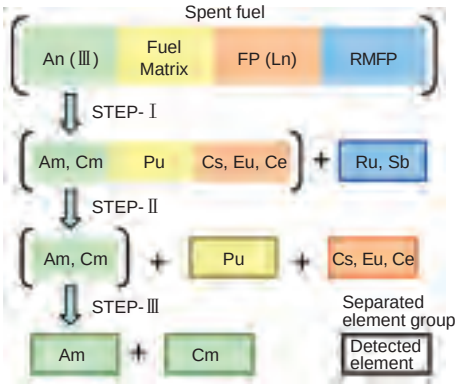

Fig.1-40 Outline of separation process
Three step separation process for each element group.

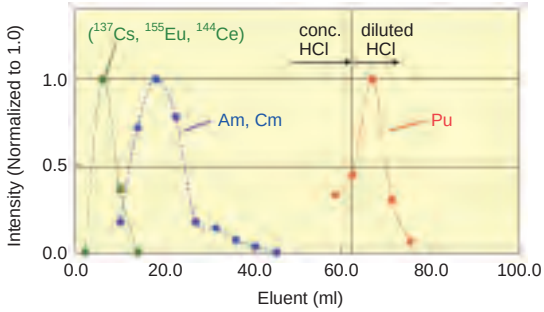

Fig.1-41 Chromatogram of STEP-Ⅱ separation process
Separation of FP(Ln), An(Ⅲ), and fuel (Pu) groups demonstrated.

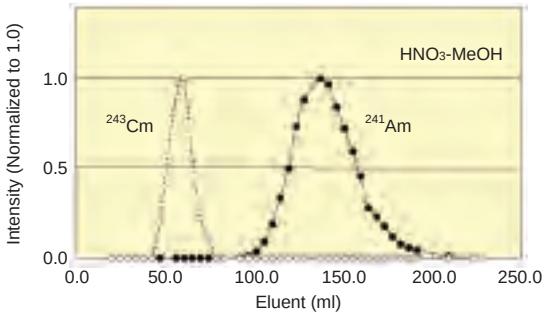

Fig.1-42 Chromatogram of STEP-Ⅲ separation process
Separation of Am and Cm demonstrated.

A separation process concept utilizing tertiary pyridine resin was applied to the separation of rare metal fission products (RMFP), trivalent lanthanides (Ln(Ⅲ)), trivalent actinides (An(Ⅲ)) and plutonium (Pu) in mixed oxide (MOX) fuel irradiated at "JOYO". Further, the mutual separation of americium (Am) and curium (Cm) was performed successfully. The study was carried out with Tokyo Institute of Technology.

The resin has the functions of a weakly basic anion-exchanger and a nitrogen soft donor ligand, and is a salt-free CHON compounds (Fig.1-39).

The separation process (Fig.1-40) can be divided as follows:

STEP-Ⅰ : Platinum group elements separation (pre-filtration)

STEP-Ⅱ : Separation of Ln(Ⅲ) and other FP, An(Ⅲ), and Pu

STEP-Ⅲ : Separation of Am and Cm

Firstly, a 85 μg HCl solution of MOX with high burnup of 140 GWd/MTM was introduced to the separation process.

STEP-Ⅰ Antimony-125 and RMFP, mainly ^{106}Ru in present experiment, were perfectly adsorbed in the resin. STEP-Ⅱ The solvent was changed to conc. HCl solution, and passed through the resin embedded in silica beads. The Ln (Ⅲ) including the other FP, such as ^{155}Eu, ^{144}Ce, and ^{137}Cs, were separated. Accordingly An(Ⅲ) were separated. After the removal of An(Ⅲ), the effluent was changed to diluted HCl to strip out Pu fraction from the resin. (Fig.1-41) STEP-Ⅲ An(Ⅲ) solution was changed to nitric acid-methanol mixed solution, and passed through the resin, separating Am and Cm. (Fig.1-42)

The recovery of ^{241}Am was more than 95% in this experiment. The Decontamination Factors (DFs) of ^{137}Cs and ^{155}Eu in the isolated Am-fraction exceeded 3.9×10^{4} and 1.0×10^{5}, respectively. The DF of ^{243}Cm from ^{241}Am was more than 2.2×10^{3}. This DF of An(Ⅲ) is higher than ever achieved. These results proved that a simplified separation process can be used in the advanced ORIENT multifunction cycle with enhanced separation, transmutation and utilization of spent fuel.

Reference

Koyama, S. et al., Development of Multi-functional Reprocessing Process based on Ion-exchange Method by Using Tertiary Pyridine-type Resin, Journal of Nuclear Science and Technology, vol.43, no.6, 2006, p.681-689.

1-17 Viewing Inside an Irradiated Fuel Assembly

— Development of a Non-Destructive Post-Irradiation Examination Technique Using High-Energy X-ray Computer Tomography —

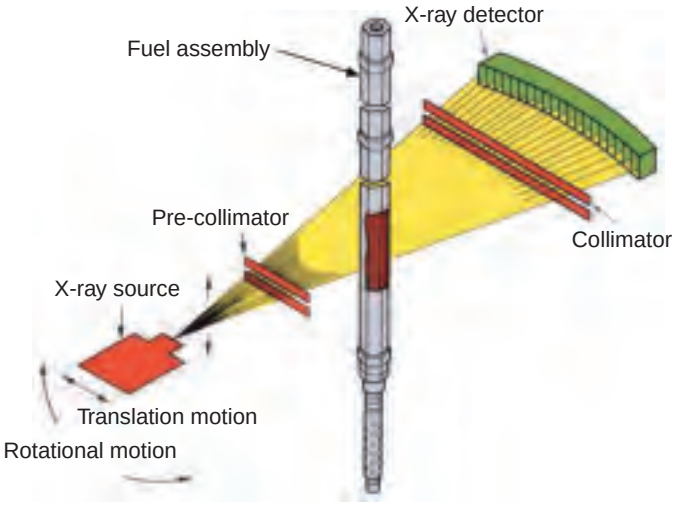

Fig.1-43 Outline of X-ray CT system
X-rays generated by the accelerator are collimated in front of specimen. An X-ray detector measures the intensity of X-ray transmitted through the specimen.

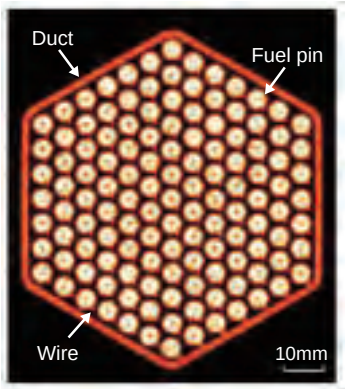

Fig.1-44 X-ray CT image of irradiated fuel assembly
The wrapper tube, cladding, fuel pins and wrapping wire can be distinctly seen in this figure.

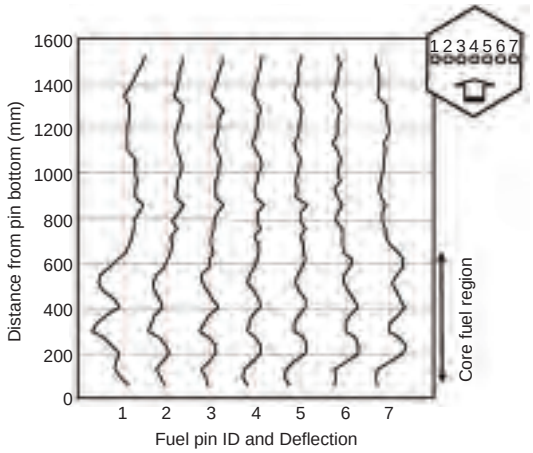

Fig.1-45 Longitudinal deformations of fuel pins
This figure shows the longitudinal deformations of an irradiated fuel assembly. The deformations of the core fuel region are significant.

In order to develop the fuels and materials to be used for a fast breeder reactor which has economic efficiency and high reliability, it is very important to confirm the irradiation performance by a Post Irradiation Examination (PIE). Non destructive PIEs for the fuel assemblies irradiated in the "JOYO" reactor are performed in the Fuel Monitoring Facility (FMF). An X-ray Computer Tomography (X-CT) apparatus was installed in the FMF in order to observe the inner condition of an irradiated fuel assembly.

In this study, the X-CT technique developed in the medical field was established to apply to the inspection of the irradiated fuel assembly (Fig.1-43). This was the first attempt at applying this technique to PIE in the world.

In order to reduce the effect of γ -ray from an irradiated fuel assembly, a high energy X-ray was selected, and the detection period of X-rays passing through the irradiated fuel assembly is synchronized the generated pulse of high energy X-rays, using $CdWO_4$ as the material of the scintillation detector because of its high sensitivity for high-energy photons.

As a result, a clear cross sectional CT image (Fig.1-44) of the fuel assembly irradiated to high burn up can be obtained. Analyzing this image enables measurement of the displacement of fuel pins in the assembly and the change of sodium flow area.

Fig.1-45 illustrates the longitudinal deformations of 7 fuel pins located in the center line of the fuel assembly. As shown in this figure, the deformations of fuel pins at the core fuel region are significant compared with the deformations of fuel pins at other regions. This behavior was caused by the irradiation creep of the core. Evaluation of the temperature effects on the fuel assembly will be aided using these data.

Reference

Katsuyama, K. et al., Application of High-energy X-ray Computer Tomography Technique for Checking Irradiated Nuclear Fuel, Proceedings of 4th World Congress on Industrial Process Tomography, Aizu, Japan, 2005.

2 Research and Development on Geological Disposal of High-Level Radioactive Waste

2-1 R&D Supporting the Technology and Reliability of Geological Disposal in Japan

Radioactive waste occurs when we utilize nuclear power. In Japan, reprocessing is done to recover uranium and plutonium remaining in spent fuel from power generating reactors for recycling into useful fuel. The liquid remaining after such retrieval is vitrified to produce a chemically and physically stable glass monolith, which is high-level radioactive waste (hereafter, HLW). Radioactivity of HLW is high initially and lasts a long time. Therefore, HLW should be isolated from human environments for a long term. International consensus has been developed that HLW can be disposed of in stable deep geological environments (geological disposal). Waste glass inserted in an overpack (e.g. carbon steel) will be emplaced with a bentonite buffer at below 300m depth in the Japanese concepts (Fig.2-1).

To ensure safe implementation of geological disposal, R&D should be carried out in various fields, i.e. geoscientific research, engineering development and study of performance assessment (PA) of the geological disposal system. JAEA and its predecessor have conducted comprehensive R&D on geological disposal technology since the 1970's. In November 1999, we compiled its R&D achievements up to that time into the second progress report (referred to "H12") and submitted it to the government. H12 presented the technical feasibility of geological disposal in Japan. The Specified Radioactive Waste Final Disposal Act (the "Act"), based on the technical achievements documented in H12, came into force in June 2000. Pursuant to the Act, the Nuclear Waste Management Organization of Japan (NUMO), with responsibility for implementing geological disposal of HLW, was established in October 2000 and the Japanese program of geological disposal moved into the implementation phase (Fig.2-1).

NUMO has defined a stepwise site selection procedure as required by the Act, and adopted a novel "volunteering" approach to siting. The stepwise site selection procedure starts with literature surveys of volunteer community areas to identify suitable Preliminary Investigation Areas (PIAs). PIAs will be investigated using surface-based techniques, including deep boreholes. Thereafter, Detailed Investigation Areas (DIAs) will be selected for more intensive characterization including studies by an underground research facility. This leads to selection of the repository site.

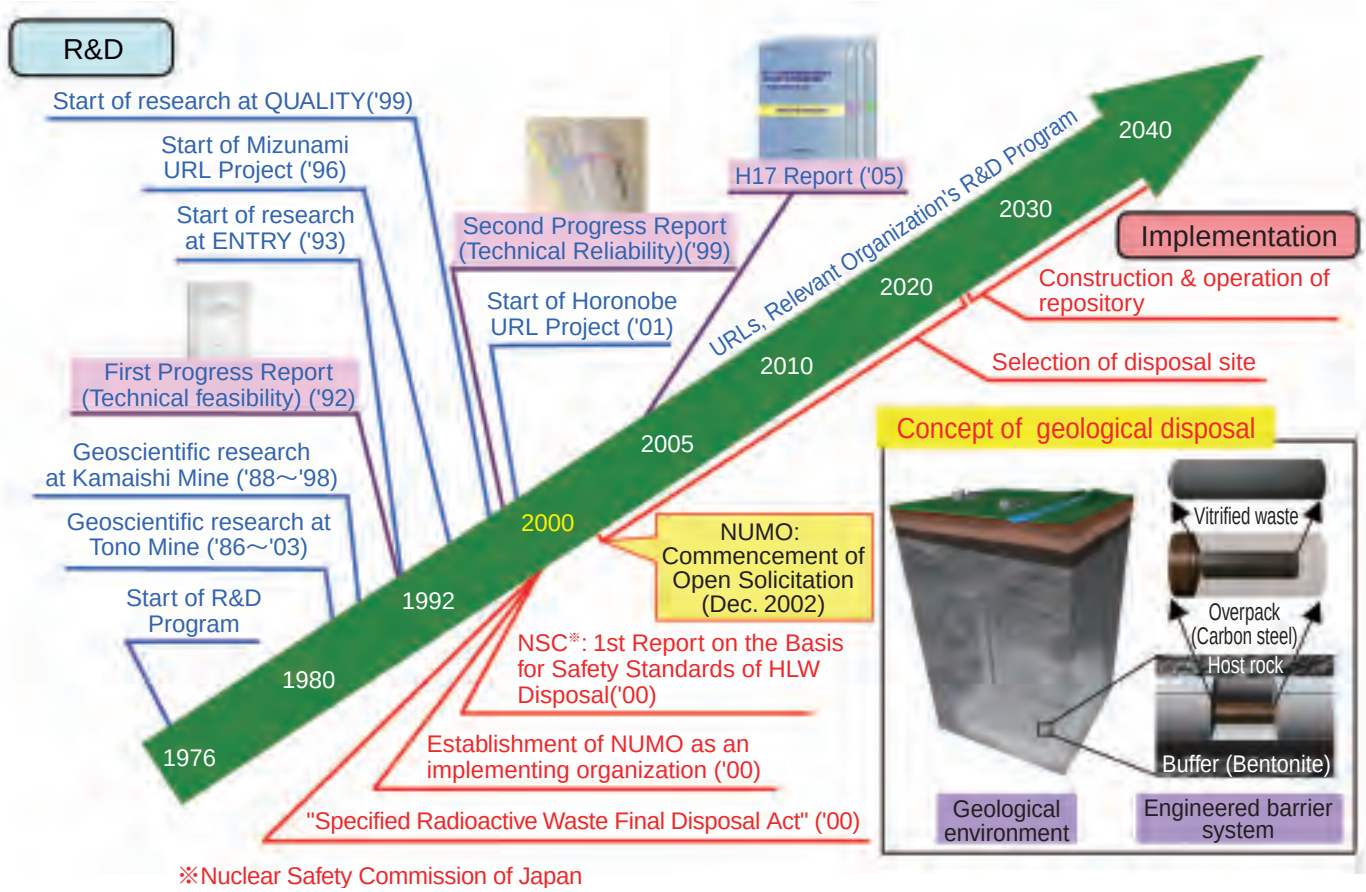

Fig.2-1 Milestones of HLW disposal program in Japan

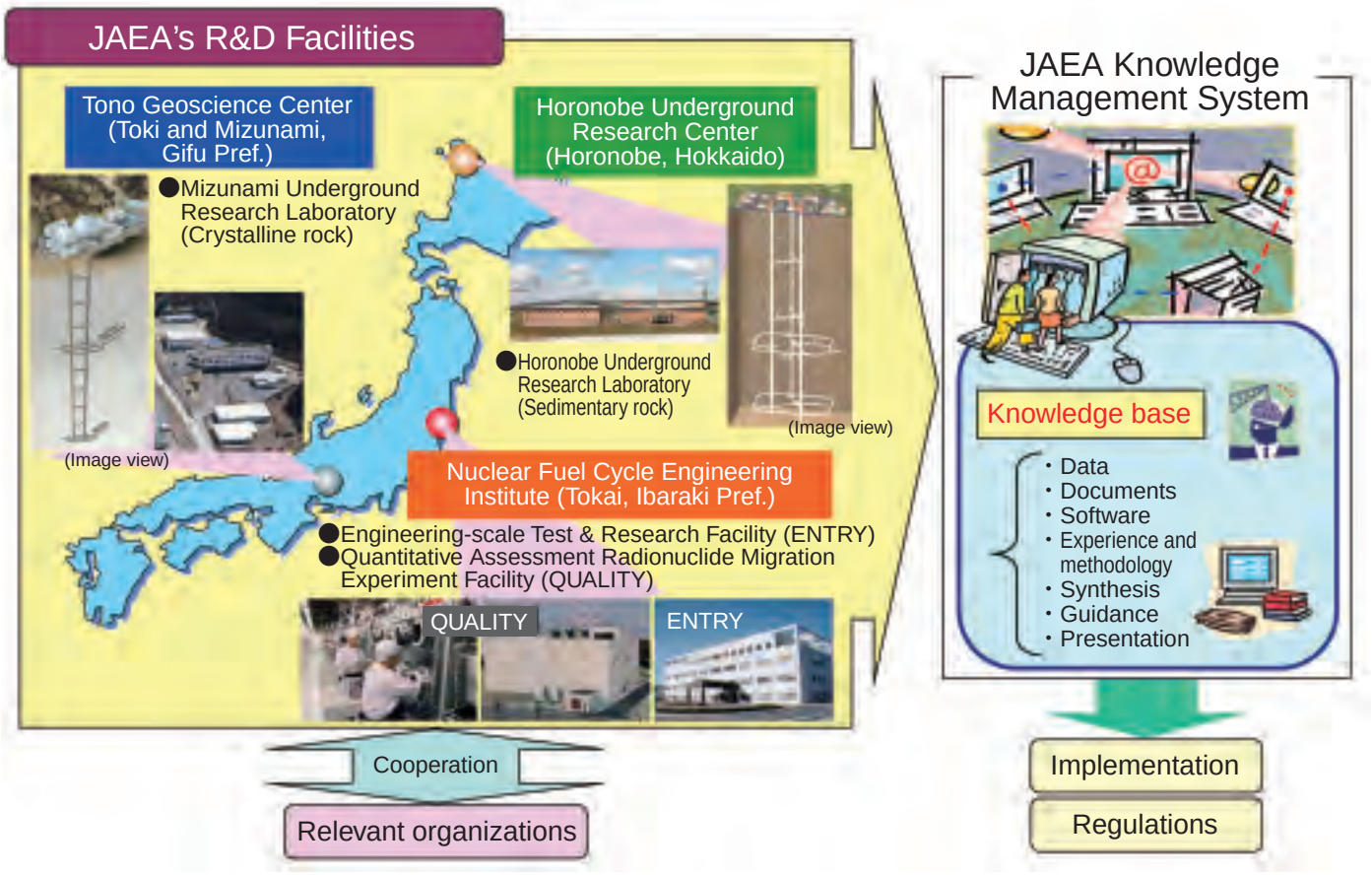

Fig.2-2 JAEA's R&D activities on geological disposal technology

The role of our R&D is to develop the technical basis for such implementation activities as well as the safety regulations with lead time. A particular our R&D activity in this implementation phase is to promote the projects of two Underground Research Laboratories (URLs): one at Mizunami city in crystalline rock and the other at Horonobe town in sedimentary rock (Fig.2-2). The URL programs are being conducted in three phases planned over a period of 20 years, i.e. investigations from the surface (Phase Ⅰ; already finished), excavation of shafts and drifts (Phase Ⅱ) and detailed investigations in the underground facility (Phase Ⅲ). In each phase, the investigation and evaluation methodologies used will be iteratively improved and integrated as necessary, and the applicability of engineering technologies for the design and construction of an underground facility will be verified.

At the same time, we are conducting laboratory experimental studies at our Engineering-scale Test and Research Facility (ENTRY) and Quantitative Assessment Radionuclide Migration Experimental Facility (QUALITY) at Tokai village. ENTRY was designed for performing a series of relatively large-scale and non-radioactive experiments and PA of the multibarrier system supported by extensive computer analysis. QUALITY was designed to obtain basic data concerning the chemical properties and migration behavior of radionuclides under geological disposal conditions. These studies are linked with the geological environment data obtained from the URLs.

Geological disposal of HLW will be a long term project of more than one hundred years. It is supported by vast quantities of information, data, experience, understanding, etc. – which can be defined broadly as "knowledge". Management of knowledge is a very important issue for this long-term disposal program. We have initiated a project to develop the next generation of novel knowledge management tools utilizing advanced electronic information management technology.

In July 2005, a "Coordination Council for R&D on geological disposal" was established to develop wide ranging R&D which is being carried out by JAEA and ANRE (Agency for Natural Resources and Energy). In this council, JAEA and related R&D organizations have discussed their respective roles, and also a co-operation framework to integrate R&D results into knowledge base and have prepared a roadmap of R&D for the implementation of geological disposal.

2-2 Development of a Novel Knowledge Management System for Geological Disposal —Fundamental Concepts and Implementation Plan—

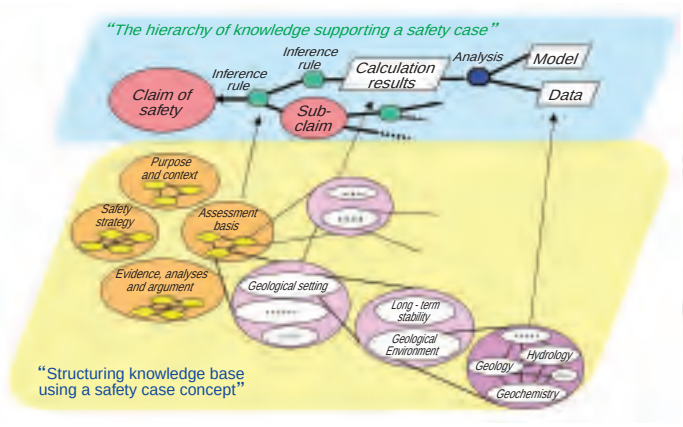

Fig.2-3 An approach to structuring knowledge based on its application to support a safety case

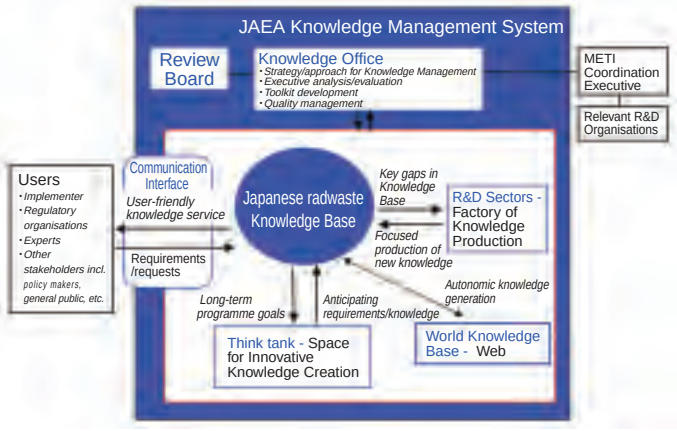

Fig.2-4 Preliminary KMS concept[2)]

The implementation process for the geological disposal of high - level radioactive waste (HLW) utilises vast quantities of information, data, experience, understanding, etc. – which can be defined broadly as "knowledge". All stakeholders, including the implementer, the regulator and political decision-makers, will use this knowledge at many decision points in the phased implementation process. In order to improve confidence in the safety of geological disposal, it is necessary to collate, integrate and quality assure appropriate knowledge, extending it where needed with focused studies – taking particular account of advances in the diverse areas of science and technology that are of relevance here.

The exponential expansion of knowledge is, however, rapidly reaching the limits of what can be handled by traditional approaches. we, therefore, have initiated a project to develop a "next generation" knowledge management system (KMS), utilising advanced electronic information management technology.[2)] Although extremely challenging and requiring development of novel technology, this seems essential to prepare for repositories which will be licensed in the 21st century.

Initially, the prototype knowledge base will follow the structure of a geological repository safety case, which will certainly be a key requirement for all implementers and will need to be evaluated by regulators (JNC, 2005).[1)] Fig.2-3 illustrates an approach to structuring knowledge, using the safety case concept. The structured knowledge is further organised within an integrated knowledge base, which contains all relevant information produced or needed by users, including raw and processed data, documents, software, experience & methodology, synthesis output, guidance and materials for presentations.[2)]

The preliminary concept for a Japanese KMS is shown in Fig.2-4. Although such a system is still at the early stages of internal discussion, it can be seen that the emphasis is on interaction – with two-way flows between the knowledge base and the central guiding knowledge office, the R&D sectors which produce focused new knowledge, the web (which is the interface to the wider international community), a think tank (which attempts to anticipate relevant future developments) and, most importantly, the end-users.

Taking account of both present requirements and possible future needs of users, we will develop a prototype of a novel KMS within the current 5-year R&D programme (up to the fiscal year 2010). The quality-assured knowledge base provided by JAEA (as an independent third party) will also integrate the R&D results from other organisations and can thus serve as a valuable technical resource for both the implementer and the regulator, allowing JAEA to play a central R&D role in the HLW disposal programme in Japan.

Although this work is focused on radioactive waste disposal, knowledge management will be one of the great challenges of coming decades and the technology developed may be transferable to many other applications.

References

1) Japan Nuclear Cycle Development Institute, H17: Development and Management of the Technical Knowledge Base for the Geological Disposal of HLW —Knowledge Management Report—, 2005, JNC TN1400 2005-022, 68p.

2) Kawata, T. et al., Knowledge Management: Emperor's New Clothes?, International High-Level Radioactive Waste Management Conference (IHLRWM) 2006, Las Vegas, Nevada, April 30-May 4, 2006, p.1236-1243.

2-3 Development of Reliable Databases for Safety Assessment of High-Level Radioactive Waste Disposal System
—Database Development for Radionuclide Migration Analysis—

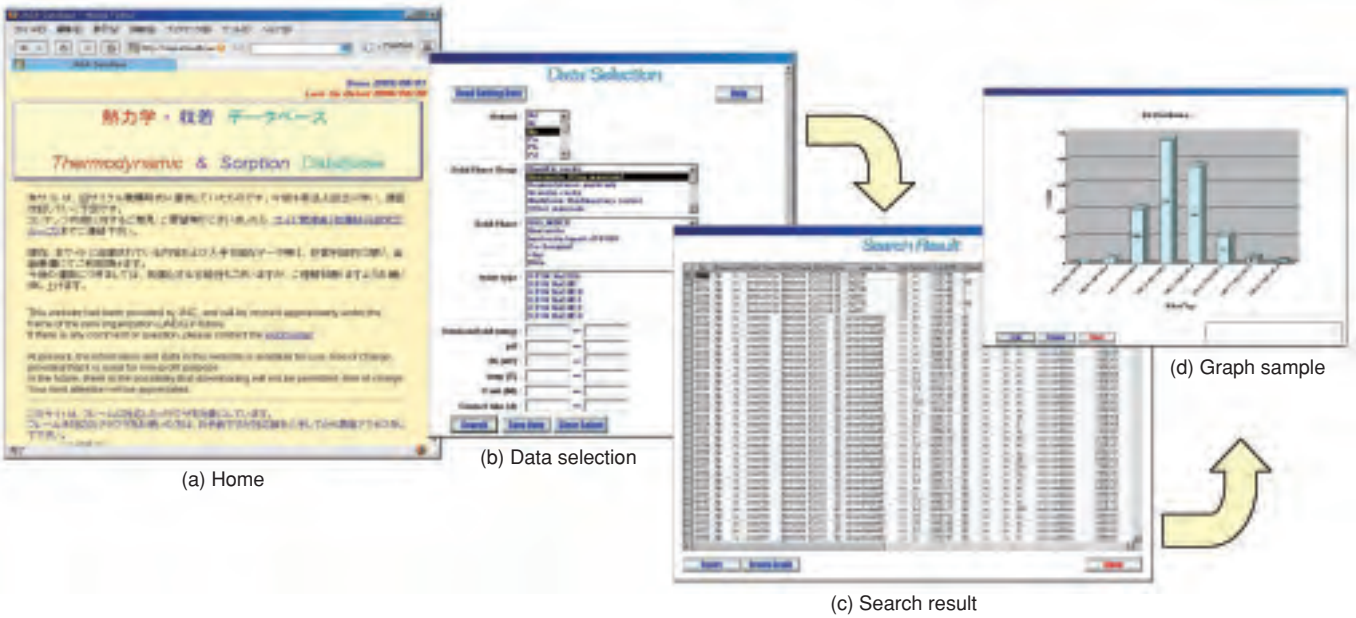

(a) Home (b) Data selection (c) Search result (d) Graph sample

Fig.2-5 Example of database for radionuclide migration analysis - Distribution coefficient of Neptunium onto Bentonite

Safety assessment of high-level radioactive waste (HLW) disposal system in Japan is based on "groundwater scenarios", where radionuclides are transported to the surface environment by flowing groundwater. For the estimation of transportation of radionuclides through buffer materials (clay minerals) and in the geosphere, it is necessary to develop basic data for solubility, sorption and diffusion of radionuclides. We have developed databases on radionuclide migration, which contain thermodynamic, sorption and diffusion databases (TDB, SDB and DDB, respectively), to provide solubility, distribution coefficient and diffusion coefficient of radionuclides. The TDB and the SDB have been released on the Web (http://migrationdb.jaea.go.jp/).[1)]

The JNC-TDB for "Second Progress Report (H12)" contains solubility products and equilibrium constants, and enables determination of solubility of important radionuclides. The JNC-TDB also contains thermodynamic data on minerals, and thus it is also useful for investigating groundwater chemistry and long-term alteration behavior of buffer materials. The JNC-TDB and the TDB developed by an international TDB project are provided on the Web and available for use in geochemical calculation programs. Since some thermodynamic data are less reliable, experimental and theoretical studies to evaluate the unreported and less reliable thermodynamic data are in progress by many institutions including JAEA. JAEA's new TDB incorporating the latest information will be published around 2010.

The SDB contains the distribution coefficients (K_d) of elements onto clay minerals and rocks under particular experimental conditions. More than 20,000 K_d values have been put in the SDB. Using the SDB, we can search and graph the K_d distribution by selecting solid phases and/or groundwater chemistry and then can estimate unreported K_d. The latest K_d values are continuously put in the SDB, and the evaluation of the reliability of K_d values has started.

DDB contains the diffusion coefficient into typical clay minerals and rocks in Japan. The DDB has been published as a JAEA technical report and will be released on the Web in 2007.

The usefulness and easy accessibility of the data on radionuclide migration have been maintained by developing and publishing the databases continuously. Revision of the database based on the needs of the users will be continued to increase the number of users in the world.

Reference

1) Sasamoto, H., et al. Current Status of System Development to Provide Databases of Nuclides Migration. Japan Nuclear Cycle Development Institute, 2005, JNC Technical Review, no.28, JNC TN1340 2005-002, p.27-33 (in Japanese).

2-4 Development of Low Alkaline Cement
－Study on Workability of Low Alkaline Shotcrete－

Table 2-1 The mix composition of concrete for shotcreting test
Cement type ; HFSC424N (OPC 40% + silicafume 20% + flyash 40%), HFSC424H(HPC 40% + silicafume 20% + flyash 40%)
OPC: Ordinary Portland Cement, HPC: High early strength Portland Cement

Cement type	Slump (cm)	W/B (%)	s/a (%)	Unit weight (kg/m³)								quick setting admixture
				W	OPC	HPC	SF	FA	S	G	water-reducing admixture	
HFSC 424N	18 ± 2	40	60	200	200	-	100	200	950	645	C×1.1%	HFSC×10%
HFSC 424H		45	60	203	-	180	90	180	975	663	C×1.2%	HFSC×10%

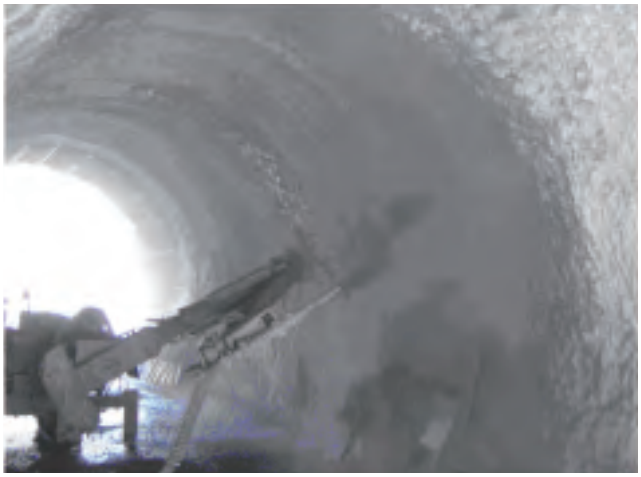

Fig.2-6 State of shotcreting in the test tunnel
The test tunnel is 5.2m wide, 4.4m high and 20m long.

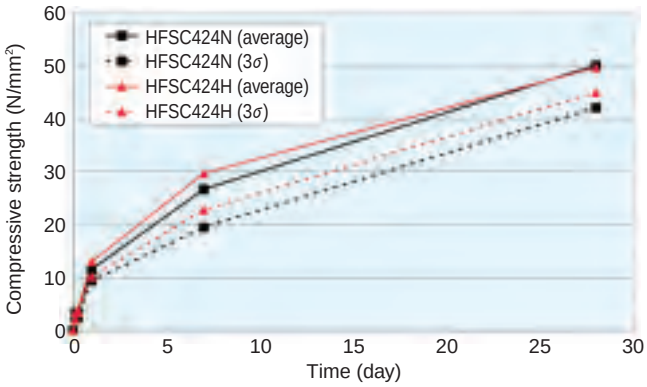

Fig.2-7 Compressive strength of shotcrete core
The mean and 3σ of compressive strength of shotcrete core are plotted against elapsed time.

To maintain stability of host rock in deep geological tunnel construction, a cement tunnel supporting system is the most promising candidate. Hyper alkaline solution with pH as high as 12.5 is used for hardening ordinary Portland cement (OPC), and may affect nearby rock and bentonite if exposed for a long period, although OPC has been used in actual construction in civil engineering field. Highly flyash containing silicafume cement, HFSC, has been developed by JAEA, and its in-situ applicability tests are planned at the Horonobe underground research laboratory (URL) starting in 2007. In this study, the mix proportion of HFSC in shotcrete was investigated and workability was assessed. Since strength of 36 N/mm2 after 28 days is desired for the supporting system, two promising mix proportions to achieve this strength were proposed (Table 2-1). A 40% water to binder ratio (W/B) was needed in the case where OPC is the base cement of HFSC, and 45% W/B is needed in the case of high early strength Portland cement (HPC) in order to achieve the design strength. The actual scale shotcreting test was carried out with a hardening accelerator admixture (Fig.2-6). The workability of both 40% and 45% W/B was good. Although many pores were observed on the surface, the density uniformity of the inner portions satisfied the design requirement. The mean core strength of both types of shotcreting is more than 48 N/mm^2 after 28 days, the required design strength (Fig.2-7). The pH of pore water from HFSC shotcreting was 12.4 after 28 days, since the pozzolanic reaction has progressed sufficiently. The mix proportion will be determined using actual materials in construction at the Horonobe URL, and assessment of long term pH change will be carried out in future work.

Reference
Konishi, K. et al., Study on Applicability of Low Alkaline Shotcrete in Horonobe URL Project, 2006, JAEA-Research 2006-040, p.1-53 (in Japanese).

2-5 Prediction of Long Term Changes at Barriers

—Development of a Coupled Thermo-, Hydro-, Mechanical, and Chemical Model—

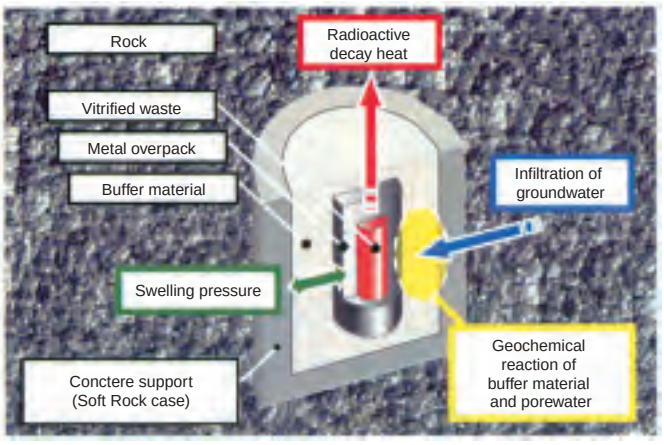

Fig.2-8 Schematic view of T-H-M-C behavior
After emplacement of the engineered barriers, coupled thermo - hydro -mechanical and chemical (T-H-M-C) processes will occur.

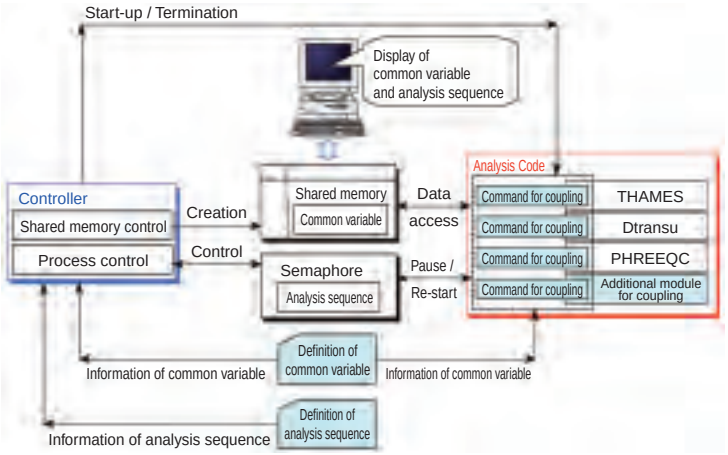

Fig.2-9 Outline of the coupled T-H-M-C code
This system is based on three existing codes, for high flexibility.

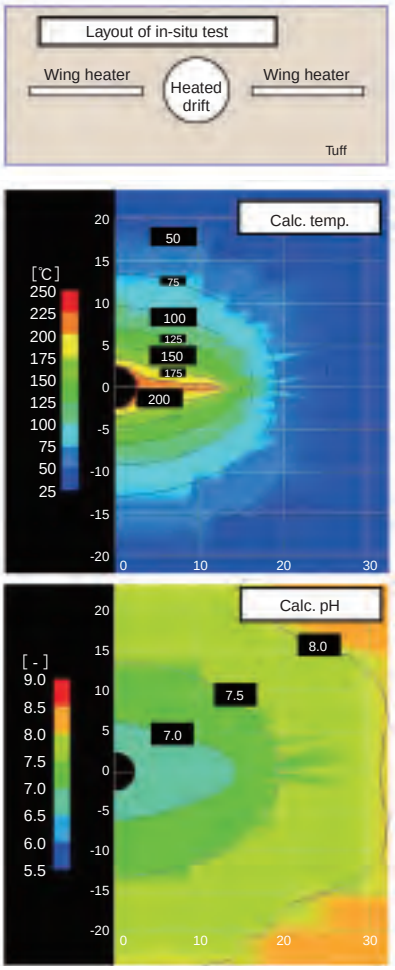

Fig.2-10 Example result of analysis by developed code
The upper fig, shows layout of in-situ test. Middle and lower graphs show the calculated temperature and pH after 4 years heating.

Near a high-level radioactive waste repository after emplacement of engineered barriers, coupled thermo-, hydro-, mechanical, and chemical (T-H-M-C) processes will occur, involving interaction among radioactive decay heat from the vitrified waste, infiltration of groundwater into bentonite, swelling pressure of bentonite due to saturation and chemical reaction between bentonite and pore water (Fig. 2-8). It is very important to predict these phenomena quantitatively in order to improve reliability in assessing the long term performance of engineered barriers. For this objective, we have developed a coupled thermo-, hydro-, mechanical, and chemical (T-H-M-C) analysis model / code. To realize the T-H-M-C analysis system, we combined the three existing codes (i.e. the coupled T-H-M code "THAMES", mass transport code "Dtransu", and geochemical code "PHREEQC") in a program which can control execution of each analysis code and can exchange data among each (Fig.2-9). This system is very effective to improve efficiency and quality of code development.

JAEA has participated in the international co-operative project (DECOVALEX) to improve the understanding of the coupled T-H-M-C processes and to validate the code we developed. In this project, we performed calculations for the in-situ test at Yucca Mountain in U.S.A., using our code (Fig. 2-10). This code makes it possible to predict quantitative changes over time and space, not only of the engineered barrier system but also near the drift. We will be incorporating new findings and precision models in the current coupled model, attempting to advance our model further and achieve realistic prediction.

Reference

Sonnenthal, E., Ito, A., Yui, M. et al., Approaches to Modeling Coupled Thermal, Hydrological, and Chemical Processes in the Drift Scale Heater Test at Yucca Mountain, International Journal of Rock Mechanics and Mining Sciences, vol.42, Issues 5-6, 2005, p.698-719.

2-6 Study Plan for Performance Assessment of High-Level Radioactive Waste Geological Disposal (5-year Plan)

— For Development of Technical Basis for System Performance Assessment in Implementation Phase —

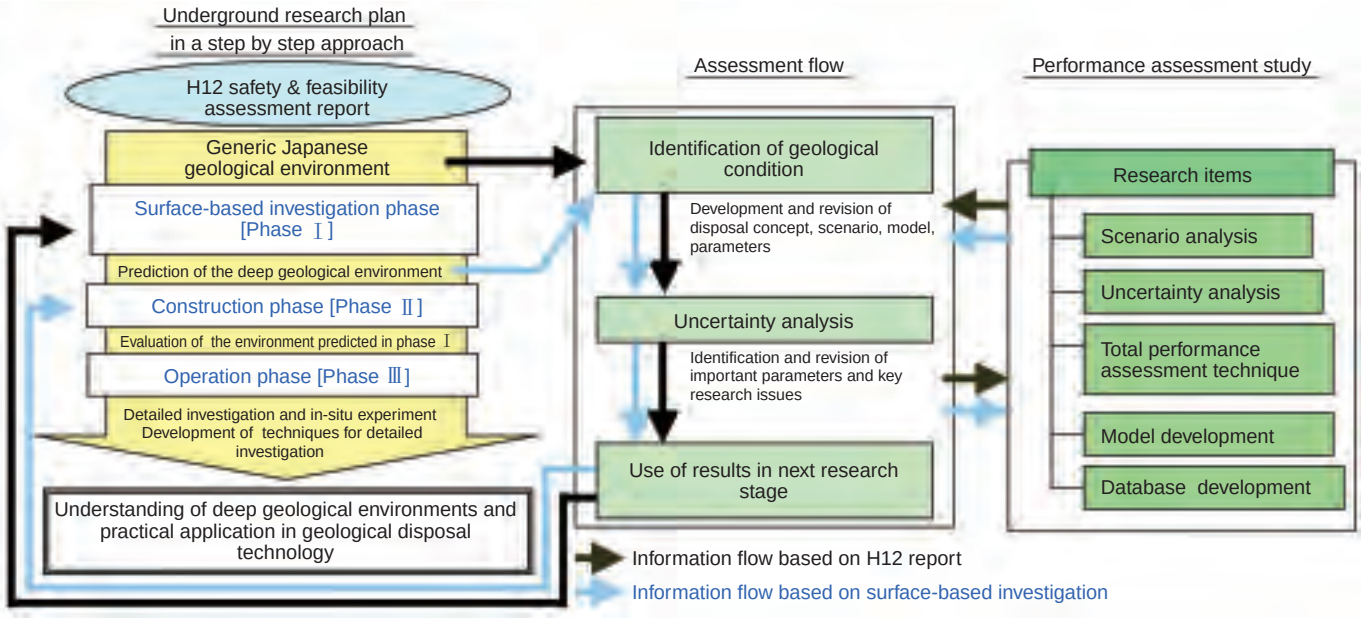

Fig.2-11 Research items of performance assessment study for HLW disposal and procedure of performance assessment in current stage

This study plan is to outline a 5-year plan of research and development (R&D) for performance assessment of geological disposal of high-level radioactive waste (HLW) in JAEA.

This 5-year plan is based on JAEA's mid-term plan which follows the R&D policy specified in "Framework for Nuclear Energy Policy" issued by the Japan Atomic Energy Commission. Moreover, research plans for safety regulation issued by the Nuclear Safety Commission of Japan should be taken into account. The contents of this 5-year plan follows a framework of R&D issues in performance assessment established in "the R&D map", i.e. the mid and long term R&D plan for geological disposal of HLW, developed by JNC and other relevant R&D organizations.

Objectives chosen according to their necessity and the significance in each research plan are clarified in the section "Objectives and the past progress", also summarizing the progress of the H12 Project in establishing the scientific and technical basis for HLW disposal in Japan (H12 report), and of H17 in development and management of a technical knowledge base for the geological disposal of HLW (H17 report). In addition, the next five year plan is described in the section "5-year plan (up to Fiscal 2010)".

The objectives of the performance assessment study are to provide examples of integrated methodologies for safety assessment and also provide as much know-how as possible, for forming a knowledge base that will reinforce the technical basis upon which implementation and safety regulations of disposal will be based.

The performance assessment study shall develop and test the approaches, tools and databases required to carry out such work for specific sites in the future. Demonstration of applicability up to now has been limited to examination of a few components of the safety assessment model chain. More extensive effort will be invested in further developing the methodology, models and databases used to quantify the long-term safety of a repository on a site-specific basis. Methodology development includes detailed examination of the significance of uncertainties associated with volcanic perturbation and with the representations and parameters used to quantify radionuclide transport in the far-field. Model development shall be focused on improving the capability of codes to reproduce the results of laboratories (e.g. ENTRY), and on field tests which attempt to simulate the behaviour of particular engineered and natural barrier systems as realistically as possible. Database effort will concentrate on the compilation and evaluation of element-specific data (e.g. fundamental thermodynamic, empirical sorption data) which can be used to determine the parameters that can quantify radionuclide release and transport (e.g. solubilities, system-specific Kds) in safety assessments. This last effort, in particular, utilizes data produced in QUALITY, which are integrated with partner databases of projects coordinated by the NEA.

Reference

Miyahara, K. et al., Study Plan for Performance Assessment of HLW Geological Disposal (5-year Plan), 2006, JAEA-Review 2006-015, 29p.

2-7 Imaging Crustal Magma beneath an Active Volcano and the Generation of High Temperature Hot Springs in a Non-Volcanic Region
—Magnetotelluric Modeling in Naruko Volcanic Region and Kii Peninsula—

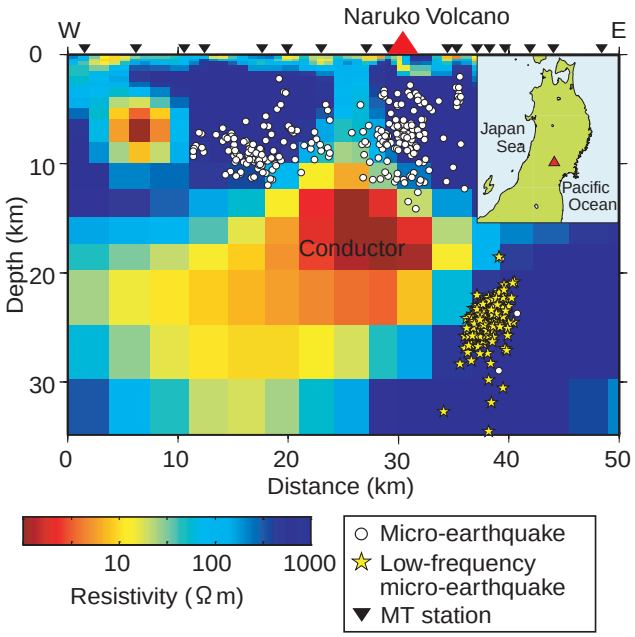

Fig.2-12 Two-dimensional resistivity model beneath Naruko Volcanic region in Japan
A prominent conductive body is visible beneath the volcano. It is due to high-temperature fluids consisting of magma and related aqueous fluids.

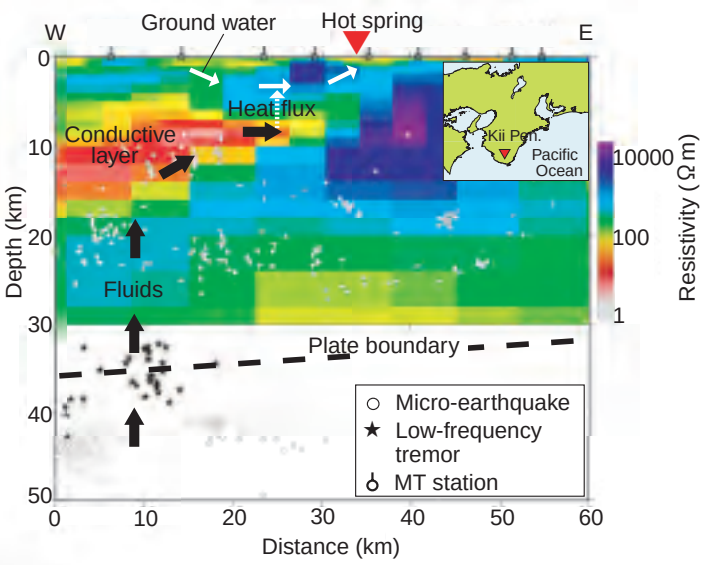

Fig.2-13 Two-dimensional resistivity model beneath southern Kii Peninsula, Japan
A prominent conductive layer is visible at depth of 10-15 km. It is related to aqueous fluids derived from the Philippine Sea plate.

Volcanism is one of the most important factors affecting the long-term stability of a geological disposal system, because the intrusion and eruption of magma could cause a dynamic destruction and subsidence of basement rocks. Therefore, development of geophysical approaches for detecting magmas and/or high temperature fluids has been carried out to evaluate the possibility of renewed volcanism in any given site. With this purpose, we characterized the subsurface structure beneath the Naruko volcano (active volcano) and the southern Kii Peninsula (active geothermal area in a non-volcanic region) using magnetotelluric (MT) soundings.

Electrical conductivity is the physical property most sensitive to the configuration of aqueous fluids and/or magmas. Fig.2-12 shows the best fit resistivity model of the crust beneath the Naruko Volcano. An anomalous conductive body (< 10 Ω m) is clearly visible at a depth of 10-30 km beneath the volcano. The cut-off depth of micro-earthquakes generally coincides with the upper boundary of the conductor, implying that the temperature of the conductor is higher than 400 °C. These results indicate that this conductor is due to the presence of partial melts in the crust. In other words, MT soundings can be a powerful tool for detecting magma and related fluids in the crust and upper mantle.

It has long been recognized that the Kii Peninsula is peculiar for a non-volcanic region, with anomalously high heat discharge values similar to those from hot springs in volcanic regions. According to the magnetotelluric soundings in this region, there is a conductive layer in the upper crust (Fig.2-13). The occurrence of micro-earthquakes and low-frequency tremors reveal that the conductive layer is caused by the presence of aqueous fluids derived from the subducting Philippine Sea plate. The high temperature hot springs in this region may be due to heat flux discharged from aqueous fluid in the upper crust.

Reference

Asamori, K., Umeda, K., Geophysical Techniques for Detecting Magmas and High-Temperature Fluids —Their Application to the Onikobe-Naruko Volcanic Region and the Southern Kii Peninsula—, Genshiryoku Bakkuendo Kenkyu, vol.11, no.2, 2005, p.147-155 (in Japanese).

2-8 Paleo-Hydrochemical Conditions Recorded in Calcite
—Long-Term Stability of Geochemical Environment Deep Underground—

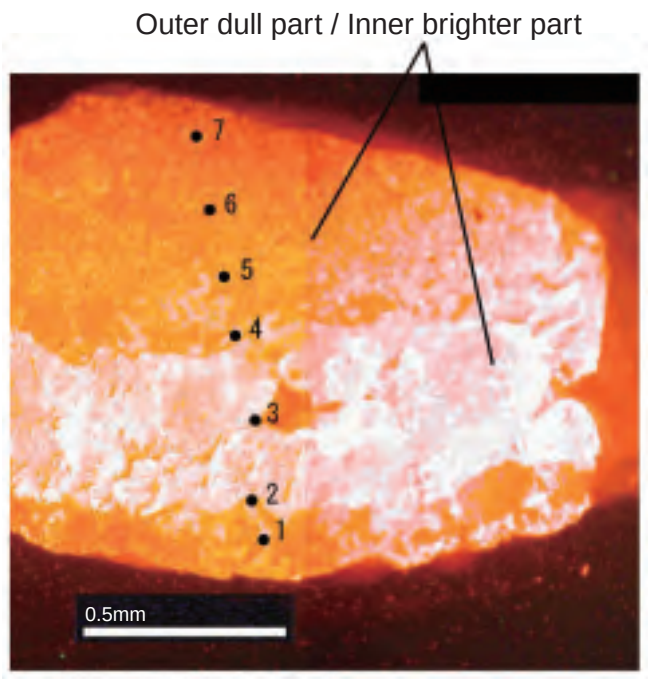

Fig.2-14 Cathode luminescence image of sampled calcite
Chemical zonal structure is made clear by cathode luminescence. In this case, the inner part of a grain is brighter than the outer part. The difference is caused by change of groundwater chemistry. Numbers show analysis point.

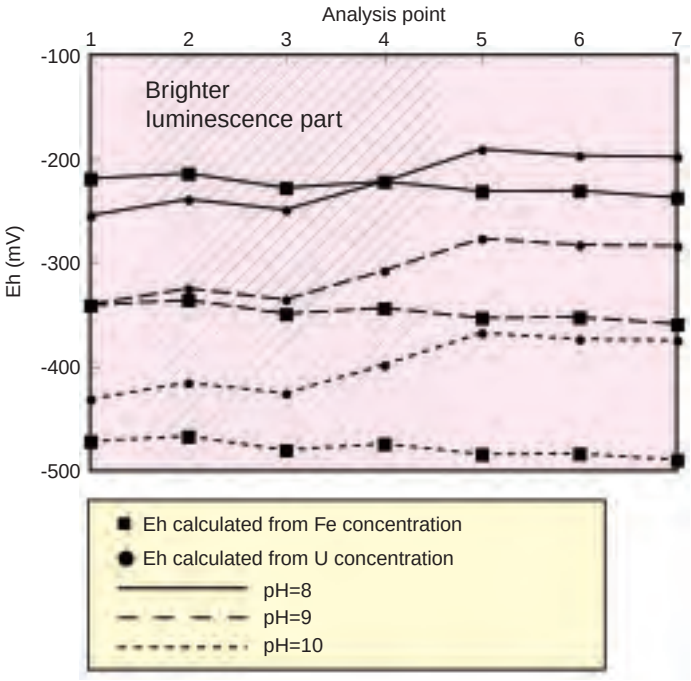

Fig.2-15 Calculation result
This figure shows the calculated result of Eh based on U and Fe concentration in calcite. Each number indicates the points in Fig.2-14. Hatched area corresponds to brighter area in Fig.2-14.

With the research and development for the long-term disposal of radioactive wastes, it is necessary to understand the nature of mass transport in natural environments. This will depend on the groundwater chemistry. Thus, evolution processes and long-term stability of groundwater chemistry should be understood to predict the change of hydrochemical conditions in the future.

In this study, to develop a methodology for assessing the paleo-hydrochemical evolution process of groundwater, especially with respect to understanding variations in redox conditions, calcite was studied. Chemical data from calcite have been found to be particularly useful for understanding chemical evolution processes of groundwater, which may affect the precipitation of calcite and thus be recorded. Such change of chemical environment will be recorded as a zonal structure in calcite grain (Fig.2-14). To calculate evolution of potential, firstly, concentration of metal element in past groundwater was calculated based on their concentration in calcite using partition coefficient. Next, redox potential was calculated based on the redox equilibrium of the metal element. In this way, we can guess the redox potential when calcite was precipitated.

Observation and quantitative analysis were carried out using 6 fracture filling calcite samples taken from basement granite. Calculated paleo-redox potential based on the concentrations of U and Fe are similar to present redox conditions (Eh: approx. -270mV to -400mV) in the case of pH=8. Based on this result, it is suggested that the redox conditions of the calcite in the evolving groundwater have varied with a range of several tens mV (Fig.2-15). Thus, the present study suggests that redox conditions in this area may have changed little. Therefore, the redox condition of groundwater likely will remain in reduction condition during calcite precipitation.

There has been no research which appraises the change of redox potential quantitatively, as in this research. This new understanding of natural phenomenon can contribute to a more realistic setting of conditions for mass transfer analysis, an so should be important knowledge in safety assessment of disposal of radioactive wastes.

Reference

Mizuno. T. et al., Long-Term Stability of Geochemical Environment at Deep Underground —Case Study of Minor Elements in Carbonate Minerals—, Chikyu Kagaku, vol.40, no.2, 2006, p.33-45 (in Japanese).

2-9 Study of Environmental Disturbance by an Underground Facility
—Estimate of Hydrochemical Disturbance Resulting from Drift Excavation—

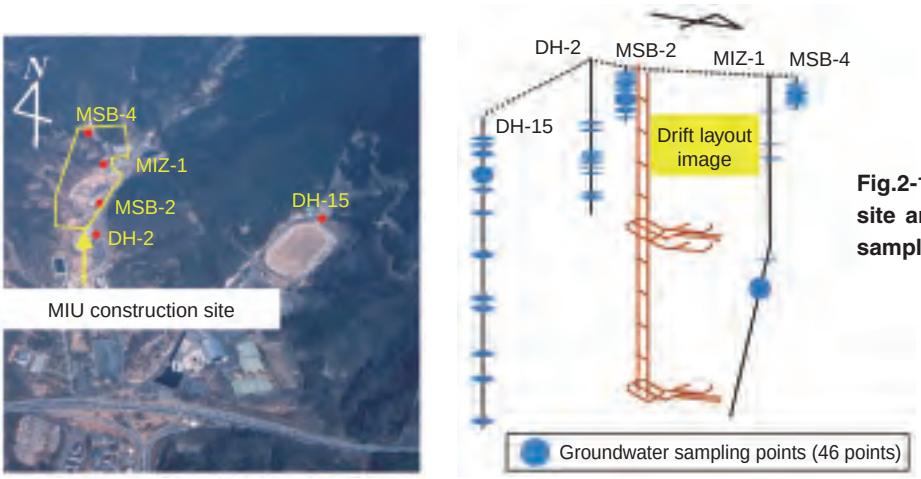

Fig.2-16 Bird's-eye view of MIU construction site and borehole location, and groundwater sampling point in each borehole.

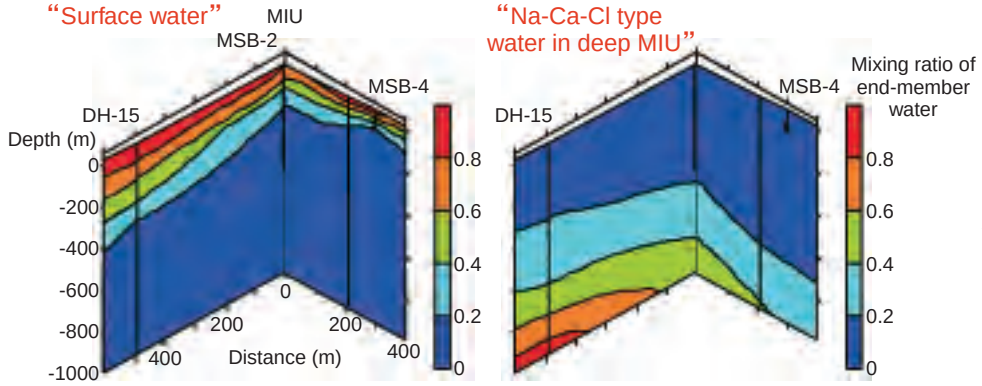

Fig.2-17 Mixing ratios of end-member water named "Surface water" and "High salinity Na-Ca-Cl water in deeper part of MIU" (Cross section of Fig.2-16).

The Japanese government has decided that the radioactive waste from atomic power plants shall be isolated in deep underground deeper than 300m below ground level. The construction and operation of such a large facility causes various environmental disturbances around it. For example, the pump up of large amounts of groundwater will change the hydraulic and chemical condition of groundwater in the local area.

This study focuses on methodology development to estimate long-term hydrochemical disturbance by a large underground facility. The analysis of principal components together with mixture and mass balance calculations was carried out at Mizunami Underground Research Laboratory (MIU: Fig.2-16) to infer the hydrochemical condition and evolution processes of groundwater prior to facility construction. The results show that the groundwater in the local area evolves by a mixing process among four end-component water types ("surface water", "Na-Ca-HCO_3 type water", "dilute Na-Ca-Cl type water in shallow part of MIU" and "concentrated Na-Ca-Cl type water in deep part of MIU") and water-rock interaction such as ion exchange reaction and precipitation / dissolution. The dominant evolution process in the vicinity of MIU is considered to be mixing between "dilute Na-Ca-Cl type water in shallow part of MIU" and "concentrated Na-Ca-Cl type water in deep part of MIU". It is possible to quantitatively describe the groundwater chemistry by the mixing ratio of the end components (Fig.2-17).

Furthermore, we attempted quantitative analysis of hydrochemical changes of groundwater around MIU during construction based on continuous hydrochemical observation. Preliminary analysis indicates that the hydrochemical change occurred several tens to several hundreds meter from the drift. This disturbed area will expand with time. Disturbance may be caused by inflow of large amounts of groundwater into drift, followed by outflow.

The procedure and methodology demonstrated by this study enable production of a "snap shot" of the hydrochemical condition at every step of facility construction. Such analysis will provide an important insight regarding disturbances around an underground facility.

Reference

Ajima, S. et al., Hydrogeochemical Modeling Around the Mizunami Underground Research Laboratory using Multivariate Analysis, Oyo Chishitsu, vol.47, 2006, p.120-130 (in Japanese).

2-10 Magnetotelluric Survey of 3-Dimensional Distribution and Hydrogeological Properties of Faults
—Development of Techniques for Investigating Geological Environment—

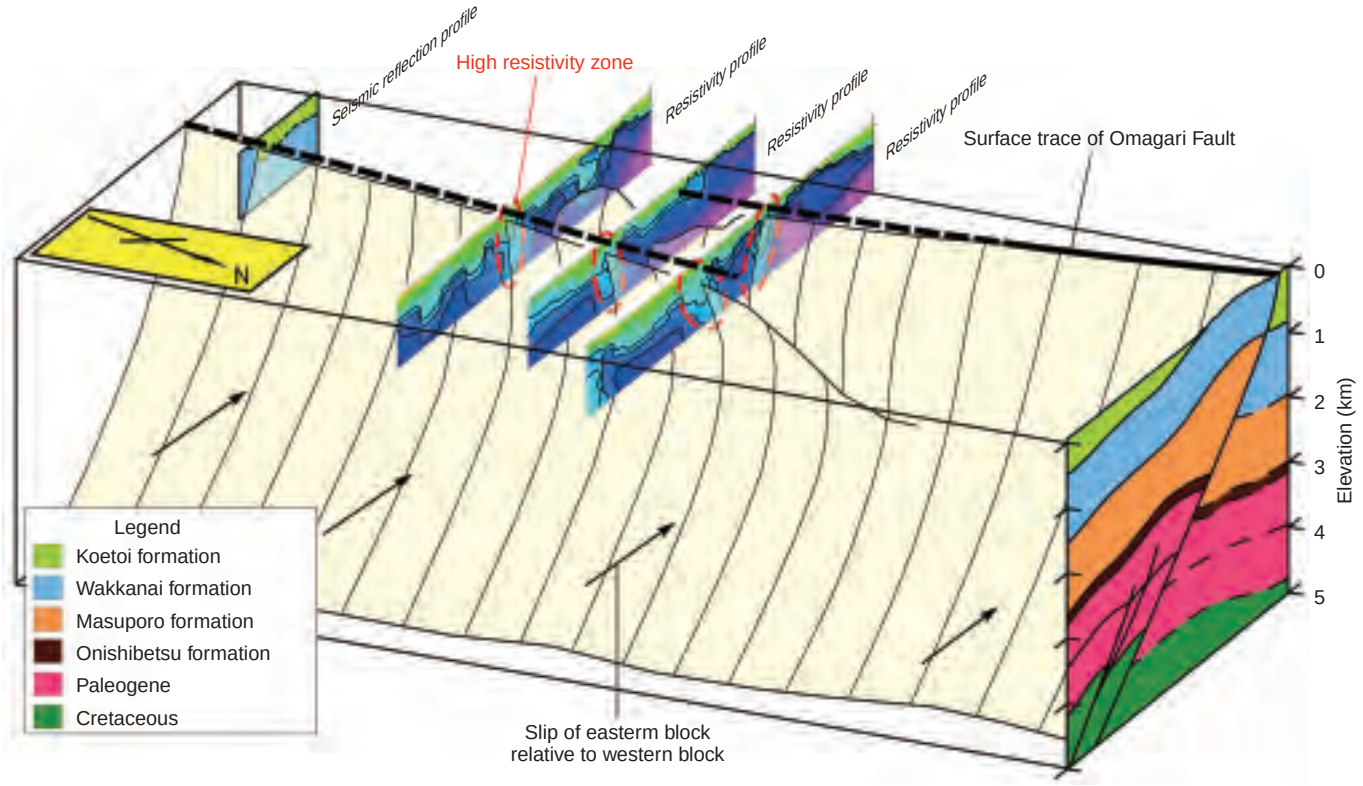

Fig.2-18 Inferred 3-D distribution of the Omagari Fault
The high resistivity zones in Fig.2-18 correlate with the rainwater infiltration zones, based on the data of resistivity and chlorinity of water taken from test boring. One of the high resistivity zones corresponds to the Omagari Fault inferred from a reflection seismic survey (not shown). Permeability along the Omagari Fault is estimated to be high, judging from outcrop occurrence along the Fault. Therefore, the high resistivity zone suggests infiltration of groundwater along the Omagari Fault and the stepped-diverging structure of the Fault shown in Fig.2-18 is inferred. The structure agrees with displacement direction of the Omagari Fault seen in outcrops.

Distributions of permeable zones in rocks influence the performance of far field barriers for the geological disposal of radioactive wastes. A fault zone composed of plural faults is a typical geologic permeable zone. For the geological disposal performance assessment, investigating distributions of the fault zone is important.

Investigation methods include geological mapping, remote sensing, airborne survey, geophysical prospecting and borehole investigation, and the best combination of methods depends on geological and social conditions.

In this study, heretofore unknown distribution and hydrogeological properties of the Omagari Fault were investigated by geological mapping, reflection seismic survey, audio-frequency magnetotelluric survey, and borehole investigations. The results showed that magnetotelluric survey in particular is effective for mapping the 3-D distribution and hydrogeological properties of a fault zone in massive rocks where both saline and fresh water exist. Uplifted marine sediments tend to exhibit distinctive resistivity due to the difference of chlorinity of formation water caused by the mixing of saline water with fresh water after uplift. Thus, distributions of fresh water zones can be searched by investigation of resistivities of the sediments. In addition, these distributions in massive rocks are largely caused by geological structures such as fault zones and their hydrogeological properties. Therefore resistivities in uplifted and massive marine sediments likely reflect the distribution and hydrogeological properties, as shown by this study.

Reference

Ishii, E. et al.. Three-dimensional Distribution and Hydrogeological Properties of the Omagari Fault in the Horonobe Area, Northern Hokkaido, Japan, Chishitugaku Zasshi, vol.112, no.5, 2006, p.301-314 (in Japanese).

2-11 Saline Concentration Indicates Groundwater Flow

— Relationship between Saline Concentration Distribution and Groundwater Flow in Sedimentary Rock —

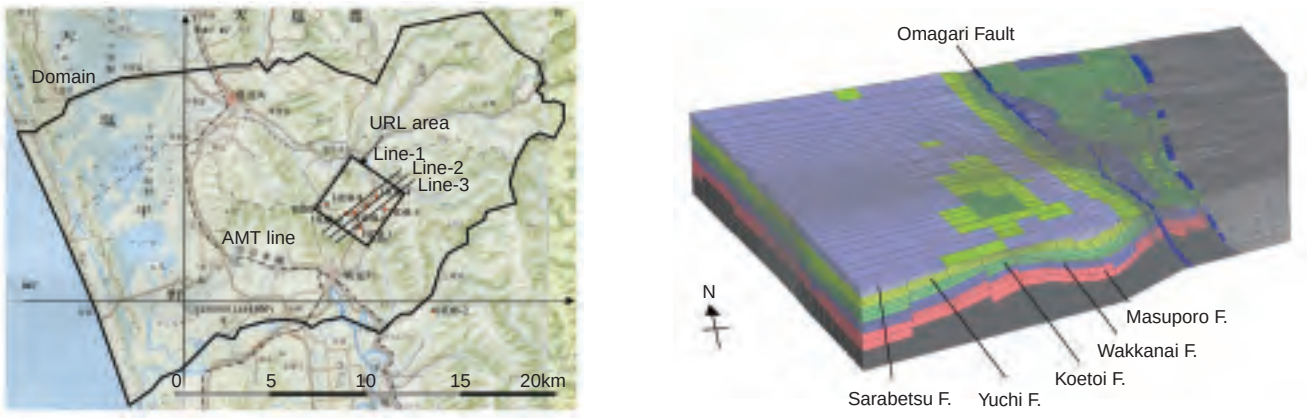

Fig.2-19 Analyzed area(left) and the finite element (FE) mesh (right)
To understand the groundwater (GW) flow system and distribution of saline concentration in and around the Horonobe URL area, GW flow and saline transport analysis by the FE method was carried out. Surrounding mountains and valleys were assumed to be impermeable boundaries and hydraulic conductivities obtained by the borehole investigations were applied to the FE mesh.

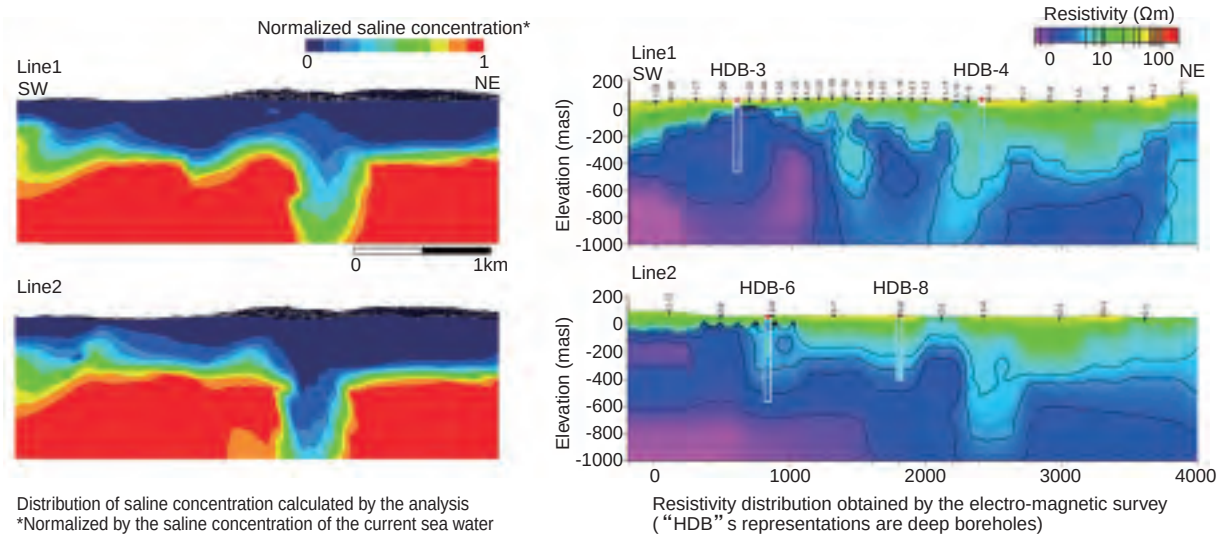

Distribution of saline concentration calculated by the analysis
*Normalized by the saline concentration of the current sea water

Resistivity distribution obtained by the electro-magnetic survey
("HDB"s representations are deep boreholes)

Fig.2-20 Distribution of saline concentration calculated by the GW flow and saline transport analysis (left) and resistivity distribution obtained by the electro-magnetic (EM) survey (right)
Highly concentrated saline GW is considered to be replaced with the infiltrating water from precipitation. This occurs especially at high permeable zones (near a permeable fault) according to the analysis. Resistivity distribution obtained by the EM survey which reflects the distribution of saline concentration correlates with the results of this analysis.

In order to understand a deep groundwater (GW) flow system, a GW flow analysis is often performed based on investigations providing the distribution of hydraulic parameters and boundary conditions. The result of this analysis is generally evaluated by comparison with measured hydraulic pressures. However, it is not effective in an area where the range of distribution of hydraulic pressure is small like Horonobe area.

Deep GW in Horonobe area has high salinity which indicates that it is old seawater confined during sedimentation. Therefore, GW flow and saline transport analysis was performed and the result was compared with measured saline concentration and distribution of resistivity which is considered to reflect the distribution of saline concentration.

In a geological environment such as this, where GW highly influences distribution of saline concentration, this analytical method focusing on the saline concentration is effective in evaluating the GW flow system.

Reference

Kurikami, H. et al., Groundwater Flow Analysis of Horonobe Underground Research Laboratory Project, 2005, JNC TN5400 2005-003, 97p. (in Japanese).

2-12 Detecting the Stress Distribution of Deep Sedimentary Rock in Northernmost Japan

— Construction of a Dynamic Model of Tertiary Siliceous Rock Based on Laboratory and In-Situ Measurement —

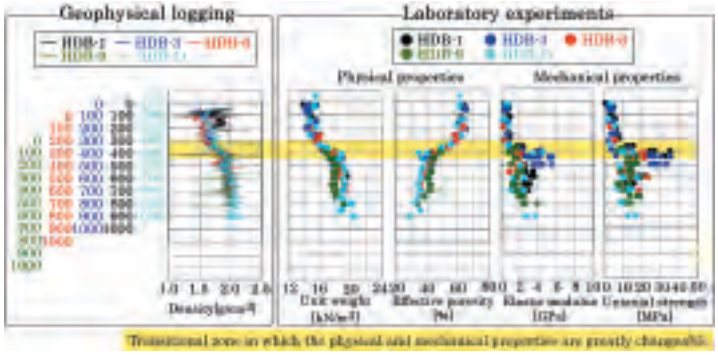

Fig.2-21 Various in-situ and laboratory experiments

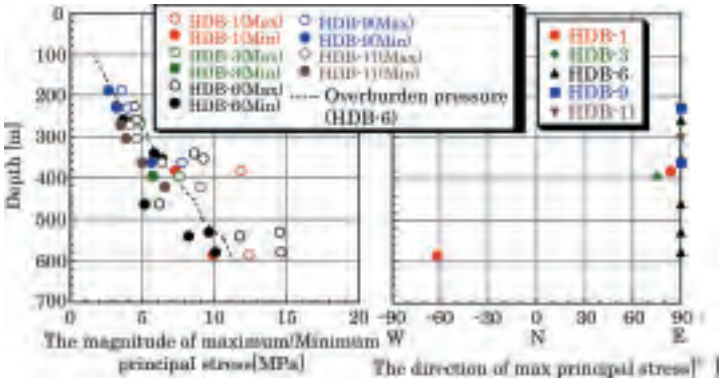

Fig.2-22 Measurement of initial stress by hydraulic fracturing test

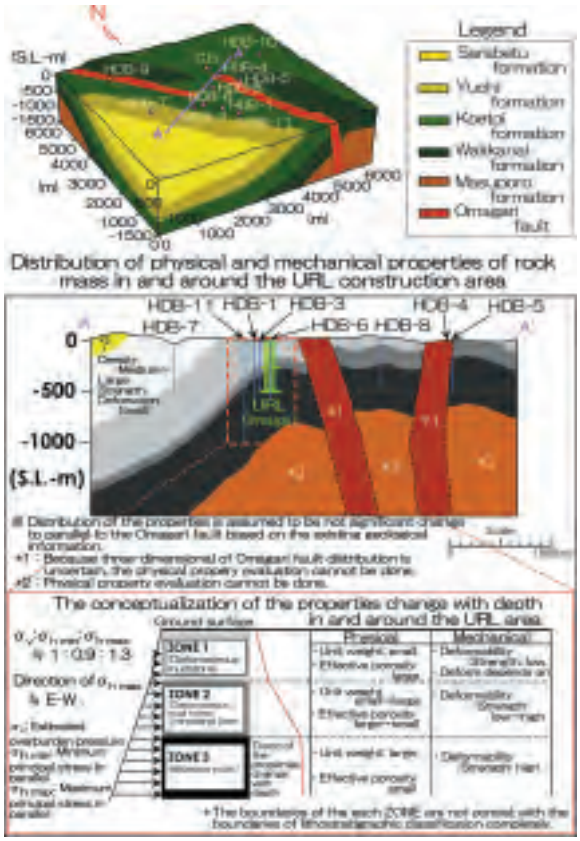

Fig.2-23 Rock mechanical conceptual model

We have carried out deep borehole of Tertiary sedimentary formations in the Underground Research Laboratory (URL) site, about 3km×3km in Horonobe-cho, Hokkaido. As the part of the investigations, laboratory and in-situ measurements of rock mechanics were carried out to select the URL site and to design the underground facility.

The URL area consists of the diatomaceous mudstone and siliceous mudstone to 1,000m depth. The origins of both rocks are mostly diatom and they show very little lithofacies change. The physical and mechanical properties of these rocks are not distinct from Tertiary sedimentary rock distributed elsewhere in Japan. However, there is a large difference between the properties of the two rocks. In addition, a transition zone, where the properties change continuously and radically, exists between both rocks. Therefore, we conceptually divided the vertical property distribution of the URL area shown in Fig.2-21 into three zones. This division can explain the features of the physical and mechanical properties of the rock in any point in the URL area.

Fig.2-22 shows the results of the in-situ stress measurements done by hydraulic fracturing in the URL area. The results indicate that the directions of $\sigma_{h\,max}$ are all close to EW up to 1,000m depth. The magnitudes of $\sigma_{h\,min}$ were almost equal the overburden pressure and the magnitudes of $\sigma_{h\,max}$ were from 1.2 to 1.65 times $\sigma_{h\,min}$. The influence of Omagari fault on the stress state in the URL area is not clear. The final conceptual model which integrates the results of previous discussions in the URL area is shown in Fig.2-23. The model describes the physical and mechanical properties including rock mass and stress state in the URL area qualitatively. The design of the URL facilities and the prediction of excavation disturbance due to URL construction were performed based on the conceptual model. We also learned the combination of the laboratory tests and geophysical logging that is effective for understanding and modeling a rock mass with little lithofacies change as in this investigation.

The verification of the conceptual model will be carried out in the investigation during construction of the URL facility. Based on the results, the methodology to understand the rock mechanics of a geological environment from the surface will be established.

Reference

Japan Nuclear Cycle Development Institute, Development and Management of the Technical Knowledge Base for the Geological Disposal of HLW, Supporting Report 1 “Geoscience Study”, 2005, JNC-TN1400 2005-014, p.4-93-4-146 (in Japanese).

2-13 Results of Transuranium (TRU) Waste Disposal Studies
－From the 2nd TRU Progress Report－

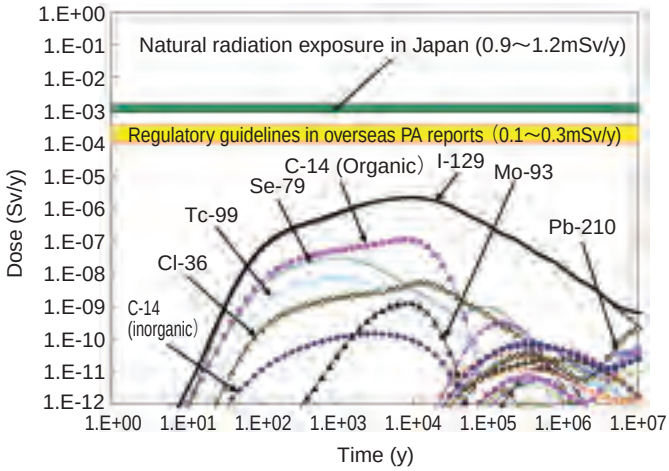

Fig.2-24 Estimated dose rate from a repository for TRU waste
Iodine-129 and Carbon-14 are dominant. Assumes a representative Japanese geologic environment.

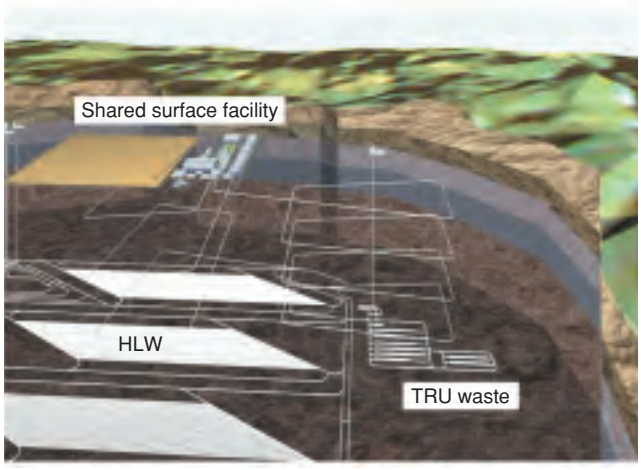

Fig.2-25 A conceptual figure of co-disposal system composed of HLW and TRU waste repository
This assessment shows that co-disposal is possible in a Japanese representative geologic environment, because setting repositories a certain distance apart prevents reciprocal influences.

Low-level radioactive waste generated during operation and dismantling of reprocessing facilities and MOX fabrication plant is called Transuranium (TRU) radionuclides bearing waste (abbr. TRU waste) in Japan (TRU waste was recently named “long half-life low heat radioactive waste”, but in this article, the term “TRU waste” is used). In order to establish a nuclear fuel cycle in Japan, a safe and feasible disposal methodology is required for TRU waste. To this end, Japan Nuclear Cycle Development Institute (in JNC, now JAEA) and the Federation of Electric Power Companies carried out an investigation of safe TRU waste disposal and summarized the results in a technical report called as the 2nd TRU progress report (hereafter TRU-2)[1]. The contents of TRU-2 are:

(1) the latest information on waste and a prediction of new waste generation
(2) detailed plans for realization of disposal concepts and safety analyses that consider the geologic conditions of Japan
(3) predictions of safety of shallow and intermediate depth disposal
(4) alternative technologies for reducing uncertainties in performance assessment and in the geologic environment
(5) and items for future study

To carry out a detailed safety assessment geologic disposal, knowledge and data were acquired and organized with respect to long-term alteration of the buffer material (bentonite) and rock near the repository which contact with cementitious material. Similarly, the influence of nitrate, organisms, gas-generation, colloids, and microbes on the disposal system and radionuclides migration were also obtained and analyzed. These data allowed improved reliable assessment models and parameter settings.

The assessment showed that for a TRU waste disposal system in a Japanese representative geologic environment, the maximum dose rate occurs about 10,000 years after disposal and is 3 orders of magnitude lower than the Japanese natural dose rate (Fig.2-24)

For performance optimization of the geologic disposal system of radioactive waste, a safety assessment was carried out for a co-disposal system composed of TRU waste and high-level waste repositories (Fig.2-25). The result shows that a co-disposal is possible if these repositories are set at a certain distance apart because then reciprocal influences, e.g. nitrate, high-alkaline plume and organic matter from the TRU waste repository, and heat from the high level waste repository, can be avoided. The Atomic Energy Commission of Japan deliberated on the result and judged that the co-disposal concept described in the 2nd progress TRU report has technical feasibility.

The 2nd TRU progress report also provides a technical basis for systematic TRU waste disposal and safety regulations.

Reference

1)The Federation of Electric Power Companies and Japan Nuclear Fuel Cycle Development Institute, Second Progress Report on Research and Development for TRU Waste Disposal in Japan －Science and Technology, Safety Assessment and Means of Implementation－, 2005, JNC TY1400 2005-013, FEPC TRU-TR2-2005-02, 556p. (in Japanese http://www.jaea.go.jp/04/below/tru/top.htm) (English version in press).

3 Nuclear Fusion Research and Development

3-1 For Practical Use of Fusion Energy

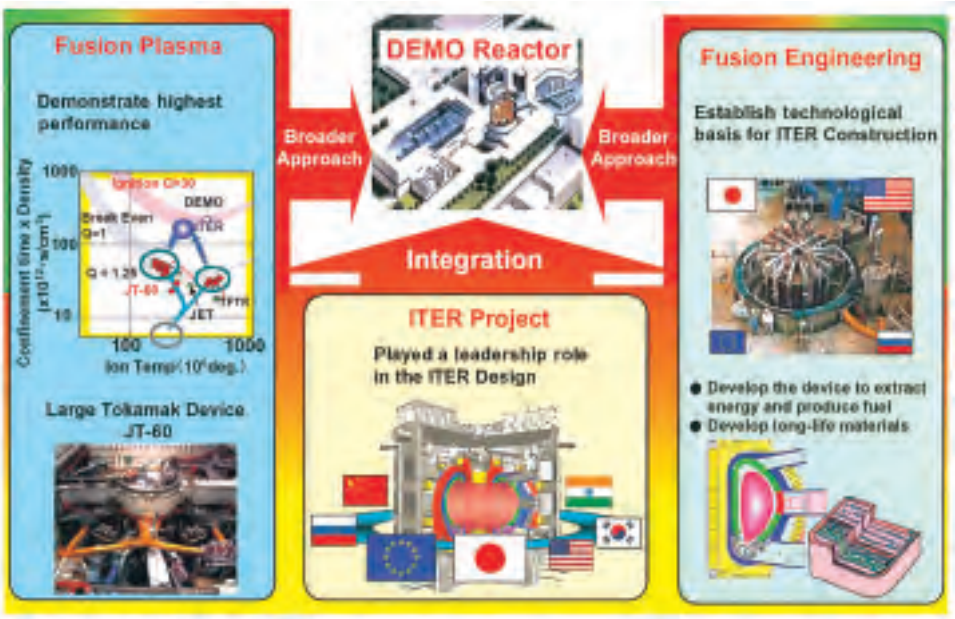

Fig.3-1 There are three important areas in fusion research. JAEA is the only research institute in the world investigating all of them

Fusion energy is one type of nuclear energy enabling permanent and sustainable development of society because the fuel is abundant, not unevenly distributed, it has fundamentally high safety, and it doesn't exhaust materials causing environmental damage, such as global warming and acid rain, in the process of power generation. In JAEA, the research and development of fusion energy have been conducted for 44 years including the period of the former JAERI. The ITER project, fusion plasma research, and fusion engineering research are keys to fusion development. JAEA is the only research institute in the world where these three areas are investigated comprehensively, as shown in Fig.3-1. In addition to the ITER project, the international cooperation between Japan and EU will be advanced over a broader area in order to realize the DEMO reactor (Broader Approach Activity).

ITER (International Thermonuclear Experimental Reactor) Project

"ITER", the next stage large tokamak, is being developed under international cooperation, originated from the U.S.-Soviet summit in November 1985. Its purpose is to realize and control extended burning plasma, and also to conduct experiments for the integration of fusion technologies.

It was decided to construct "ITER" at Cadarache in France and the critical role of Japan and the EU as well was agreed upon in the summit of June 2005 in Moscow. Formal participation of India was decided in December 2005 and the participants of ITER project grew to 7: Japan, EU, US, Russia, China, Korea and India, more than half of the world population. Kaname Ikeda, the former ambassador to Croatia, was elected as Director-General Nominee of ITER Organization, and the infrastructure of the organization is being developed. The joint implementation agreement of ITER was initialed in May 2006, and will be ratified after each party signs it in fiscal 2006, after which the ITER project enters the construction phase. Japan will make the second greatest contribution in procurement and staffing, following EU, the host party. JAEA is to be the domestic agency of ITER project in Japan, and will play a critical role to the ITER project.

Fusion Plasma Research

The large tokamak device "JT-60" started its operation in 1985 as one of the three large tokamak devices in the world. "JT-60" has been the first in the world with many results, such as the achievement of world's highest ion temperature, 520 million degrees, the world's highest energy multiplication factor, 1.25, and the discovery of the thermal insulation layer and the current hole. Recently, research into the long pulse operation of "ITER" and reduction of the cost of power generation, by such measures as long sustainment of high pressure plasma, and simulation research to clarify the characteristics of plasma are being pursued.

Fusion Engineering Research

Research and development of various advanced technologies which enable the utilization of fusion energy have been conducted. JAEA was hosted three of the seven ITER large R&D projects, and has established the technological basis for "ITER" construction. A breeder blanket and reduced activation ferritic steel etc. are now being developed by JAEA.

Broader Approach Activities

In the process of international negotiation regarding the determination of "ITER" site, Japan and EU agreed to implement the broader research and development (Broader

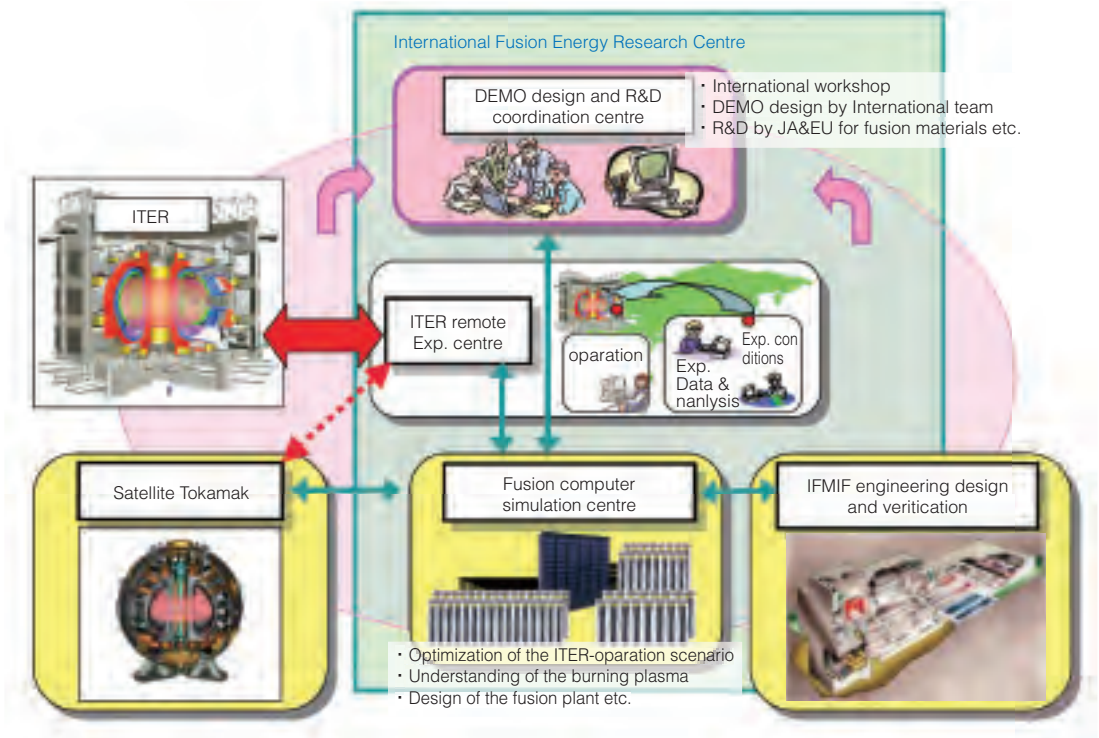

Fig.3-2 Broader Approach activities

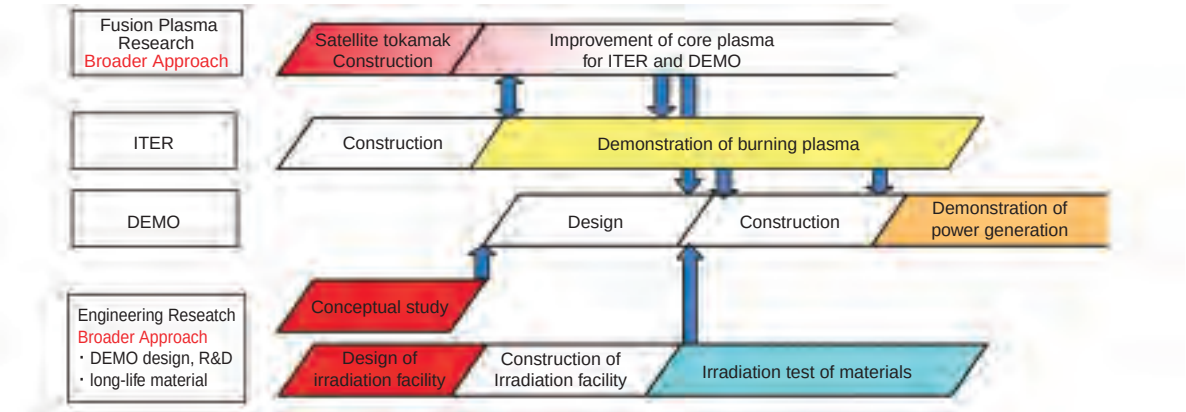

Fig.3-3 Development step of fusion research aiming to practical use in the midst of 21 century

Approach activities) that are necessary for "ITER" and DEMO with the two parties making equal contributions, in parallel with ITER implementation by the seven parties. The projects of Broader Approach activities are decided by MEXT, referring to the opinion of domestic specialists etc. as shown in Fig.3-2: (1) International Fusion Energy Research Center for computer simulation, remote experiment, DEMO design and R&D etc., (2) Engineering design and verification of the International Fusion Materials Irradiation Facility (IFMIF), (3) Satellite Tokamak. Technological meetings were held many times with EU to discuss the proposal from Japan, and the activities to be carried out and the allotment of work were agreed upon. Japan is now conferring with EU to ratify an agreement on EU-Japan fusion cooperation at the same time as the ITER agreement. JAEA is to be the Japanese implementing agency of the Broader Approach activities.

Future Research and Development

In the ITER project, about 20 years of experiment will be performed after the 10 years of construction phase. The control of burning plasma and the steady-state operation will be demonstrated, and the various fusion engineering technologies necessary for fusion reactors will be examined comprehensively in order to establish the technological basis for DEMO construction. On the other hand, in the fusion plasma research, the Broader Approach activities will be utilized as much as possible, and the research guiding the ITER project will be advanced, and the establishment of a steady-state operation with high-pressure plasma to realize compact fusion reactors is aimed. In the fusion engineering research, conceptual design of the DEMO reactor and the R&D necessary to utilize fusion energy will be advanced and the prospect to develop long-life materials will be obtained through the design of irradiation facility for materials. JAEA aims at the utilization of fusion energy in the middle of the 21st century, through a comprehensive approach to research including fusion plasma and fusion engineering technologies centering on the ITER project.

3-2 Prospects of Reduced Cost of Electricity from Fusion Power Plants
—Energy-Saving Operation for Fusion Power Plants in JT-60—

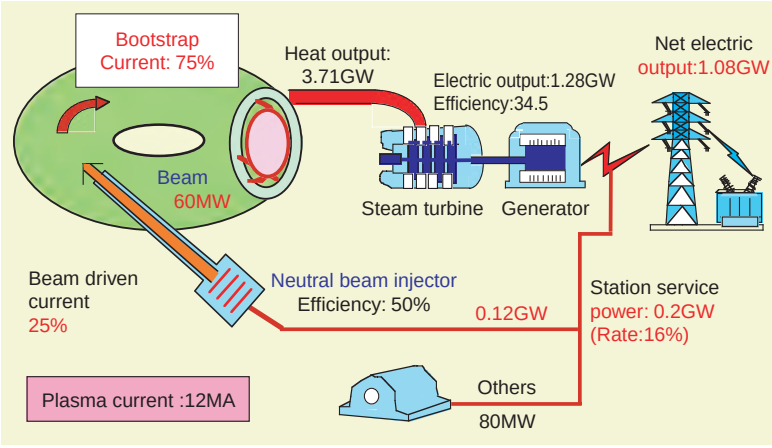

Fig.3-4 The flow of the electric power in an energy-saving operation with bootstrap current fraction of 75%
The capacity of neutral beam injector becomes 1/4 in comparison with that without bootstrap current. The ratio of station service power to fusion output reduces from 42% to 16%, making it a high-efficiency plant.

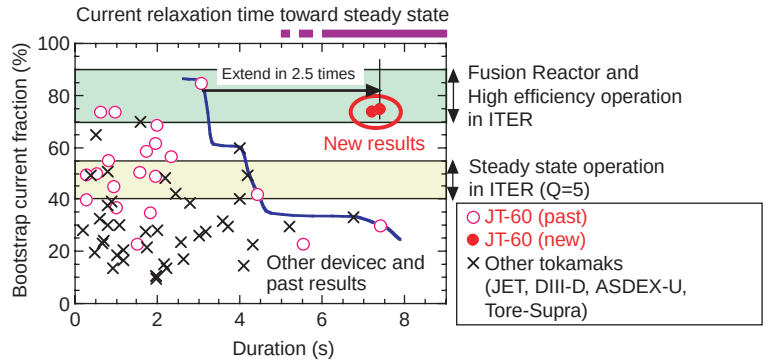

Fig.3-5 Progress in sustaining high bootstrap current fraction
The world's longest sustained operation at the bootstrap current fraction necessary for fusion reactor and the high efficiency operation of ITER was attained.

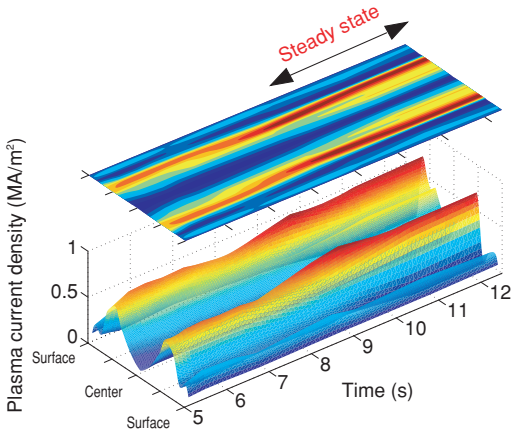

Fig.3-6 Changes in current density profile
In tokamak, profile becomes concave when bootstrap current fraction increases.

For reduction in the cost of electricity (COE) produced by fusion power plants, the electric power for operation (station service power) must be reduced, while at the same time raising the plasma pressure to increase the fusion power. In tokamak devices, a plasma current is necessary to confine the plasma. In present-day long pulse operation of tokamaks, most of the plasma current is driven by injection of radio-frequency (RF) waves and/or neutral beams, which requires a large amount of electric power and thus increases the station service power. Therefore, to reduce the station service power, development of the high-efficiency operation mode, in which a large fraction of the plasma current is driven by a self-generated bootstrap current, had been desired (Fig.3-4). We were the first in the world to start development of this high-efficiency operation, after recognizing its importance. In our studies, however, sustained duration was hampered by plasma instability, which was not controlled, and plasma conditions (pressure profile and current profile) did not reach stationary conditions. A strong linkage between pressure profile and current profile characterizes the plasmas with large bootstrap current fraction. Therefore, extending the plasma duration is an key issue, and it is important to ensure that the plasma with a large bootstrap current fraction stabilizes within a certain time.

We successfully avoided the plasma instability by the control of the pressure profile by changing the plasma flow with the "JT-60" neutral beam injection system which has a variety of injection directions. As a result, we maintained a high- temperature plasma with a bootstrap current fraction of 75% for 7.4 s (Fig.3-5), confirming that the current profile and the pressure profile reached nearly stationary conditions, (Fig.3-6), i.e. a steady state, for the first time in the world. This result demonstrates the technical feasibility of the high-efficiency operation mode and opens up prospects for reducing the COE of fusion power plants. Thus, the high-efficiency steady-state operation of burning plasma with a bootstrap current fraction of 50% which is desired for "ITER" is feasible.

Reference

Sakamoto, Y. et al., Stationary High Confinement Plasmas with Large Bootstrap Current Fraction in JT-60U, Nuclear Fusion, vol.45, no.7, 2005, p.574-580.

3-3 Insulator Generated in High-Temperature Plasma
—Anomaly of Current Profiles Observed in JT-60—

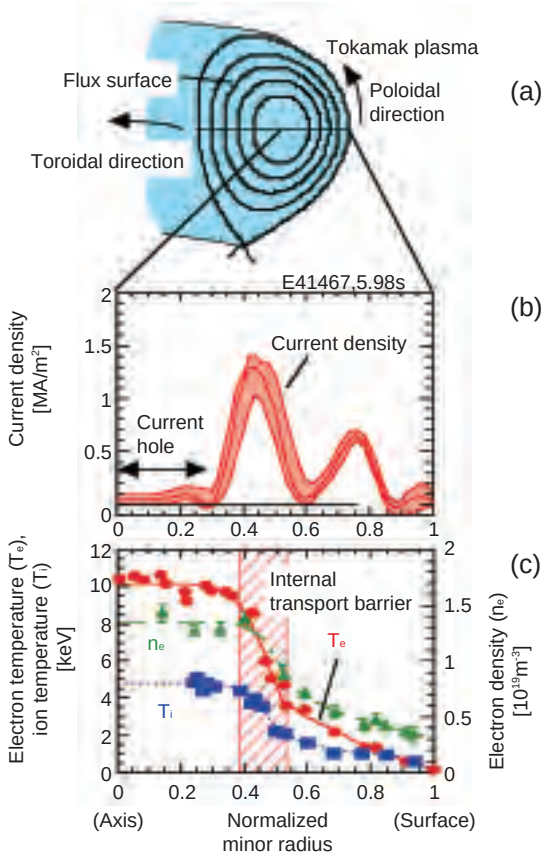

Fig.3-7 Current hole in tokamak plasma
A current hole, a region with nearly zero current density, appears in the central region of a donut-shaped tokamak plasma.

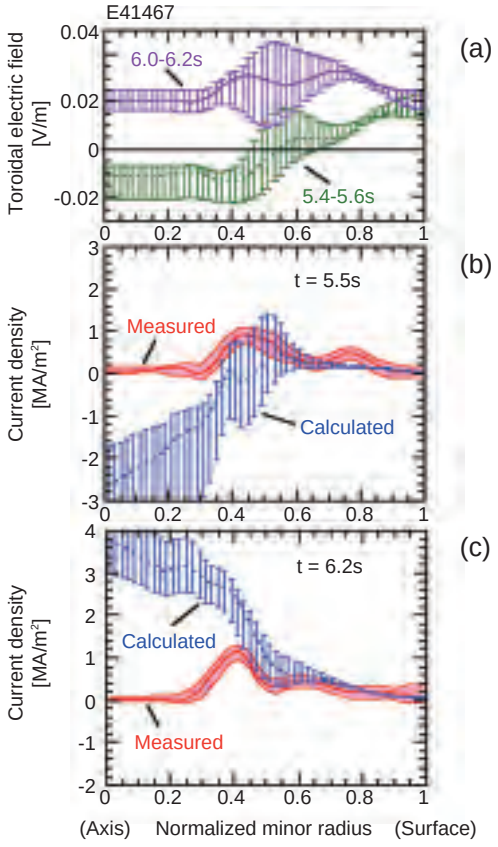

Fig.3-8 Application of electric field to a current hole
The current hole is maintained even when a positive or a negative electric field is applied.

Electric conductivity is one of fundamental material properties; materials may be a good conductor, an insulator, or a semiconductor. A plasma, which consists of ions and electrons, is a good conductor since an electric current is easily generated by motion of ions and electrons. The higher the electron temperature, the more easily the current flows. The conductivity of plasma with 13 million K electron temperature is close to copper.

We observed stable plasma sustained for several seconds in the "JT-60" tokamak with nearly zero magnetic field in the poloidal direction and hence nearly zero toroidal current in a substantial central region ("current hole") (Figs.3-7 (a) and (b)). A very-high-temperature plasma with an electron temperature of 10 keV (1.16 billion K) is confined stably in a current hole (Fig.3-7 (c)).

It was not known why a current hole is maintained in a very-high-temperature plasma with high conductivity. Is it because the current driving source such as an electric field becomes zero, or because some mechanism opposes the current driving force and keeps the current around zero? To find the answer, the response of a current hole to change in the driving source has been studied, precisely measuring the inductive electric field in the plasma. When the inductive field was changed by starting and stopping current drive and electron heating with electron cyclotron waves outside the current hole, a finite inductive electric field was generated in the central portion of the plasma (Fig.3-8 (a)). A large current is predicted, based on the theoretical value of electric conductivity of plasma ("Calculated" in Figs.3-8 (b) and (c)), but the measured current remained close to zero ("Measured"). Furthermore, current drive with electron cyclotron waves also failed to generate the current and destroy the current hole.

From these results, it has been shown experimentally for the first time that some mechanism works to keep the current density at zero level once it reaches that level in the central region. An insulator appears to be created in the central region of tokamak plasma, which generally has high conductivity. This observation reveals an anomaly of current profiles in the tokamak plasma, namely, in certain cases the profile is determined as a whole structure, not by driving force alone as has been thought. This is a new and remarkable phenomenon of structure formation in high-temperature plasma.

Reference

Fujita, T. et al., Current Clamp at Zero Level in JT-60U Current Hole Plasmas, Physical Review Letters, vol.95, no.7, 2005, p.075001-1-075001-4.

3-4 Mechanism of Confinement Improvement in Tokamak Plasmas
—Control of Turbulent Transport by Zonal Flow Modification—

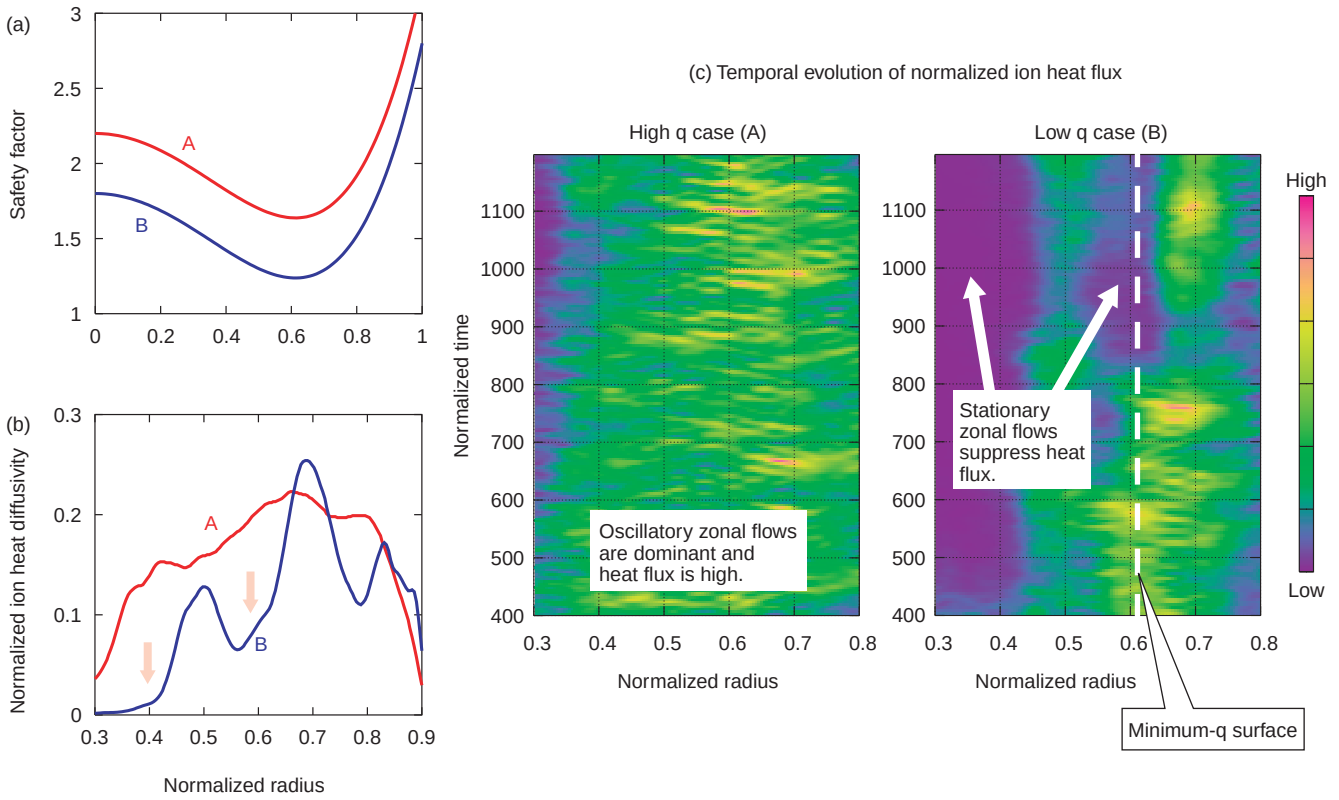

Fig.3-9 Effect of safety factor profile on ion turbulent heat transport
(a) Safety factor (q) profile used in simulation. (b) Normalized ion heat diffusivity. For low q, the heat diffusivity decreases around the circumference where q is minimum. (c) Temporal evolution of normalized ion heat flux. For high q, the heat flux is high and oscillates in time due to oscillatory zonal flows. On the other hand, the heat flux is suppressed by stationary zonal flows which strengthen when q is low.

In magnetically confined fusion plasmas, a pressure gradient generates turbulence. The turbulence causes loss of heat and particles and plasma confinement deteriorates. In recent years it has been shown experimentally that the plasma confinement is improved by control of plasma safety factor (q) profile. It is important to find a mechanism of confinement improvement for realization of efficient nuclear fusion power generation.

So far, theoretical and numerical simulation studies have shown that zonal flows (ZFs) are generated nonlinearly from microturbulence in the plasma, and can suppress the turbulence. ZFs are also observed in the atmosphere of Jupiter and Earth. Two kinds of ZFs, stationary ZFs appearing in a low q region and oscillatory ones in a high q region which are called geodesic acoustic modes (GAMs), are possible in tokamaks like “JT-60U”.

In the Numerical Experiment of Tokamak (NEXT) research, simulation of microturbulence driven by ion temperature gradient was performed. It was found that ion turbulent heat transport can be controlled by the change of ZF behavior accompanying change in the q profile.

Fig.3-9 shows effect of the q profile on the ion turbulent heat transport. In a high q case, the GAMs are dominant throughout the plasma. Since the GAMs are less effective in suppressing the turbulence than the stationary ZFs, the turbulent heat transport is high over a broad radial region. When q is decreased, the GAMs are damped at the minimum q region and the stationary ZFs become dominant instead. The stationary ZFs suppress the turbulence effectively and the heat transport is reduced. Outside the minimum q region, the GAMs are still dominant, so the turbulent heat transport is high.

Thus, control of the q profile is effective in changing the zonal flow behavior and thereby restraining the ion turbulent transport.

Reference

Miyato, N. et al., Study of a Drift Wave-Zonal Mode System Based on Global Electromagnetic Landau-fluid ITG Simulation in Toroidal Plasmas, Nuclear Fusion, vol.45, no.6, 2005, p.425-430.

3-5 Image of Radiation from 1/4 of a Donut Plasma
—Development of an Infrared Imaging Bolometer in JT-60U—

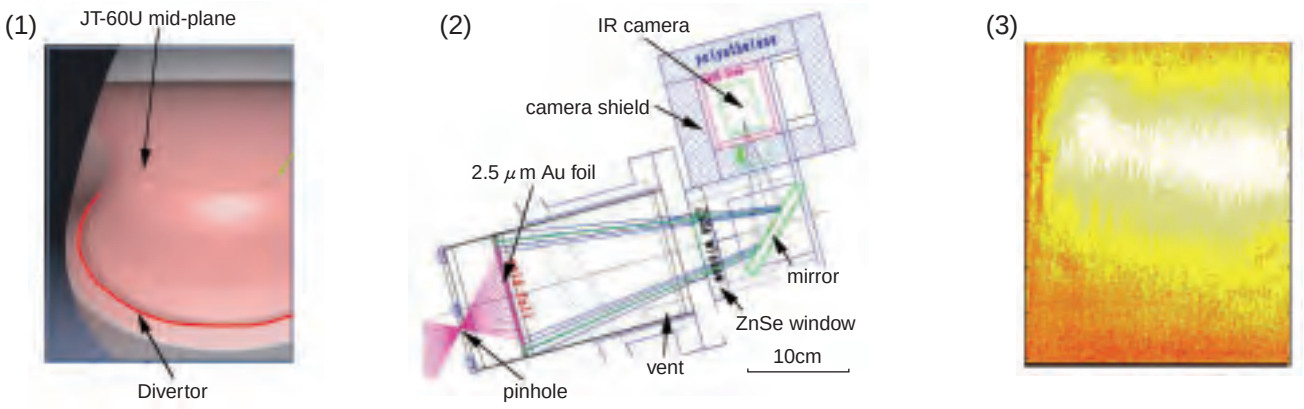

Fig.3-10 (1) IRVB views JT-60U plasma (pink) tangentially (2) IRVB: radiation mapped on a foil through a pinhole and observed by a shielded IR camera (3) unstable plasma about to disappear with strong radiation, disruption.

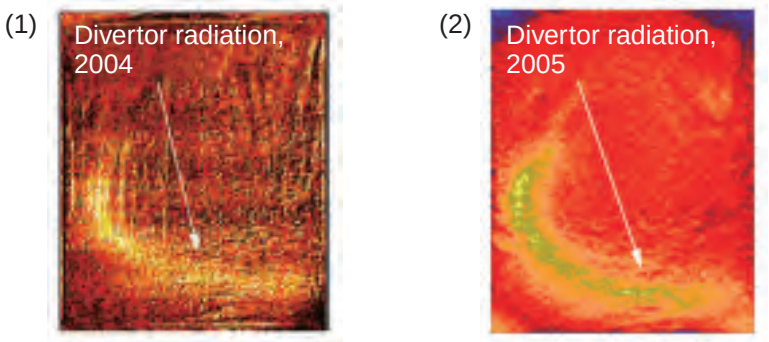

Fig.3-11 Curved belt of divertor radiation along 1/4 of donut ring is visible as an image (1) analog data during initial hydrogen experiment and (2) digital data during high power deuterium experiment. Enhanced shield and digital system improved images.

A bolometer is an instrument to diagnose plasma radiation. A thin metal foil of the bolometer receives radiated power from the plasma, impurities and hydrogen being the primary radiators, and the resulting temperature rise of the foil is measured. So-called resistive bolometers have been used up until now. A resistor is attached on the back of the foil and the temperature is given as a function of that resistance. However, this method requires many detectors and electronic circuits. Recently, compact and advanced infrared (IR) cameras have become available. The foil temperature can be measured directly by an IR camera outside of the vacuum window. This is the IR imaging video bolometer, IRVB. The IRVB can provide a wide view equivalent to hundreds of resistive bolometers. In order to test IRVB feasibility under burning plasma conditions, an IRVB was installed on the JT-60U tokamak (Fig.3-10 (2)). The field of view (Fig.3-10 (1)) was designed to cover a wide area of the donut plasma by looking tangentially from an upper port of "JT-60U". The 2.5-micron gold foil in IRVB has proved to be durable for more than three years of tokamak operations. The brightest radiation, i.e. highest foil temperature image, is seen during an abrupt plasma termination called a disruption, as shown in Fig.3-10 (3). An enormously strong radiation belt was recorded on the foil when the high temperature plasma became a huge radiator. Under normal operation, radiated power peaks only near the target tiles of the divertor. A curved radiation belt along the divertor, a red line in Fig.3-10 (1), is visible on the foil in Fig.3-11. Improvement of the neutron shielding and digital data system allowed clearer images even during high power deuterium discharges. Radiated power from 1/4 of big donut plasma with diameter of 6 meters was taken successfully as an image. There has been no such attempt like this before. A simple unanswered question, whether tokamak radiation is uniform along the donut ring, can be addressed with this diagnostic. (This is a collaborative research between JAEA and the National Institute for Fusion Science and was partly supported by a Grant-in-Aid for Scientific Research from JSPS, Nos. 16560729 and 16082207.)

References

Konoshima, S. et al., Radiated Power Profile Observed by a Tangentially Viewing IR Imaging Bolometer in JT-60U Tokamak, Europhysics Conference Abstracts, 2005, vol.29C, P-4.092 in CD-ROM attached.

Parchamy, H., Peterson, B.J., Konoshima, S. et al., Detailed In-Situ Laser Calibration of the Infrared Imaging Video Bolometer for the JT-60U Tokamak, Review of Scientific Instruments, 2006, vol. 77, no.10, p.10E515-1-10E515-4.

3-6 Concept for a Reduced Cost Fusion Reactor
—Compact Reactor Allowing Early Realization of Fusion Power—

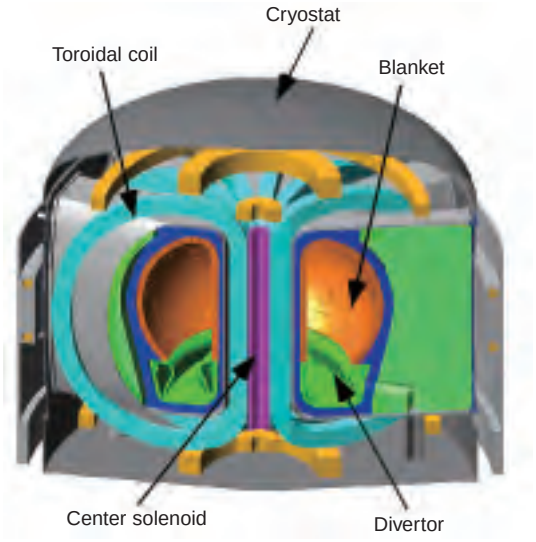

Fig.3-12 Conceptual view of Fusion DEMO reactor, which is designed to produce 1 GW of net electric output.

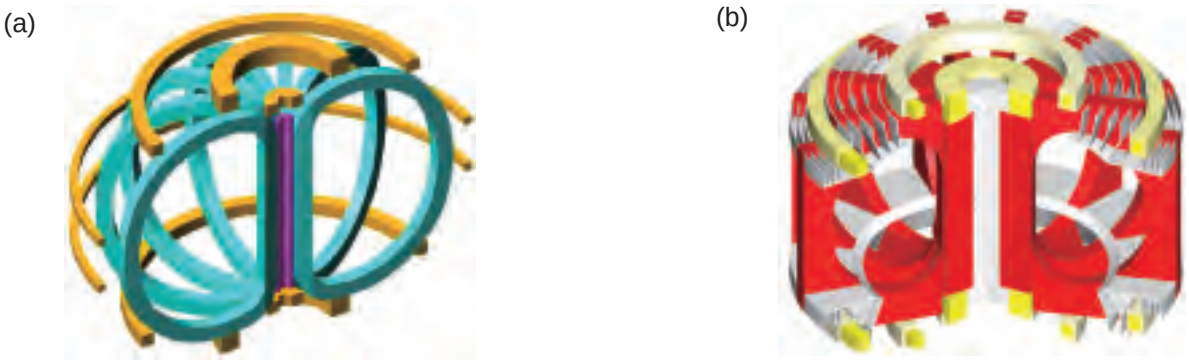

Fig.3-13 Comparison of superconducting coil system in (a) the proposed DEMO reactor and (b) conventional tokamak reactor
(a) with a low aspect ratio has a coil system with very low magnetic energy, allowing such a thin coil support assembly.

Nuclear fusion is a promising innovative energy option for the future because of its superiority over safety and environmental aspects. On the other hand, a reduction of the construction cost is an important issue to be addressed for commercialization. We have developed a design for a fusion DEMO plant which can resolve the cost issue.

It is required that the fusion DEMO plant generate a commercial scale electric output of 1 GW. Additional missions of the DEMO plant are economic viability as well as operational reliability. To meet these requirements, we have been envisaging a DEMO reactor which has reduced size in comparison with conventional fusion power reactors (Fig.3-12). One of the most striking features of the reactor is that the electric output of 1 GW is attainable with the relatively conservative plasma technology foreseeable in the 2020's, despite its compactness. What allows such a reactor design is 1) a thin superconducting coil system producing high magnetic field, and 2) a low aspect ratio regime (corresponding to a fat plasma shape) which has not received attention so far because plasma experiments in this regime have been scarce. Based on recent progress in experimental and theoretical studies, a low aspect regime is likely to be adequate for advanced tokamak operation. Fig.3-13 shows a comparison of superconducting coil system of the proposed DEMO and a conventional tokamak reactor design. The coil system, which is usually the most expensive components of a fusion reactor, is very thin in this DEMO, so that there is significant cost reduction. Furthermore, low aspect ratio has the advantages of lowering requirements for plasma conditions, and mitigation of outboard blanket design conditions for blocking the electromagnetic forces acting on a disruption, etc.

Our evaluation indicates that this fusion reactor concept is basically viable and has good impact on cost reduction. The next challenge in the design study is to make the concept concrete by combining various fusion technologies being available in the near future.

Reference

Tobita, K. et al., Design Study of Fusion DEMO Plant at JAERI, Fusion Engineering and Design, vol.81, 2006, p.1151-1158.

3-7 Achievement of 1000 s High Power Radio-Frequency
—Establishment of Gyrotron Technology for Stable & Steady State Operation—

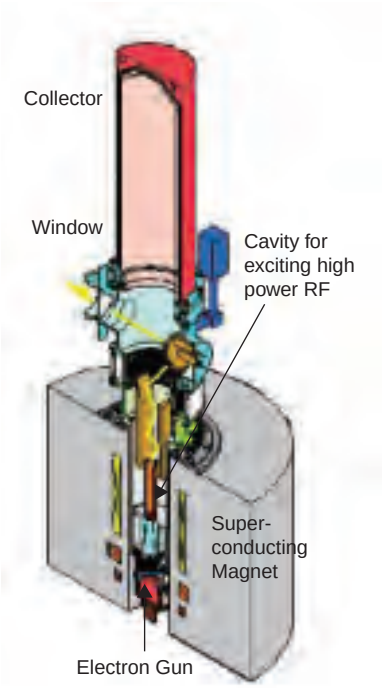

Fig.3-14 Schematic view of high-power gyrotron for fusion
Height is ~3 m, weight is ~800 kg. The gyrotron is installed in a superconducting magnet weighing ~7 T. The major three breakthrough technologies used were: high order mode cavity for high power oscillation, artificial diamond window for long pulse operation and an energy recovery system for high efficiency.

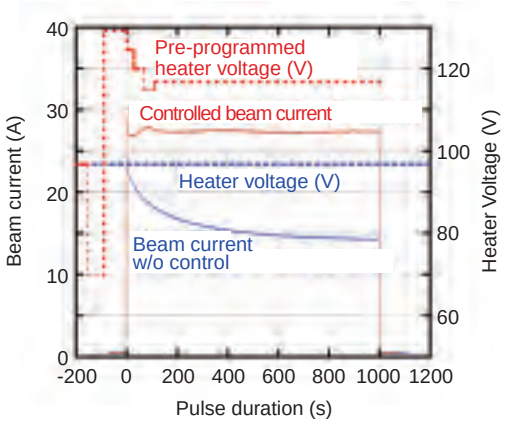

Fig.3-15 Comparison of beam current and applied cathode voltage in 1000 s operation without oscillation. Red shows operation with pre-programming control, blue shows operation without control.
By the control of the voltage of the cathode heater during the shot, the temperature of the electron emitter can be stabilized and the beam current decrease is suppressed.

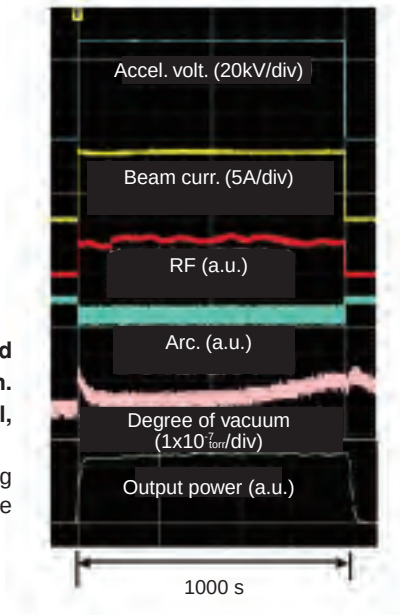

Fig.3-16 Typical waveform of stable gyrotron operation during 1000 s
Steady state operation of 1000 s was achieved, far exceeding 400 s standard operation time of "ITER". By control of beam current, arcing in the gyrotron was eliminated, the vacuum pressure was lowered, and the average output power measured by the dummy load was very stable during the oscillation.

A 170 GHz gyrotron for International Thermonuclear Experimental Reactor ("ITER"), a high power Radio-Frequency (RF) source used for plasma heating and current drive, achieved 1000 s operation, far exceeding the 400 s standard operation time for "ITER" plasma burning, thus establishing gyrotron technology for a stable and steady state oscillation.

A gyrotron (Fig.3-14) is a microwave tube that utilizes the electron-cyclotron resonance maser effect and a weakly relativistic electron beam (<100kV) through gyro-motion. It can generate high output of millimeter waves of 100 GHz band with high efficiency. The "ITER" requires a 170 GHz high-power gyrotron system with total output of 24 MW, for electron cyclotron heating, current drive and suppression of plasma instabilities. Intensive development of the 170 GHz gyrotron (1 MW, CW, and 50% efficiency) is under way in JAEA. The magnetron injection gun makes a hollow beam of gyrating electrons with an energy of ~80 keV, which is injected into a cylindrical cavity. A $TE_{31,8}$ mode RF wave is excited in the cavity, output through the diamond window, and converted to a Gaussian beam by a quasi-optical mode converter.

A significant issue was the large beam current decrease caused by the emission cooling of the cathode for the long pulse operation. The rapid slump of beam current caused oscillation mode change and limited the pulse extension (Fig.3-15). Consequently, the power decreased.

To suppress the beam current decrease, pre-programming control of the cathode heater power was applied to keep the cathode temperature constant and thus stabilize the beam current. As a result of stabilization of the beam current, the stable and steady state oscillation of 1000 s with 0.6 MW output power was achieved by the 170 GHz ITER gyrotron (Fig.3-16). It appears that the beam current control by pre-programming of cathode heater power will enable long pulse, high power operation up to 1MW. With this successful steady state operation for 1000 s, one of the issues for the ITER gyrotron was solved. In the future, the development of high performance 170 GHz gyrotrons with 1MW output and 50% efficiency will be carried out.

Reference

Kasugai, A. et all., Long Pulse Operation of 170GHz ITER Gyrotron by Beam Current Control, Fusion Engineering and Design, vol.81, 2006, p.2791-2796.

3-8 Reduction of the Heat Load on Acceleration Grids in the Negative Ion Based Neutral Beam Injector —A Step Toward Long Pulse Beam Injection—

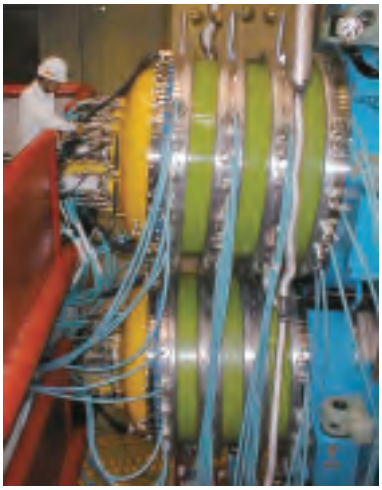

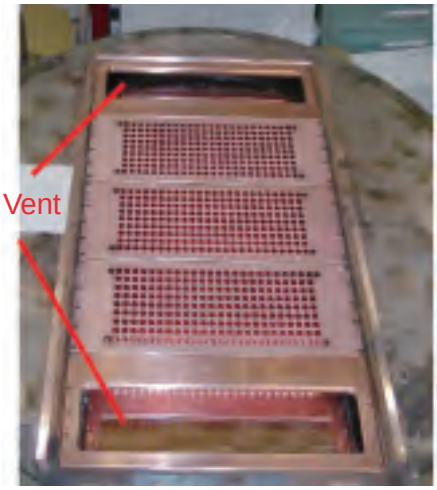

Photo3-1 (left)
Negative ion source for JT-60U
22A Deuterium negative ion beam at 500 keV is produced.

Photo3-2 (right)
Vent of acceleration grid
Vents are made on both sides of five grid segments in order to reduce the pressure in the accelerator.

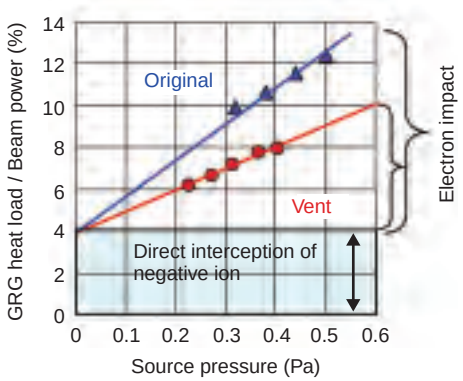

Fig.3-17 Dependence of the grounded grid (GRG) heat load on source pressure
This shows the ratio of GRG heat load to beam power. The ion source is normally operated at 0.3 Pa. With vents, the heat load by electron impact is improved about 40%.

A negative ion based neutral beam injector (NNBI) was desired to extend pulse duration from the design value of 10 s up to 30 s, maintain the plasma characteristic of "JT-60U" for a long period. Photo3-1 shows the negative ion source for "JT-60U". The pulse duration has been restricted by the temperature rise of cooling water. To extend pulse duration, it was necessary to reduce the heat load on the acceleration grids. There are two causes of the grid heat load. One is the direct interception of accelerated negative ions and the other is electrons co-accelerated with negative ions. In this research the reduction of heat load by electrons was attempted. Many electrons are generated by being stripped from negative ions when the negative ions collide with residual gas molecules in the accelerator. The electrons produced there are accelerated and collide with the acceleration grids. These stripped electrons can be reduced by decreasing pressure in the ion source. However, the pressure in the source chamber needs to be around 0.3 Pa so as to extract large negative ion current. In order to reduce pressure in the accelerator while keeping the pressure in the source chamber at 0.3 Pa, the structure of the acceleration grid segment is modified as seen in Photo3-2. Acceleration grids are composed of five segments, and in the original design, negative ions are extracted from all five segments. To lower pressure in the accelerator, vent grids were added to both sides of acceleration grid segments. In this case, the upstream plasma grids are masked so that negative ion beam are not extracted as they pass through vent grids. Fig.3-17 shows the dependence of the grounded grid (GRG) heat load ratio per beam power on the source pressure. In this figure, the GRG heat load ratio increases with the source pressure. This increase seems to be caused by electron impact, whereas the heat load ratio which is present regardless of pressure, around 4%, is negative ion interception. By decreasing pressure at the accelerator with the vent grids, the production of stripped electron is restrained, and the heat load ratio due to electron impact is reduced about 40%. This leads to restraint of the temperature rise of cooling water by about 35 degree under steady state condition more than 10 s. The pulse duration of one ion source was extended up to 25 s.

Reference

Umeda N. et al., Recent Progress of Negative Ion Based Neutral Beam Injector for JT-60U, Fusion Engineering and Design, vol.74, 2005, p.385-390.

3-9 Uniform Production of H⁻ Ions in a Large Ion Source
—Technology for High Power Neutral Beam Injection System—

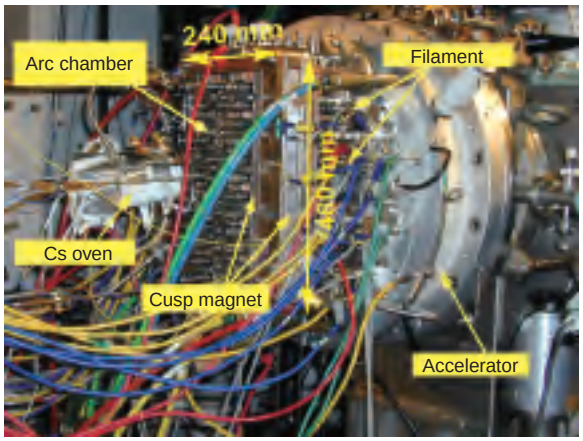

Fig.3-18 JAEA 10 A negative ion source
JAEA has succeeded in developing the world's first negative ion beam of ampere class.

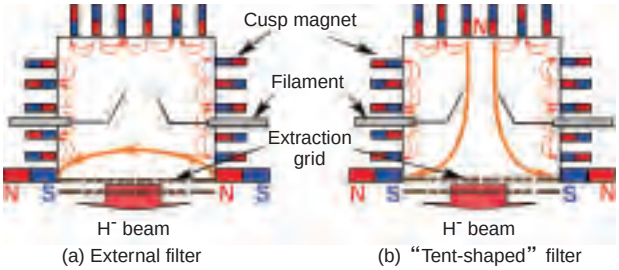

Fig.3-19 The magnetic configuration of 10 A negative ion source
The "tent-shaped" filter was used to improve the uniformity of negative ion production.

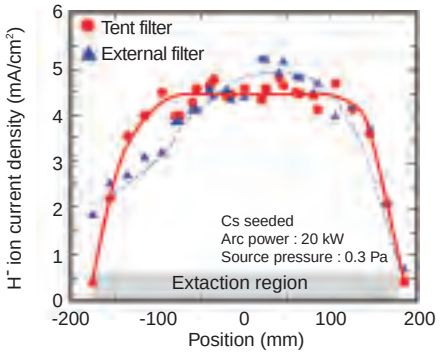

Fig.3-20 The H⁻ ion beam intensity
By using the "tent-shaped" filter, the deviation of the beam profile was reduced from 16% to 8%.

In a high energy neutral beam injection (NBI) system for fusion reactors, a large size negative ion source is required. However, in the negative ion source for a large fusion experimental reactor such as "JT-60U", non-uniformity of the extracted negative ion current density over the wide area of the source is observed. This causes poor optics of the beams and limits beam pulse length of the system, due to high heat loads placed on the acceleration grids and the beam line components.

To overcome this problem, experimental studies have been performed using the JAEA 10 A negative ion source whose magnetic configuration is similar to that of the large negative ion source of the JT-60 N-NBI (Fig.3-18).

In negative ion sources, hydrogen arc discharge produces dissociated H0 and/or H+. By seeding a small amount of Cesium (Cs) into the source, work function of the plasma grid is lowered, H0/H+ being converted to H- on the plasma grid surface (surface production). In the original H- source, a transverse magnetic field called a "magnetic filter" is formed to keep a low electron temperature around the extraction region (Fig.3-19 (a)). However, from the result of the 3D electron trajectory calculation, it was found that the residual magnetic filter field around the filament cathode causes a drift of the fast electrons emitted from the filaments. Due to this electron drift, the source plasma is localized and the ion beam becomes non-uniform.

Based on these results, the magnetic configuration of the JAEA 10 A negative ion source was modified in order to improve the beam uniformity. Instead of an external filter field, a tent-shaped filter field as shown in Fig.3-19(b) was employed between a cusp magnet on the source back plate and the large magnets placed outside of the aperture area of the plasma grid. This "tent filter" is effective to suppress co-extraction of electrons. Fig.3-20 shows the longitudinal beam profile before and after the modifications. The beam profile with the external filter configuration exhibited a non-uniform profile with the deviation of 16%. In the tent filter configuration, the uniformity of the extracted beam was drastically improved, the deviation of the beam profile reducing to 8%. The co-extracted electron current was suppressed to a level equivalent to that of the H- ion current.

Reference

Hanada, M. et al., Improvement of Beam Uniformity by Magnetic Filter Optimization in a Cs-seeded Large Negative-Ion Source, Review of Scientific Instruments, vol.77, no.3, 2006, p.03A515-1-3.

3-10 Pioneering Material for ITER Superconducting Wire
—Success in Mass Production of High Performance Nb_3Sn Strands—

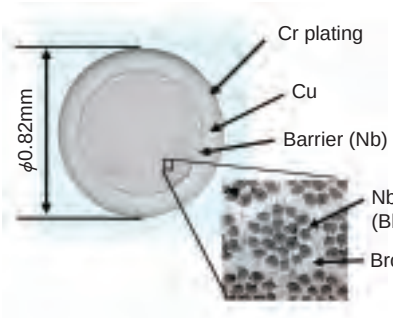

Fig.3-21 Cross section of bronze processed strand
Tin is contained in bronze and an increase of tin content in bronze has enhanced critical current density.

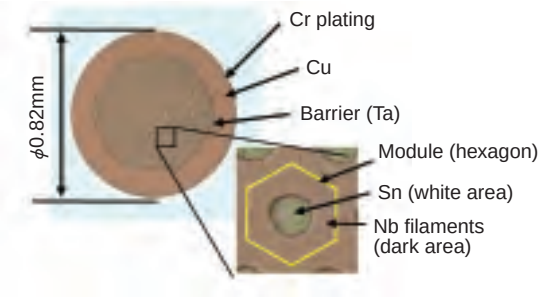

Fig.3-22 Cross section of internal tin processed strand
Tin rod is embedded in a module. The targets are reached by downsizing of the module and optimizing the ratio of niobium to tin.

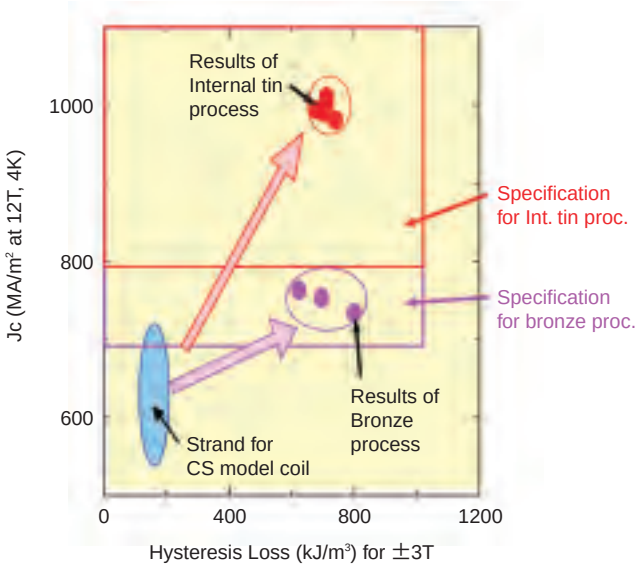

Fig.3-23 Performance of the developed strand
The important parameters are critical current density (Jc) and hysteresis loss. Strands satisfying these requirements were fabricated by both bronze and internal tin processes.

Magnetic fields of 12 to 13 T are required to generate and confine plasma for International Thermonuclear Experimental Reactor ("ITER"). To generate such high magnetic fields, huge amounts of high performance Nb_3Sn strand must be produced. The strand is required to have not only high critical current density (Jc), but also low hysteresis loss in a varying field. These are contradictory characteristics for a strand and therefore, it is necessary to develop a new technology to achieve both requirements.

Typical methods to fabricate Nb_3Sn strand are the bronze process and the internal tin process. In the bronze process, Niobium (Nb) filaments are embedded in bronze (Fig.3-21), and Nb_3Sn is produced by a heat treatment at 650℃ for 200 hours. A major barrier to improving Jc is the low tin content in a strand. Recently good quality of high tin content bronze has become available and adopting this bronze has realized the enhancement of Jc.

In the internal tin process, Nb filaments and tin (Sn) rods are embedded in copper (Fig.3-22). It is relatively easy to increase tin content in this strand and to enhance Jc, but hysteresis loss drastically increases due to the formation of superconducting rings by the joining of filaments near Sn rods upon heat treatment. A hexagon, in which a large number of filaments and a single Sn rod are embedded, is called a "module." Downsizing the module and optimizing the ratio of Nb to Sn have restrained this increase in the hysteresis loss because diameter and thickness of the ring are reduced. Consequently, both high Jc and low hysteresis loss have been satisfied.

0.1-tons strands fabricated through both processes have been demonstrated to satisfy the specifications, as shown in Fig.3-23. While Jc specifications at 4K are different between the two processes, they are the same value at the operating condition of the "ITER" (12 T, 5.7 K and strain of -0.76%). JAEA has achieved these Nb_3Sn fabrication results ahead of the other "ITER" participants, and thus JAEA will be make the largest contribution in strand supply among the "ITER" parties.

Reference

Okuno, K. et al., From CS and TF Model Coils to ITER: Lessons Learnt and Further Progress, IEEE Transaction Superconductivity, vol.16, 2006, p.880-885.

3-11 New Stainless Steel for High Performance Superconducting Coil
—Development of ITER Central Solenoid Conductor Conduit Material—

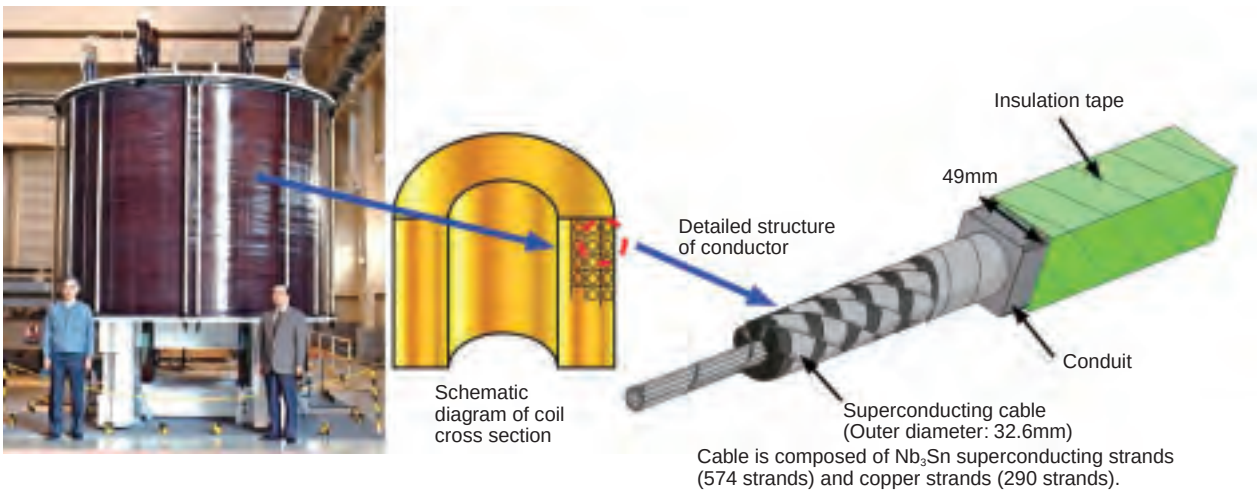

Fig.3-24 Model coil to demonstrate the "ITER" Central Solenoid (CS) (left), schematic diagram of coil cross section (center) and superconducting conductor cable unit (right)
The length of the conductor in the CS is about 900 m. The conductor is wound into a coil and then given heat treatment at 650 ℃ x 240 h in furnace to produce superconducting Nb_3Sn.

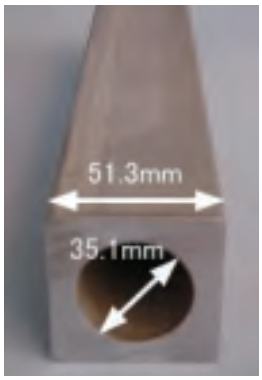

Fig.3-25 Photo of full size CS circle-in-square conduit made of improved JK2
In inspection, ITER requirement for size precision was satisfied. After insertion of superconducting cable into conduit, the conduit is compacted to 49 mm square.

We have developed a new stainless steel (SS) as a conduit material for the Central Solenoid (CS) conductor of "ITER" (Fig.3-24). Since a superconductor is brittle, it is required that niobium (Nb) and tin (Sn) are reacted to produce the superconductor Nb_3Sn by heat treatment (HT) at 650 ℃ × 240 h after forming the conductors into a coil shape. The conduit should have high strength and toughness, but the toughness of conventional SS deteriorates under HT. In addition, the CS should be compressed by the SS structure from top and bottom at room temperature to support large electromagnetic forces. Therefore, the conduit should have lower thermal contraction coefficient than that of the SS structure, so as not to relax compression forces due to shrinkage during cooling of CS.

JK2 steel, developed by JAEA, has suitable strength (0.2% yield strength: 1000 MPa) and thermal expansion coefficient (2/3 of conventional SS) to be used as a conduit, but improvement of toughness after HT was required.

One idea to solve this problem was to reduce the precipitation at grain boundaries generated during HT, by adding boron (B) and reducing nitrogen (N) and carbon (C). To verify this idea, a JK2 samples with changed chemical composition were produced and mechanical tests were performed at 4 K. It was found that fracture toughness was increased by a factor of 2 in JK2 samples which have low C (less than 0.03%), low N (less than 0.2%) and adding B (10-40ppm), meeting the "ITER" requirement. In the trial conduit fabrication, the obtained dimension accuracy satisfied the "ITER" requirement (Fig.3-25).

Reference

Hamada, K. et al., Optimization of JK2LB Chemical Component for ITER Central Solenoid Jacket Material, Teion Kogaku, vol.41, no.3, 2006, p.131-138 (in Japanese).

3-12 Compact Fusion Reactor Using Advanced Shield Materials
—Application of Hydrogen-Rich Hydride to the Shield of Fusion Reactor—

Table3-1 Hydrogen density of various materials
The anticipated hydrogen concentration of $Mg(BH_4)_2$, which is a new candidate shielding material, is as high as 1.32 x 10^{29} H-atoms/m^3, surpassing those of already known TiH_2 (9.1 x 10^{28} H-atoms/m^3), polyethylene and water.

Material	Appearance	Mass number	Density (10^3kg/m^3)	H density (10^{28}/m^3)
$Mg(BH_4)_2$	powder	53.99	1.48	13.2
TiH_2	powder	49.88	3.77	9.1
ZrH_2	powder	93.24	5.6	7.2
Polyethylene	Solid	14.03	0.90	7.7
H_2O	liquid	18.02	1.00	6.7

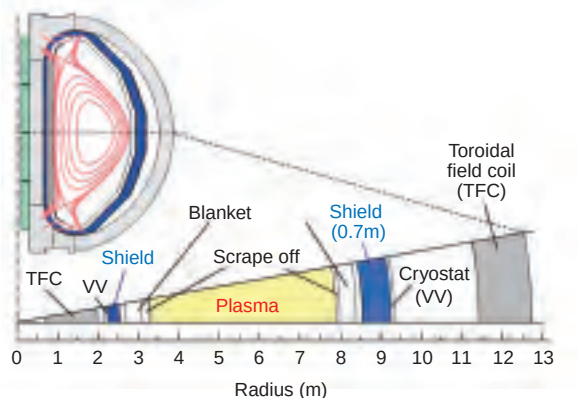

Fig.3-26 Cross section and 1-D calculation model of a low aspect ratio tokamak reactor
Neutron transport calculations of the 0.7 m-thick outboard shields were performed in order to evaluate the neutron shielding capability.

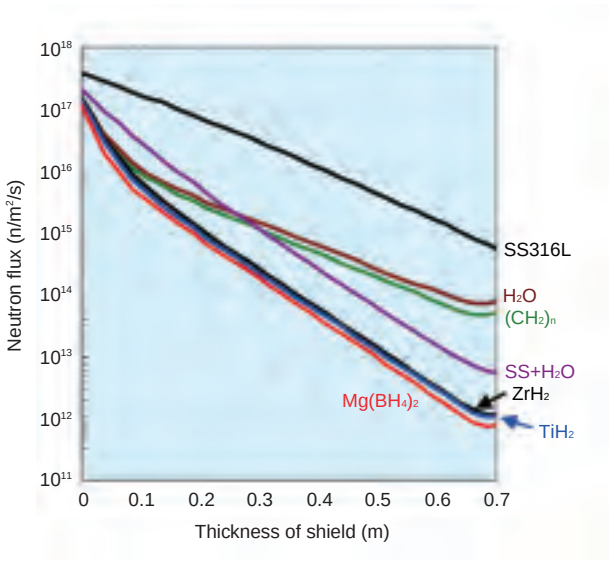

Fig.3-27 Attenuations of fast neutron fluxes in 0.7 m-thick shields made from various materials
The hydrogen-rich hydrides show superior neutron shielding capability compared to the conventional materials. Neutron transport calculations of the 0.7 m-thick outboard shields indicated that $Mg(BH_4)_2$, TiH_2 and ZrH_2 can reduce the thickness of the shield by 23%, 20% and 19%, respectively, compared to the combination of steel and water.

To demonstrate economical power generation with a compact reactor, the fusion DEMO studies at JAEA focus on a low aspect ratio (A) tokamak. It is important to reduce the nuclear heating caused by both neutron and gamma interactions in order to maintain the superconductive state of toroidal field coils (TFC); this is done with a compact neutron shield. Such an excellent shield also can be also used to protect outer structural materials from serious activation, and can lead to a dramatic reduction of radwaste.

This paper presents for the first time a new candidate neutron shielding material, magnesium borohydride ($Mg(BH_4)_2$), which is one of the most promising materials for storage of large amounts of hydrogen. Table3-1 gives several metal hydrides, borohydride and their properties. The anticipated hydrogen concentration of $Mg(BH_4)_2$ is as high as 13.2×10^{28} H-atoms/m^3. It is notable that some hydrides have considerably higher hydrogen content than polyethylene or water.

Neutronics calculations were carried out in order to assess the capability of $Mg(BH_4)_2$ and metal hydrides such as titanium hydride (TiH_2) and zirconium hydride (ZrH_2) which are candidates for the new shield material. Fig.3-26 shows the poloidal cross section and a 10° sector model of the low aspect ratio tokamak.

Fig.3-27 shows the calculated attenuation of fast neutron (E>0.1 MeV) flux in outboard shields made from various materials. The mixture of SS and H_2O consisting of 70% stainless steel SS316L and 30% water, which is presently one of the main shielding materials in fusion device design such as ITER, also was calculated. The thickness of a shield of $Mg(BH_4)_2$, TiH_2 and ZrH_2 can be respectively 23%, 20%, and 19% less than the combination of SS and water. Also, though the γ-ray shielding capability of only $Mg(BH_4)_2$ is low, mixing $Mg(BH_4)_2$ with steel significantly improves gamma-ray shielding.

The hydrogen-rich hydrides exhibit superior neutron shielding capability. Neutron transport calculations of the 0.7 m-thick outboard shields indicate that some hydrides allow the shield to be more than 20% thinner than the combination of SS and water.

Reference

Hayashi, T. et al., Neutronics Assessment of Advanced Shield Materials using Metal Hydride and Borohydride for Fusion Reactors, Fusion Engineering and Design, vol.81, 2006, p.1285-1290.

3-13 Measurement of Hydrogen Depth Profile Using Fast Neutrons
—Materials Analysis with Deuterium and Tritium Fusion Neutrons—

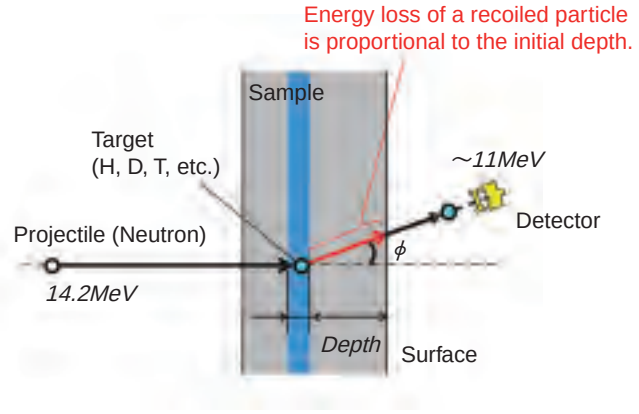

Fig.3-28 Principle of neutron elastic recoil detection analysis
Depth profile of target particles in a sample is estimated from the measured energy spectrum of recoil particles, i.e. target particles elastically scattered by incident neutrons. Since the energy loss of a recoil particle is proportional to the initial depth of that particle, the depth and atomic density can be calculated from the detection energy and yield of recoil particles, respectively.

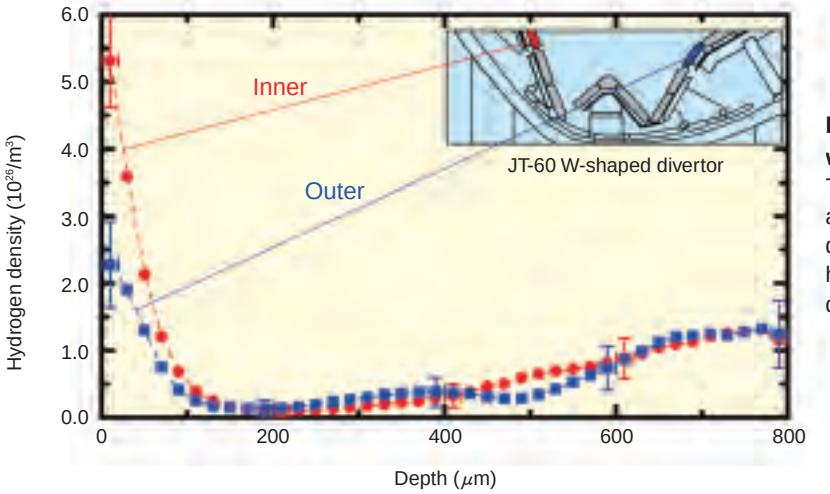

Fig.3-29 Hydrogen depth profile of JT-60 from wall into the plasma
The PFC samples were prepared from the inner and outer baffle plates placed at the W-shaped divertor region in JT-60. We could measure hydrogen profiles from the wall surface to 800 μm deep.

The surface of plasma-facing components (PFC) is eroded due to plasma-surface interaction in fusion devices. The dusts generated redeposits on the surface and forms layers of more than 100 μm thickness in some areas. Since the redeposited layers contain hydrogen isotopes such as fuel deuterium (D) and tritium (T), their retention must be estimated for the design of plasma control, the safe management of tritium inventory, etc. Conventional analytical methods enable measurements of hydrogen isotope retention on PFC surfaces, but begin to have difficulty measuring in the depth range of 100～1000 μm.

We have developed Neutron Elastic Recoil Detection Analysis (NERDA) using a 14 MeV fast neutron beam produced by D + T fusion reaction to measure hydrogen isotopes in these deeper regions. This method is essentially based on the conventional elastic recoil detection analysis with an ion beam, which utilizes the elastic scattering between a projectile and target. In addition, the electrical neutrality of neutrons allows beam-induced degradation of hydrogen isotopes to be minimized because kinetic energy of neutron transfers to the substrate by nuclear interaction only, not by electronic interaction.

In the experiment, the energy spectrum of recoil charged particles from a sample irradiated by a neutron beam from the DT fusion neutron source is recorded. A response function including charged-particle transport in the sample and geometrical configuration of the experimental setup is calculated by a Monte Carlo method. A depth profile is computed from the spectrum numerically processed with this response function (Fig.3-28).

Hydrogen depth profiles of inner and outer baffle plates exposed to DD plasma in "JT-60" were measured as an application of NERDA. We could measure the profiles from the surface to 800 μm (Fig.3-29). It is found that hydrogen is denser in the region of more than 200 μm depth.

In future, we will apply NERDA to measurements of deuterium and tritium depth profiles for analysis of fusion reactor materials.

Reference

Kubota, N. et al., Ion and Neutron Beam Analyses of Hydrogen Isotopes, Fusion Engineering and Design, vol.81, Issues 1-7, 2006, p.227-231.

3-14 Accelerator Development for International Fusion Materials Irradiation Facility(IFMIF)

— A Key to Strong, Steady Beam Acceleration is Precise Radio-Frequency Property Adjustment —

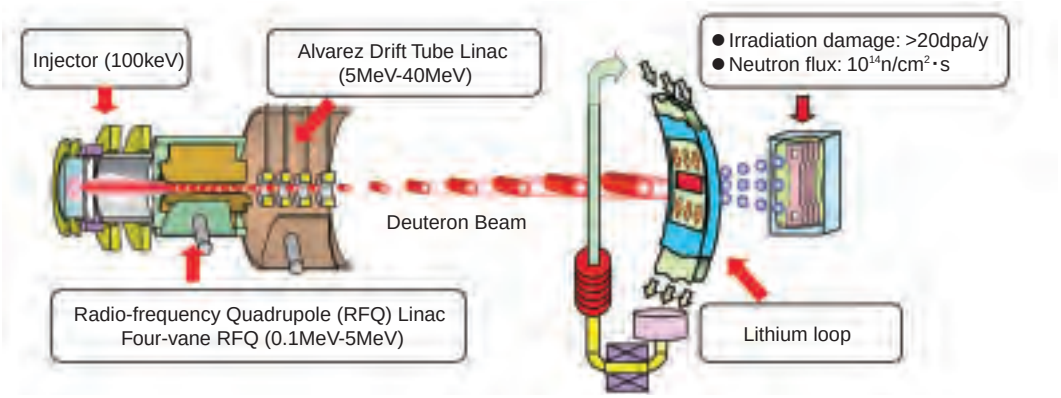

Fig.3-30 Configuration of International Fusion Materials Irradiation Facility (IFMIF)
A 40MeV deuteron beam with a current of 250mA is injected into liquid lithium flow, and a 14MeV neutron field similar to D-T fusion reactor is produced by D-Li stripping reaction. With these neutrons, materials are irradiated to evaluate robustness for use in fusion reactors.

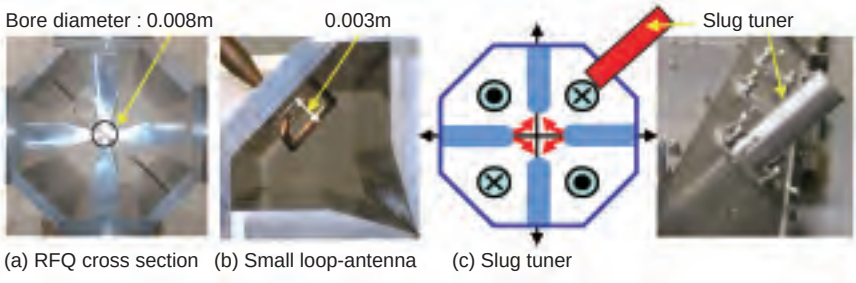

Fig.3-31 Photographs of RFQ mock-up modules
(a) Actual size cross section of 175MHz RFQ mock-up module, length and breadth 0.35m x 0.35m, (b) a small loop antenna to attain phase differences of less than a few degrees for the RFQ operation mode, (c) A slug tuner to control precisely the RF power-balance in the RFQ cavities.

For the development of a demonstration fusion reactor, an evaluation of feasibility of fusion reactor materials using 14MeV neutron irradiation is indispensable. For this purpose, the International Fusion Materials Irradiation Facility (IFMIF) is being jointly planned by Japan, the European Union, the United States and the Russian Federation under the auspices of the IEA (International Energy Agency). In IFMIF, a neutron field is produced by the deuteron (d)-lithium(Li) stripping reaction. The realization of a deuteron beam that can be accelerated and injected into liquid lithium, is a key issue (Fig.3-30). In this accelerator facility, two beam lines of 125mA are used. CW operation is also required, making this the world's first attempt at developing such a high-current beam CW linac.

One beam line consists of an ion injector, an Radio-Frequency Quadrupole (RFQ) Linac and a Drift Tube Linac (DTL), their output energies are designed to be 0.1, 5.0 and 40.0 MeV, respectively. We developed a new RFQ, since the RFQ had many technical issues to be overcome for the realization of the high-current and CW operation in this configuration.

In this RFQ design, a lower operation frequency of 175MHz is used to accelerate to the high-current of 125mA. By this frequency, a world record 12.5m-long RFQ is needed, and extremely precise control of RF properties (RF power-balance and phase difference among all cavities) is required.

In this study, RF properties using a real size RFQ mock-up module (Fig.3-31) are evaluated to establish the precise control of RF properties. Specially, an important key element technology is a loop antenna to inject RF power into the RFQ. Deteriorations of phase differences caused by inserting the antenna are analyzed by a 3-D simulation code to determine the specifications of the antenna. The deterioration could be suppressed to less than a few degrees by suitably arranging four small loop antennas in the RFQ quadrants. The power-balance can be controlled and withstanding voltage can be also moderated, which is indispensable for CW operation. Additionally, slug tuners are fabricated to maintain the power-balance, compensating for fabrication errors of the 12.5m-long RFQ and positioning errors of the multi-loop antenna, and thus a key technology for power-balance control has been established. With these results, there are prospects for a development of the world's first 175MHz RFQ prototype with extremely precise control of RF properties.

Reference

Maebara S. et al., Power-balance Control by Slug Tuner for the 175MHz Radio-Frequency Quadrupole (RFQ) Linac in IFMIF Project, Fusion Science and Technology, vol.47, 2005, p.941-945.

3-15 R&D of New Detritiation System Using Bacteria
—Incubating Tritium Oxidizing Bacteria from the Forest Soil—

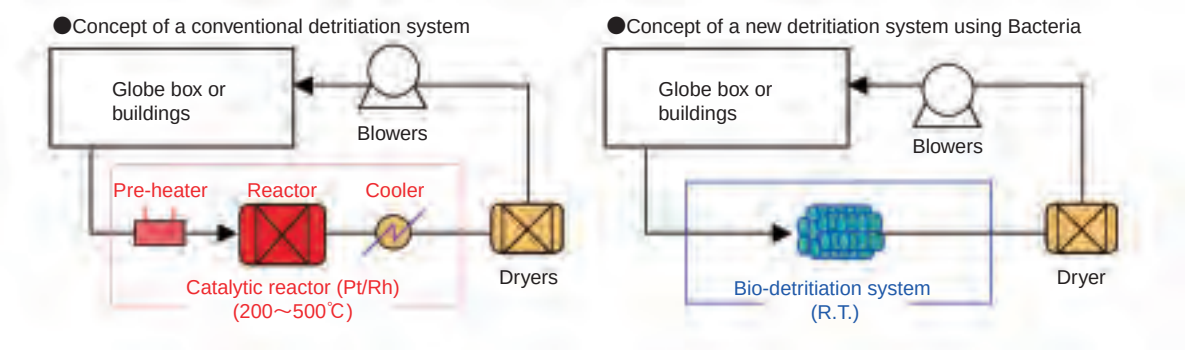

Fig.3-32 Comparison of detritiation system concept using catalyst and bacteria
The conventional system requires catalytic reactor to always be at high temperature, so capital & operation cost is high, and the replaced catalyst becomes tritiated waste. The new system can be operated at room temperature. The bio-reactor cost will be about 1/10 that of the catalyst set. Bio-reactor can be burnt for waste minimization.

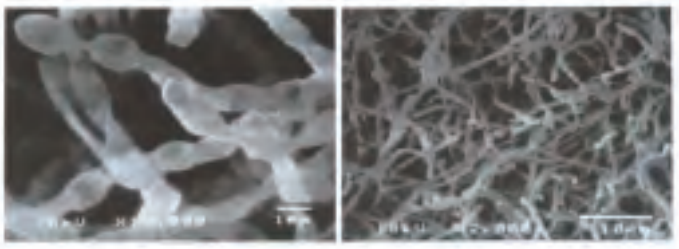

Fig.3-33 Typical tritium oxidizing bacteria (by SEM)
Left:x 10000, Right:x 2000 (*Kitazatospora*)

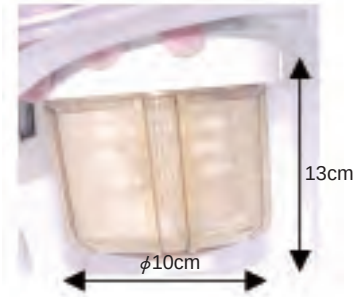

Fig.3-34 Bio-reactor for detritiation
The bacteria was incubated under 307K for 10 days on a filter in the reactor cassette.

A fusion reactor uses deuterium and tritium (^{3}H) as a fuel. ^{3}H is a radioisotope, emits a weak β-ray, and decays to ^{3}He with a half-life of 12.3 years. It can be handled safely in a multiple confinement system, because it has characteristics similar to hydrogen. In fusion facilities like "ITER", the confinement functioning is always checked. Also, even if some ^{3}H leaks into the buildings, that ^{3}H is oxidized by a high temperature catalytic reactor and the tritiated water vapor is recovered by a dryer, in order to avoid ^{3}H release to the environment as much as possible. This conventional detritiation system has been used extensively, but it requires keeping an expensive catalyst bed at high temperature (Fig.3-32). Therefore, R&D has been continuing at JAEA to develop a more efficient system. In this study, we took notice of research at Ibaraki Univ. (Prof. Ichimasa et al.), in which the almost all the hydrogen in an environment was oxidized by ordinary bacteria in the soil at room temperature. Recently, for the first time in the world, we succeeded in efficient atmosphere detritiation using bacteria which can be an alternative detritiation technology.

Traditionally, bacteria have been used extensively for fermentation in food, and medical products industries, but here we investigated the original idea that the special function of bacteria can be used for fast oxidation of hydrogen in atmosphere. We succeeded in finding and incubating bacteria with high ^{3}H oxidation ability from the forest soil (Fig.3-33), and identifying the conditions making this bacteria active. Using this bacteria, a bio-reactor was fabricated (Fig.3-34), and tested it by connecting it to the Caisson Assembly for Tritium safety Study (CATS). We developed a bio-reactor that could oxidize atmospheric ^{3}H in the same way as the catalytic reactor, with a detritiation factor of more than 85%. The ITER requirement of 99% should be attainable using multiple bio-reactor connection series. Further, the bacteria maintained about 70% of their ^{3}H oxidation activity even after one year storage under 4 ℃. From the above accomplishments, we see a good possibility that the bio-reactor can be used for an alternative detritiation system. If this technology is used, a high temperature catalytic reactor would not be required, and the fabrication & operation cost and waste volume would be decreased. For the future practical use of bio-reactors, we will investigate their long-term performance, and also attempt using bacteria for processing of gas other than tritium.

Reference

Ichimasa, M. et al., Tritium Elimination System Using Tritium Gas Oxidizing Bacteria, Fusion Science and Technology, vol.48, 2005, p.759-762.

4 Quantum Beam Science Research

4-1 Pioneering R&D of Quantum Beam Technology

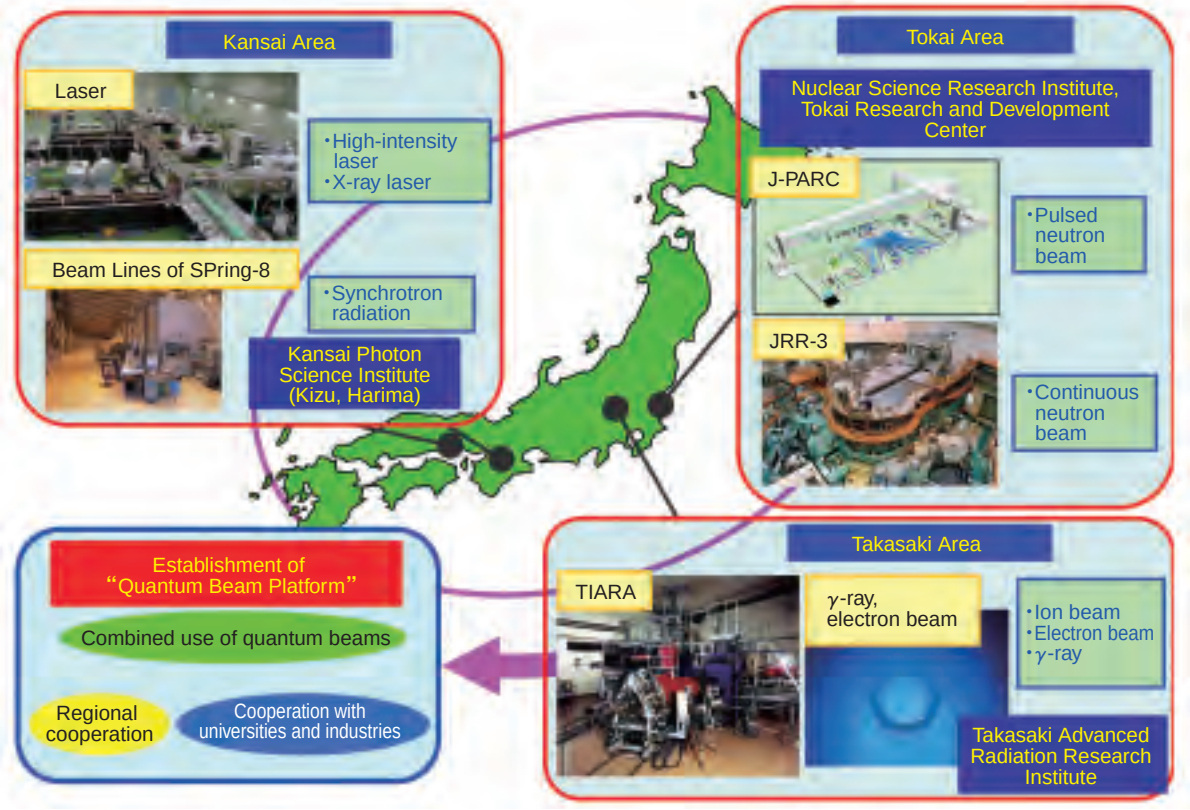

Fig.4-1 Quantum beam facilities in JAEA
J-PARC: Japan Proton Accelerator Research Complex (scheduled to start operation in FY2008; the Material and Life Science Facility of J-PARC is drawn in the figure.), JRR-3: Japan Research Reactor No.3, TIARA: Takasaki Ion Accelerators for Advanced Radiation Application, SPring-8: Super Photon ring 8 GeV.

We are carrying out research and development of "Quantum Beam Technology" utilizing the intrinsic characteristics of neutrons from reactors, ion particles and electrons from accelerators, γ-rays from radioisotopes, intense ultra-short pulsed lasers from table-top high power laser equipment and synchrotron radiation from SPring-8 (Fig.4-1).

These quantum beams have wave-particle duality. As waves, the wavelengths of these quanta are a nano-meter or less, depending on the beam energy. Consequently, one quantum acts on a part of matter of similar size at one time. Since the distance between an atom and the neighboring one in matter is also a nano-meter or less, the quantum beams make it possible to observe atomic arrangement and electronic state, and to identify elements in matter. They can also be used for ultra-fine manufacturing and special chemical reaction initiation, by cutting the bond between atoms i.e. molecular chain scission (Fig.4-2).

Hence the quantum beams become a powerful tool to "observe" with "nano eyes" and "create" with "nano hands". By making full use of the quantum beams' characteristics, we have been promoting research and development focusing on key issues: 'life sciences', 'information and communication technology', 'environmental sciences' and 'nanotechnology

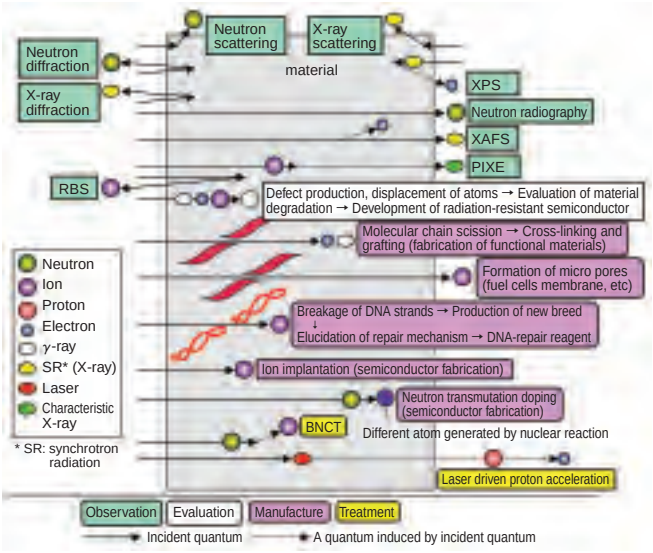

Fig.4-2 Interactions between quantum beam and material, and their applications
The figure shows how the various interactions of quantum beam and material are applied as tools for the R&D activities at JAEA (RBS: Rutherford Backscattering Spectrometry, XPS: X-ray Photoelectron Spectroscopy, PIXE: Particle Induced X-Ray Emission, XAFS: X-ray Absorption Fine Structure, BNCT: Boron Neutron Capture Therapy).

and materials' in 'Four Priority Fields to be Promoted', and 'energy' in 'Four Fields to be Promoted', as described in 'The 3rd Science and Technology Basic Plan' (Fig.4-3).

In addition to the above areas, proton and heavy particle irradiation have been developed as a cancer therapy 'without scalpel' in Japan. We have carried out fundamental research starting from the fact that protons can be accelerated by the localized huge electric field induced by an intense ultra-short pulsed laser bombardment onto material. The application of this technique is expected to reduce the size and the cost of the medical treatment machines (Fig.4-2, Fig.4-3).

Among the above quantum beams, expectations for the intense pulsed beams of neutrons in particular have grown, stimulating the construction of new facilities worldwide. We have been constructing "J-PARC", the Japan Proton Accelerator Research Complex in cooperation with the High Energy Accelerator Research Organization, aiming at the commencement of operation in fiscal 2008, and has been producing neutron experiment equipment used at "J-PARC" (Fig.4-4). The facilities are expected to produce neutrons and other secondary particles of very high intensities leading the world, by proton bombardment onto a target. The objective of this project is the utilization of these particles for a variety of areas in science and technology from materials science, life science and particle physics to industrial applications. The completion of the facilities will open new prospects for advanced applications of quantum beams like neutrons.

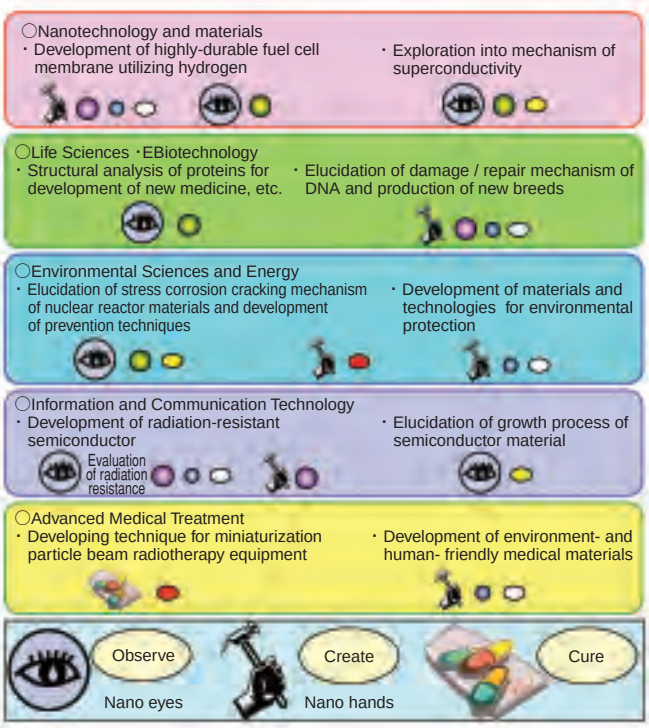

Fig.4-3 Contribution of quantum beam technology to "prioritized" areas
Under the R&D items in each area are shown which of the three quantum functions (to "observe", "create" and "cure") are exploited and which quantum beams are utilized. The quantum symbols are the same as shown in Fig.4-2

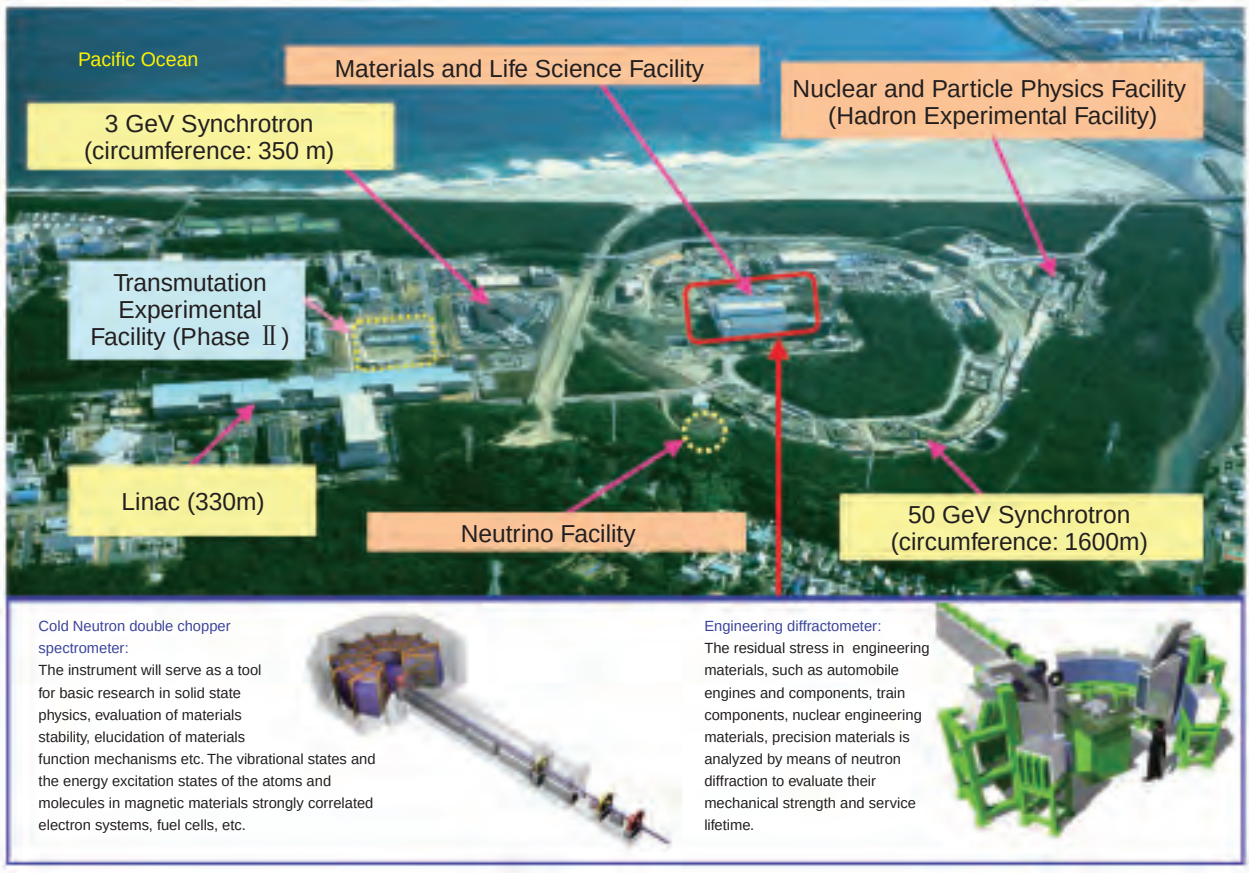

Fig.4-4 Aerial view of J-PARC under construction and schematics of two experimental instruments to be established at the Material and Life Science Facility

4-2 Hydrogen Separation by Nano Hole Ceramics

— Development of Heat and Corrosion Resistant Hydrogen Separation Silicon Carbide Based Membrane —

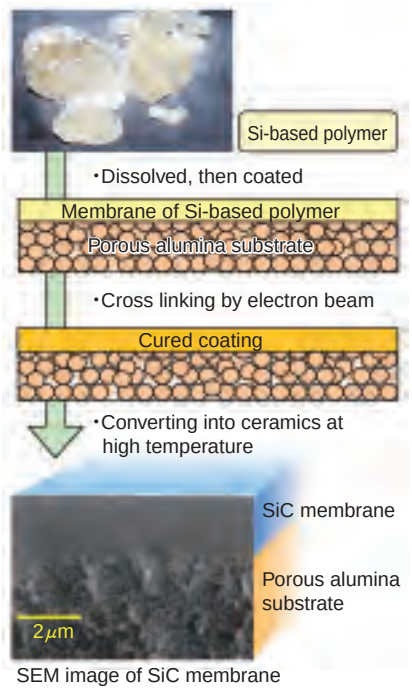

Fig.4-5 Fabrication process of silicon carbide (SiC) membrane
The Si-based polymer is coated on the porous alumina substrate and cross linked by electron beam irradiation, which prevents melting during further heat treatment. Afterwards, it is converted into SiC ceramic by pyrolysis at high temperature in inert gas.

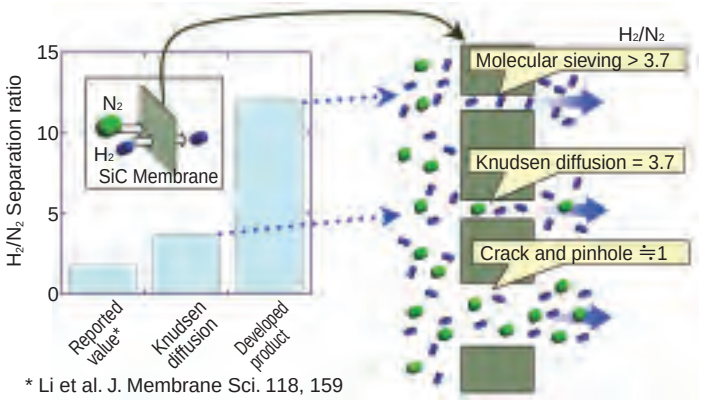

Fig.4-6 Gas separation ratio and separation mechanism of the SiC membrane
The gas separation ratio was measured by comparing the penetration amount of hydrogen (H_2) with that of nitrogen (N_2). The hydrogen separation, $H_2/N_2 > 3.7$, by the molecular sieving mechanism was confirmed.

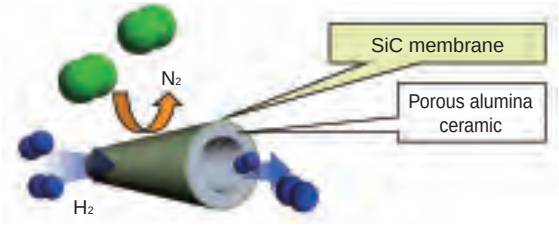

Fig.4-7 Tubular hydrogen separation membrane with SiC coating
Faster permeation sought by bundling many tube filters for large surface area.

To develop into a society that doesn't exhaust greenhouse effect gases, we are researching and developing the hydrogen fuel cell and a new thermo chemical process of hydrogen production using nuclear energy. For the fuel cell, removal of impurities from hydrogen is necessary. In the latter process, hydrogen is separated in a strong acid at over 500℃, and therefore the separation membrane material should have heat and corrosion resistance, stable for several thousand hours. Ceramics materials are the best for such applications.

JAEA succeeded in the development of silicon carbide (SiC) ceramic fiber that has high strength and heat resistance over 1700℃, by the method of converting Si-based polymer fiber to ceramics by firing after electron beam irradiation for cross linking, which prevents melting. Further, we found that there is amorphous area in that SiC ceramics, with an atomic network in which nano-holes are formed. The Knudsen diffusion mechanism controls separation of gases when both the smaller and the bigger gas molecules can penetrate through the nano hole membrane. In such case, H_2/N_2 separation ratio is 3.7. On the other hand, it is possible to reduce the diameter of nano holes to the size that promotes permeation of only hydrogen having the smaller molecules. This hydrogen separation membrane that functions based on the molecular sieve mechanism has high separation ratio.

Now, we are advancing the development of the SiC membrane by the fabrication process shown in Fig.4-5. In this method, it was difficult to decrease the crack formation because of the volume of Si-based polymer shrank over 50% during conversion of Si-based polymer into ceramics by firing. The volume shrinkage was reduced by electron beam crosslinking which increases the ceramic conversion rate. In addition, the formation of pinholes was lowered by mixing two kinds of Si-based polymer, to improves precursor fluidity.

Fig.4-6 shows the separation mechanism of hydrogen and nitrogen by the SiC membrane made by this method. The separation ratio of the SiC membrane developed in this research is larger than that fabricated by thermal oxidation and the theoretical value of perm-selectivity controlled by the Knudsen diffusion mechanism. In the future, we plan to improve hydrogen permeability by increasing the number of nano holes of the optimal size and the development of the cylindrical SiC membranes to produce the tilter module as shown in Fig.4-7.

Reference

Wach, R.A., Sugimoto, M. et al., Development of Silicon Carbide Coating on Al_2O_3 Ceramics from Precursor Polymers by Radiation Curing, Key Engineering Materials, vol.317, 2006, p.573-576.

4-3 Development of New Monitoring Technology for the Utilization of Hydrogen as a Clean Energy Source
—Optical Hydrogen Sensors Using Gasochromic Phenomenon—

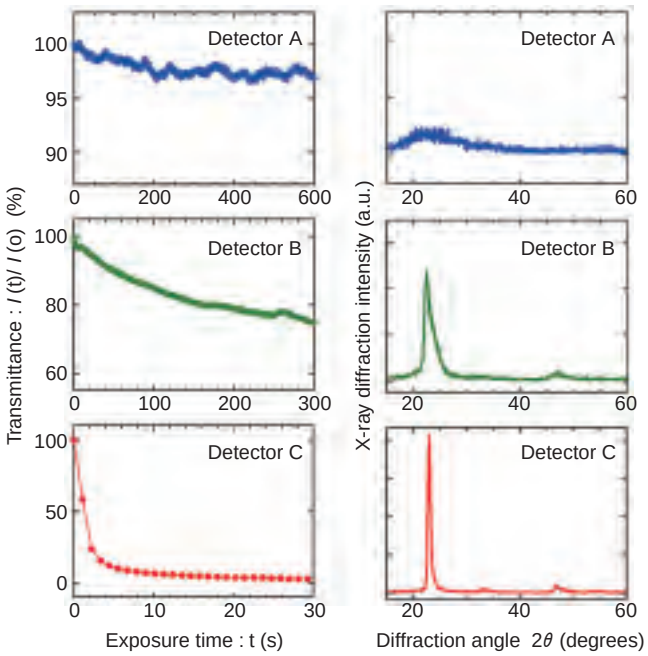

Fig.4-8 Response for hydrogen and structure of the tungsten oxide in the detectors
The transmittance of 630 nm light in the detector decreases with time, during the exposure of 1 % hydrogen. The response in Detector A is slow, but that in Detector C is fast. The tungsten oxide in Detector A has an amorphous pattern, and those in Detector B and C have X-ray diffraction peaks. The crystal of the tungsten oxide in Detector C orients to the (001) monoclinic plane.

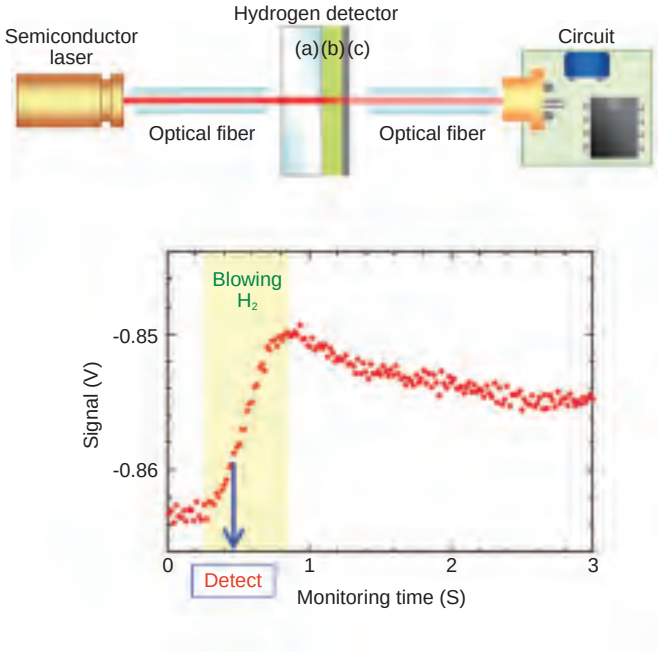

Fig.4-9 Developed optical hydrogen sensor
The detector consists of (a) quartz glass substrate, (b) oriented tungsten oxide film, and (c) palladium coating. The intensity of 650 nm light transmitted from the detector is converted into a voltage signal by the circuit at the end of the optical fiber. Received signals when 1 % hydrogen is blow on the detector are shown. Hydrogen can be recognized from a received signal which is more than double intensity of the noise width.

The concentration of lower explosive limit (LEL) in hydrogen (H_2) is 4 vol.% at room temperature in ambient air. Therefore, the development of technology to detect a leak of H_2 with low cost, but reliably and safely, is required for the production, the storage, the transport, and the use of H_2. Optical hydrogen sensors without an electric current and a heating in the detector have been proposed as safer and cheaper sensors. The detector consists of transparent substrate, a coloration layer of tungsten oxide thin film, and catalyst layer of palladium. Leakage of H_2 is detected by decrease in the intensity of transmitted light from the detector, using the gasochromic phenomenon that tungsten oxide changes color from yellow to blue when it adsorbs H_2 catalyzed by palladium. The detection time is required to be the less than 1 second in the standard which is proposed by U.S. Department of Energy (DOE). But the coloration rate of tungsten oxide for H_2 is usually slow, on the order of minutes. In this study, the tungsten oxide thin films with rapid coloration rate were investigated. It was found that the response in the detector using oriented crystal tungsten oxide is faster, as shown in Fig.4-8. A sensor was constructed with the detector inserted between conventional optical fibers. It was verified that the sensor can detect 1 % H_2 in ambient air within 1 second, as shown in Fig.4-9. Using the optical fiber networks, the sensor can be applied to a centralized monitoring system for large pipe layouts or complex plants of production and storages.

Reference

Takano, K. et al., High Sensitive Gasochromic Hydrogen Sensors using Tungsten Oxide Thin Films, Transaction of the Material Research Society of Japan, vol.31, no.1, 2006, p.223-226.

4-4 Novel Technique for Characterization of Chemical Modification of Internal Surface of Nano-Pores
—Fabrication of Functional Polymer Materials Using Ion Beams—

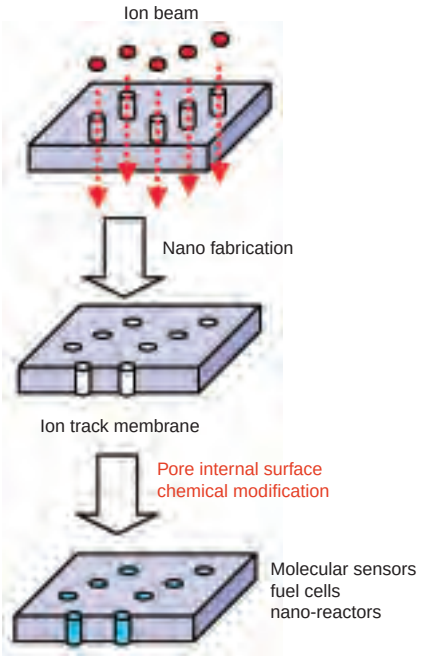

Fig.4-10 Creation of functional thin films using the chemical modification of the internal surfaces of nano-pores in ion track membranes
By using ion beams, ion track membranes with size controlled nano-pores can be prepared. Characteristics of the internal surfaces of the nano-pores can be controlled by chemical modification, resulting in nano-layers for molecular recognition, electrolytes, or catalysts. These membranes can be applied to molecular sensors, fuel cells, and nano-reactors.

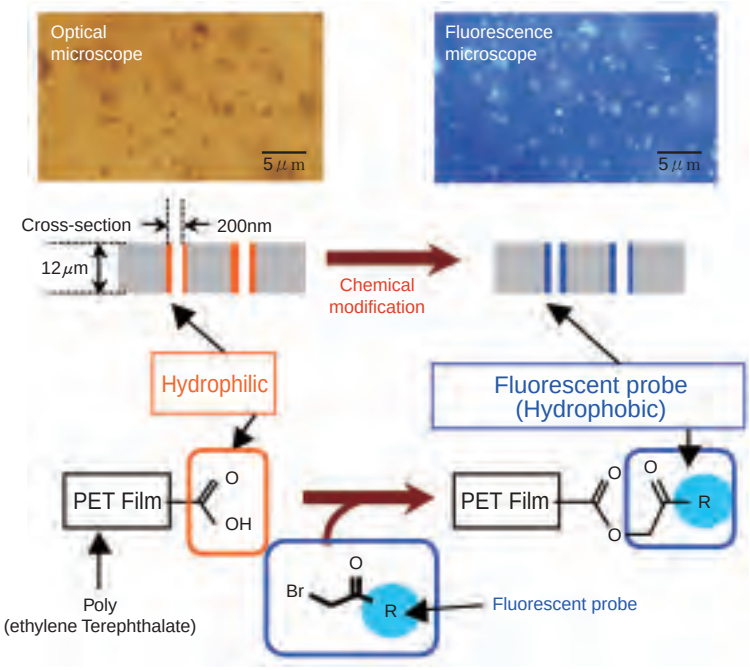

Fig.4-11 Direct observation of internal surfaces of nano-pores using fluorescent probes
By attaching fluorescent probes to the hydrophilic groups on the internal surfaces of pores in ion track membranes consisting of poly (ethylene terephthalate) (PET), internal pore surfaces can be changed from hydrophilic to hydrophobic. The process of the chemical modification can be directly characterized by emission from pore internal surface using a fluorescence microscope.

When polymer membranes are irradiated by swift ion beams, ion track membranes with size controlled nano-pores can be prepared (Fig.4-10). By development of modification techniques of chemical structures and surface properties of the nano-pores (pore internal surface chemical modification), electrolyte layers necessary for fuel cells can be prepared. However, until now the chemical modification of the internal surfaces could not be practically controlled because there was no method to observe the internal pore surfaces. Here, we noticed that hydrophilic internal pore surfaces are subject to the alkylation reaction. Using alkylation reagents with fluorescent probes, the extent of chemical modification can be observed by the emission from the probes at pore internal surfaces. Thus, this method should allow a direct observation of the condition of pore internal surfaces.

We prepared the ion track membranes of poly(ethylene terephthalate) (PET) by ion irradiation followed by chemical etching in an alkaline solution. By introducing the solution of alkylation reagent having fluorescent probes into the pores with 200 nm in diameter in the PET, the hydrophilic internal pore surfaces can be modified chemically to a hydrophobic character. The probe emissions can be observed in the fluorescence microscope image of the membranes, from which the positions of the pores can be located; Emissions from the ion track membranes could not be observed before alkylation reactions (Fig.4-11). Furthermore, the emission and excitation intensities of the membranes increased proportionally with increases of the pore surface areas. Thus, we can make semi-quantitative estimation of the degree of chemical modification of the pore internal surfaces.

Accordingly, by adding the fluorescent probes to the alkylation reagents, a direct observation method can be established to estimate the extent of the chemical modification of the internal pore surface of ion track membranes. This method should be of use in the efficient creation of nano-layers for molecular recognition, electrolytic and catalytic properties; these materials are key component for molecular sensors, fuel cells, and nano-reactors.

Reference

Maekawa, Y. et al., Chemical Modification of the Internal Surfaces of Cylindrical Pores of Sub-micrometer Size in Poly(ethylene terephthalate), Langmuir, vol.22, 2006, p.2832-2837.

4-5 Confirming Cost Estimations of Uranium Collection from Seawater
—Assessing High Function Metal Collectors for Seawater Uranium—

Fig.4-12 Preparing braided adsorbent for mooring on sea bottom
Polyethylene fiber is given a chemical structure of high affinity to uranium in seawater by radiation - induced graft polymerization. Adsorbent is formed into a lace by twisting the resulting polyethylene fibers. The braided adsorbent can be lifted from the sea bottom and moored, since floats are incorporated in it. The braid type adsorbent was pulled up after soaking in seawater for 60 days. The adsorbed uranium on the adsorbent was collected by elution with acid solution.

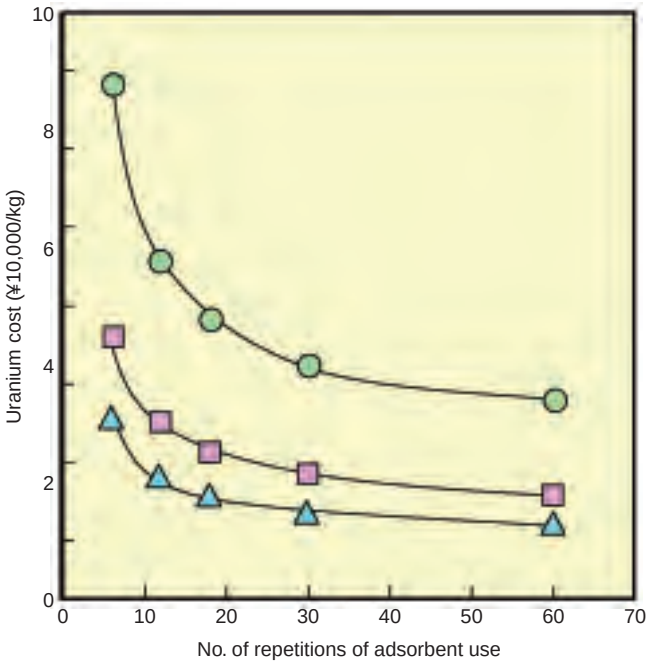

Fig.4-13 Effect of repeated usage of the braided adsorbent on the cost of uranium collection
(●) 2 g-U/kg-adsorbent and (■) 4 g-U/kg-adsorbent and (▲) 6 g-U/kg-adsorbent
Uranium cost means the price when uranium resources are collected from seawater using the braid type adsorbent.

All the necessary uranium fuel for power generation in Japan is imported, though nuclear power generation supplies 34% of the electric power in Japan. When the collection of uranium in seawater is commercialized, the energy security of our country would become stronger, and would allow extra time for the completion of an ideal nuclear fuel cycle system.

The total amount of uranium in seawater is 4.5 billion tons though the concentration is very low, 3.3 ppb (3.3mg-U in one ton of seawater). This total amount is 1000 times of all the underground uranium. Moreover, the annual amount of the uranium carried by the Black Current, flowing near Japan, is estimated at 5.2 million tons. When 0.2% of this uranium is collected, it would be enough for all the nuclear power generation in Japan.

The collection of uranium from seawater has been developed by JAEA. A pilot scale experiment in the sea revealed that a braided adsorbent was effective to achieve a reasonable cost for the uranium collection from seawater. The adsorption ability of the braided adsorbent (Fig.4-12) was evaluated in the sea area of Okinawa to obtain the necessary data for cost estimation. The collection cost of uranium from seawater was calculated at the present and the expected level of adsorbency (Fig.4-13). In this estimation, the annual scale of uranium collection was set to 1200 t/y which corresponds to the uranium amount consumed by six nuclear plants.

If 2g-U/kg-adsorbent is submerged for 60 days at a time and used 6 times, the uranium cost is calculated to be 88,000 yen/kg-U, including the cost of adsorbent production, uranium collection, and uranium purification. When 6g-U/kg-adsorbent and 20 repetitions or more becomes possible, the uranium cost reduces to 15,000 yen. This price level is equivalent to that of the highest cost of the minable uranium. The lowest cost attainable now is 25,000 yen with 4g-U/kg-adsorbent used in the sea area of Okinawa, with 18 repetitionuses. In this case, the initial investment to collect the uranium from seawater is 107.7 billion yen, which is 1/3 of the construction cost of a one million-kilowatt class nuclear power plant.

Reference

Tamada, M. et al., Cost Estimation of Uranium Recovery from Seawater with System of Braid Type Adsorbent, Nippon Geshiryoku Gakkai Wabun Ronbunshi, vol.5, no.4, 2006, p.358-363 (in Japanese).

4-6 Elucidation of the Gene Activation Mechanism and Application to Visualization of DNA Strand Breaks —DNA Repair Promoting Protein PprA—

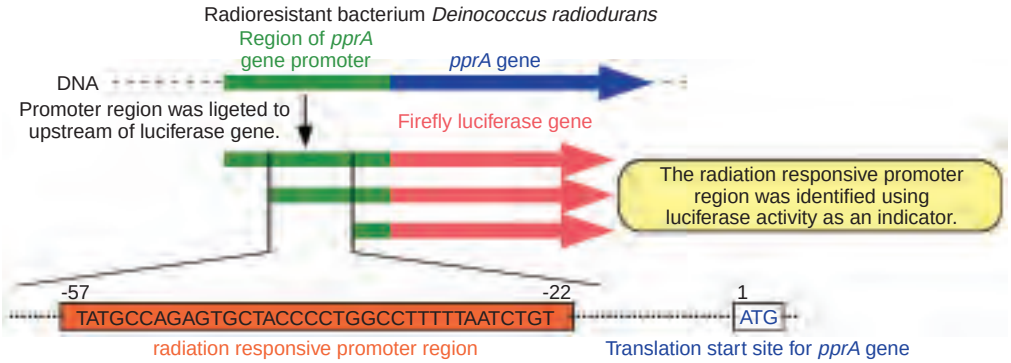

Fig.4-14 Identification of the radiation responsive promoter region of *pprA* gene
The promoter region of *pprA* gene was ligated upstream of firefly luciferase gene. The luciferase activity was monitored as an index of gene promoter activity. This result revealed that the radiation responsive promoter region was located between positions -57 and -22 from the start codon of the *pprA* gene.

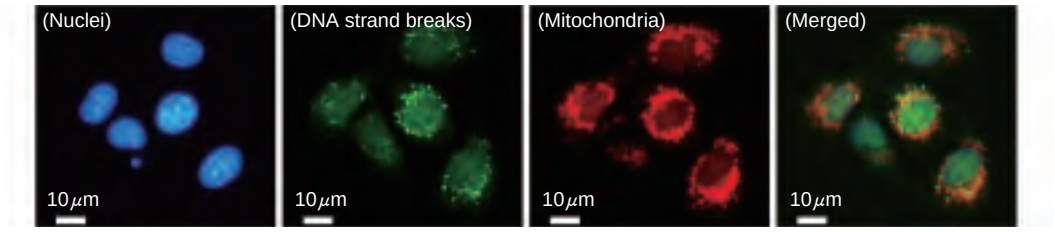

Fig.4-15 DNA strand breaks in mitochondria of mammalian cells following γ ray irradiation
Radiation-induced DNA strand breaks in mitochondria of mammalian cells were visualized by employing PprA protein using an immunofluorescence technique. Colocalization of fluorescence breaks and mitochondria was observed in the image merging the two (right panel). This image suggests that DNA strand breaks existing in mitochondria were effectively detected by utilizing DNA strand break binding ability of PprA protein.

Deinococcus radiodurans (*D. radiodurans*) possesses extraordinary resistance to ionizing radiation, which has been attributed to its highly proficient DNA repair capacity. We have identified the novel gene (*pprA* gene) from this bacterium, and revealed that the gene product (PprA protein) preferentially binds to DNA strand breaks and possesses DNA repair promoting activity. However, the radiation responsive DNA region (promoter) which is essential for the *pprA* gene expression has not been located. Moreover, though visualization of DNA damage utilizing the ability of PprA protein is promising, this detection technology has not been established.

To identify the radiation responsive promoter region, DNA fragments which may include the *pprA* gene promoter were ligated upstream of firefly luciferase gene. The luciferase activity was then monitored following γ irradiation as an index of gene promoter activity. It was revealed that the radiation responsive promoter region was located between positions -57 and -22 upstream from the *pprA* gene (Fig.4-14). Identification of the radiation responsive promoter is very useful finding to delineate the DNA repair network mechanism of *D. radiodurans*.

In mammalian cells that are sensitive to ionizing radiation, several DNA strand breaks result in cell death. Therefore, it is important to assess intracellular distribution and generative frequency of DNA strand breaks directly for the evaluation of radiation effect in mammalian cells. Certain DNA strand break visualization methods using proteins in mammalian cells associated with their own DNA repair have been developed. However, these methods have disadvantage that is difficult to detect initial DNA damage immediately following γ irradiation. To overcome this disadvantage, we developed a new detection method to visualize the initial DNA damage by utilizing the *D. radiodurans* PprA protein, which possesses an ability to bind to DNA strand breaks specifically. In this method, initial DNA damage can be visualized using fluorescence-labeled anti-PprA antibody bound to PprA protein (Fig.4-15). This detection method of DNA strand breaks with increased sensitivity will be useful in evaluating radiation effect in mammalian cells, and widely applicable to genotoxic tests in environmental and pharmaceutical fields.

Reference

Ohba, H. et al., The Radiation Responsive Promoter of the *Deinococcus radiodurans pprA* Gene, Gene, vol.363, no.9, 2005, p.133-141.
Satoh, K. et al., Method for Detecting DNA Strand Breaks in Mammalian Cells using the *Deinococcus radiodurans* PprA Protein, Mutation Research/Fundamental and Molecular Mechanisms of Mutagenesis, vol.596, no.1-2, 2006, p.36-42.

4-7 Plants Become More Tolerant to Ultraviolet (UV) Light by Increasing Nuclear DNA Content

—Discovery of Novel UV Resistance Mechanism in Plants—

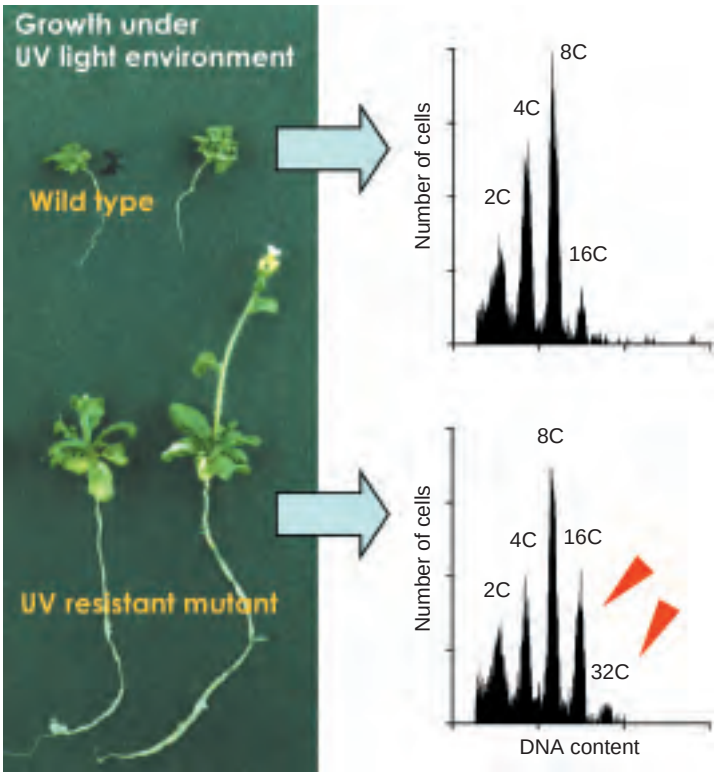

Fig.4-16 Growth of UV resistant mutant and the wildtype under UV light environment and their ploidy profiles
The UV resistant mutant has higher fraction of cells with higher nuclear DNA content (arrowhead). This suggests that increased gene copy number confers UV tolerance. 2C stands for diploid DNA content.

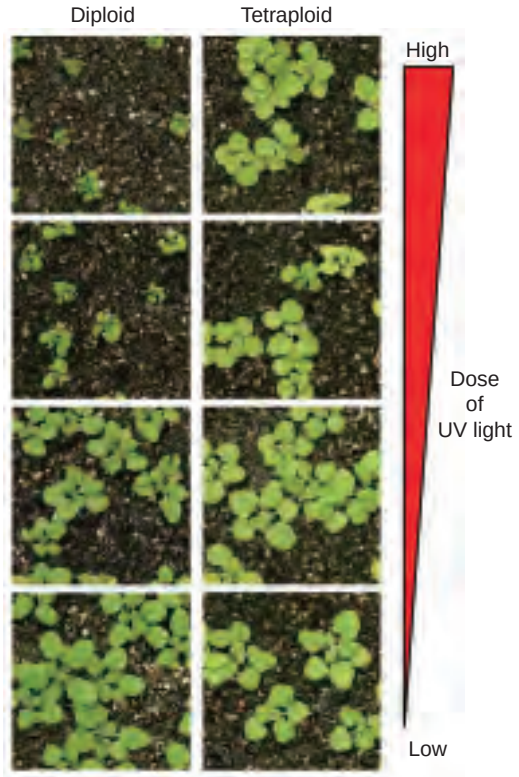

Fig.4-17 Comparison of UV sensitivity between diploid and tetraploid Arabidopsis
Tetraploid plants with double the DNA of the wild type (diploid) are hyper-resistant to UV light. This indicates that the DNA content is an important factor for UV tolerance.

Since plants utilize energy from sunlight, they are inevitably exposed to solar ultraviolet (UV) light. The UV light cause significant damages to plants, as seen in crop yield reduction and leaf burn. Furthermore, the UV light that we experience has increased due to the depletion of the ozone layer.

Plants possess various protective mechanisms to cope with UV light. UV absorbing compounds such as flavonoid pigment attenuate the damaging solar UV light. The UV light that is not shielded by the UV absorbing compounds induces DNA damage, predominantly pyrimidine dimers. The pyrimidine dimers are efficiently repaired by the repair enzyme photolyase. Previous studies have revealed various mechanisms for this, but we thought there might be other unidentified mechanisms protecting against UV light.

We succeeded in isolating Arabidopsis mutants that are hyper-resistant to UV light using ion beams as a mutagen. The fresh weight of the mutant plants grown under UV light was more than twice that of the wild-type plants (Fig.4-16). We found that the mutant had a mutation in the gene named *UVI4*. This mutation resulted in an increased nuclear DNA content in the leaf and stem cells (Fig.4-16). Therefore, it is thought that the increased gene copy number due to the increased DNA content confers UV tolerance. Supporting this idea, tetraploid plants that have double the nuclear DNA content of diploid plants are hyper-resistant to UV light (Fig.4-17).

From these results, we concluded that nuclear DNA content is an important factor in tolerance to solar UV light. These results will provide a clue to understand how plants adapt to UV light environments. This mechanism might be utilized in various plant species to increase the crop yield or to protect them from leaf burn.

Reference

Hase, Y. et al., A Mutation in the *uvi4* Gene Promotes Progression of Endo-Reduplication and Confers Increased Tolerance Towards Ultraviolet B Light, The Plant Journal, vol.46, no.2, 2006, p.317-326.

4-8 Elucidation of the Mechanism of Granulocytopenia Drug
—Tertiary Structure Analysis of Human GCSF with its Receptor—

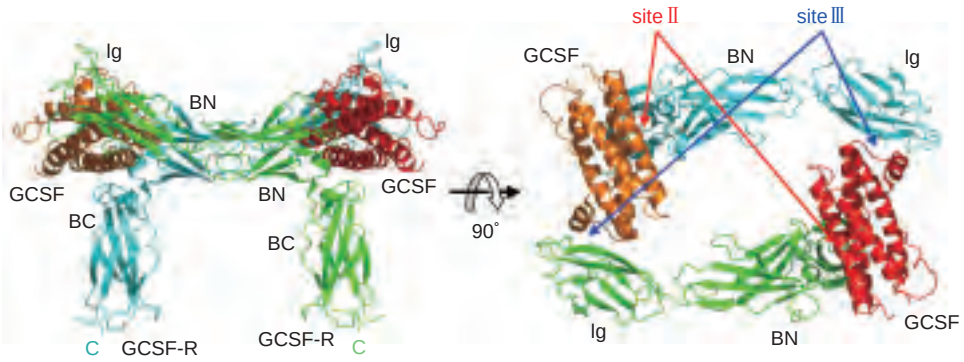

Fig.4-18 Overall structure of the signaling complex consisting of human GCSF and human GCSF-R
Left: side view. Right: top view. Two human GCSFs (red and orange) and two human GCSF-Rs (cyan and green) associate through the two binding sites (site Ⅱ and Ⅲ).

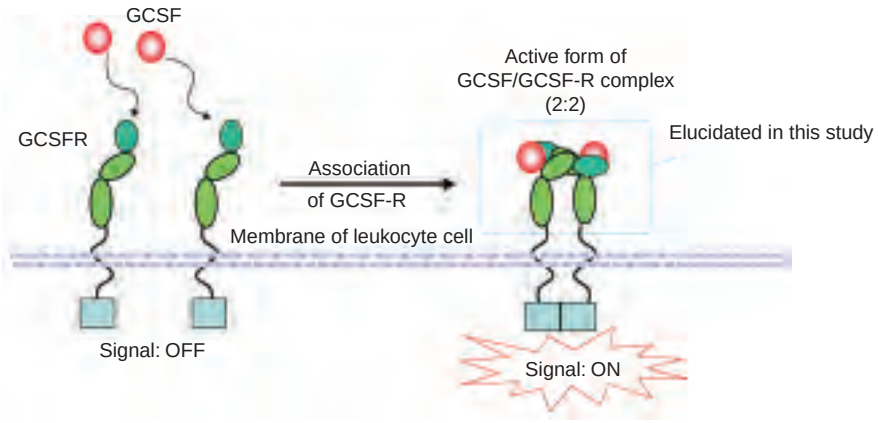

Fig.4-19 Activation mechanism of GCSF-R
Binding of GCSF to GCSF-R triggers association of GCSF-Rs with each other, resulting in activation of a signaling cascade for proliferation of leukocyte (granulocyte) cell.

The crystal structure of the signaling complex of human granulocyte colony-stimulating factor (hGCSF) and ligand binding region of hGCSF receptor (hGCSF-R) has been determined (Fig.4-18). The hGCSF is a glycoprotein consisting of about 180 amino acids, and is a cytokine for medical treatment of patients suffering from granulocytopenia which acts by causing the maturation proliferation, and differentiation of the precursor cells of neutrophilic granulocyte. Binding of hGCSF to the extracellular region of its receptor triggers receptor association, resulting in activation of a signaling cascade. Although hGCSF is an important protein not only for basic science but also for therapeutic use, the detailed activation mechanism of hGCSF-R has not been clarified.

We have already succeeded in preparation of the extracellular region of hGCSF-R, and demonstrated a 2:2 stoichiometry of the stable hGCSF/hGCSF-R complex in solution by thermodynamic analysis. Moreover, we have succeeded in crystallization of this sample and determined its tertiary structure by X-ray crystallography. The crystal structure revealed the atoms involved in the molecular positioning and recognition for the 2:2 complex; there is ligand-receptor interaction at two locations (site Ⅱ and Ⅲ) (Fig.4-18). Thus, the homodimerization of receptors by this 2:2 complex is elucidated to be an important feature for hGCSF-R activation (Fig.4-19).

This structural information may allow us to synthesize an agonist more efficiently. This study was cooperative research with Kirin Brewery and was partly supported as a Pilot Applied Research Project for the industrial use of space by Japan Space Utilization Promotion Center and Japan Aerospace Exploration Agency, and supported by the Protein 3000 Project and a Grant-in-Aid for Scientific Research (C) from Ministry of Education, Culture, Sports, Science and Technology, Japan.

Reference

Tamada, T. et al., Homodimeric Crossover Structure of the Human GCSF-Receptor Signaling Complex, Proceedings of the National Academy of Sciences of the United States of America, 103, 2006, p.3135-3140.

4-9 Observation of Electronic Structure Utilizing Synchrotron Radiation X-rays
—Electronic Excitations by Resonant Inelastic X-ray Scattering—

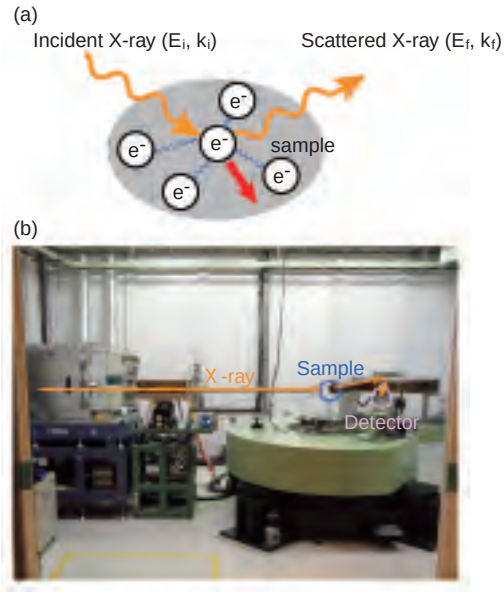

Fig.4-20
(a) Schematic diagram of inelastic X-ray scattering
One of the electrons interacting each other by strong Coulomb repulsion (blue lines) is scattered by X-rays.
(b) Spectrometer for inelastic X-ray scattering installed at BL11XU of SPring-8.

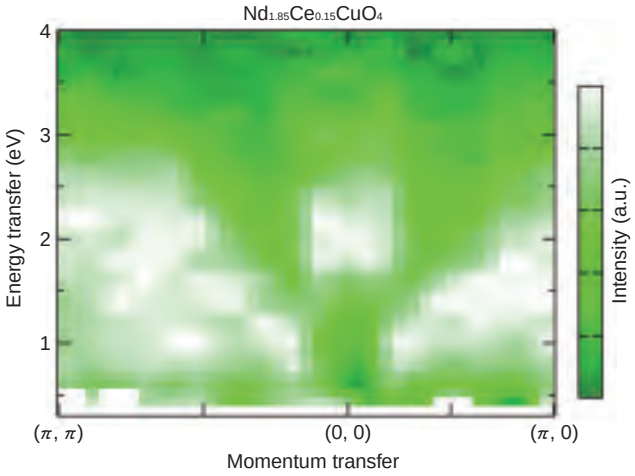

Fig.4-21 Resonant inelastic X-ray scattering spectra of $Nd_{1.85}Ce_{0.15}CuO_4$

One of the important tasks of materials science is to understand electronic properties of a material from the observation of its electronic structure, namely energy and momentum of the electrons. Resonant Inelastic X-ray scattering (RIXS) which has been developed recently utilizing brilliant synchrotron radiation X-rays enables us to measure momentum and energy of the electron simultaneously, which was impossible by conventional photon scattering and absorption methods. Fig.4-20(a) shows a schematic diagram of inelastic X-ray scattering. Energy transfer (E_i-E_f) and momentum transfer (k_i-k_f) during the scattering process reflects the character of the electron. We have installed a specially designed spectrometer for inelastic X-ray scattering at the JAEA beam line of "SPring-8" and have used it to measure electronic excitation spectra.

A target of our research is strongly correlated electron systems exhibiting phenomena such as superconductivity with high transition temperature and colossal magnetoresistance. Electrons in the system interact with each other by strong Coulomb repulsion which exceeds their kinetic energy. Investigation of the electronic structure of these systems is a starting point for the understanding of their properties and it is an important subject in recent condensed matter physics.

Fig.4-21 shows RIXS spectra of the superconducting cuprate $Nd_{1.85}Ce_{0.15}Cu_{O4}$. The 2-eV feature at momentum (0,0) is an excitation across the energy gap due to the strong Coulomb repulsion. On the other hand, shifts to higher energy with momentum transfer from (0,0) to (π,0) and (π,π) originate from the mobile electrons in the material. The latter excitation is closely related to the electronic properties and we found that its character agreed with theoretically calculated dynamical charge correlation function relating the energy and momentum between two electrons in the material. Though dynamical charge correlation function is an important and fundamental physical quantity, we have had no experimental method to measure it until now. Our result demonstrates that RIXS can be a tool to measure it and this is the first observation of the dynamical charge correlation function of strongly correlated electrons.

Reference

Ishii, K. et al., Momentum Dependence of Charge Excitations in the Electron-Doped Superconductor $Nd_{1.85}Ce_{0.15}CuO_4$: A Resonant Inelastic X-ray Scattering Study, Physical Review Letters, vol.94, no.20, 2005, p.207003-1-207003-4.

4-10 Residual Stress Measurement of Internal Materials Using Synchrotron Radiation
—Stress Analysis Technique with a New Strain Scanning Method—

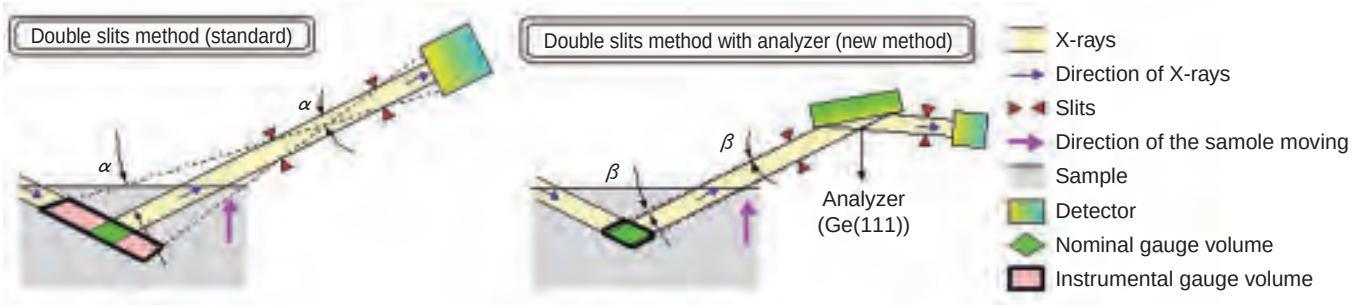

Fig.4-22 (Upper) Optics of strain scanning method
In the strain scanning method, the distribution of the strain or stress beneath the surface can be determined by scanning the gauge volume in the depth direction of the specimen. In the standard method, the instrumental gauge volume is much larger than the nominal gauge volume and the measurement error is large. On the other hand, in the new method, the instrumental gauge volume is equal to the nominal gauge volume and the measurement error is much less.

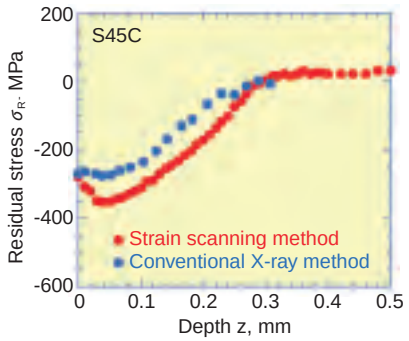

Fig.4-23 (Left) Distribution of residual stress measured by new type strain scanning method
The red circles indicate the in-plane residual stress at each depth of S45C (steel with 0.45% carbon) which was shot-peened to introduce a compressive residual stress in the surface layer. The blue circles indicate the out-of-plane residual stress obtained in our previous study, where the surface layer of the shot-peened specimen was removed successively by electropolishing and the stress measurement by the $\sin^2\psi$ method using Cr-Kα radiation was repeated. The strain scanning method is a useful alternative to the conventional X-ray method because the stress distribution below the surface is obtained non-invasively and in a short time with the same accuracy.

To guarantee the reliability of structural component service, a non-destructive method is required to determine a precise distribution of the residual stress in materials. A strain scanning method based on X-ray diffraction method using synchrotron radiation is used to measure the strain and the stress. We improved this method, attempting to measure the residual stress of a local internal area of a material with high precision.

In order to measure the residual stress of a local area with the high precision, X-rays with high brilliance, high flux and high energy, and optics with high resolution are necessary. An original monochromator for high energy X-rays and an undulator in which permanent magnets are arranged in the straight section of the accelerator so that their south pole and the north pole alternate vertically were installed to obtain such X-rays. To achieve high resolution in the optics, a single crystal called an analyzer was installed (Fig.4-22). The analyzer is suited to measure with high resolution because it reflects monochromatized X-rays over a very small angle range, but the problem occurs that the X-ray intensity diffracted by the analyzer greatly decreases. Our proposed method enables a high space-resolution evaluation of the stress distribution which takes a few hours, whereas the conventional X-ray method takes several days (Fig.4-23).

The strain scanning method developed in this study can determine the stress distribution with the spacial resolution of several hundreds μm^2 around a crack in internal material by using high energy synchrotron radiation X-rays. Furthermore in - situ stress measurement under high temperature or high pressure can be carried out because the measurement time of the strain scanning method is very short.

This newly developed method can be applied to various problems of concern to JAEA, such as stress corrosion cracking, development of materials for nuclear power generating plants, and the container for mercury target of "J-PARC". Furthermore, in the industry - academia - government collaboration, this method is applicable to research vital to the energy problem, for example, thermal barrier coating for a high efficiency jet turbine and solid oxide fuel cells.

Reference

Shobu, T. et al., High Space-resolutive Evaluation of Subsurface Stress Distribution by Strain Scanning Method with Analyzer Using High-energy Synchrotron X-rays, JSME International Journal Series A, vol.49, no.3, 2006, p. 376-381.

4-11 Synchrotron X-rays Revealing Crystal Growth Front at the Atomic Level
—Monitor for Gallium Arsenide Growth Using Synchrotron X-rays—

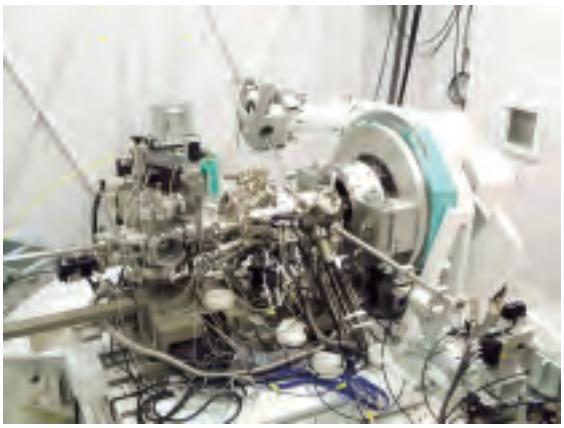

Fig.4-24 X-ray diffractometer integrated with a molecular beam epitaxy chamber

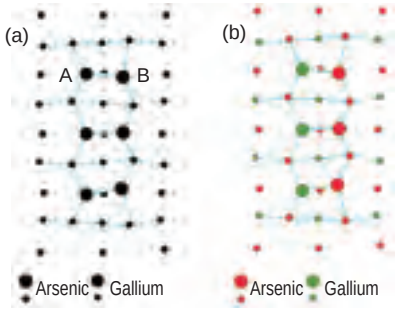

Fig.4-25 Surface structure of gallium arsenide under growth conditions
Atoms A and B cannot be distinguished as gallium and arsenic by the ordinary method (a), but can be distinguished by this method (b).

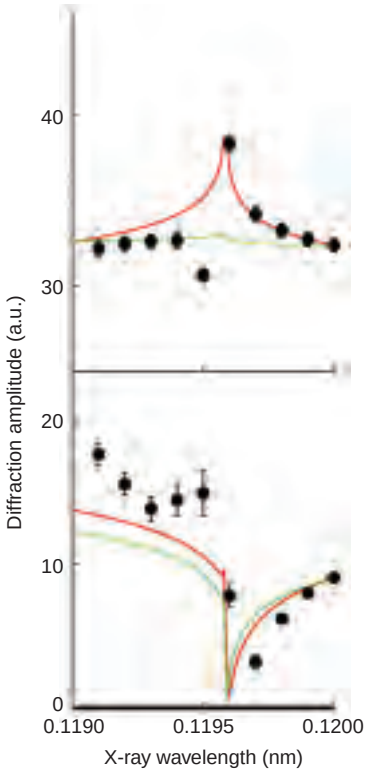

Fig.4-26 Diffraction amplitude as a function of X-ray wavelength
Experimental results (black circles) agree with the simulation corresponding to the case where A and B aer gallium and arsenic (red lines) rather than the case where both atoms are arsenic (green lines).

Gallium arsenide is a semiconductor showing excellent performance in optoelectronic and high-frequency devices. It is playing a critical role in today's highly-networked society as widely used in cell phones and optical communication lasers. For these applications, atomically-controlled device structures are grown using state-of-the-art techniques called molecular-beam epitaxy (MBE) and metalorganic chemical vapor deposition (MOCVD). These techniques need detailed knowledge about surface structures during growth.

We have developed an X-ray diffractometer integrated with an MBE chamber (Fig.4-24) at "SPring-8" for surface studies during crystal growth. The intense X-rays of "SPring-8" have speeded up the measurements of surface X-ray diffraction, which is weaker than the diffraction from bulk crystals by several orders of magnitude. Moreover, a wide spectrum of SPring-8 X-rays has enabled the determination of the species of surface atoms as well as their coordinates.

Fig.4-25(a) shows the top view of the gallium arsenide surface investigated in the present work. Conventional surface analysis techniques have difficulty in differentiating between gallium and arsenic because the numbers of electrons possessed by gallium and arsenic are fairly close, being 31 and 33, respectively. In fact, in Fig.4-25(a), each atom is indicated by a circle whose radius is proportional to the number of the electrons it has, but the difference is subtle. In the present study, We investigated the variation of X-ray diffraction intensity as a function of X-ray wavelength. As shown in Fig.4-26, the experimental results (filled circles) agree better with the model in which the topmost layer consists of both gallium and arsenic (red lines) than the counterpart in which only arsenic is present on the surface (green lines). In the sense of using multiple wavelengths, this method is equivalent to taking a color picture like Fig.4-25(b), in which gallium and arsenic atoms can be distinguished easily.

The X-ray technique is suitable for industry-oriented MOCVD growth as well because X-rays can propagate even in high ambient pressures which are typical for MOCVD. This method is expected to accelerate the development of novel devices through precise control of semiconductor processes.

Reference

Takahashi, M. et al., Element Specific Surface X-Ray Diffraction Study of GaAs(001)-c(4x4), Physical Review Letters, vol.96, no.5, 2006, p.055506-1-055506-4.

4-12 Attempt to Control Quantum Dot Size
—Measurement of the Number of Atoms in a Nanocluster—

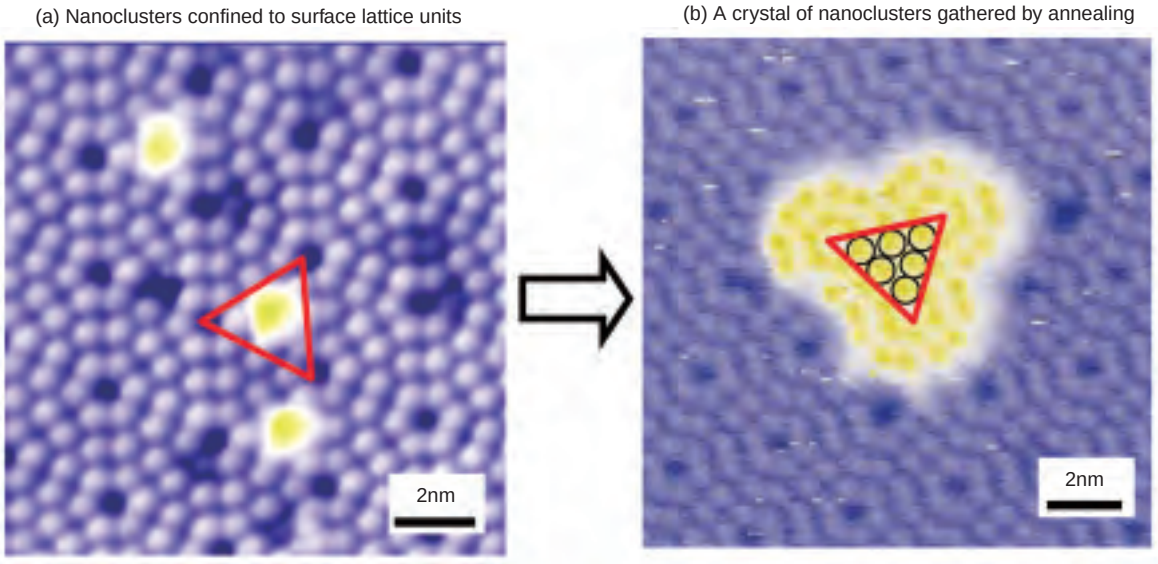

Fig.4-27 Scanning tunneling microscopy (STM) images of Germanium (Ge) nanoclusters in surface lattice units of Ge(111) and a nanocluster crystallized by annealing
Nanoclusters which are precursors for quantum dots in the initial growth stage are confined to half of the surface lattice unit (red triangle in (a)). The atoms in the nanoclusters (yellow mass at the center of red triangle in (a)) could not be recognized separately. We present a method for measurement of the average number of atoms in a cluster by using nanoclusters crystallized by annealing to make atoms directly recognizable.

Quantum dots are well known to confine electrons to a dot of quasi-zero dimension. This confinement leads to discrete energy levels, much like an atom, so that they are sometimes called "artificial atoms". The energy levels can be controlled by changing the size and shape of the quantum dot. As a result, they are researched for use in future applications such as diode lasers and solid-state quantum computation. The quantum dots nucleate spontaneously under certain conditions during molecular beam epitaxy (MBE), when elements with different lattice constants are grown on a substrate. The resulting strain produces self-assembled nanodot islands on top of a two-dimensional layer. However, it is difficult to control quantum dot size by using such a crystal growth mode. We tried to determine the number of atoms in a nanocluster, which is a precursor for a dot, to control the dot size quantitatively.

The confinement of the clusters to half of a surface lattice unit (red triangle at Fig.4-27(a) will result in a limitation of the size of the clusters to a maximum value. However, the atoms in the nanoclusters could not be individually recognized. We present a method for measurement of the average number of atoms in a cluster by crystallizing nanoclusters. To determine the number of the atoms, the amount of deposited material per area has to be divided by the number of clusters per area. The number of clusters per area can be easily determined from STM images such as the one presented in Fig.4-27(b). More difficult thing is the reliable measurement of the deposited amount of material. Fig.4-27(b) on the right shows a STM image of a crystal of nanoclusters gathered by annealing. In half of the surface lattice unit (red triangle in left figure), 6 atoms can be recognized separately. This structure is well known to have 45 atoms under the surface 6 atoms. As a result, we found that 8 atoms exist in the cluster in Fig.4-27(a), and the number of atoms in a cluster depends critically on the size of the surface lattice unit. And also the cluster size was found to be largely independent on the cluster material. These results have opened up a way to control quantum dot size by using quantitatively determined nanoclusters.

Reference

Asaoka, H. et al., Size of Small Si and Ge Clusters on Si (111) and Ge (111) Surfaces, Surface Science, vol.588, 2005, p.19-25.

4-13 Toward a Practical Small Proton Cancer Therapy Machine
—Discovery of Optimum Conditions for Laser Driven Proton Acceleration—

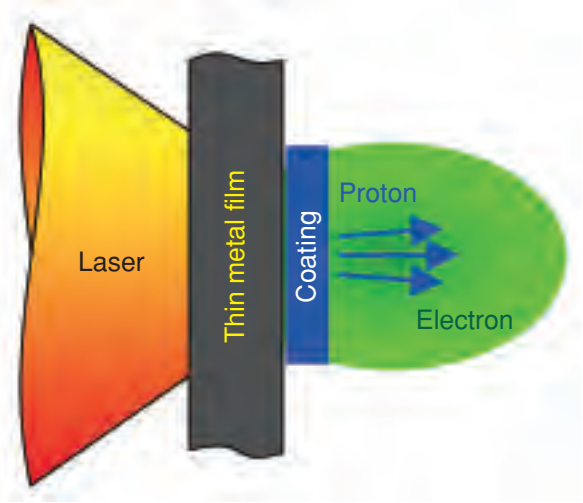

Fig.4-28 Schematic diagram of the double layer target
Via laser irradiation of a thin film target e.g. of metal (heavy atoms) coated by hydrogen, electrons are accelerated, a strong electric field is generated, and finally protons are efficiently accelerated.

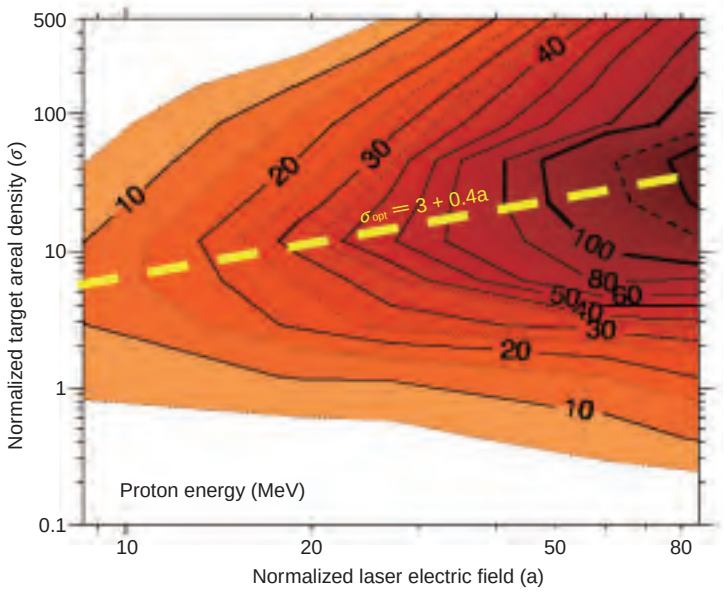

Fig.4-29 Multiparametric simulation results
The proton energy is depicted in the plane of the laser electric field (a) and the target areal density (σ). a = 8.5 (λ/1 μm) (I/10^{20} W/cm^2)$^{1/2}$; λ the laser wavelength; I the laser intensity. $\sigma = (I/\lambda)(n_e/n_c)$; l the target thickness; n_e the electron density; n_c the critical density at which the laser pulse is reflected.

The method of laser acceleration by using intense laser light is very attractive, since the acceleration performance is markedly higher than standard large accelerators and the device size could be much more compact (1/10～1/100) than present facilities in existence. Currently, proton acceleration experiments using high power lasers close to petawatt levels are going on vigorously all over the world to develop a compact cancer therapy machine. Finding the optimum conditions for the laser parameters and designing targets of micron order thickness only by experiments are, however, very difficult.

Therefore, in this study a simulation program has been developed to thoroughly survey the optimum laser and target conditions by using super computers at JAEA.

Fig.4-28 is a schematic diagram of the double layer target adopted in our simulation. The double layer target as a tool for hadron therapy, which was first suggested by S.V. Bulanov and V.S. Khoroshkov, is composed of a coating of light matter (low atomic number (Z)) on the back side of a thin metal film target. Due to laser irradiation of the target, high energy electrons are generated. As a result, an electrostatic field is induced and low-Z matter (protons in this case) can be efficiently accelerated.

Fig.4-29 shows multiparametric simulation results of the proton energy with the laser intensity and the target thickness and electron density as parameters. Contour lines of the proton energy are plotted in the plane of the laser strength (a) and the target areal density (σ) which is the product of the thickness and the electron density. It has been found that to attain a given proton energy the necessary laser strength (a) can be minimized by appropriately choosing the target areal density (σ) and that the optimum relation between a and σ is given by the scaling law of $\sigma_{opt} \simeq 3+0.4a$.

The present result, indicating that the laser intensity needed to trigger the proton energy generation can be reduced, leads us closer to the realization of a laser driven cancer therapy machine. Further research and development to achieve more realizable experimental parameter values and laser systems for the realization of a small laser driven cancer therapy machine will be undertaken at JAEA.

Reference

Esirkepov T., Yamagiwa, M. et al., Laser Ion Acceleration Scaling Laws Seen in Multiparametric PIC Simulations, Physical Reviwe Letters, vol.96, no.10, 2006, p.105001-1-105001-4.

4-14 Quasi-Monoenergetic Electron Beam Generation by Using an Intense Laser Pulse
—High Quality Electron Beam Source by Laser Acceleration—

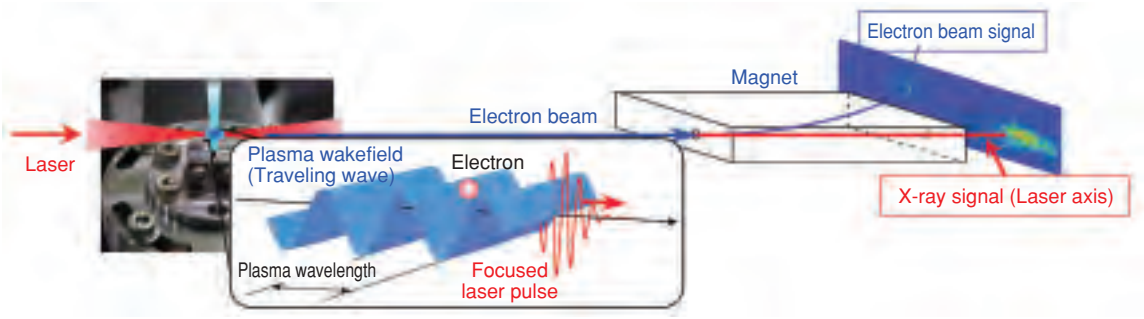

Fig.4-30 Schematic of laser acceleration
The intense laser pulse generates a plasma wake in the laser-produced plasma. The extremely high electric field of the wake is a traveling wave. A compact short pulse electron beam source is made by the wake due to the high field and the short wavelength of the plasma wake.

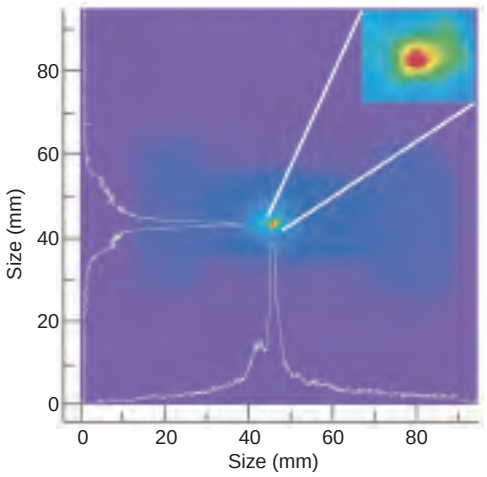

Fig.4-31 Profile of generated electron beam
Measured by a screen and a CCD camera. The electron beam is in a very small angle of 7.5 mrad.

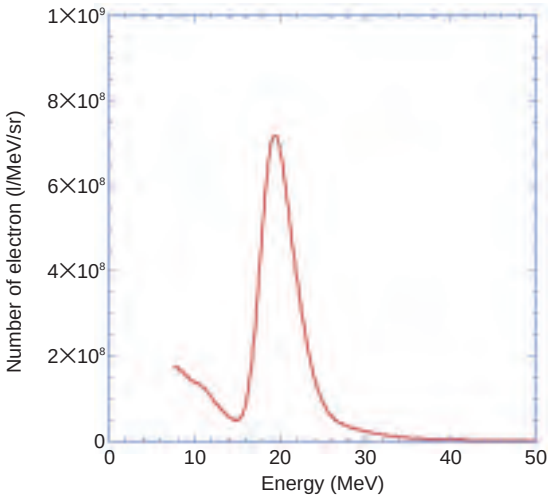

Fig.4-32 Energy spectrum of the electron beam
The quasi-monoenergetic electron beam is generated. The peak energy is 20 MeV, and the charge is 0.8 pC/shot.

The plasma wakefield generated by an intense laser pulse accelerates plasma electrons (laser acceleration: Fig.4-30). The laser acceleration becomes a compact short pulse electron beam source. This electron beam is suited for the next generation high quality electron beam injector and measurement of a structure change of molecules.

An electron beam generation experiment was conducted with a Ti:Sapphire laser, which has a pulse width of 70 fs (femto second: femto = 10^{-15}) and a power of 3 TW (tera watt: tera = 10^{12}). The electron beam profile and the energy spectrum are shown in Fig.4-31 and Fig.4-32, respectively. In this experiment, 20 MeV of quasi-monoenergetic electron beams are generated in the angle of 7.5 mrad. The emittance of the electron beam is 0.4 π mm mrad and the charge per laser shot is 0.8 pC (pico coulomb: pico = 10^{-12}). The electron beam source is smaller and of higher quality than conventional accelerators. This is the world's first quasi-monoenergetic electron beam generation with a laser of intensity as low as 10^{18} W/cm^2. The generated electron beam is about 10 fs due to the very short plasma period of a few tens fs, and can be used for the measurement of high-speed phenomena.

In order to use the electron beam for applications, it is necessary to generate a stable electron beam. We conducted a theoretical analysis and a particle-in-cell simulation to solve the problem of the unstable electron beam. The electron beam produced by one laser pulse is sensitive (unstable) to the parameters of laser intensity and the plasma density. In order to generate a stable electron beam, we propose a head-on collision of two laser pulses. The head-on collision can generate a high-quality stable electron beam due to wide stable range.

This study realized a compact high-quality electron beam source by laser-plasma interaction, which should enable various applications.

Reference

Mori, M. et al., Transverse Dynamics and Energy Tuning of Fast Electrons Generated in Sub-Relativistic Intensity Laser Pulse Interaction with Plasmas, Physics Letters A, vol.356, 2006, p.146.

4-15 Demonstration of Ultrafast Selective Excitation with Quantum Interference
—Toward a New Method of Isotope Separation—

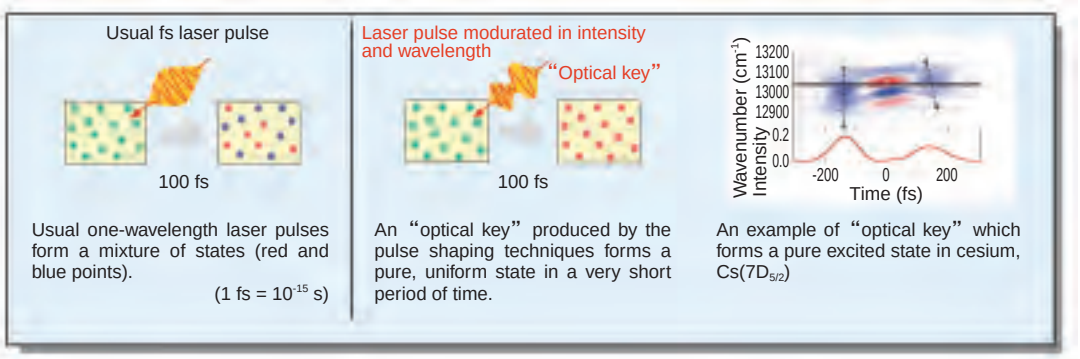

Fig.4-33 Ultrafast selection with the "optical key"

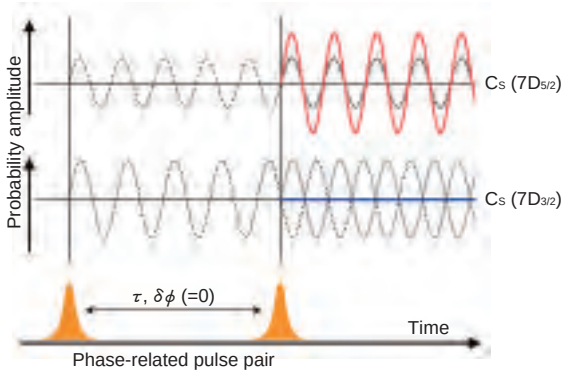

Fig.4-34 Mechanism of the ultrafast selection
Two waves in each state Cs(7D5/2) or Cs(7D3/2) created by a phase-related pulse pair interfere with each other so that one state vanishes (lower) while the other survives (upper).

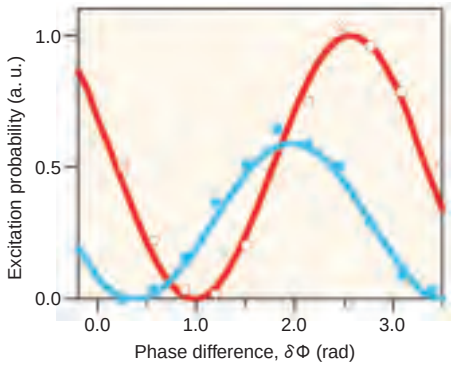

Fig.4-35 Phase difference dependence of the excitation probabilities to the two states
Selection is possible, since the phase differences where the population reach zero are different.

The quantum computer concept is attracting much attention as a future technology for ultrafast computers. Using the same quantum mechanical principle, a new method to control materials is being studied by physical chemists. Here, materials are cut or joined utilizing their wave character at the microscopic level of atoms and molecules. This method utilizes light, which also behaves as a wave. The wave form of light is molded into an "optical key" which induces the reaction fitting the key (Fig.4-33).

In a fundamental experiment to establish this technique, we tried to control the probability of photoexcitation of cesium to one state, applying the pulse shaping technique which was learned during development of the ultra high peak power laser at the Kansai Photon Science Institute (Fig.4-34). We were able to selectively generate one out of two states which have nearly the same energy, in a very limited time. This ultrafast selection could be done with an ultra-short phase-related pulse pair (Fig.4-35). This figure indicates that complete selection of one state, rejecting the other state, is possible with a delay time of 300 fs. The generation ratio between the two states was more than a hundred times greater than in the case of conventional laser pulses. The principle of this selection is the quantum mechanical interference and, thus, totally different from the usual method.

We believe that this ultrafast selection will ultimately lead to a breakthrough in the isotope separation which is required of nuclear wastes, semiconductors, and medical regents. In nuclear waste disposal, long lived fission products (LLFP) like cesium must be separated according to their isotopes. LLFPs are to be transmutated in a fast reactor to reduce the future dose to the public. However, for some species, the transmutation was found not to be feasible economically without isotope separations. Therefore, the development of isotope separation techniques of these species can help to reduce the future load to the environment. Additionally, isotope separation of valuable noble elements like paradium is desired to extract them from nuclear wastes. The present results should contribute basic understanding needed to achieve such a separation process.

Reference

Yamada, H., Yokoyama, K. et al., Selective Transition to the Closely-Lying States Cs(7D3/2 and 7D5/2) by Femtosecond Laser Pulses, Physical Review A, vol.72, no.6, 2005, p.063404-1-063404-5.

4-16 R&D of High Power Neutron Sources
—Micropit Formation by Pressure Wave in Mercury Target—

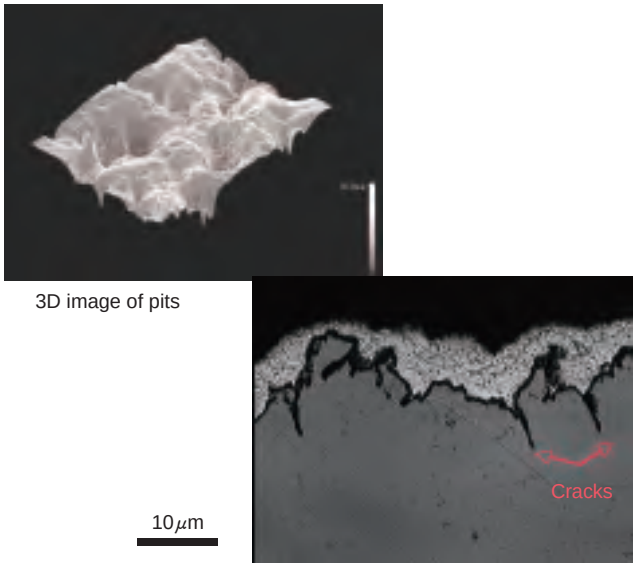

Fig.4-36 Micrographs taken by a laser microscope
The pitting damage was observed after 10^6 pulses whose amplitude is equivalent to the pressure pulse induced by MW-class proton beam injection. Cracks were propagated under the bottom of pits.

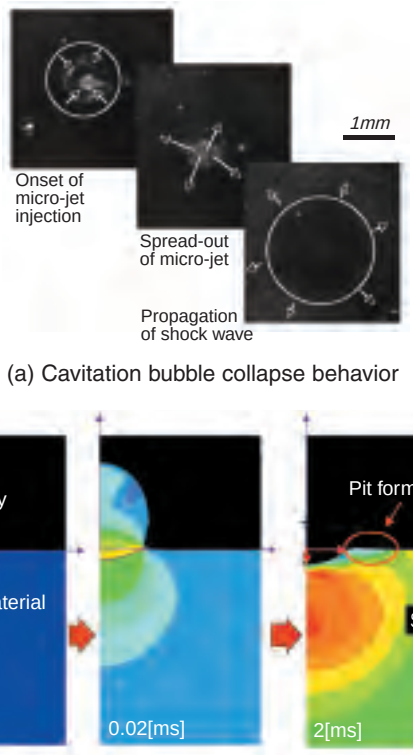

Fig.4-37 Micro-jet impact analysis with impact velocity (*ca.* 200 m/s) estimated from observing bubble collapse behavior describes well the pit formation.

Innovative researches will be performed at Materials & Life Science Experimental Facility in "J-PARC", in which a mercury target system will be installed in a MW-class pulse spallation neutron source. Proton beams will be injected into mercury target to induce the spallation reaction. At the moment the intense proton beam hits the target, pressure waves are generated in the mercury because of the abrupt heat deposition. The pressure waves interact with the target vessel leading to negative pressure that may cause cavitation along the vessel wall. Localized impacts by micro-jets and /or shock waves which are caused by cavitation bubble collapse impose pitting damage on the vessel wall. Fig.4-36 shows micrographs of the pitting damage caused by mechanically creating the pressure waves in mercury. Such pitting damage is a crucial issue for high power mercury targets. The cavitation bubble collapse behavior was observed by using a high-speed video camera, and also simulated numerically (Fig.4-37). Localized impact was quantitatively estimated through comparison between numerical simulation and experiment. A novel surface treatment technique that consists of carburizing and nitriding processes was developed. The treatment condition was optimized to achieve an improved surface layer with a suitable hardness gradient that can mitigate the pitting damage due to localized impacts, taking into account the stress distribution evaluated by micro-jet impact simulation. This surface improvement increases the lifetime of the mercury target vessel: the number of pulses before pitting damage becomes pronounced increases from 10^6 to 10^7.

Reference

Futakawa, M. et al., Mico-Impact Damage Caused by Mercury Bubble Collapse, JSME International Journal, vol.48, 2005, p.234-239.

4-17 Development of High Performance Neutron Supermirror
－For Higher Fluxes at the Spallation Neutron Source of J-PARC－

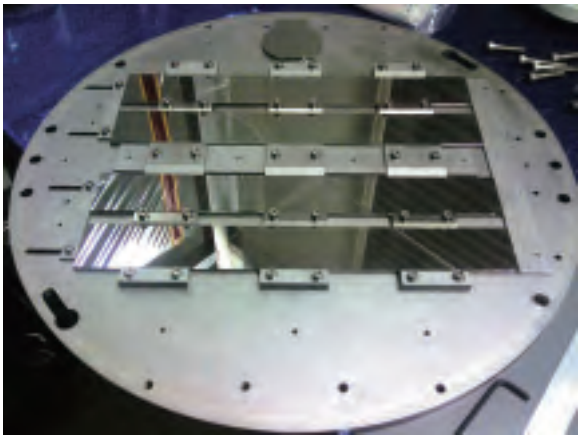

Fig.4-38 Photograph of the substrate holder (500 mm ϕ) of the IBS instrument installed in JAEA and the float glass substrates (50×400 mm) on it.

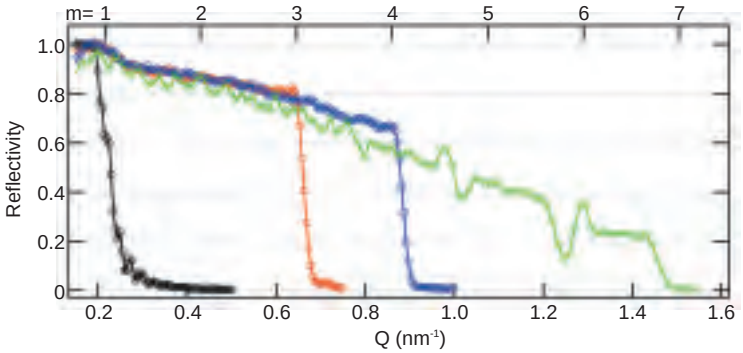

Fig.4-39 The measured neutron reflectivities of the supermirrors fabricated with the IBS instrument
The red, blue, and green lines indicate the reflectivities of the supermirrors with *m*=3, 4, and 6.7, respectively. The reflectivities at their respective critical angles (Q=0.645, 0.86, and 1.44 nm^{-1}) are 82%, 66%, and 23%.

Neutron scattering is a useful source of information about the positions, motions, and magnetic properties of condensed matters. Neutron scattering is important because it provides valuable information that can not be obtained using other techniques such as X-ray scattering. In order to study a wide range of problems in material and life science with a much higher neutron intensity, a new spallation neutron source (Japan Proton Accelerator Research Complex, "J - PARC") is now under construction. The development of high performance neutron supermirrors with high reflectivity and large *m*, the ratio of the effective critical angle of the supermirror to that of natural nickel (Ni), is important for the J-PARC project since it greatly increases the available neutron intensity. For example, supermirror neutron guide with $m=k$ would bring about a gain factor of k^2 in the neutron flux at the end of the guide when it is used instead of the Ni guide. Neutron supermirrors consist of alternating layers of two materials with different refractive indices for neutrons.

We have developed neutron supermirrors by employing the ion beam sputtering (IBS) technique because it enables the production of layers with high density and small grain size. An ion polishing technique is combined with IBS deposition in order to suppress the interface roughness, which is an important problem in the fabrication of supermirrors with large *m*, and the efficiency of this combined IBS technique has been confirmed. Although the IBS technique produces high quality layers, its disadvantage is that the deposition area and rate are relatively small. Based on the results of our development, a new IBS instrument with a large effective deposition area of 500 mm diameter (Fig.4-38) has been designed and installed at the JAEA. The difference in the deposition rate over the entire deposition area has been confirmed to be less than 4%.

Ni/titanium(Ti) supermirrors with *m*=3 and 4, for use as neutron guides in the J-PARC project, have been fabricated using the IBS instrument. The total number of layers is 403 and 1201, respectively. The neutron reflectivities of mirrors with *m*=3 and 4 at their critical angles are 82% and 66%, respectively (Fig.4-39). Ni/Ti supermirror with *m*=6.7, which is a record breaking critical angle, has also been fabricated. The total number of the layers is 8000. The neutron reflectivity at the critical angle is 23% (Fig.4-39). Thus, we can contribute to the J-PARC project in which the production of neutron guides, benders, and other devices using supermirrors is planned.

Reference

Maruyama, R. et al., Development of Neutron Supermirror with Large-Scale Ion Beam Sputtering Instrument, Physica B, in press.

5 Nuclear Safety Research

5-1 Role and Scope of Nuclear Safety Research

To ensure the safety of nuclear installations, the regulatory authorities conduct strict investigations and inspections. Nuclear safety research is necessary to improve the safety regulations. The latest scientific and technical knowledge is essential for the development and improvement of the safety guidelines and regulatory criteria.

The Nuclear Safety Commission (NSC) proposed a "Prioritized Plan for Nuclear Safety Research" in July 2004, to be carried out in order to meet the future regulatory needs. The major research activities expected the JAEA are shown in Fig.5-1.

The results of nuclear safety research contribute to the maintenance and improvement of safety of the nuclear facilities and also to fostering public confidence in nuclear safety.

The experimental approach is usually used in nuclear safety research to investigate the phenomena occurring during accidents and to confirm the effectiveness of safety systems. The data obtained from these experiments are used to develop safety evaluation methods. The major test facilities are shown in Fig.5-2.

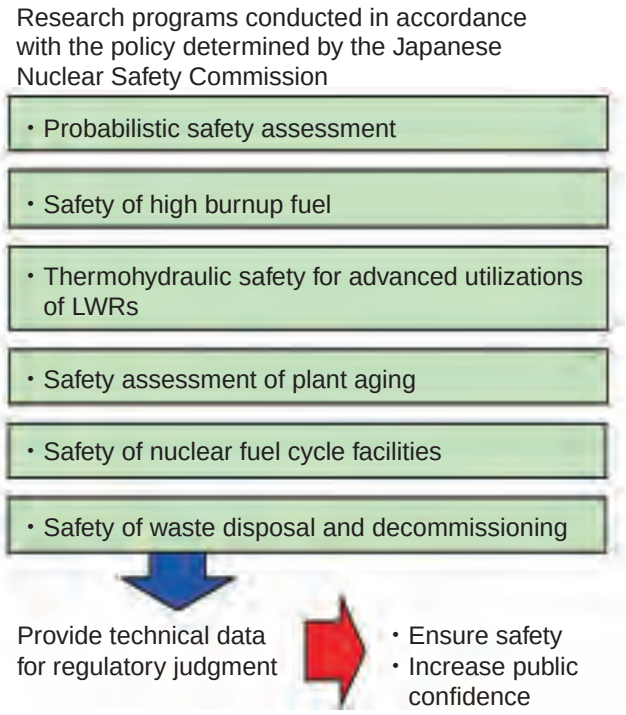

Fig.5-1 Major subjects and tasks of safety research

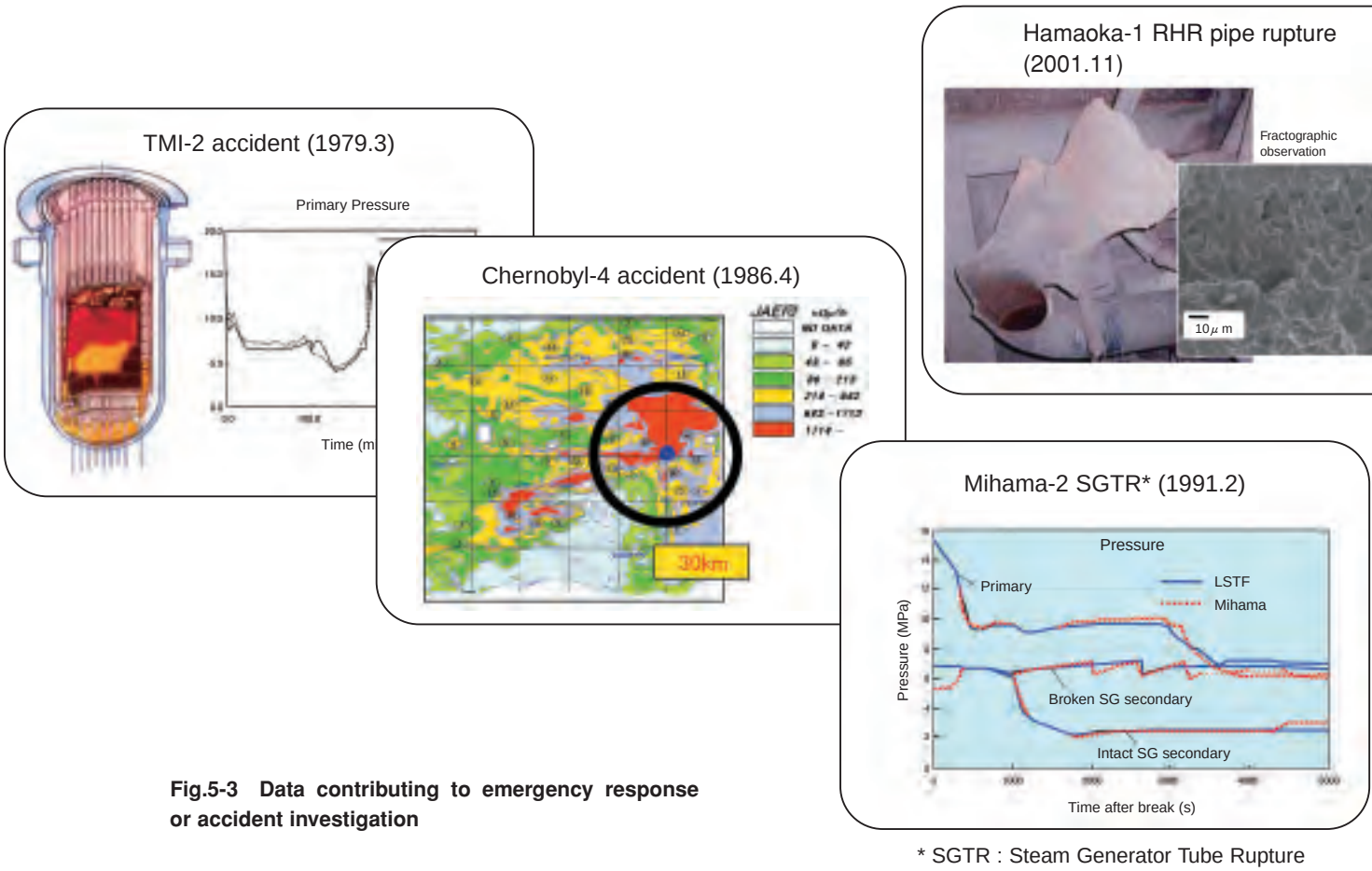

Fig.5-3 Data contributing to emergency response or accident investigation

* SGTR : Steam Generator Tube Rupture

Nuclear Safety Research Reactor (NSRR) :
NSRR is a research reactor to conduct fuel irradiation experiments with pulse operation. Experiments are performed to establish safety guidelines and regulatory criteria for fuel failure threshold under reactivity-initiated accident (RIA) conditions.

Large Scale Test Facility (LSTF) :
LSTF is the largest test facility in the world to simulate responses during loss of coolant accidents and abnormal transients of PWR. The components are 1/48-scale in volume and full-scale in height. The OECD/NEA/ROSA Program is being conducted using the LSTF.

Nuclear Fuel Cycle Engineering Research Facility (NUCEF) :
NUCEF is a facility for research and development of the nuclear fuel cycle including radioactive waste disposal. The research results contribute to establish safety guidelines and criticality databases.

Fig.5-2 Major facilities for nuclear safety research

Moreover, when accidents or trouble occurred at nuclear facilities, the JAEA played a responsible role by providing technical experts to assist the government or local government in conducting accident investigations or emergency responses, in such cases as the JCO criticality accident and the Mihama-3 secondary pipe rupture (Fig.5-3).

Stress corrosion cracking of BWR core shroud and piping (2002.8)

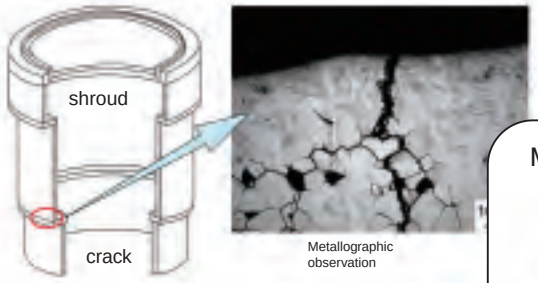

Mihama-3 secondary pipe rupture (2004.8)

JCO criticality accident (1999.9)

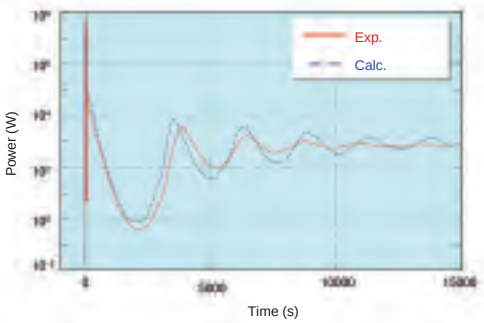

Cracking in BWR hafnium blade type control rod at Fukushima I-3 (2006.1)

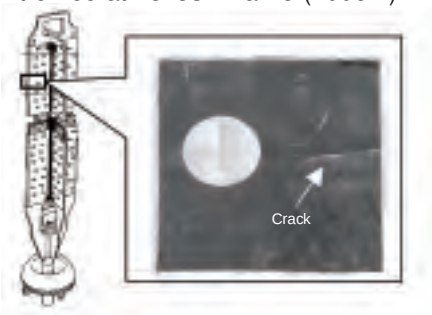

5-2 Toward Risk-Informed Safety Management of Nuclear Fuel Facilities

— Development of Probabilistic Safety Assessment Procedures for MOX Fuel Fabrication Facilities —

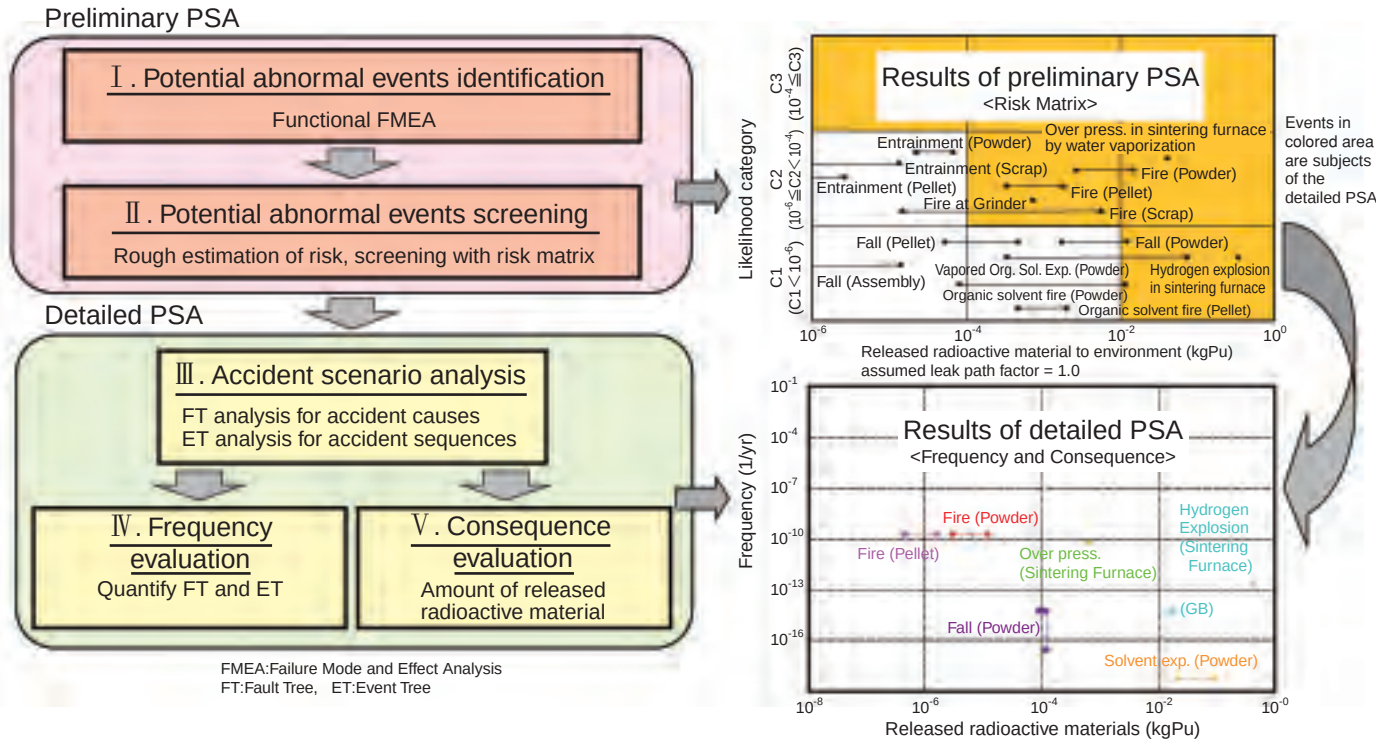

Fig.5-4 PSA procedures and analysis results of a typical MOX fuel fabrication facility
The preliminary PSA is carried out through Ⅰ) exhaustive identification of potential abnormal events and Ⅱ) efficient screening of those events using a risk matrix. In the detailed PSA, Ⅲ) Accident scenario analysis is carried out to analyze causes and event sequences of each abnormal event by drawing a fault tree (FT) and event tree (ET) respectively. Ⅳ) Accident frequencies are evaluated by quantifying FT and ET. Finally, Ⅴ) radioactive material releases to the environment are evaluated as the accident consequence using a five factor formula calculating the release amount from five material-specific factors.

Probabilistic safety assessment (PSA) has the advantage that it can give valuable information for reasonable decision-making on safety measures for nuclear installations with considering their effects and inferences that are assessed systematically and quantitatively by the PSA. Compared with the PSA for the nuclear power plant, however, the PSA for nuclear fuel facilities seems to be immature. In order to assist the regulatory review, in FY2001, a five-years research project was launched at the former JAERI to develop a PSA procedure applicable to a MOX fuel fabrication facility under the entrustment from the Ministry of Economy, Trade and Industry (METI).

One of the features of MOX fuel fabrication facilities is that nuclear materials exist in various physical forms at different areas in the facility. It is supposed that a variety of accidents may occur with different energy release at those areas. Therefore, it is important to identify potential abnormal events exhaustively and to screen those events efficiently from the point of risk significance. After screening, detailed risk assessment is also important for frequency of occurrence and radioactive material release to environment of various accident sequences.

The developed PSA procedure consists of two stages, “Preliminary PSA” and “Detailed PSA” which include five major analysis steps as shown in Fig.5-4. In the Preliminary PSA, the screening of the potential abnormal events identified by the hazard analysis is carried out by using a two dimensional matrix (called as risk matrix) based on the rough estimation of likelihood and unmitigated release of radioactive material. The selected events are the subjects of the Detailed PSA in which major procedures are as same as for the nuclear power plant PSA.

The applicability of proposed PSA procedure was demonstrated through a trial PSA for a model MOX plant in which risk-significant accident scenarios, systems and components were identified with risk profile derived from the results of accident frequency and amount of released radioactive materials.

Reference

Tamaki, H., Yoshida, K. et al., Development of Probabilistic Safety Assessment Method for Mixed Oxide Fuel Fabrication Facilities, Nippon Genshiryoku Gakkai Wabun Ronbunshi, vol.5, no.2, 2006, p.125-135 (in Japanese).

5-3 Safety Evaluation of Long-Term Irradiated Light Water Reactor Fuels
—High Burnup Fuel Behavior in a Reactivity Initiated Accident—

NSRR at pulse operation

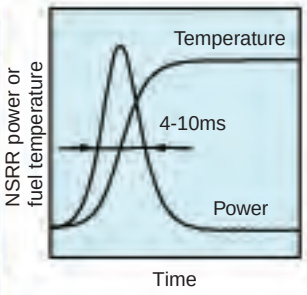

Histories of NSRR power and fuel temperature during pulse operation

Failed fuel rod in NSRR experiment (78 GWd/t)

Fig.5-5 Pulse irradiation experiment at NSRR
Pulse operation of the Nuclear Safety Research Reactor (NSRR) can simulate a Reactivity Initiated Accident (RIA) which is hypothesized in light water reactors. High burnup fuel behaviors under RIA conditions are thereby investigated and conditions of fuel failure are quantified.

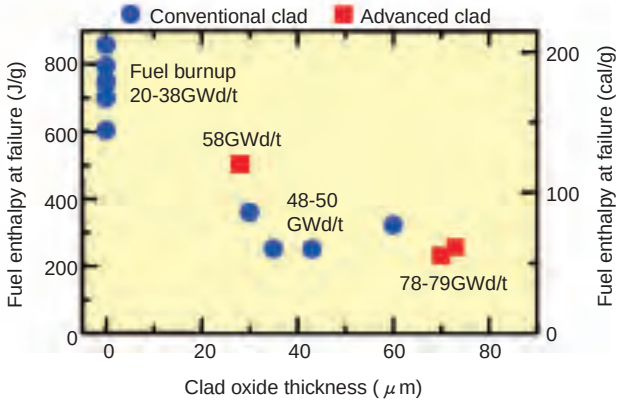

Fig.5-6 Relation between clad corrosion and safety performance
The vertical axis denotes fuel enthalpy at which fuel failure occurs. Hence, this is an index for the fuel safety performance in RIA. The period of fuel irradiation in a power producing reactor is indicated with the fuel burnup in GWd/t. This figure shows that fuel safety performance has a stronger correlation with clad oxide thickness, which is an index for clad corrosion, than with fuel burnup.

Extending the utilization period of reactor fuel, i.e. burnup extension, is being promoted worldwide for efficient use of natural resources and reduction of spent fuels. The burnup extension, however, leads to higher corrosion of fuel clad and larger accumulation of fission products in fuel pellets. Accordingly, fuel safety at high burnups must be confirmed under accident conditions as well as under normal operation conditions. To clarify fuel behavior and failure mechanisms in a reactivity initiated accident (RIA), power burst tests simulating RIA are carried out at the NSRR on high burnup fuels which have been irradiated in power producing reactors (Fig.5-5).

The NSRR tests showed that fuel rods with corroded clad could fail due to mechanical load generated by pellet thermal expansion at a power burst. The fuel enthalpy at failure is used as the index of fuel safety in an RIA. It has been clarified that fuel rods with higher burnup could fail at lower fuel enthalpies. These results were incorporated in the Japanese safety regulatory guides for power producing reactors.

The current regulatory guides are based on the test results of conventional fuel rods. However, advanced clad alloys with higher corrosion-resistance have been introduced. The fuel rods with such improved claddings sustained higher fuel enthalpies than the conventional rods in the latest NSRR tests. Fig.5-6 shows the relation between the clad oxide thickness, representing the corrosion level, and fuel enthalpy at failure. It can be clearly seen that fuel enthalpy at failure correlates with the oxide thickness better than with burnup. Hence, the oxide thickness is an effective index for fuel safety margin against failure in RIA.

Currently, further extension of burnup, extensive utilization of plutonium and improvement of pellet and cladding are being promoted simultaneously. The NSRR test program continues to support safety regulatory authorities by providing advanced safety evaluation methods and tools based on the experimental data and understanding of key phenomena.

The tests with 78-79GWd/t fuels were sponsored by the Nuclear and Industrial Safety Agency of the Ministry of Economy, Trade and Industry.

Reference

Fuketa, T. et al., NSRR RIA-simulating Experiments on High Burnup LWR Fuels, Proceedings of the 2005 Water Reactor Fuel Performance Meeting, Kyoto, Japan, Oct. 2-6, 2005, p.633-645.

5-4 Is Safety Maintained in Loss-Of-Coolant Accident even with Long-Term-Used Fuel?
—Evaluation of Light Water Reactor Fuel Behavior under LOCA Conditions—

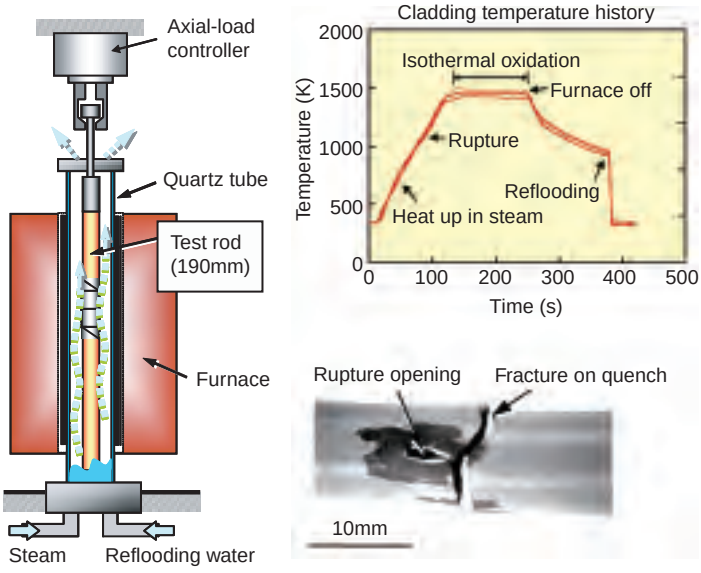

Fig.5-7 LOCA-simulated experiment
Test rod is heated to 1200 – 1500 K in flowing steam with the furnace. After isothermal oxidation, the test rod is cooled and quenched with flooding water. The photograph shows post-test appearance of irradiated fuel cladding.

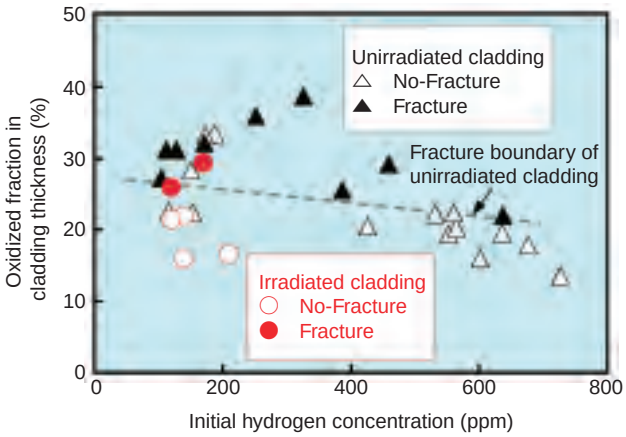

Fig.5-8 Fracture map, relevant to oxidized fraction and initial hydrogen concentration
Results with unirradiated cladding (triangles) show that fracture preliminary depends on oxidized fraction and slightly on hydrogen concentration. Results with irradiated cladding (circles) show that fracture boundary is not reduced significantly by irradiation at the examined burnup level.

The loading period of fuel (fuel burnup) is being increased step by step in light water reactors (LWRs) for efficient use of natural resources and reduction of spent fuels. This should be achieved without degrading the safety. We perform experiments under simulated accident conditions to investigate effects of longer-term irradiation on fuel behavior during accidents and confirm fuel safety.

In a postulated loss-of-coolant accident (LOCA), fuel temperature is increased for several minutes until the emergency core cooling system (ECCS) recovers the coolability of the reactor core. Fuel cladding, composed of zirconium-based alloys, becomes brittle if it is severely oxidized during the high-temperature period, and may fracture by thermal shock during the emergency core cooling. Heat removal may not be possible in the case that fragments from the fractured fuel accumulate in the lower part of the reactor core. To maintain coolable geometry of the reactor core, the Japanese LOCA criteria require that the peak clad temperature shall not exceed 1473 K (1200ºC), and the oxidized fraction shall not exceed 15% of the cladding thickness. The 15% criterion is based on fracture/no-fracture boundary conditions determined by laboratory - scale experiments simulating LOCA conditions. Since most of the previous experiments used only unirradiated cladding, information regarding irradiated cladding was insufficient. Hence, we devised a simulating apparatus (Fig.5-7) in a hot-cell and performed the LOCA-simulating experiments with cladding that had been irradiated for a long term (burnup: 39 to 44 GWd/t) in a commercial pressurized water reactor (PWR). As a result, important information was obtained on overall behavior and fracture conditions of irradiated cladding under LOCA conditions. Fig.5-8 shows that fracture conditions of the irradiated cladding are identical to those of unirradiated cladding which has been equivalently pre-hydrided simulating hydrogen absorption that occurs during reactor irradiation. Accordingly, the fuel safety in a LOCA is not degraded by long-term irradiation of the examined range, though the fracture boundary oxidation value is reduced by hydrogen absorption to some extent. The obtained information is used in the regulatory judgment by the government.

Reference

Nagase, F. et al., Fracture Behavior of Irradiated Zircaloy-4 Cladding under Simulated LOCA Conditions, Journal of Nuclear Science and Technology, vol.43, no.9, 2006, P1114-1119.

5-5 Analysis of Rod Failure Mechanism in Accident Conditions
—Development of the RANNS Code—

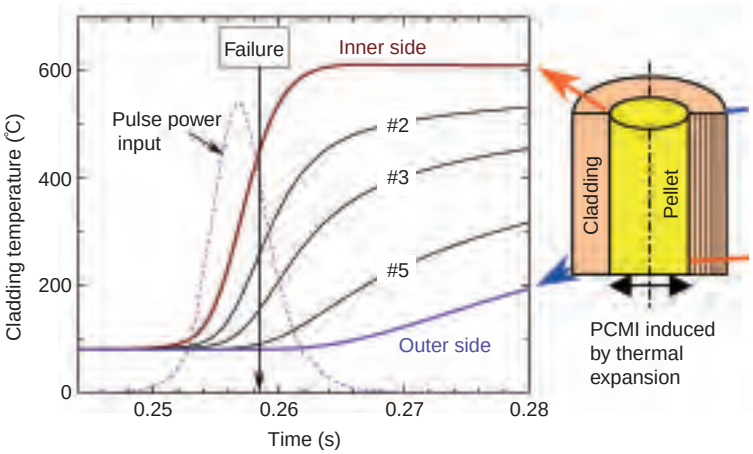

Fig.5-9 Calculated temperature distribution of cladding
#2, #3 and #5 are ring elements between the inner and outer sides. Upon pulse power input, the temperature rises faster in the inner region than the outer region. PCMI-failure time was observed. Temperature difference between the inner and outer sides is as much as 400C at the failure instant.

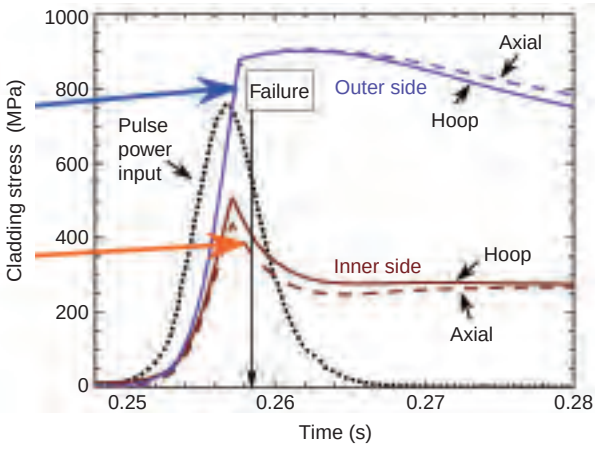

Fig.5-10 Axial and hoop stresses in the inner and outer sides of cladding, analyzed in FK-10 experiment
Stress is mitigated in the inner side of cladding by thermal expansion, and stress in the outer side is relatively higher. The rod failed when a slight plastic deformation occurred, indicating a low-strain breakage mechanism.

The RANNS code was developed for the analysis of thermal and mechanical behavior of high-burnup LWR fuel rod in reactivity-initiated accident (RIA) conditions and in loss-of-coolant accident (LOCA) conditions. Its primary purpose is to investigate the mechanism underlying the observations made during a limited number of accident-simulating experiments, and to support the determination of failure threshold of rods for the purpose of enhancing the credibility of safety evaluation. In high burnup fuel rods, pellet-clad gap is closed, which generates a "bonding layer". Also, cladding ductility is reduced by radiation damage and waterside oxidation (hydrogen absorption). In these rod conditions, when an abrupt power increase occurs in an RIA, thermal expansion of the pellet directly pushes the cladding outward and gives severe mechanical loading. Focusing on such pellet-clad mechanical interaction (PCMI), the RANNS model was designed to have multi-layer ring elements in both the pellet stack and cladding to perform an accurate evaluation of stress and strain in the radial direction and distributions of temperature. Numerical analysis of the RIA-simulating experiments in the NSRR (Nuclear Safety Research Reactor) with high burnup BWR rods showed that the cladding inner side is heated up rapidly upon pulse power input, while the temperature rise in the outer side is much delayed (Fig.5-9). Consequently, thermal expansion is larger in the inner region, which relieves the PCMI-induced tensile stress of cladding significantly, and the stress is relatively higher in the outer region (Fig.5-10). Considering that a failure crack occurs at the outer surface of cladding in many experiments, it is obvious that this quantitative analysis can successfully explain such observation. Also, as shown by the broken lines in Fig.5-10, the code predicts that axial stress also occurs, and the cladding fails in bi-axial stress state. The above analyses demonstrate the usefulness of the RANNS code in the study of high burnup fuel behavior in RIA conditions, particularly in PCMI, and the code allows a quantitative clarification and evaluation instead of qualitative interpretation of experimental data. Besides, RANNS can analyze the fuel behavior in postulated conditions. If the pulse power input does not bear a sharp shape as shown in Fig.5-9 and Fig.5-10 but has a broader shape, or the pulse has a lower peak value, it is anticipated that the cladding temperature gradient and PCMI-induced stress are mitigated. In such situation, the code can predict specific cladding conditions and evaluate the threshold level of failure. In the near future, subjects of analysis will be expanded, and practical failure prediction capability will be studied.

In addition, since the RANNS code can calculate the cladding high temperature oxidation and thermal stress generated in a rapid temperature transient, the code will be applied to the analysis of the fuel rod behavior in quench phase of a LOCA.

Reference

Suzuki, M. et al., Analysis on Split Failure of High Burnup BWR Rods in Reactivity-Initiated Accident Conditions by RANNS Code, Nuclear Engineering and Design, vol.236, 2006, p.128-139.

5-6 Verified Effectiveness of Pressurized Water Reactor Severe Accident Management
—Even When Break Is at the Worst Location in PWR Primary Coolant System—

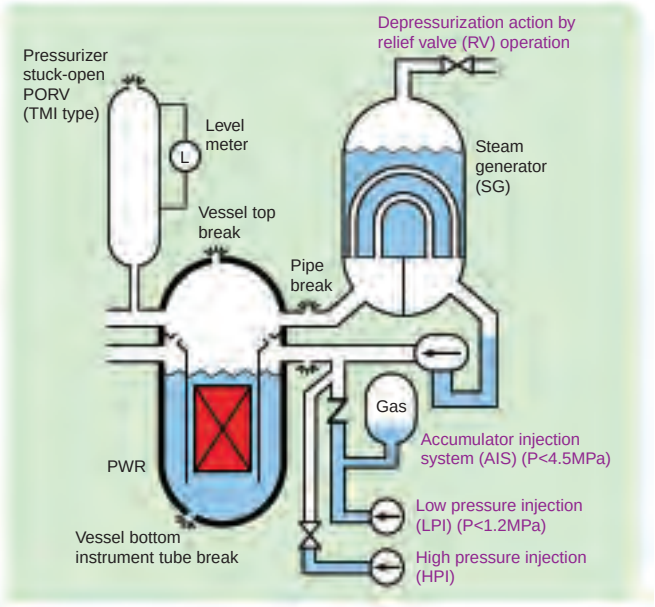

Fig.5-11 Simulated AM measures for various PWR/LOCAs
Various LOCA tests were conducted at LSTF, the world's largest plant simulator with the same height and 1/48 volume of a 3423 MWt PWR, to examine the effectiveness of accident management (AM) measures if there is severe loss of coolant. In case of HPI total failure, it is important for operators to depressurize the primary coolant system by opening SG relief valves (RVs) to activate the AIS and LPI system. The tests verified the effectiveness of this AM measure even in a LOCA caused by vessel bottom break which is the worst break location. A code analysis also confirmed the effectiveness.

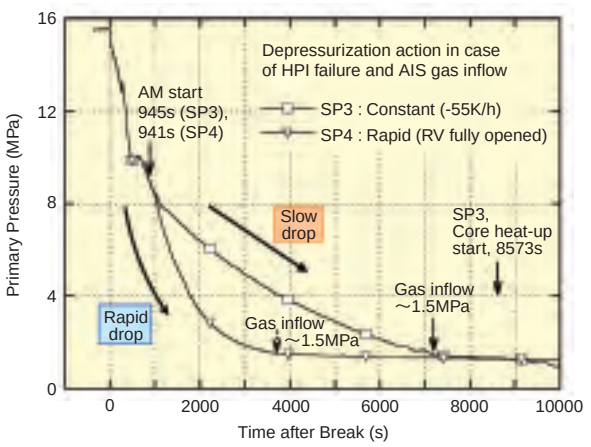

Fig.5-12 Core cooled by rapid-depressurization after bottom breakage with HPI failure and gas inflow

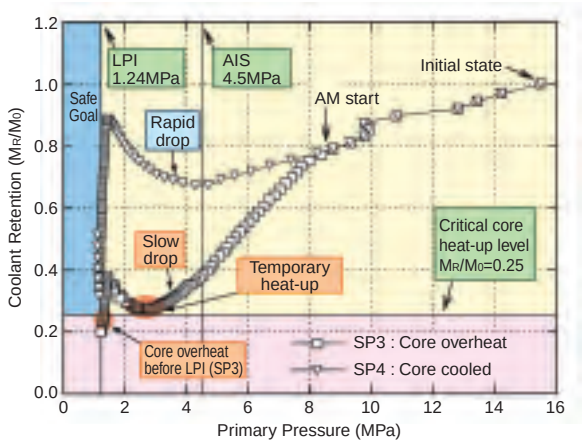

Fig.5-13 P-M map display useful for PWR/LOCA detection
This shows the difference in retained coolant in two tests of different AM actions (SP4 achieved the goal).

Pressurized water reactors (PWRs) are most common type of nuclear power plants in the world. The ROSA-V program has conducted small break loss-of-coolant accident (SBLOCA) tests with a break at various locations in the Large Scale Test Facility (LSTF) to study coolant behavior and to improve analysis code capability.

Following a study on effectiveness of accident management (AM) measures for SBLOCAs at the primary loops, we verified effectiveness of AM measures for SBLOCAs at the reactor vessel bottom caused by instrument tube nozzle failure (Fig.5-11). An indication of coolant leakage around two instrument tubes was newly found at the South Texas Project reactor in USA, and effectiveness of AM measures during a bottom break LOCA became one of priority issues of the OECD/NEA ROSA project initiated by JAEA in 2005.

We conducted two tests of vessel bottom break equivalent to a 0.2% cold leg break with total HPI failure and gas inflow from the AIS tanks taking different SG depressurization actions. Fig.5-12 compares their primary pressure transients and shows that the rapid depressurization in SP4 test achieved adequate core cooling irrespective of the gas inflow while a slow and constant cooling rate at -55 K/h in SP3 test resulted in core heat-up. A reason for these different core cooling results is clear in the Fig.5-13 chart showing dependence of coolant retention on primary pressure. In the SP4 test the conditions for LPI actuation were achieved maintaining coolant amount over the critical core heat-up level by the rapid depressurization, while coolant in the SP3 test decreased to the critical level, the larger coolant discharging due to higher pressure than in the SP4 test.

Reference

Suzuki, M. et al., Effects of Secondary Depressurization on Core Cooling in PWR Vessel Bottom Small Break LOCA Experiments with HPI Failure and Gas Inflow, Journal of Nuclear Science and Technology, vol.43, no.1, 2006, p.55-64.

5-7 Evaluating the Risk of Steam Explosions
—Simulation of Fuel-Coolant Interactions—

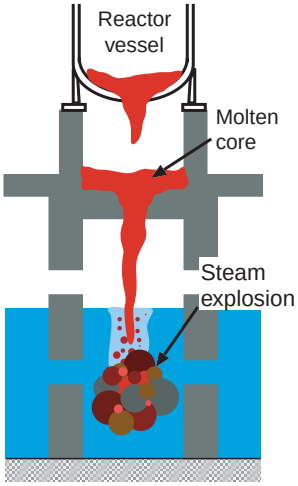

Fig.5-14 A steam explosion during a severe accident of a light water reactor
A steam explosion may occur if the core is melted and drops into water in the reactor vessel or the containment vessel.

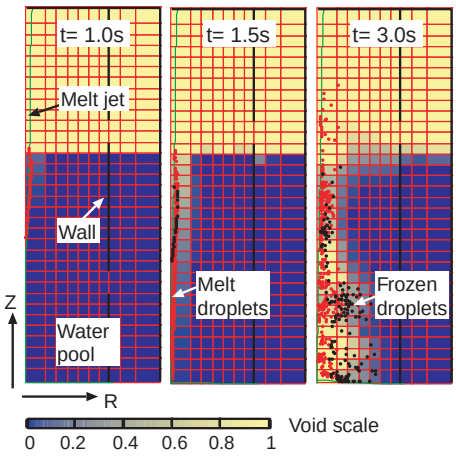

Fig.5-15 Simulation of the premixing process by the JASMINE code
Break-up of the molten core jet and formation of the premixture. The part of the molten core that is well mixed with water and kept molten contributes to the following explosion process.

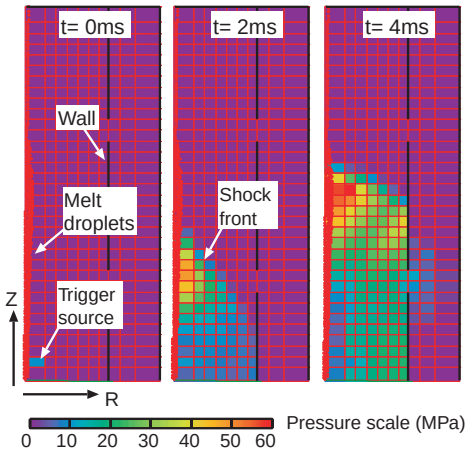

Fig.5-16 Simulation of the explosion process by the JASMINE code
Development of the shock wave of the steam explosion that is triggered by an assumed pressure pulse near the bottom, with the premixture condition taken from the result at t=1.5s in Fig.5-15. The steam explosion load on the structure is evaluated by this calculation.

A steam explosion, an extremely rapid production of high pressure steam, occurs when a hot liquid (e.g. molten metal) drops into water. It may occur in severe accidents of nuclear power plants (involving core melt down; e.g. Three Mile Island accident in U.S.) when the molten core drops into water. (Fig.5-14) If the shock load by the explosion breaks the containment vessel, radioactive material may leak into the environment. Thus, the steam explosion has been regarded as a cause of a large release and has been studied intensively for a long time. It is now accepted that the frequency of a steam explosion is very low so that its contribution to the public risk (product of the frequency and radiological consequences) is small in the probabilistic safety assessment (PSA). However, the uncertainty of the steam explosion risk is a remained issue.

Although much research has been done to clarify the mechanism and the load of steam explosions, such knowledge could not be directly applied to plant scale assessment due to differences in scale and material between experiments and real plants. We needed something that bridges this gap, and so developed a steam explosion simulation code, JASMINE, and applied it for the evaluation of the containment failure probability which is necessary for the risk analysis.

Fig.5-15 and Fig.5-16 are example calculations by JASMINE. In a steam explosion, the molten core breaks-up in the water and mixes with water and steam, “premixing” (Fig.5-15), which is followed by the explosion where rapid steam generation causes a high pressure in a few milliseconds (Fig.5-16). JASMINE models such phenomena by an extended multiphase flow simulation method, conventionally used for the analysis of reactor cooling system and so on.

We applied JASMINE in a probabilistic framework to evaluate the containment failure probability. We made calculations for sets of initial/boundary conditions and model parameters sampled by reflecting their probability distributions, and obtained the probability distributions of the loads. The results were compared with fragility curves of the containment vessel to evaluate the containment failure probabilities. The containment failure probabilities obtained by this method were in the range 0.01~0.1 (mean, per explosion triggering), in agreement with the values used in PSAs in the past. To get the frequency of radioactive release by a steam explosion, this result should be multiplied by the core damage frequency and the probability of the steam explosion occurrence after core damage.

This method, combining a mechanistic simulation and a probabilistic framework, gives a clear explanation for the basis of PSA results, and helps the clarification of uncertainty sources.

This work includes a part of a contract research project sponsored by Ministry of Education, Culture, Sports, Science and Technology (MEXT).

Reference

Moriyama, K. et al., Evaluation of Containment Failure Probability by Ex-Vessel Steam Explosion in Japanese LWR Plants, Journal of Nuclear Science and Technology, vol.43, no.7, 2006, p.774-784.

5-8 Containment Protection Using Natural Force

— Experiment Using Horizontal Heat Exchanger for Passive Containment Cooling System (PCCS) —

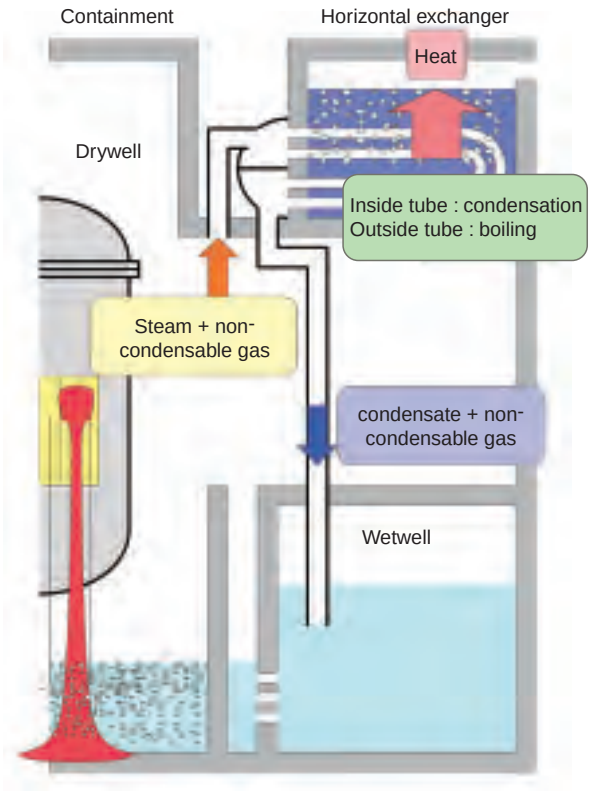

Fig.5-17 Schematic view of PCCS using horizontal heat exchanger
The steam in the drywell flows into heat exchanger driven by the pressure difference between the drywell and wetwell. The condensation in the heat exchanger suppresses the containment pressure increase. The reliability of the PCCS is so high because of the natural force that continues with steam generation in the drywell.

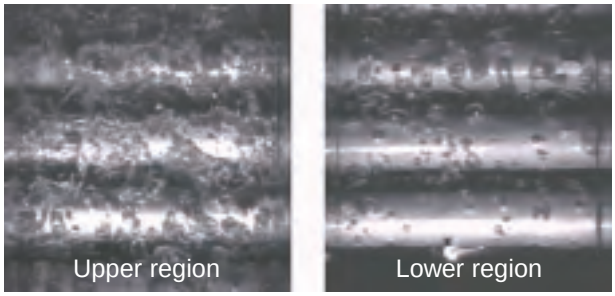

Fig.5-18 Secondary-side flow at heat exchanger
The secondary-side flow fluctuates greatly in the heat exchanger upper region, but is merely bubbly in the lower region. Three horizontal objects in each figure are condenser tubes.

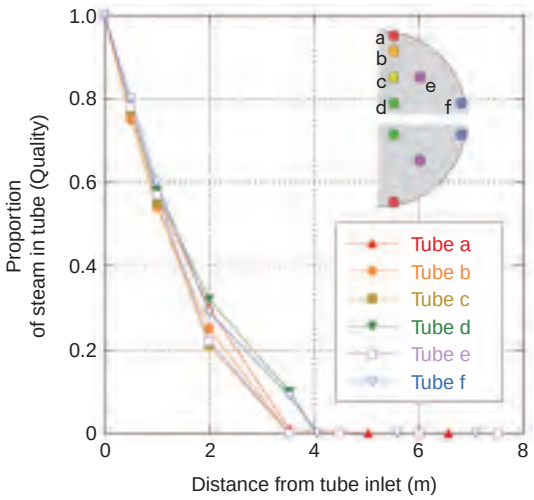

Fig.5-19 Proportion of steam in tube (Quality)
Steam condenses independently of the tube location in the tube bundle which is shown at the upper right of the figure.

The containment of a light water reactor confines radioactive materials inside. To assure this function, the containment has a safety spray system using pumps to suppress the containment pressure increase even if large amount of steam is generated in the containment. This safety feature is very important, but it may fail during a severe accident. A Passive Containment Cooling System (PCCS, Fig.5-17) that is driven by natural forces has been invented as the backup system. A PCCS drives the steam in the drywell to the PCCS heat exchanger using pressure difference, and condenses the steam utilizing pool water outside the containment to suppress the containment pressure increase. We proposed a new type PCCS that employs a horizontal heat exchanger, and confirmed the capability of the new PCCS.

The uniformity of the condensation distribution among the condenser tubes of the horizontal heat exchanger was experimentally confirmed using a prototypical-size test facility. A non-uniform condensation distribution would reduce the total heat removal capability of the heat exchanger, since some steam would flow out without condensation. Although the heat exchanger has a non-uniform distribution in the secondary-side flow due to boiling as shown in Fig.5-18, the effect on the local heat removal rate is slight, as shown in Fig.5-19. The effect of non-uniform boiling heat transfer is reduced by thermal conductivity across tube wall, resulting in rather uniform heat transfer to the non-uniform secondary-side flow among the tubes.

We confirmed that the thermal hydraulic characteristics of the horizontal heat exchanger fully satisfy the design requirements for a PCCS heat exchanger.

Reference

Kondo, M. et al., Confirmation of Effectiveness of Horizontal Heat Exchanger for PCCS, Proceedings of 13th International Conference on Nuclear Engineering (ICONE13), May16-20, Beijing, China, 2005, 50691 in CD-ROM.

5-9 Evaluating the Failure Probability of Aged Piping under Seismic Motion —Structural Reliability Evaluation of Aged Components in Nuclear Power Plants Based on Probabilistic Fracture Mechanics (PFM)—

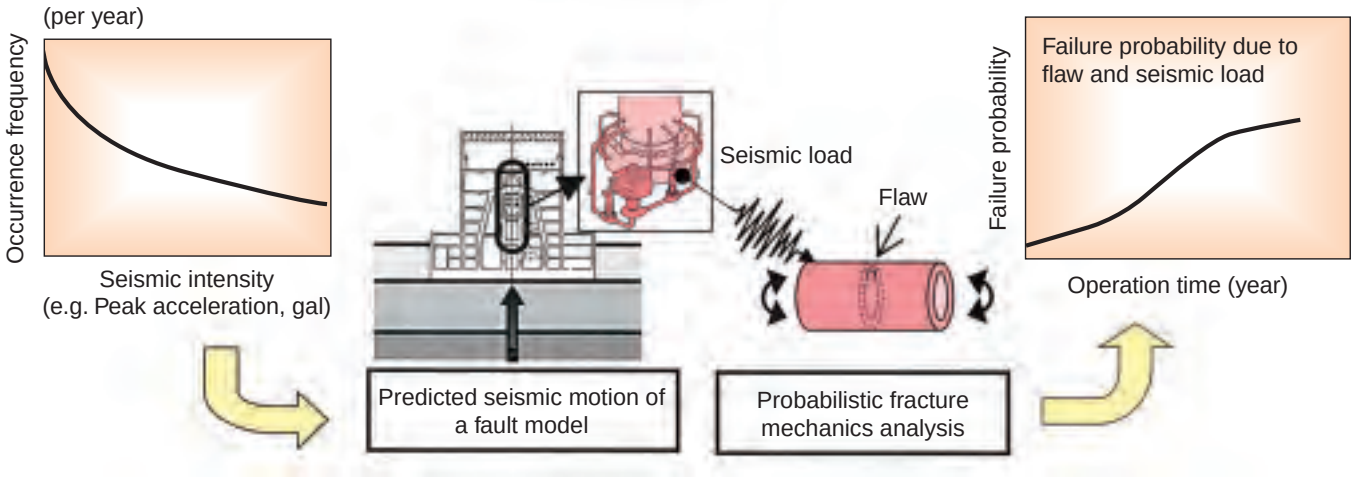

Fig.5-20 The flow of the failure probability evaluation of aged piping under seismic motion
The structural reliability of components such as aged piping during long-term operation is evaluated by PFM analysis method considering aging degradation and the relationship between seismic intensities and their occurrence frequencies (seismic hazard).

Older light water reactors (LWRs) in Japan have been operating for over 30 years. Measures need to be taken against decreases in the structural reliability induced by aging phenomena such as stress corrosion cracking (SCC). The safety evaluation based on seismic hazard for aged plants has also been an important issue. In order to evaluate the structural reliability of aged components in LWRs, the probabilistic fracture mechanics (PFM) analysis is a rational method, most suitable because the uncertainties in aging degradation and predicting seismic motion can be quantified.

We have developed a failure probability analysis method for aged piping based on PFM analysis and the latest knowledge on aging, and a seismic hazard analysis method which takes into consideration the uncertainty in predicting seismic motion. Although these methods were developed separately, we have recently established a structural reliability evaluation methodology merging them together as shown in Fig.5-20. In the first phase, the seismic hazard, i.e., occurrence frequencies of seismic motion of various intensities are evaluated based on the information on past seismic histories around LWR plants and the prediction values of seismic intensity at the plant (e.g. peak ground acceleration) upon occurrence of an earthquake. This seismic intensity is predicted by a fault model, made considering the break process of a fault and propagation characteristics inside the crust. In the next phase, failure probabilities of aged piping for various seismic motions are calculated by PFM analysis. In this analysis, SCC and fatigue crack extension under seismic load are calculated considering the scatter and uncertainties in crack initiation and growth rate, residual stress and material properties. Failure probability is calculated with the random variables expressing uncertainty by a Monte Carlo method. The structural reliability of aged piping against seismic motion can be evaluated by multiplying the failure probability as a function of seismic strength by earthquake probabilities obtained from their frequencies.

In the structural reliability evaluation of aged components under seismic motion, the prediction of the occurrence of very large seismic motion which might cause severe damages to the components is very important even if the occurrence probabilities are very small. This evaluation method developed here makes this possible.

We are going to establish more practical evaluation methods which consider the effectiveness and accuracy of in-service inspection, and will contribute to revisions of codes and standards.

Reference

Sugino, H., Itoh, Y., Onizawa, K. et al., Development of Structural Reliability Evaluation Method for Aged Piping Considering Uncertainty of Seismic Motions, Nippon Genshiryoku Gakkai Wabun Ronbunshi, vol.4, no.4, 2005, p. 233-241 (in Japanese).

5-10 Safe and Efficient Criticality Control of Spent Fuels
—Development of Calculation Code and Database for Burnup Credit—

Fig.5-21 The spent fuel isotopic composition database – SFCOMPO
SFCOMPO is now operated by OECD/NEA to obtain and evaluate new isotopic composition data of spent nuclear fuel under an international collaborative framework.
URL http://www.nea.fr/html/science/wpncs/sfcompo/

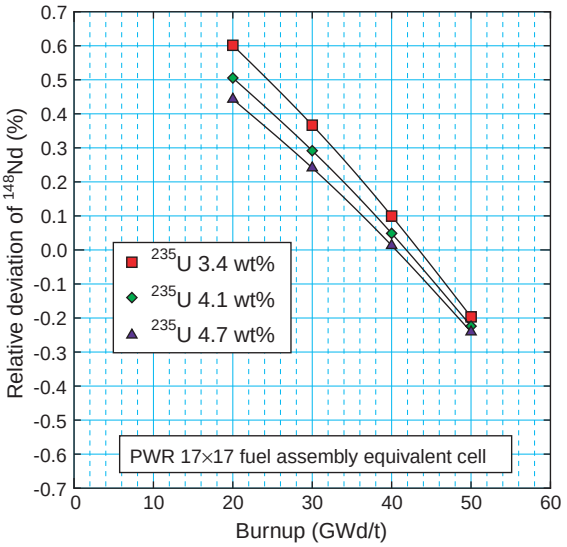

Fig.5-22 Effect of Neutron Capture Reactions of ^{147,148}Nd on ^{148}Nd (From the reference)
Burnup of spent fuel is evaluated by measurement of ^{148}Nd quantities. This figure shows that the abundance of ^{148}Nd is affected by neutron capture reactions of ^{147}Nd and ^{148}Nd. It enables us to conduct quantitative evaluation of the ^{147}Nd and ^{148}Nd effect in burnup calculations.

One of the most important issues in safety evaluation of fuel cycle facilities is to prevent a criticality accident. The neutron multiplication factor of the nuclear fuel in fuel cycle facilities decreases as the fuel burnup proceeds. In Japan, instead of burnt fuel, un-irradiated fuels are assumed in the criticality safety evaluation of fuel cycle facilities except a commercial spent fuel reprocessing plant. This is because assuming fresh fuel composition is conservative and simple. However, the economical disadvantage is large because of the excessive safety margin. For example, the number of fuel assemblies that can be transported in one time as well as stored in a facility will be decreased.

JAEA has conducted studies on burnup credit, a concept taking into account the decrease in the neutron multiplication factor with the burnup of fuel into the criticality safety evaluation.

We developed the integrated burnup calculation code system SWAT in order to evaluate isotopic composition accurately. This is because the isotopic composition of SF is a key issue in the burnup credit. SWAT will be a kernel of an integrated criticality safety evaluation code system under development for a comprehensive criticality safety evaluation including burnup calculation.

We also developed the spent fuel isotopic composition database "SFCOMPO" which arranges and archives isotopic composition data to be used for benchmarking of burnup calculation codes including SWAT. We widely distributed such data to researchers through the framework of OECD/NEA (Fig.5-21). For precise evaluation of burnup calculation codes, we evaluated error of burnup estimation by measuring changes in Neodymium-148 which are induced by neutron capture reactions. (Fig.5-22)

In summary, we are developing calculation codes and collecting experimental data which are required for expanding use of the burnup credit concept in Japan. These results are used in JAEA as well as in industries and Japan Nuclear Energy Safety Organization (JNES).

Reference

Suyama, K. et al., Effect of Neutron Induced Reactions of Neodymium-147 and 148 on Burnup Evaluation, Journal of Nuclear Science and Technology, vol.42, no.7, 2005, p.661-669.

5-11 Durability of Vitrified Concrete and Incinerator Ash

—Checking for Dissolution of Vitrified Radioactive Waste Form in Disposal Environments—

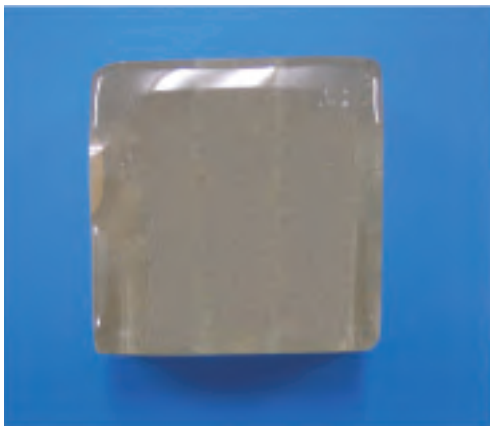

Fig.5-23 SiO_2-CaO-Al_2O_3-B_2O_3 slag sample, produced to investigate dissolution behavior
The slag sample was prepared by melting a mixture of four kind of metal oxides, silicon oxide (SiO_2), aluminum oxide (Al_2O_3), calcium oxide (CaO), and a trace amount of boron oxide (B_2O_3) at 1,600 ℃. SiO_2, Al_2O_3 and CaO represent the main components of concrete and incinerator ash.

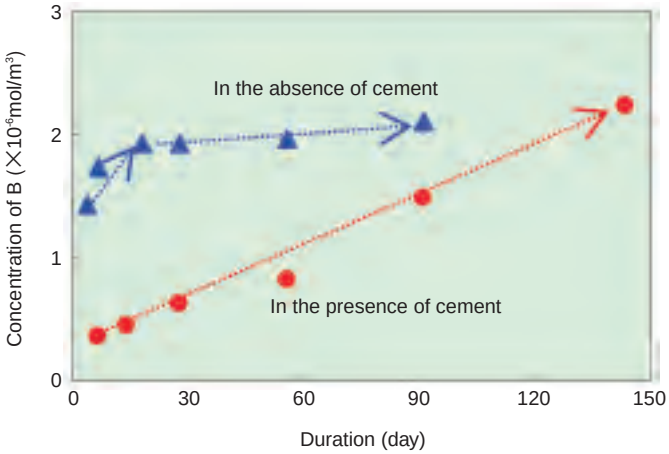

Fig.5-24 Effects of cement on dissolution of slag
Time evolution of boron (B) concentration in aqueous solutions with two leaching samples is compared. The concentration of B is used as the index of the amount of dissolved slag; B is soluble and non-sorbing so that all of the dissolved B is stably present in aqueous solutions. In the absence of cement, the amount of dissolved slag is five times higher than that in the presence of cement for the first several days, and in around 30 days the amount of dissolved slag becomes constant (2×10^{-6}mol/m^3). In the presence of cement, the dissolution rate of slag is constant through test runs of 150 days, and this trend seems to continue even longer.

Radioactive wastes of different properties are generated from nuclear facilities. The radioactive wastes contain non-metallic wastes such as concrete, incinerator ash and filters. Non-metallic wastes are molten at about 1,500 ℃ and then cooled, yielding a vitrified waste form (slag). Fig.5-23 shows a slag sample specimen prepared from simulated waste (a mixture of SiO_2, Al_2O_3, CaO and B_2O_3). This solidification (vitrification) method is advantageous in volume reduction, chemical homogenization of waste form and immobilization of radionuclides in the waste form. This method has been already introduced in the former JAERI and some nuclear power plants. We investigated durability of the vitrified waste form in the disposal environment. The acquired data will be available for safety assessment of waste disposal.

It is considered that the long-term chemical durability of slag is affected by alkaline components leached from extensively used cementitous materials in the envisaged disposal environment. Therefore, we studied the effects of alkaline environments on slag dissolution. We conducted lab-scale leaching tests for slag specimens in the presence and the absence of cement. The ordinary Portland cement, widely used in civil engineering and construction work, was employed in the tests. It is found that, in the absence of cement, the dissolution of slag rapidly increased for the first several days and leveled off (Fig.5-24). This is because the leached silicon (Si), the main component of slag matrix, reached saturation in the contacting aqueous solution during the first several days, and then the dissolution was depressed. However, in the presence of cement, the dissolution of slag continued at a constant rate through the test period (Fig.5-24). This trend can be interpreted as follows. Silicon leached from the slag interacts with calcium supplied from cement to form precipitates of calcium silicate hydrates. The precipitation consumed Si from the aqueous solution and the concentration of Si was kept lower than saturation. This experimental result indicates that dissolution of slag possibly continues over a long time period at a constant dissolution rate in a disposal environment with a large quantity of cement.

The information acquired in this study will help in constructing a source term model of safety assessment computer codes where a longer-term, constant-dissolution rate of slag waste form is taken into account.

Reference

Maeda, T. et al., Dissolution Behavior of Slag in the Presence of Cement, Nippon Genshiryoku Gakkai Wabun Ronbunshi, vol.4, no.4, 2005, p.242-247 (in Japanese).

6 Advanced Science Research

6-1 Advanced Basic Research to Create the Future

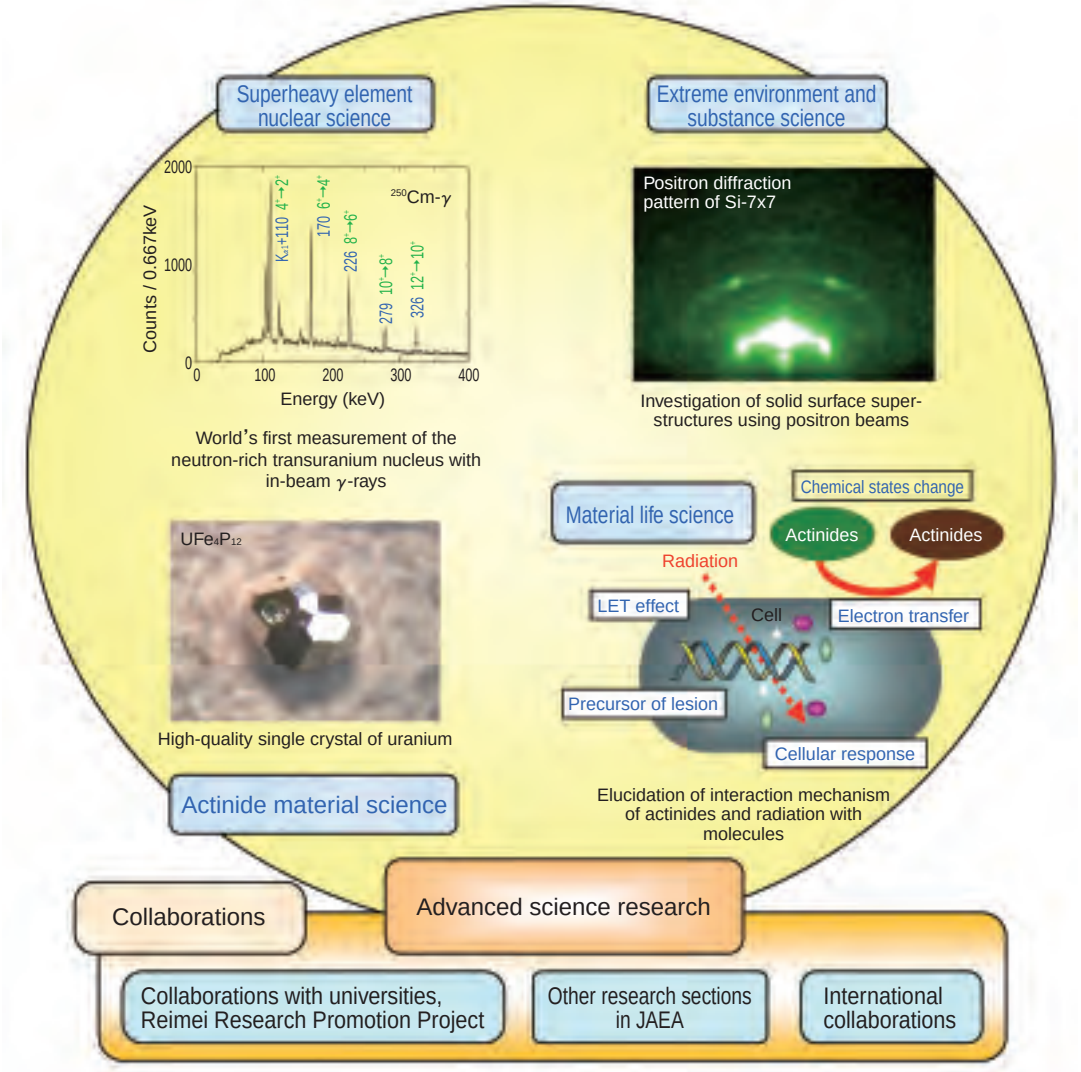

Fig.6-1 Four research fields in Advanced Science Research Center

In the Advanced Science Research Center, new frontier research of nuclear energy and ionizing radiation in the future is conducted to discover new principles and phenomena, and furthermore to create new materials and technologies. In order to achieve these aims, we have four basic policies; (1) to pursue research for which the high level research capability (researchers and facilities) in JAEA is effectively used and which is difficult to do in other research organization, (2) to achieve results ahead of the rest of the world, (3) to nurture a new basic research area until it becomes fruitful, (4) to explain and apply the research, thus fulfilling our responsibility to society, in conformity to the Third Science and Technology Basic Plan.

The following research is going on: nuclear physics and nuclear chemistry of superheavy element, the nuclear shell structure, reaction dynamics and electrochemistry using heavy-ion beam of accelerator; synthesis of uranium and transuranium compounds and measurement of their macroscopic quantities and electronic structure; clarification of magnetic structure, magnetic excitation, and the mechanism of superconductivity by using NMR, μSR, neutron scattering, and theoretical methods; design of novel materials using mega - gravitation and nano - particle deposition; topmost surface studies using bright and coherent positron beams; study on information transmittance among hierarchical structure in strongly correlated supermolecular systems; elucidation of interaction mechanism of heavy elements and ionizing radiation with cells and molecules by spectroscopy.

In order to promote this research, we are collaborating with other research sections in JAEA and several international collaborations are ongoing. In addition, we accept new research subjects based on public suggestions within the framework of the Reimei Research Promotion project of JAEA.

6-2 Investigation of Stability of the Nucleus through Deformed States
—Observation of Rotational States in the Neutron-Rich ^{250}Cm Nucleus—

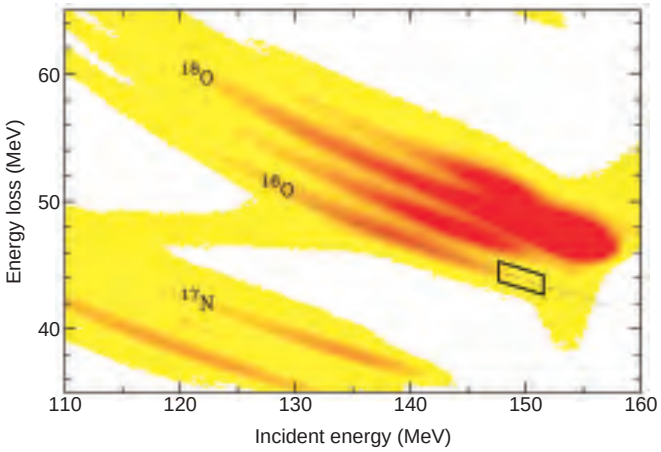

Fig.6-2 Distribution of scattered particles
Particles emitted by the reaction of ^{18}O(162MeV) + ^{248}Cm were measured by a Si ΔE-E detector. When the ^{16}O particle has the kinetic energy indicated by the enclosed area, ^{250}Cm emits no neutrons.

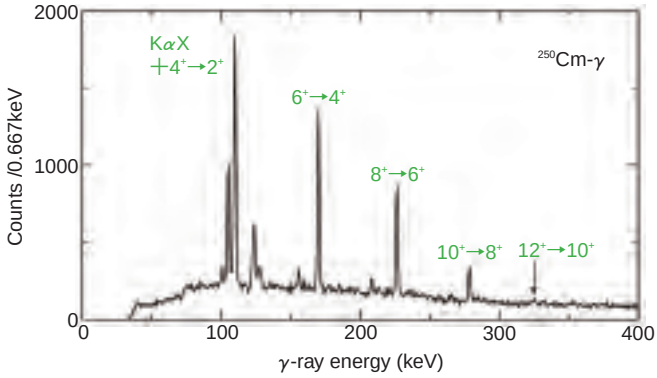

Fig.6-3 Energy spectrum of γ-rays in ^{250}Cm
This spectrum was obtained at the same time as the ^{16}O particle emission in the enclosed area in Fig.6-2. This energy spectrum shows a characteristic of the rotational band - almost equal energy spacing between the γ-rays.

Nuclei used for atomic energy, such as uranium and plutonium, are known to be spheroidal in shape. A shell structure emerges in such deformed nuclei as well as in spherical nuclei. Which nucleus has a closed shell? This is one of the most important issues in nuclear physics, a quantum many-body problem involving protons and neutrons.

The nuclear structure of neutron-rich transuranium nuclei has not been studied because of experimental difficulties. We have studied the neutron-rich nucleus curium-250 (^{250}Cm) produced by the two-neutron transfer reaction with an oxygen-18 (^{18}O) beam and a ^{248}Cm target using the tandem accelerator. Deformed states in ^{250}Cm were revealed by measuring the prompt γ-rays emitted at the reaction.

It is essential to distinguish γ-rays from ^{250}Cm from those of an enormous amount of other reaction products. We have, therefore, developed a high-resolution transmission-type Si detector (ΔE) to distinguish reaction products; energy loss in the Si ΔE detector is proportional to mass number and squared atomic number and inversely proportional to kinetic energy of the incoming particle. As shown in Fig.6-2, scattered particles are clearly separated by mass and atomic number. When the ^{16}O particle is emitted, the residual nucleus of ^{250}Cm is produced. Fig.6-3 shows the γ-ray spectrum at the same time as the ^{16}O particle emission in the enclosed area indicated in Fig.6-2, where the excitation energy of ^{250}Cm is below the neutron separation energy. This spectrum shows a typical rotational band up to 12^+, with almost the same energy differences between neighboring γ-rays. The ^{250}Cm nucleus has the largest neutron number among nuclei whose high-spin states were observed.

The moment of inertia of a rotational band, derived from the excitation energies, gives information about a closed shell. On the surface of deformed nuclei, superfluid states, which do not contribute to the moment of inertia, are formed owing to the parings of nucleons. In the deformed nucleus with a closed shell, the pairing strength is weakened, and thus, the moment of inertia becomes larger. The moment of inertia for $^{250}Cm_{154}$ was found to be significantly smaller than that of $^{248}Cm_{152}$. This indicates that Cm nucleus has a closed shell where N=152. We will further study the dependence of this closed shell on atomic number and elucidate the mechanism of evolution of the shell structure.

Reference

Ishii, T. et al., Ground-State Band of the Neutron-Rich Transuranium Nucleus $^{250}Cm_{154}$, Journal of the Physical Society of Japan, vol.75, no.4, 2006, p.043201-1-043201-4.

6-3 How Far Does the Area of Superheavy Elements Extend?
－Decay Modes of Heavy and Superheavy Nuclei－

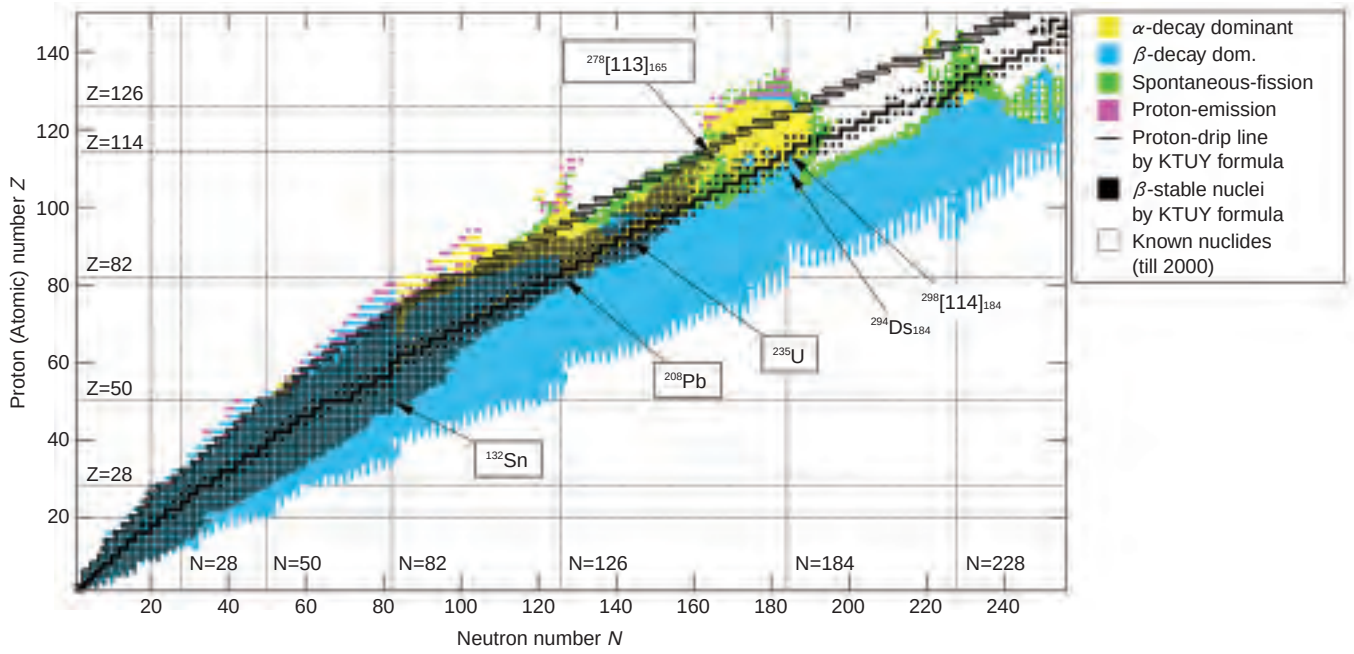

Fig.6-4 Dominant decay mode of nuclei: α-decay, β-decay, spontaneous fission or proton emission
The nuclear decay mode with the shortest partial half-life among probable nuclear decays, the dominant decay mode, is shown for each nucleus. We consider four decay modes, namely, α-decay, β-decay, proton emission and spontaneous fission in this calculation. Only nuclides with half-lives of 1 nanosecond or longer are plotted.

Nucleus is a composite system consisting of protons and neutrons, and approximately 3000 nuclides have been identified. However, the existence of much more nuclides is postulated theoretically. How far the area of nuclei extends is an essential and important question in nuclear physics.

We have developed an original model based on the macroscopic and mean-field models to describe the global features of nuclear masses, called the KTUY (Koura-Tachibana-Uno-Yamada) nuclear mass model. By using the KTUY model, we have studied decay modes for α-decay, β-decay, proton emission and spontaneous fission ranging from light nuclei to superheavy nuclei including unknown ones, and estimated the dominant nuclear decay modes as shown in Fig.6-4. This figure shows the existence of an "island of stability for the superheavy nuclei" around $^{298}[114]_{184}$. We also could obtain the nucleus with the longest total half-life among neighboring nuclei, $^{294}Ds_{184}$ (Z=110), which is on the β-stability line of our model. This is an α-decay-dominant nucleus, and has a half-life on the order of 100 years.

We also estimated decay modes of nuclei beyond the superheavy ones and find the next "island of stability" on *N*=228 line in the neutron-deficient region. This is caused by the larger fission-barrier height due to the shell closure with 228 neutrons. Another region with similar tendency is found near *N*=126 outside the proton-drip line. On the neutron-rich side, nuclei are mostly β-decay dominant and have relatively long total half-lives, at least on the order of 1 ms.

References

Koura, H. et al., Nuclidic Mass Formula on a Spherical Basis with an Improved Even-Odd Term, Progress of Theoretical Physics, vol.113, no.2, 2005, p.305-325.

Koura, H. et al., How Far does the Area of Superheavy Elements Extend? －Decay Modes of Heavy and Superheavy Nuclei Predicted by a Mass Formula－, Nippon Butsuri Gakkai-shi, vol.60, no.9, 2005, p.717-724 (in Japanese).

6-4 First Identification of Quantum States in Superheavy Nuclei

—Nuclear Structure Studies for Superheavy Nuclei through α-γ Spectroscopy—

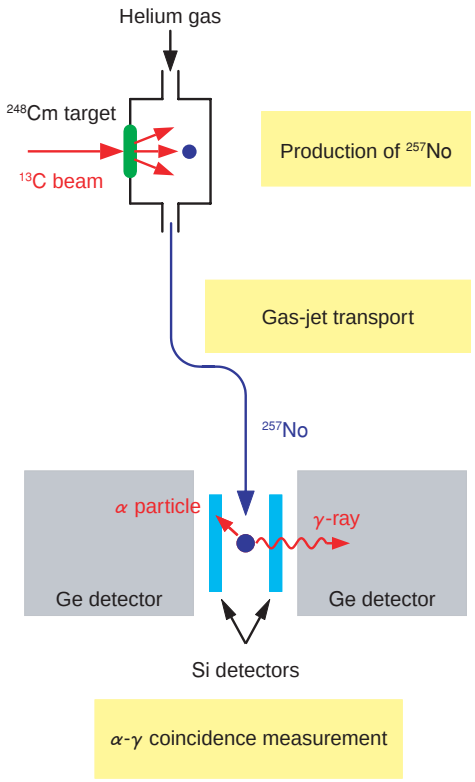

Fig.6-5 Production of ^{257}No and α-γ coincidence measurement
The ^{257}No nuclei were produced by bombarding a ^{248}Cm target with a ^{13}C beam, and transported into a detector station within 1 s using the gas-jet transport technique. α-particles and γ-rays were detected with high efficiency using Si and Ge detectors, respectively.

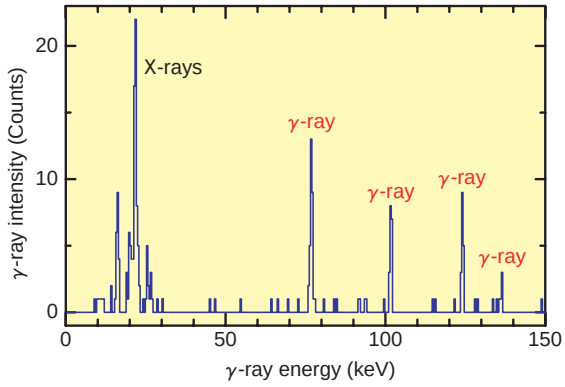

Fig.6-6 γ-ray spectrum of ^{257}No
Four γ-rays and characteristic X-rays associated with the α decay of ^{257}No were observed.

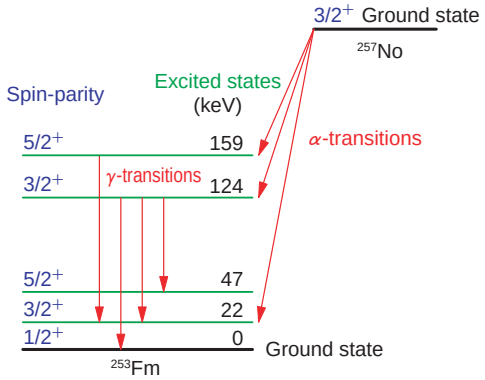

Fig.6-7 Quantum states in ^{257}No and ^{253}Fm
Energies and spin-parities of excited states of ^{253}Fm as well as the ground state of ^{257}No were identified for the first time.

The very heavy nuclei containing more than 100 protons are called "superheavy nuclei". The superheavy nuclei are very unstable because of Coulomb repulsion among the many protons. Thus, they cannot exist without an additional stabilizing effect that originates from nuclear shell structure. How heavy nuclei can exist? How stable are they? The answers strongly depend on the shell structure of superheavy nuclei.

Since the production of superheavy nuclei is extremely difficult, the discovery of the superheavy nuclei was the first aim in previous studies. However, beyond this, if excited states of superheavy nuclei are investigated in detail, the shell structure of superheavy nuclei can directly be clarified. In this work, we have successfully measured γ-rays from the α decay of nobelium-257 (^{257}No), an isotope of the 102nd element, and investigated its quantum level structure. This is the first detailed spectroscopic study of superheavy nuclei.

The ^{257}No nuclei were produced by bombarding a curium-248 (^{248}Cm) target with a carbon-13 (^{13}C) beam accelerated by the JAEA Tandem Accelerator. The ^{257}No nucleus decays with an α-particle emission with a half-life of 25 s, and its α-particles and accompanying γ-rays were measured with high efficiency (Fig.6-5). In previous studies for superheavy nuclei, only a few or at most 100 α-particles could be detected. In this study, we have detected 5000 α-particles of ^{257}No and observed 4 γ-transitions in coincidence with these α-particles (Fig.6-6). As a result, excited states of the daughter nucleus fermium-253 (^{253}Fm) have been established as shown in Fig.6-7, and spin-parities of the ground state of ^{257}No as well as the excited states of ^{253}Fm have been identified for the first time.

This is the first successful γ-ray measurement and first spin-parity assignment for such heavy nuclei. The present result revealed that the spin-parity of the ground state of ^{257}No is different from that expected. The experimental identification of quantum states in superheavy nuclei enables us to test the validity of various theoretical calculations. This is a great advance in elucidating the shell structure of superheavy nuclei.

Reference

Asai, M. et al., Experimental Identification of Spin-Parities and Single-Particle Configurations in ^{257}No and Its α-decay Daughter ^{253}Fm, Physical Review Letters, vol.95, 2005, p.102502-1-102502-4.

6-5 Investigation of New Plutonium-Based Superconductor

—Identification of Exotic Superconducting State by Nuclear Magnetic Resonance—

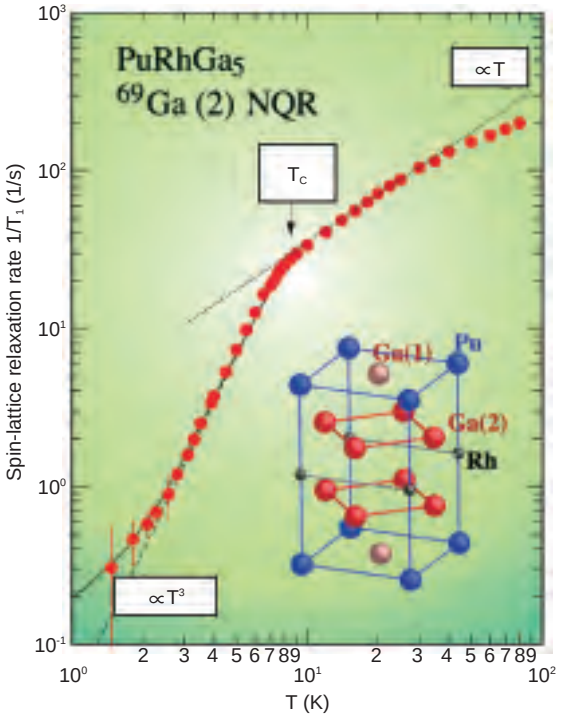

Fig.6-8 T-dependence of spin-lattice relaxation rate ($1/T_1$) in superconducting $PuRhGa_5$
No coherence peak appears just below T_c, and $1/T_1$ is proportional to T^3 below T_c, indicating non-conventional superconductivity. The tetragonal crystal structure is shown in the inset.

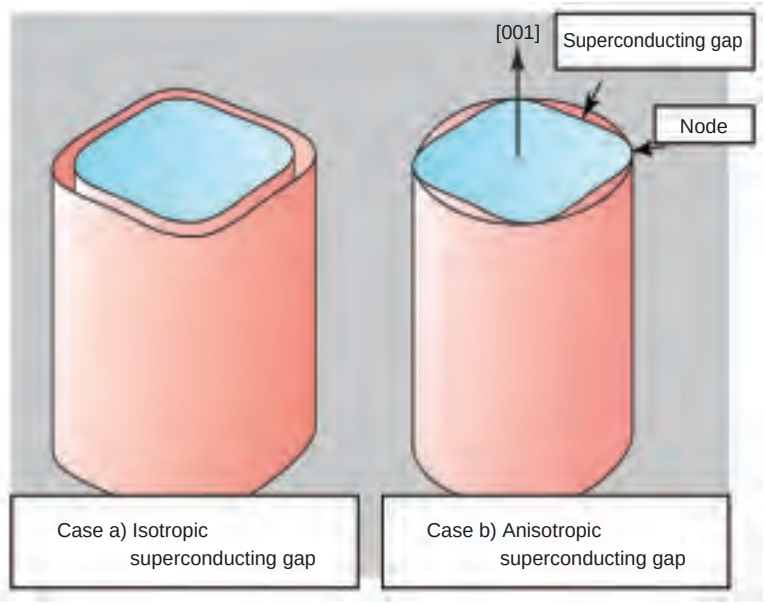

Fig.6-9 Two dimensional Fermi surfaces with d - wave superconducting gap
In the non-conventional superconductor, the superconducting gap has nodes.

In uranium and transuranium compounds, many exotic magnetic and superconducting states due to strong correlation of electrons have been found. We have synthesized a single crystal of a new superconductor $PuRhGa_5$ for the first time and clarified its exotic superconducting state by the nuclear magnetic resonance (NMR) measurements. In order to clarify the superconducting state, the spin-lattice relaxation rate ($1/T_1$) is particularly important. The BCS model theory for ordinary superconductors is well established, since measurements of ($1/T_1$) show the coherence peak just below T_c predicted by the BCS model.

In the present study, the nuclear quadrupole resonance of ^{69}Ga nuclei has been observed at zero field. Because of the zero field measurement, no distribution of superconducting order parameter due to the mixed state occurs. Fig.6-8 shows the T-dependence of $1/T_1$. The important point here is that no coherence peak just below T_c is observed, $1/T_1$ decreasing with decreasing T in the superconducting state. This fact indicates that the superconducting state in this compound is a non-conventional one with an anisotropic superconducting gap. In ordinary superconductors, $1/T_1$ is proportional to $\exp(-\Delta/T)$ below T_c. In contrast, T-dependence of $1/T_1$ shows a power law behavior: $1/T_1 \propto T^n$ in a non-conventional superconducting state. In $PuRhGa_5$, n is estimated as 3. The value of n reflects the type of anisotropy in the superconducting gap. From measurements of the upper critical field H_{C2}, it was revealed that the Fermi surface has a two dimensional nature. Combined with this fact, the observed T-dependence can be well reproduced by a model of two dimensional Fermi surfaces whose gap disappears at some points (nodes) (Fig.6-9) and a residual density of states due to defects.

As described above, we have identified an exotic superconducting state in a Pu-based new superconductor and now we will be investigating this origin of the non-conventional superconductivity.

Reference

Sakai, H. et al., Anisotropic Superconducting Gap in Transuranium Superconductor $PuRhGa_5$: Ga NQR Study on a Single Crystal, Journal of the Physical Society of Japan, vol.74, no.6, 2005, L1710-1713.

6-6 Magnetism of Plutonium-Metal Probed by μSR
—An Unsolved Problem of Solid State Physics—

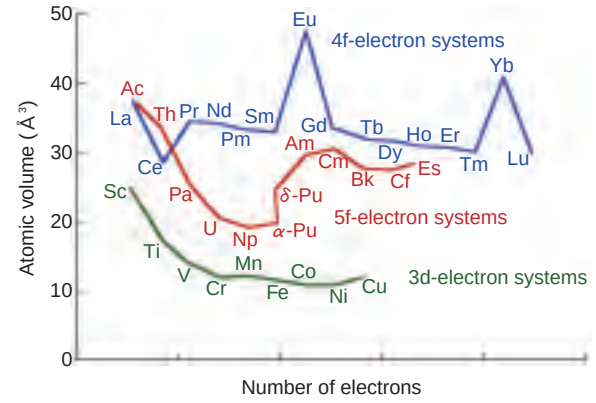

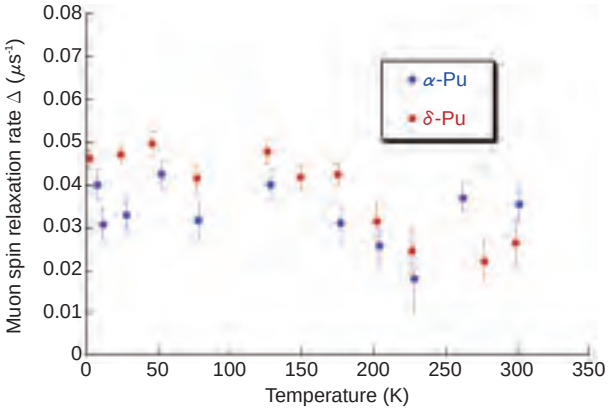

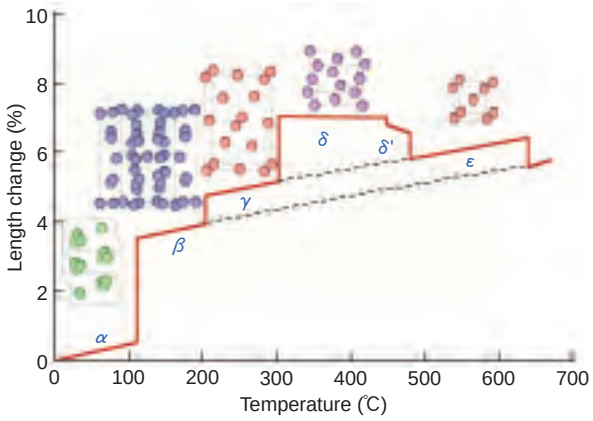

Fig.6-10 (upper left) Atomic volume in 3d, 4f and 5f-electron systems
The systematic changes in volume reflect the degree of electron localization.

Fig.6-11 (upper right) Structural Change of Plutonium
The six-distinct solid state phases of plutonium. Plutonium's 5f-electrons play a dominant role in this complexity.

Fig.6-12 (lower left) Temperature dependence of the muon spin relaxation rate
These results indicate the absence of long- or short range magnetic ordering in either δ-Pu or α-Pu.

Actinide compounds (5f-electron systems) possess atomic volumes intermediate between 3d- and 4f-electron systems (Fig.6-10). Since this volume helps to determine the strength of electron localization, studies of the electronic properties of 5f-electron systems are quite important for a systematic understanding of solid state materials. Generally, 5f-electron systems are less studied than other systems, and, therefore, many unsolved actinide problems exist. Among them, one of most interesting is whether or not plutonium (Pu) metal is magnetic. Pu exits in six different allotropic phases as a function of temperature and volume (Fig.6-11). Interest has centered on the δ-phase, which has a unit cell volume which is 26 % larger than the α-Pu. Theoretical calculations attribute the large volume increase in δ-Pu to the partial localization of the 5f-electrons. Because of this partial localization many theories of the electronic structure in δ-Pu have predicted magnetic order. There is, however, a clear lack of experimental evidence for such ordering in the ground state of δ-Pu.

Given this situation, we undertook μSR experiments on α-Pu and Ga-stabilized δ-Pu (4.3 at. % Ga) designed to answer the question: can magnetism, either ordered or disordered freezing of the spins, be completely eliminated in Pu metal? μSR is an excellent probe to address this issue because of its high sensitivity to weak magnetism.

The temperature dependencies of the muon relaxation rates Δ in α-Pu and δ-Pu under zero applied magnetic field are shown in Fig.6-12. The rates are small and independent of temperature below about 100 K; the reduction in Δ above 150 K is due to muon diffusion. The uniform ordering of Pu moments of any significant size, or the disordered spin freezing of such moments, would produce either a precessing μSR signal below the ordering temperature (which is not observed) or a temperature-dependent, exponential rate ten times that which is observed. The fundamental conclusion from our experiments is, therefore, that *there is no evidence for any magnetic ordering in Pu metal whatsoever down to T ≅ 4 K*. Thus, our results are incompatible with any theories predicting magnetism in δ-Pu for T ≥ 4 K. Currently, the electronic structure in δ-Pu incompletely understood. These results reflect the complexity of 5f electron systems.

Reference

R.H. Heffner et al., Limits for Ordered Magnetism in Pu from Muon Spin Rotation Spectroscopy, Physical Review B, vol.73, 2006, p.094453-1-094453-5.

6-7 New Surface Structures Found with Bright Positron Beam
—Surface Dynamics Revealed by Positron Total Reflection—

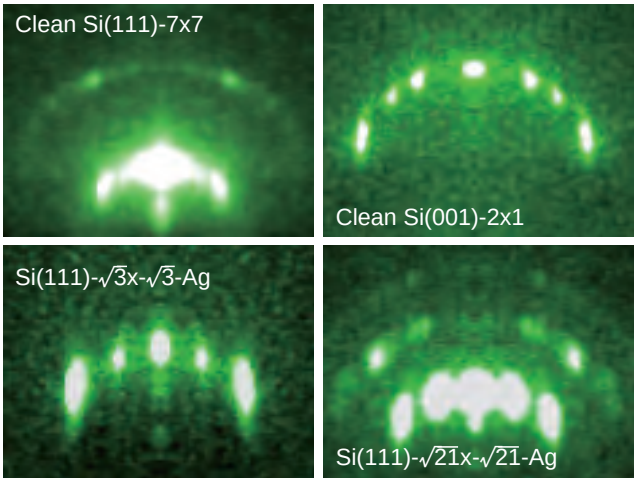

Fig.6-13 Positron diffraction patterns from various surface super-structures obtained for the first time, by a bright positron beam
The Clean Si(111)-7x7 is formed during cooling of a heated Si(111) surface. The clean Si(001)-2x1 is formed during cooling of a heated Si(001) surface. Si(111)-$\sqrt{3}\times\sqrt{3}$-Ag is formed by depositing 1 ML of silver atoms on a Si(111) surface. Si(111)-$\sqrt{21}\times\sqrt{21}$-Ag is formed by depositing 0.14 ML of silver atoms on a Si(111)-$\sqrt{3}\times\sqrt{3}$-Ag surface.

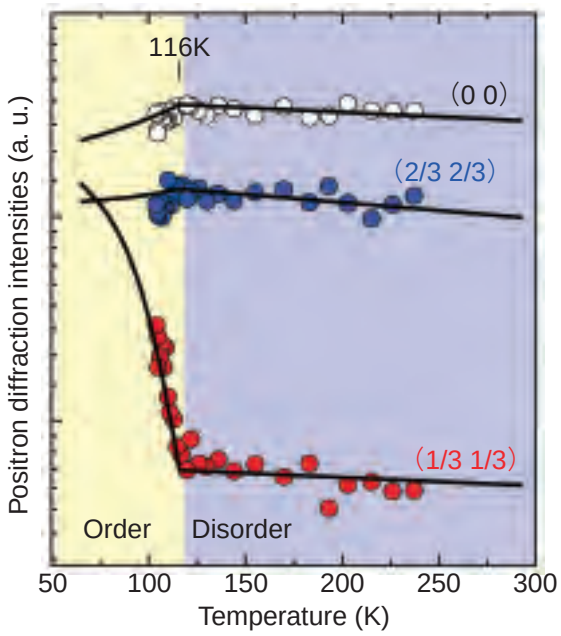

Fig.6-14 Temperature dependences of positron diffraction intensities from a silver super-structure on Si
The silver super-structure on Si is formed by 1 ML silver deposition onto a Si-7x7 surface. The positron diffraction intensities from this surface dramatically change at a critical temperature of 116 K. By a detailed analysis, this phase transition is interpreted as a order-disorder phase transition.

Positron is the anti-particle of an electron. Its rest mass and spin magnitude are the same, but the charge is positive. A well-collimated and highly parallel positron beam is totally reflected at a material's surface with negligible penetration into the bulk at small enough glancing angles. Since the total reflection intensity of a positron beam is sensitive to the surface state, one should be able to study material surfaces in greater detail than existing methods.

To observe positron diffraction patterns of total reflection, we need to have a brighter positron beam. Traditional positron beams generated using simple extraction grids and electrostatic lenses are insufficient. We attempted to generate a positron beam using an immersion lens system composed of several pinhole electrodes, and electro-magnetic lenses similar to those in electron microscopes. Consequently, we obtained a positron beam whose brightness is one order of magnitude greater. Using this positron beam, we succeeded in observing the positron diffraction patterns produced by total reflection from some surface super-structures for the first time (Fig.6-13). Currently, we are probing several surface super-structures by the bright positron beam. Here, we introduce our study of phase transition of silver super-structure on Si as an example.

By depositing 1 ML silver atoms onto a Si-7x7 surface, a silver super-structure having a new periodicity is formed. Conventional electron and X-ray diffraction methods cannot determine the silver coordinates precisely due to their low surface sensitivities. The mechanism of the phase transition of silver super-structure on Si has not yet been clarified. We investigated the temperature dependences of positron diffraction intensities from the silver super-structure on Si (Fig.6-14). Here, (0 0), (1/3 1/3) and (2/3 2/3) are diffraction spots. The (1/3 1/3) spot intensity exhibits a dramatic change at T=116K. This indicates phase transition. In the phase transition models proposed based on electron and X-ray diffraction studies, the above result is not explained. By detailed analysis, we found that the observed temperature dependences are well reproduced by an order-disorder phase transition. This settles the long debate on the phase transition of the silver super-structure on Si.

Thus, we demonstrated that diffraction of a bright positron beam is useful to reveal new aspects of material surfaces.

Reference

Kawasuso, A. et al., A Coherent Positron Beam for Reflection High-Energy Positron Diffraction, Review of Scientific Instruments, vol.75, 2004, p.4585-4589.

6-8 Mineralization of Uranium by Yeast

—Elucidation of Mechanism of Uranium Mineralization by Microorganism—

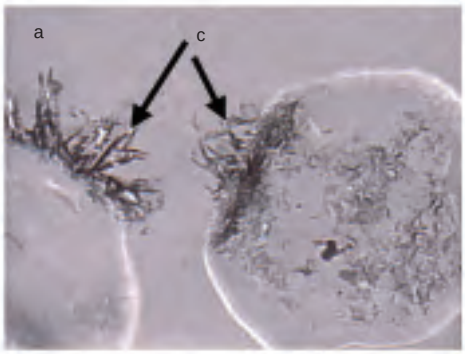

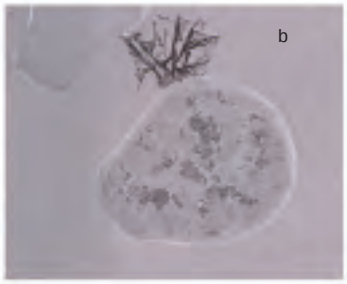

Photo 6-1 Transmission electron microscopy photographs of yeast cells exposed to a uranium solution (a, b)
Yeast cells are the ellipsoidal shapes. Cell size is several μm. Arrow c shows the needle-like uranyl-phosphate minerals developed outward from the cell surface; part of the uranium minerals intrude inside of the cells.

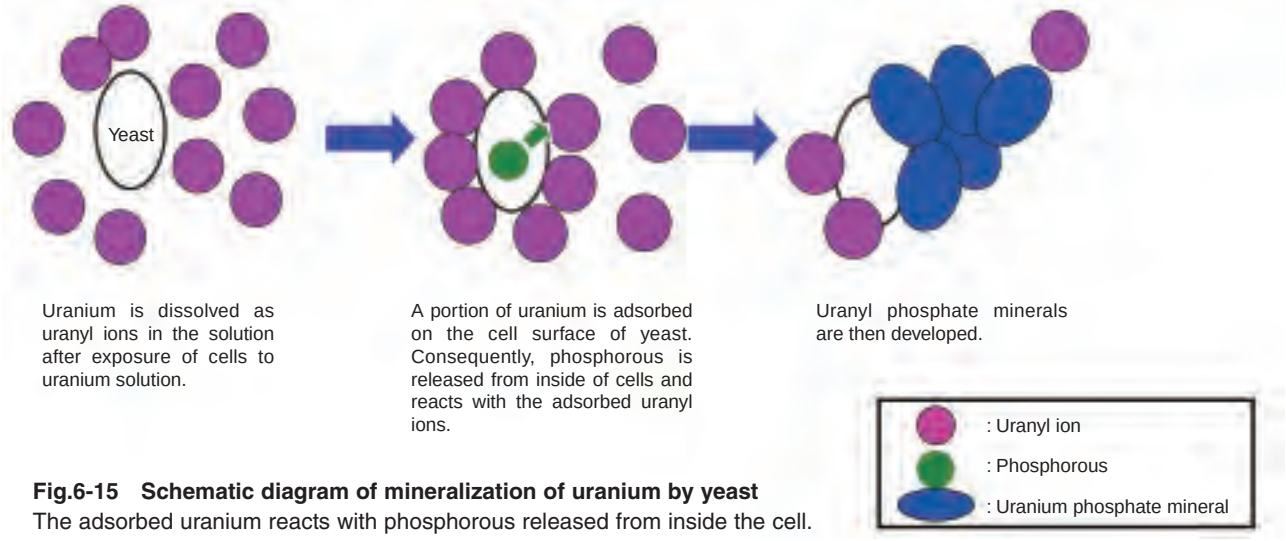

Fig.6-15 Schematic diagram of mineralization of uranium by yeast
The adsorbed uranium reacts with phosphorous released from inside the cell.

"Yeast" is a single-celled fungus which multiplies by budding, associated with wine, beer, Japanese sake, and bread, but there is more to this organism. We have been conducting research to elucidate the interaction mechanisms of heavy elements with microorganisms. Through this research, we found that a strain of wine yeast mineralized uranium on the cell surface. We clarified the mechanism of the mineralization. Although this strain of wine yeast is presently just waste after the brewing of wine, it can used for long term confinement of uranium contained in naturally occurring radioactive material (NORM).

On the cell surface of yeast, adsorbed uranium reacts with phosphorous released from inside the cells. Consequently, uranyl phosphate minerals develop on the cell surface. It is known that uranyl ions are precipitated on the cell surface of microorganisms. However, the mechanism of the precipitation is not fully understand. We carried out an experiment exposing the cells of a strain of wine yeast to a uranium solution. We monitored change of uranium concentration with exposure time. The results showed that some uranium accumulated on the yeast cells. We analyzed yeast cells by transmission electron microscopy (TEM), and found that uranium bearing materials had developed on the cell surface (Photo 6-1). TEM, electron diffraction patterns and UV visible spectrometry indicated that uranyl phosphate minerals had developed on the cell surface, and that part of the minerals were in the intracellular region. On the contrary, no mineral was distinguished on the cells grown in a phosphorous starved medium. These results strongly suggest that uranyl phosphate minerals are formed at the cell surface by the reaction of the adsorbed uranium with phosphorous released from inside of the cells (Fig.6-15). Interestingly, concentrations of uranium and phosphorous and pH were below saturation levels for formation of uranyl phosphate minerals. These results indicate that cell surface creates specific conditions different from the bulk solution, where local saturation generating the minerals is attained.

Yeast is a eucaryote whose DNA sequence analysis has been completed. We are planning to identify the proteins which accumulate uranium in order to elucidate the accumulation mechanism of uranium at the molecular level.

Reference

Ohnuki, T. et al., Mechanisms of Uranium Mineralization by the Yeast Saccharomyces cerevisiae, Geochimica et Cosmochimica Acta, vol.69, 2005, p.5307-5316.

7 Nuclear Science and Engineering Research

7-1 Formation of Basis for R&D on Nuclear Energy, and Creation of Innovative Nuclear Energy Utilization Technology

Fundamental nuclear science and engineering research is being conducted to form a base for Japan's R&D on nuclear energy, and to create innovative technologies applying nuclear energy. The fundamental engineering activities have the following four roles.

(1) Formation of the basis for innovative nuclear energy technology (such as high - temperature gas - cooled reactor/hydrogen production, and partitioning and transmutation)
(2) Support of development of applications and technology, and governmental policy regarding nuclear energy inside and outside JAEA (such as nuclear safety basis formation, technology for non-proliferation analysis)
(3) Provision of platform of nuclear energy R&D to industry and academia
(4) Organization of technology forming the basis of these activities mentioned above, and provision of it to society (such as nuclear data, nuclear/thermal design code, environment technology)

In order to carry out these roles, nuclear data and reactor engineering, fuel and material engineering, environment and radiation science, nuclear transmutation technology and nuclear applied heat technology are being studied.

Nuclear Data and Reactor Engineering

Various types of research are being performed to investigate the feasibility of advanced and innovative nuclear systems and to establish technical bases for these systems, comprising nuclear data, advanced nuclear, thermal design methods, etc.

An advanced reactor physics code system is being developed to establish nuclear design methods, which do not need large-scale mockup tests, for advanced LWRs (light water reactors) and innovative reactors. The Japanese Evaluated Nuclear Data Library (JENDL) has been developed, especially for minor actinides (MA) and fission products (FP), as basic data used in nuclear research and development fields. Nuclear reaction mechanism and structure have been studied to get reliable and accurate nuclear data for MA and long life fission products by utilizing high-resolution and high-sensitivity gamma ray detection techniques.

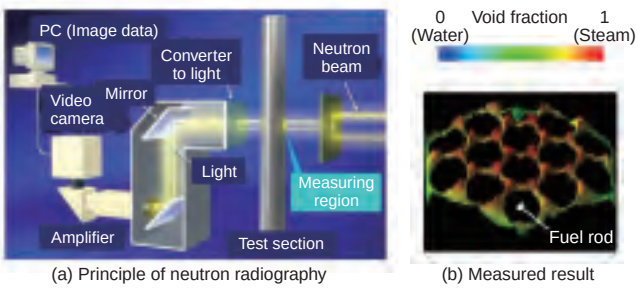

(a) Principle of neutron radiography (b) Measured result

Fig.7-1 Void fraction profile in a fuel assembly measured by NRG
Neutrons are absorbed well by water, poorly by metal. The void fraction profile inside a complicated test section such as fuel assembly can be measured by neutron radiography (NRG).

Detailed two-phase analysis codes with supercomputing technology as well as model experiments for code validation are being developed to establish new thermal design methods which do not need large-scale thermal hydraulic tests. Three-dimensional thermal-hydraulic measurement with neutron radiography has been developed to build a detailed database for code validation(Fig.7-1).

Fuels and Materials Engineering

To form the basis of an advanced nuclear fuel cycle and safety & reliability of nuclear power plants, fuels and materials research are carried out.

In the advanced nuclear fuel cycles, minor actinides (MA: Np, Am, Cm), which are classified as high level radioactive wastes in the current nuclear fuel cycle, are to be recycled to reduce the burden of waste disposals. To develop this technology, understanding and controlling of MA behaviors in the system are necessary. R&D on new extractants for MA separation based on actinide solution chemistry, fundamental technology for advanced aqueous MA separation processes, pyrochemical process for treating MA-bearing fuel, and fabrication technology and property measurements of MA-bearing fuels (Fig.7-2) are being made in advanced experimental facilities.

The materials used for nuclear reactors and reprocessing plants should maintain their integrity under irradiation and corrosive environments. For the advanced reactors, the materials are needed to have resistance against still more severe environments. R&D on irradiation effects of materials for nuclear reactors, the mechanism of stress corrosion cracking of reactor structural materials, and corrosion mechanism of reprocessing plant materials are being carried out.

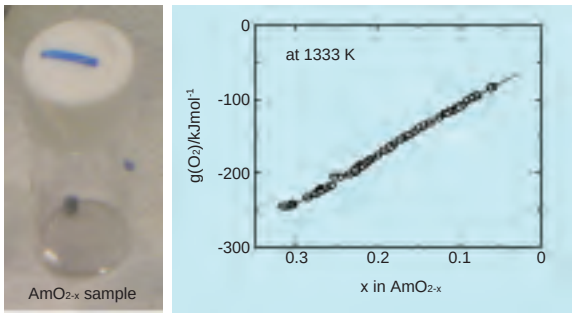

Fig.7-2 AmO_{2-x} sample and its oxygen potential ($g(O_2)$).
The oxygen potential of AmO_{2-x} was measured as a function of oxygen deficiency (x). This fundamental property is needed to evaluate and predict behaviors of MA-bearing fuels during irradiation and fabrication.

Environment and Radiation Sciences

The R&D on environmental behavior, radiation protection and technology for non-proliferation are carried out to contribute the promotion of nuclear energy.

In environmental research, the elucidation and prediction of the behavior of materials in atmospheric, oceanic and terrestrial regions (Fig.7-3) are studied. For radiation

protection, research on molecular mechanisms of biological low-level dose radiation effects, radiation dosimetry of neutrons from high-energy accelerators, and shielding evaluation for various radiations are performed. To support non-proliferation, technology for safeguards and CTBT (Comprehensive Nuclear-Test-Ban Treaty) is being developed.

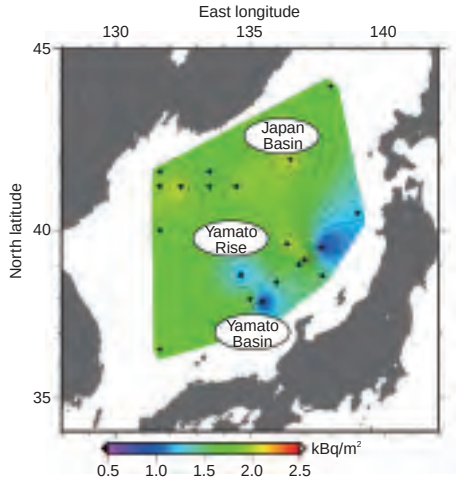

Fig.7-3 Distribution of the inventory of ^{137}Cs in seawater originating from global fallout due to atmospheric nuclear weapons testing

This map is based on a 10-year survey of the Japan Sea. This map shows no traces of radioactive waste disposal to the Japan Sea by the former Soviet Union and provides important information on seawater circulation and numerical modeling.

Nuclear Transmutation Technology

R&D on transmutation technology for long-lived nuclides are being conducted so as to reduce the burden of the radioactive waste management.

To achieve the transmutation of MA effectively and intensively, an Accelerator- Driven System (ADS) is being studied. As shown in Fig.7-4, the ADS consists of an MA-fuelled subcritical core coupled with a spallation neutron source driven by a superconducting proton accelerator. Various research and design studies are under way for the accelerator, the spallation target and the subcritical core using lead-bismuth eutectic as the primary coolant.

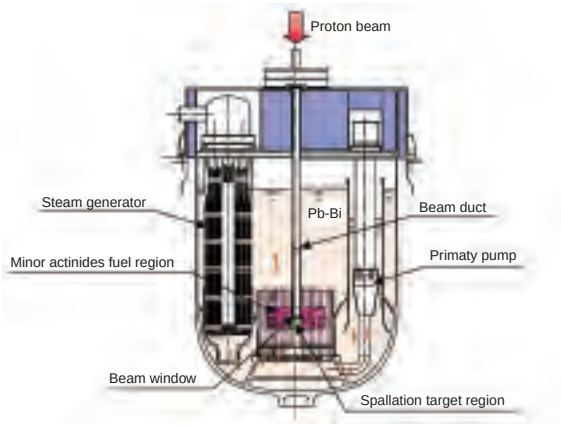

Fig.7-4 Concept of Accelerator-Driven transmutation System (ADS)

One ADS (800MWth) unit driven by a 30MW proton beam can transmute 250kg of minor actinides annually, equivalent to production in 10 LWR (1GWe) units.

Nuclear Applied Heat Technology

To expand nuclear energy application to heat process industries, we have continued extensive efforts of development for high-temperature gas-cooled reactor (HTGR) technology and for hydrogen production system using the nuclear heat from HTGR. Using the High Temperature Engineering Test Reactor ("HTTR"), which is the sole HTGR in Japan, reactor performance and safety demonstration tests have been conducted as planned to establish data base essential for commercial HTGR electricity/hydrogen cogeneration system (Fig.7-5). The reactor outlet temperature of 950°C indispensable to the HTGR cogeneration system was successfully achieved in 2004, demonstrating the highest temperature reactor operation in the world.

For hydrogen production as heat utilization technology, we have been carrying out R&D on thermo-chemical splitting of water by the "Iodine-Sulfur process" (IS process), which emits zero CO_2 greenhouse gas. The IS process involves reactions iodine and sulfur compounds to decompose water molecules into hydrogen and oxygen using heat at about 900°C. In 2004, one-week continuous operation of the IS process was successfully demonstrated using a bench-scale apparatus with hydrogen production rate of ca. 30 L/h. In 2006, a mock-up model of a sulfuric-acid decomposer was also successfully test-fabricated with ceramics. We are leading the world R&D on the IS process.

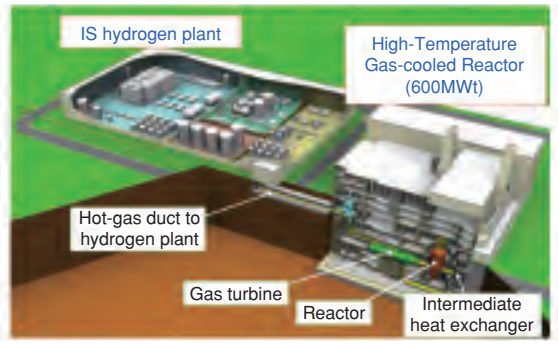

Fig.7-5 Concept of commercial HTGR cogeneration system

Sequential utilization of nuclear heat of 950℃ enables the production of hydrogen and electricity generation.

Collaboration with external organizations

We have built a "Nuclear Energy Research Collaboration Center" for playing the role of supplying platform to reinforce collaboration with industry and to promote R&D that meets the need of society. Presently, collaborative research activities in several fields, such as upgrading of structural material used in reprocessing facilities, thermal flow of light water reactors, and non-invasive detection of U and Pu in waste drums have been started. In addition, various collaborative research projects with academia/business are progressing, and we contribute to human resource development through collaboration with Nuclear professional school of the University of Tokyo.

7-2 Predicted Two-Phase Flow Behavior in Nuclear Reactors
－Development of Detailed Two-Phase Flow Simulation Method－

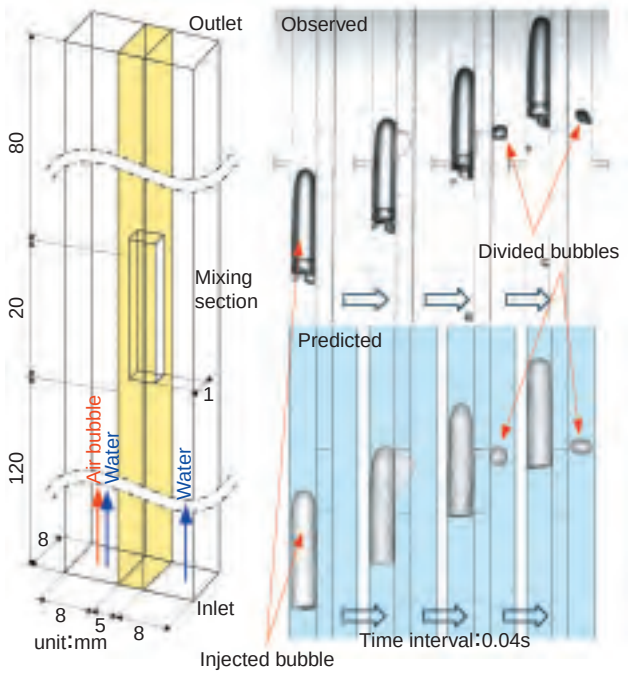

Fig.7-6 Predicted dynamics of bubbles moving through a mixing section
Air and water flow upwards from the bottom of the test channel. A part of the bubble shifts at the gap between the ducts due to the pressure difference. The predicted result agrees well the observed results.

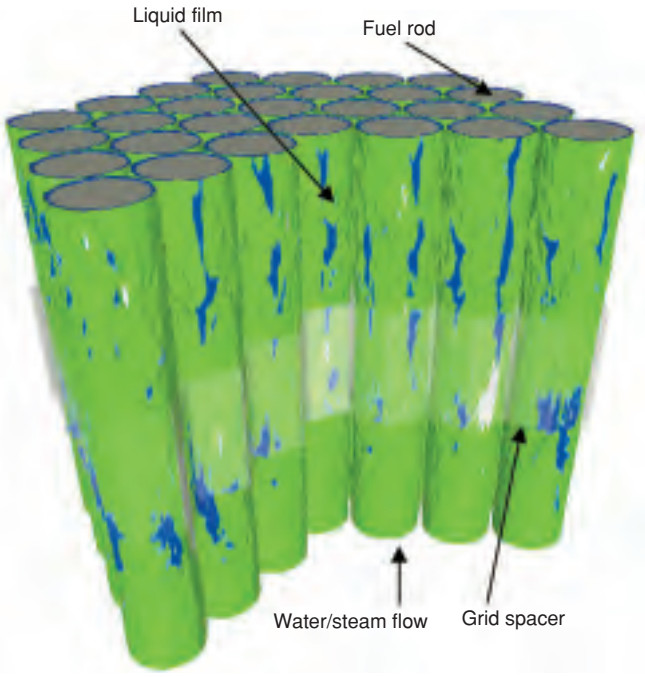

Fig.7-7 Predicted two-phase flow behavior in the tight-lattice rod bundle
This geometry and dimensions simulate an axial part of the tight- lattice fuel bundle. Each fuel rod is enclosed by a water film with very thin thickness, and vapor flows on the outside.

Thermal-hydraulic design of the current boiling water reactor (BWR) is performed by correlations with empirical results of actual-size tests. Then, when the reactor of new design is developed, an actual size test that simulates its design is required to confirm or modify the correlations. Development of a method that enables the thermal-hydraulic design of nuclear rectors without these actual size tests is desired, because these tests take a long time and entail great cost.

For this reason we developed an advanced thermal-hydraulic design method for BWRs using innovative two-phase flow simulation technology. For this, the following are required: (1) an advanced simulation method with high accuracy prediction, (2) verification of simulation method; and, (3) capability to analyze enormous amounts of data.

We are developing an advanced interface tracking method which improves fluid volume conservation, to enable high accuracy prediction of two-phase flow. It was incorporated in the detailed two-phase flow simulation code: TPFIT. We tried to verify the TPFIT code comparing with experimental results.

In one test, the TPFIT code was applied to the 2-channel air-water mixing (Fig.7-6). The fluid mixing was observed at a gap between ducts in the experiment. Bubble dynamics through the gap and cross flow behavior could be effectively predicted by the TPFIT code.

The parallel computation of TPFIT code was conducted for the large-scale simulations. The TPFIT code was applied to the two-phase flow analysis of a tight -lattice rod bundle and its high adequateness capacity for large scale simulations was confirmed (Fig.7-7).

This paper contains some results obtained within the task “Development of Fuel Assembly for Very High Burnup Water-cooled Breeding Reactor” entrusted from the Ministry of Education, Culture, Sports, Science and Technology of Japan.

Reference

Yoshida, H. et al., Current Status of Thermal/Hydraulic Feasibility Project for Reduced-Moderation Water Reactor(2)－Development of Two-Phase Flow Simulation Code with Advanced Interface Tracking Method－, Nuclear Engineering and Technology, vol.38, no.2, 2006, p.119-128.

7-3 Development of Organic Material for the Recovery of Transuranium Elements
—The Novel Strong Ligand, Diglycolamide, for Total Recovery of Minor Actinides—

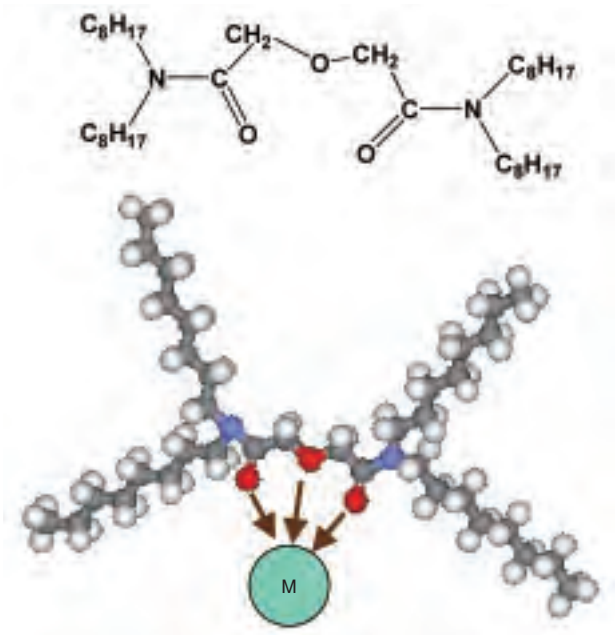

Fig.7-8 Structure of TODGA
TODGA is a tridentate ligand containing three oxygen donors (red color atoms). The analogs of TODGA were synthesized and their hydrophilic and lipophilic properties can be changed.

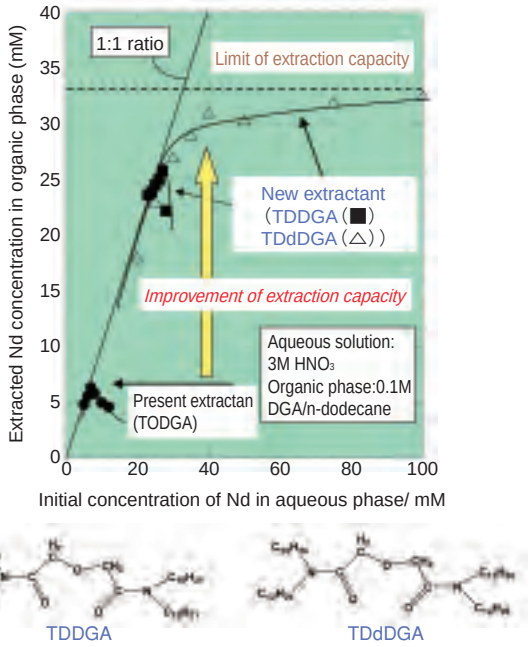

Fig.7-9 Loading capacity of DGA compounds
The highest value of the vertical line indicates the loading capacity of the extractant. The structures of TDDGA and TDdDGA are drawn below.

There are long lived minor actinides (MA), e.g., neptunium (Np), americium (Am) and curium (Cm) in spent nuclear fuel (SF), and these MA are present in the high level radioactive liquid waste (HLW) remaining after recovery of uranium and plutonium. In order to reduce the long-term environmental risk, the transmutation of the radioactive nuclides has been proposed and strong extractants for the recovery of MA have been investigated. We have developed TODGA (*N,N,N',N'*-tetraoctyl-3-oxapentanediamide, Fig.7-8) for the total recovery of MA. This extractant has three oxygen donors and behaves as a tridentate ligand. The tridentate extractants have never been studied in the chemical treatment of SF and HLW. TODGA has a powerful ability to separate tri- and tetra-valent metals, and higher extraction capability than other representative extractants.

In a series of the process adaptation work, the extraction capacity of TODGA was measured (Fig.7-9). The extraction capacity is indispensable to determine the optimal conditions for the planned process. Improving on TODGA, we synthesized TDDGA (*N,N,N',N'*-tetradecyl-3-oxapentanediamide, Fig.7-9) and TDdDGA (*N,N,N',N'*-tetradodecyl-3-oxapentanediamide, Fig.7-9), which have 4-5 times higher extraction capacity than TODGA, and suppress the third phase formation.

We also synthesized water-soluble DGA as masking reagents. These materials have the following advantages, (1) high solubility in water, (2) strong complexation with MA, and (3) neutral donor which can be used in acidic solution. These new ligands have been tested for the reverse extraction of MA. Testing is in progress, and the results suggest that this ligand will be a useful reagent for a planned innovative separation method of MA from HLW.

Not only the novel extractant, TODGA, which has very powerful complexing ability, but also improvements on TODGA, TDDGA and TDdDGA showing higher extraction capacity and water-soluble DGA with high ability to reverse-extract MA have been developed.

Reference

Sasaki, Y. et al., A Method for the Determination of Extraction Capacity and Its Application to *N,N,N',N'*-Tetraalkylderivatives of Diglycolamide-Monoamide/*n*-dodecane Media, Analytica Chimica Acta, vol.543, 2005, p.31-37.

7-4 Preparation of Nitride Fuel in the Pyrochemical Reprocessing of Spent Fuel

—Technological Development of Renitridation of Plutonium Recovered in Liquid Cathode—

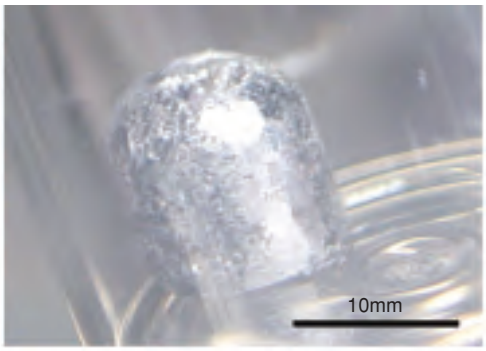

Fig.7-10 Liquid Cd cathode after electrorefining
In the pyrochemical reprocessing of nitride fuel, actinides are recovered in liquid Cd cathode by molten salt electrorefining.

Fig.7-11 PuN powder obtained by nitridation - distillation combined reaction
Experiments are carried out in Ar-atmosphere gloveboxes.

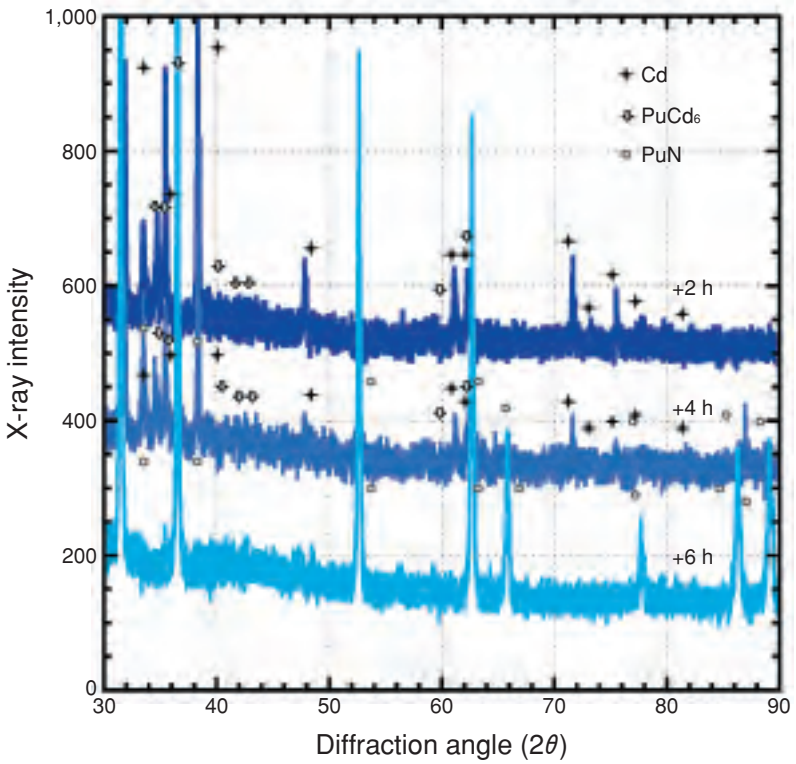

Fig.7-12 Change of X-ray diffraction patterns during the reaction
With the progress of distillation of Cd in the alloy, PuN is formed by the reaction of $PuCd_6$ and N_2 gas. After heating for 6h, almost the single phase of PuN is identified.

R&D on transmutation of minor actinide (MA) by Accelerator Driven System (ADS) is in progress in JAEA in order to lessen the long term radiotoxicity in high level waste and enhance the rational final geological disposal. Nitride fuel containing MA as a principal component is proposed for ADS and a pyrochemical process is proposed for the treatment of spent nitride fuel with high dosage radiation and decay heat. In the pyrochemical reprocessing of nitride fuel, actinides are recovered in a liquid cadmium (Cd) cathode by molten salt electrorefining, followed by renitridation of actinides in Cd for preparation of recycled fuel.

In this study, renitridation of plutonium (Pu) recovered in liquid Cd cathode (Fig.7-10) was developed by the nitridation-distillation combined reaction. In this method, high-purity PuN powder was recovered by heating the Pu-Cd alloy obtained by electrorefining at 973K in N_2 gas stream (Fig.7-11). The nitridation- distillation combined reaction is characterized by the simultaneous nitridation of Pu and distillation of Cd in the same stage. Although the nitridation of Pu in liquid Cd phase is difficult because of high thermodynamic stability, PuN was formed by the reaction of Pu-Cd binary intermetallic compound and N_2 gas during the distillation of Cd. Here the nitridation of Pu also promoted the distillation of Cd (Fig.7-12). According to the experimental results, mass balance of Pu and Cd during the experiments was good, and recovery and recycling of the evaporated Cd will be possible. The nitridation-distillation combined reaction seems to be technologically feasible.

Further, we tried the renitridation of Pu and uranium (U) and small amounts of rare earth (RE) elements contained in the Pu-U-RE-Cd alloy obtained by electrorefining. It was found that Pu and U were converted to mononitride and RE elements were also dissolved in the (Pu,U)N phase. Since RE elements have thermodynamic properties similar to MA in liquid Cd cathode, the nitridation-distillation combined reaction should be applicable to MA-bearing Cd alloy. In addition, preparation of nitride fuel pellets from the recovered nitride powder is planned.

This study was carried out within the task “Technological development of a nuclear fuel cycle based on nitride fuel and pyrochemical reprocessing” entrusted by the Ministry of Education, Culture, Sports, Science and Technology (MEXT) of Japan.

Reference

Arai, Y. et al., Fabrication and Electrochemical Behavior of Nitride Fuel for Future Applications, Journal of Nuclear Materials, vol.344, 2005, p.180-185.

7-5 Investigations of Irradiation Assisted Stress Corrosion Cracking (IASCC) Behavior for Reactor Materials —Achievement of In-Pile SCC Tests at JMTR—

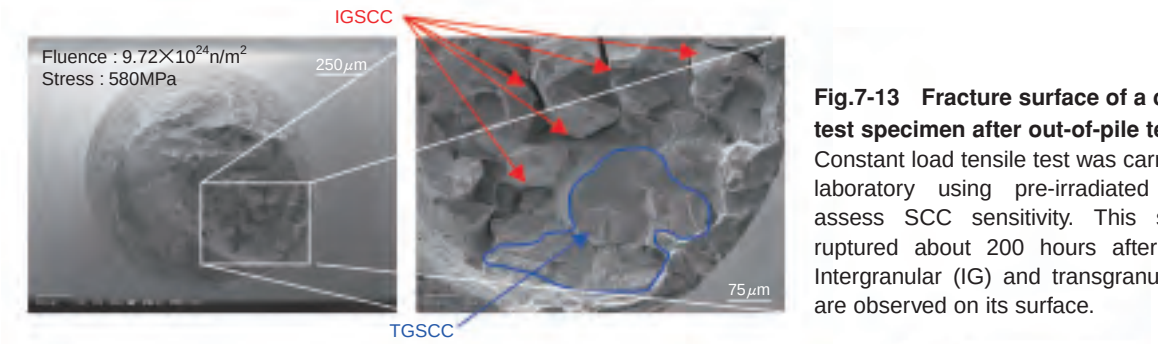

Fig.7-13 Fracture surface of a crack initiation test specimen after out-of-pile test
Constant load tensile test was carried out in a hot laboratory using pre-irradiated specimen to assess SCC sensitivity. This specimen was ruptured about 200 hours after loading start. Intergranular (IG) and transgranular (TG) SCCs are observed on its surface.

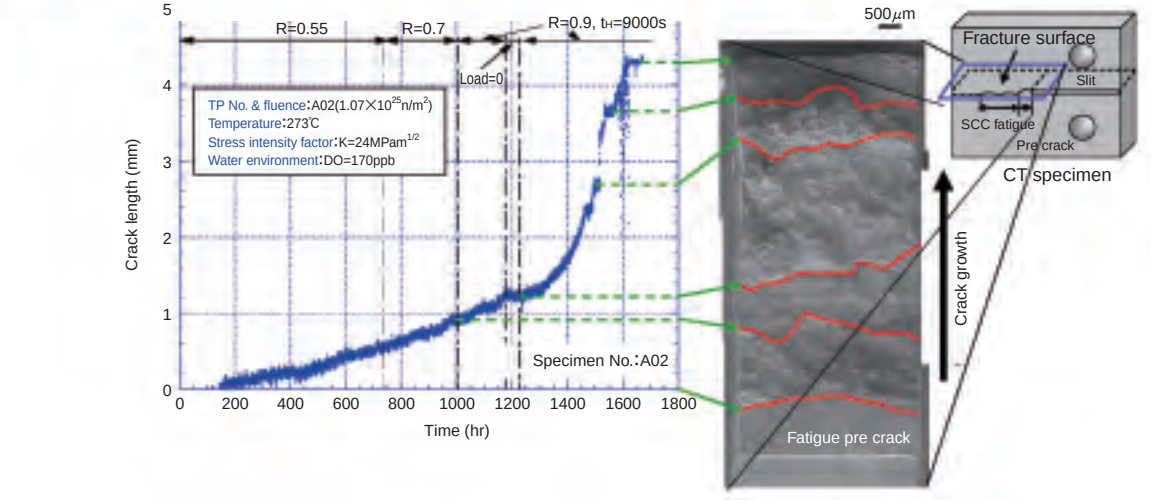

Fig.7-14 Measurement of crack length on in-pile crack growth test and fracture surface of specimen
Changes of crack length on in-pile test could be measured by direct current potential drop (DCPD) method using pre-irradiated compact tension (CT) specimen. (Fatigue pre crack was introduced by cyclic loading before in-pile test. R is the ratio and t_H is a holding period.)

Irradiation assisted stress corrosion cracking (IASCC) is one of the critical concerns when stainless steel components have been in service in light water reactors (LWRs) for a long period. It is, however, considered that the reproduced IASCC by the post-irradiation examinations (PIEs) must be carefully compared with the actual IASCC in nuclear power plants, because the actual IASCC occurs in the core under simultaneous effects of radiation, stress and high temperature water environment. Hence there are many difficulties in SCC tests under neutron irradiation. We have embarked on a development of the test technique to obtain information concerning effects of applied stress level, water chemistry, irradiation conditions, etc. The results of this study will be reflected to the evaluation of PIE data and the construction of guidelines for the IASCC research project of METI (Ministry of Economy, Trade and Industry).

With crack initiation test, in the case that the fluence was about 1×10^{25}n/m^2 and loading stress was equal to the yield stress of the specimen (at the above-mentioned fluence, it is about 580MPa), occurrences of SCC (intergranular and transgranular SCC) were recognized (Fig.7-13), but there was no clear indication that SCC was accelerated considerably under irradiation.

With crack growth test, there was good correlation between changes of the stress ratio of loading to unloading and circumstances of the fracture surface, it was possible to measure the change of crack length using direct current potential drop method under irradiation (Fig.7-14). About the simultaneous effect of irradiation for crack growth rate, it is considered that the influence of irradiation is almost small because electrochemical corrosion potential is almost equal between PIE data under the conditions of 32ppm dissolved oxygen and in-pile test data.

This study was conducted as a joint research program of JAEA and Japan Atomic Power Company from fiscal 2000 to 2005.

Reference

Ugachi, H. et al., Development of Test Techniques for In-Pile SCC Initiation and Growth Tests and the Current Status of In-Pile Testing at JMTR, Proceedings of 12th International Conference on Environmental Degradation of Materials in Nuclear Systems-Water Reactors, Salt Lake City, USA, 2005, p.319-325 in CD-ROM.

7-6 Distribution Maps of Anthropogenic Radionuclides in the Japan Sea
—Transport Processes of Radionuclides in the Japan Sea—

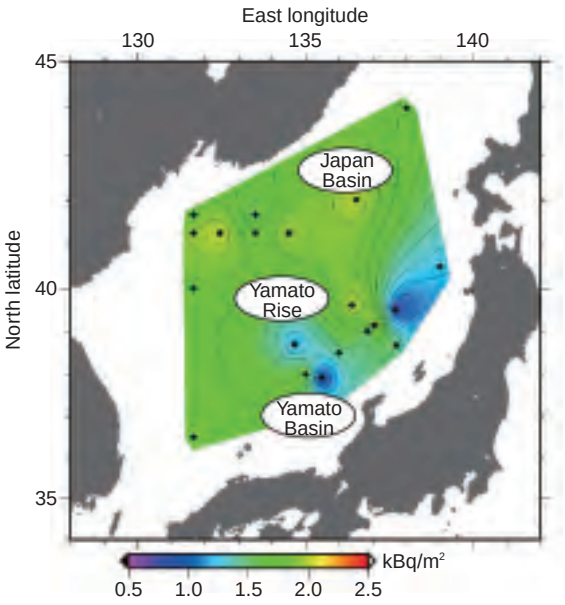

Fig.7-15 Distribution of the inventory of cesium-137 (^{137}Cs) in seawater originating from global fallout due to atmospheric nuclear weapons testing

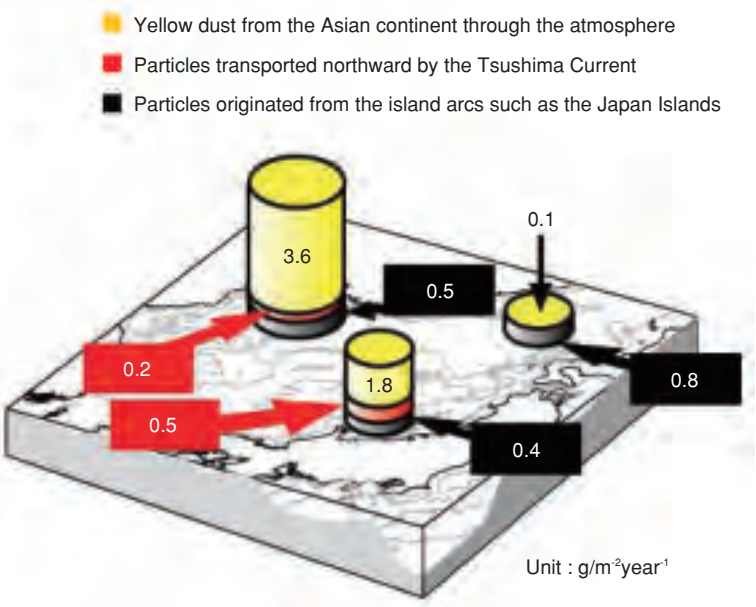

Fig.7-16 Settling flux and the origin of aluminum at three regions in the Japan Sea
(1) off Vladivostok, (2) off the Noto Peninsula, and (3) off Okushiri Island ("Settling flux" is defined as the quantity of particles collected per unit area and in set collection time. In the figure, settling fluxes are measured at a depth of 1 km.)

We have carried out expeditions in the Japanese and Russian exclusive economic zones (EEZ) of the Japan Sea for 10 years to clarify seawater circulation and transport processes of materials in the sea. As a result, for the first time, we have made distribution maps of anthropogenic radionuclides in the Japan Sea and outlined the transport processes of radionuclides in the sea. The Japan Sea expeditions by JAEA started with its participation in the Japanese-Korean-Russian joint expeditions of 1994 and 1995. Through 18 expeditions, JAEA succeeded in covering almost all areas of the Japan Sea that can be observed at present.

The results of these expeditions are summarized below.

(1) Concentrations of anthropogenic radionuclides in seawater vary over regions and depths. Distributions of radionuclides in middle-deep layers of the sea show a southeastward lateral transport of radionuclides from the Japan Basin to the Yamato Basin, detouring around the Yamato Rise due to seawater movement (Fig.7-15). Vertical convection of seawater in winter plays an important role in transport of radionuclides to the lower depths of the northwestern Japan Sea.

(2) Studies of settling particles reveal accumulation of particulate radionuclides in the seabed from lateral transport of particles originating in the East China Sea and the Japan Islands, as well as from yellow dust from the Asian Continent via the atmosphere (Fig.7-16).

(3) Anthropogenic radionuclides detected in seawater and seabed sediments are inferred to originate from global fallout from atmospheric nuclear weapons testing. The radiological consequences of these radionuclides on human physiology are negligible.

These findings enable understanding of seawater circulation and transport processes of materials in the sea. Furthermore, the dataset on the distribution of anthropogenic radionuclides established by this study provides background data in assessing the radiological consequences in cases of radioactive waste disposal in the sea or nuclear emergency response to accidental releases of radionuclides in or near the Japan Sea.

Reference

Togawa, O. et al.(eds.), Japan Sea Expeditions for Studies on Water Circulation and Transport Processes of Radionuclides, 2006, JAEA-Research 2006-004, 132p.

7-7 DARWIN

—Dose Monitoring System Applicable to Various Radiations with Wide Energy Ranges—

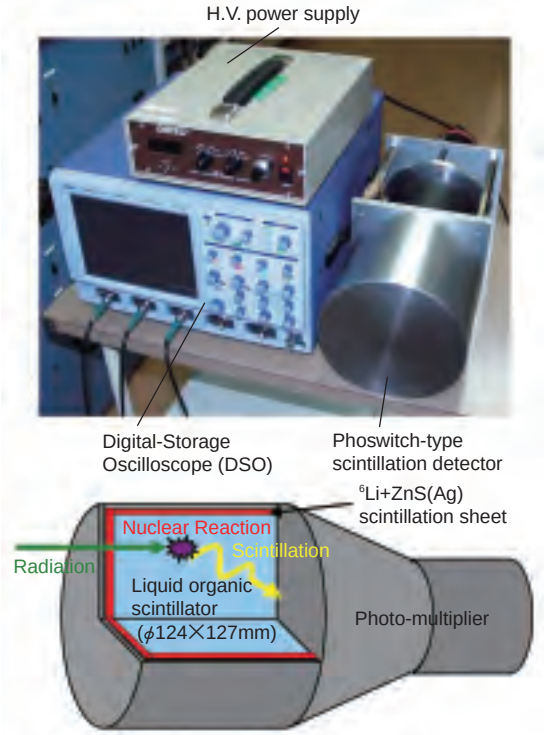

Fig.7-17 Picture of DARWIN (above) and schematic view of the phoswitch-type scintillation detector (below)

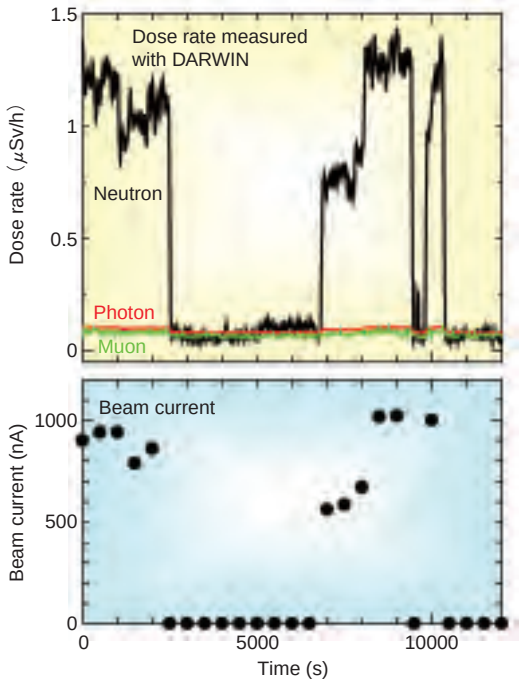

Fig.7-18 Dose rates measured with DARWIN in a high energy accelerator, and the accelerator beam current

Workers in high energy accelerator facilities are potentially exposed to high energy neutrons, photons and muons because of their high penetrability through radiation shielding. Measurement of doses from these particles is therefore of great importance for assuring radiation safety in the facilities. However, none of the existing devices are able to measure doses from all of these particles with satisfactorily accuracy.

With this specific problem in mind, we have developed a new device for monitoring doses in workspaces and environments surrounding high energy accelerator facilities, calling it DARWIN (Dose monitoring system Applicable to various Radiations with WIde energy raNges). DARWIN is composed of (1) a phoswitch-type scintillation detector, which consists of liquid organic scintillator BC501A coupled with ZnS(Ag) scintillation sheets doped with ^{6}Li, (2) a data acquisition system based on a Digital-Storage Oscilloscope (DSO), (3) and a high-voltage power supply. The picture of the system together with the schematic view of the phoswitch-type scintillation detector is shown in Fig.7-17. DARWIN is capable of monitoring doses from neutrons, photons and muons with energy ranges from thermal energy to 1 GeV, 150 keV to 100 MeV, and 1 MeV to 100 GeV, respectively, in real-time.

The performance of DARWIN was examined experimentally in several radiation fields. For example, the dose rates measured with DARWIN in the neutron detection room in the 800MeV proton accelerator facility LANSCE at Los Alamos National Laboratory is depicted in Fig.7-18, together with the beam current of the accelerator. It is apparent from the figure that the neutron dose rates correspond almost exactly to the beam current, indicating the accuracy and rapid response of DARWIN. It is also found from various experiments that DARWIN is superior to conventional radiation dose monitors in terms of accuracy, sensitivity, and applicable radiation types and their energy ranges. With these properties, DARWIN is expected to play a very important role for assuring radiation safety in high energy accelerator facilities.

Reference

Sato, T. et al., Development of Dose Monitoring System Applicable to Various Radiations with Wide Energy Ranges, Journal of Nuclear Science and Technology, vol.42, no.9, 2005, p.768-778.

7-8 Towards Treatment of Toxic Materials and Utilization of Radioactive Wastes

—A Novel Method for Non-Toxic Treatment of Cr(Ⅵ) Wastes by Using Ionizing Radiation—

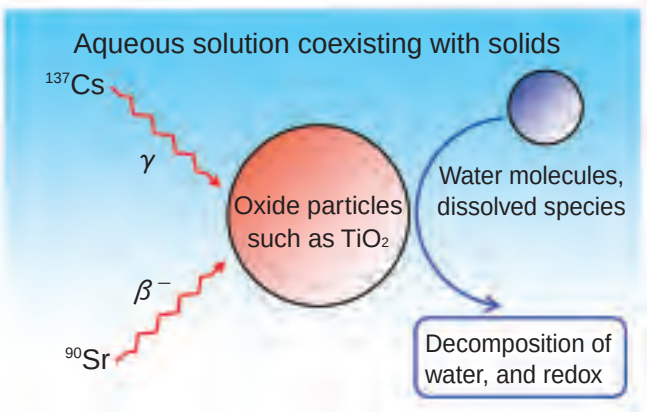

Fig.7-19 Promotion of reaction in aqueous solution by solids under irradiation

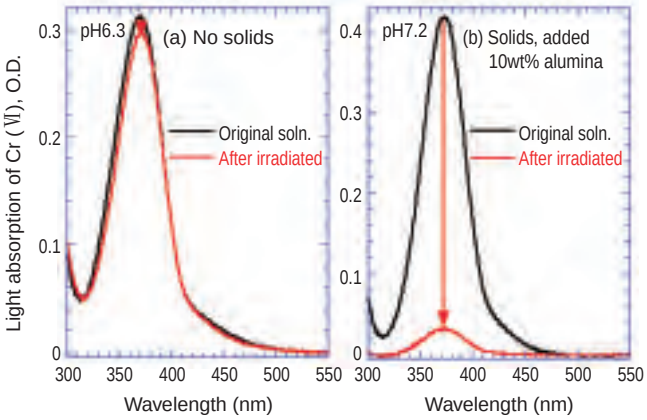

Fig.7-20 Absorption spectra of Cr(Ⅵ) ion in aqueous solution

In aqueous solution at pH conditions like liquid waste and environmental water, Cr(Ⅵ) is not reduced by irradiating radiations (a). When a small amount of solids are added to the solution, Cr(Ⅵ) is remarkably reduced (b).

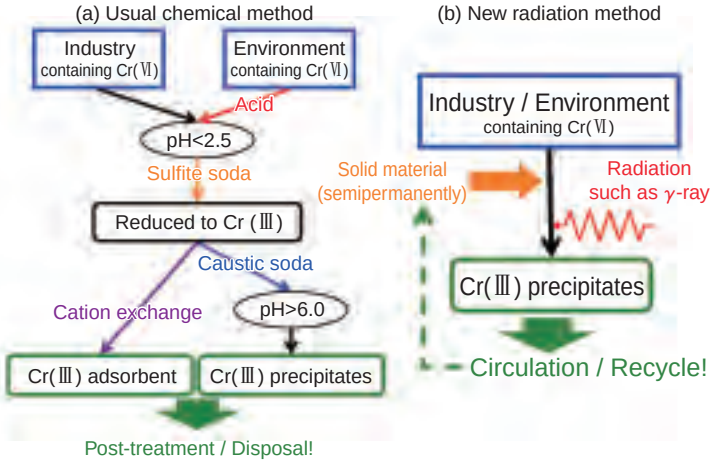

Fig.7-21 Schematic diagram of non-toxic treatment

The usual method (a) needs a large amount of dangerous reductants, acids and alkalis, and thus has many issues such as high cost and post-treatment. The new method (b) is simple and environmentally friendly because those chemicals are not needed.

When a medium (liquid and gas) containing solids such as oxide particles is irradiated by radiations, chemical reactions of ions or molecules in the medium are sometimes promoted without the consumption of solids (Fig.7-19). We have applied this promotive effect to practical systems, and developed a novel method for non-toxic treatment of chromium(Ⅵ), Cr(Ⅵ). Cr(Ⅵ) is so harmful to cause cancer, but is useful as industry for surface finishing of metal, production of colorants, etc. Its discharge to the environment must therefore be limited. To develop this method, we investigated how to treat Cr(Ⅵ) using radiation instead of a large amount of chemicals, though in aqueous solution like industrial liquid wastes and environmental water, Cr(Ⅵ) is hardly reduced by radiation.

Compared with the usual method, our novel one has several advantages: (1) Cr(Ⅵ) concentration after treatment is reduced under the emissions standard, without using a large amount of the chemicals (Fig.7-20), (2) the treated chrome materials can be recycled usefully into fire-retardant bricks, catalysts etc. without discharge into the environment, and (3) easy operation and easy maintenance (Fig.7-21).

In order to further make the novel method fit for practical use, we are developing treatment technology of industrial wastes such as electroplating waste liquids and polluted soils, jointly with a local factory and with a corporation. Since the promotive effect is also effective for treatment of other heavy metals and organic compounds which are social issues, and for generation of hydrogen gas as a clean energy, we are simultaneously conducting R&D of these applications.

We require radiation sources for this novel method, and are now using cobalt-60 γ-ray and electron beams. We also expect to utilize high-level radioactive wastes as the sources in the near future. When this utilization is possible, a highly sustainable reaction process "for the waste by the waste" will be realized. We are also doing some investigations by using the practical radioactive wastes.

This work is a part of the results of the project "Search for Radiation-induced Catalysts and Clarification of Reaction Mechanism in the Heterogeneous Systems" given a Grants-in-Aid for Scientific Research (Kakenhi) by JSPS.

Reference

Nagaishi, R. et al., Radiation-Induced Catalytic Reduction of Chromium(Ⅵ) in Aqueous Solution Containing TiO_2, Al_2O_3 or SiO_2 Fine Particles, Radiation Physics and Chemistry, vol.75, no.9, 2006, p.1051-1054.

7-9 Towards Reducing Tritium Concentration in the Hydrogen Produced by Very High Temperature Reactors —Permeability of Hydrogen of Operating Reactor Measured for the First Time—

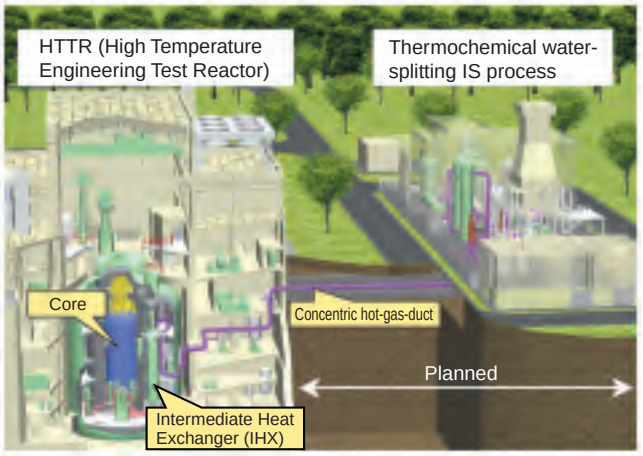

Fig.7-22 Hydrogen production by the HTTR (HTTR-IS system)
Demonstration of hydrogen production by the HTTR-IS system is planned in the near future. The IS process coupled to the reactor will be built with non nuclear standards. One of the concerns for adapting non nuclear standards is tritium becoming mixed with produced hydrogen.

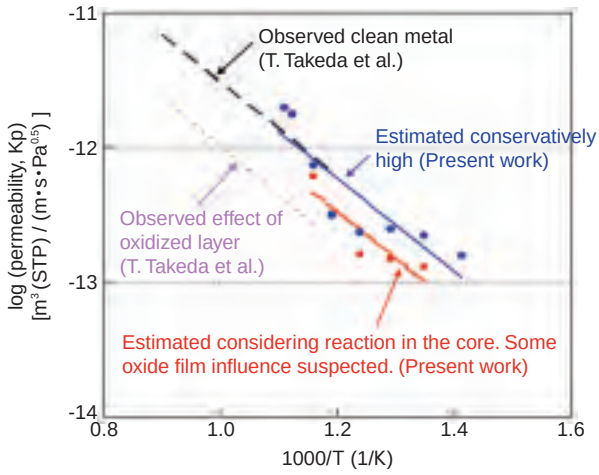

Fig.7-23 Hydrogen permeability of Hastelloy XR
Permeability of hydrogen in an operating reactor was measured for the first time. Comparing conservative evaluation (blue line) and realistic one (red line) it is implied that an oxidized layer was formed at the surface of the heat transfer pipes of the intermediate heat exchanger.

The HTTR (High Temperature Engineering Test Reactor) - IS (Iodine-Sulfur) hydrogen production system is planned to demonstrate nuclear powered hydrogen production (Fig.7-22). A non-nuclear IS process is planned, and a problem for this is admixture of tritium in the produced hydrogen.

It is well known that hydrogen and its isotope permeate through metallic materials and that the adsorption and desorption at the surface and diffusion in the metal are dominant phenomena. Because diffusion velocity of tritium is about $1/\sqrt{3}$ times that of hydrogen, the permeation of tritium can be estimated from that of hydrogen. Hydrogen permeation through Hastelloy XR, the material of the HTTR IHX (intermediate heat exchanger) heat transfer tubes, has been measured in the laboratory and it was found that an oxidized layer can reduce permeation of hydrogen efficiently. Also, the smallest possible tritium purification system is desired to reduce cost. Nuclear powered hydrogen production is being researched worldwide, but there has been no measurement of hydrogen permeation in an actual reactor, and the effect of oxidized layer on permeation has been unknown.

In this study, we could acquire the hydrogen permeation coefficients for the first time by using the impurity data during the HTTR 950°C operation.

The valuable permeation coefficients were obtained from macro experimental data as follows. Initially, the permeability was evaluated conservatively high for the safety case study. During the HTTR first 950°C operation, more hydrogen was found in the secondary system than in the primary. This indicates that hydrogen permeated from secondary to primary. Hydrogen is not considered to be generated in the core in the conservative evaluation and hence the amount of hydrogen that permeated was equal to that removed by the helium purification system (Blue line of Fig. 7-23). As a result, the activation energy and pre-exponential factor were 65.8kJ/mol and 7.8×10^{-9}m^3 (STP)/(m·s·Pa$^{0.5}$), respectively, at 707-900K. Then, the permeability was evaluated realistically, considering the chemical reaction in the core ($H_2O+C\rightarrow H_2+CO$). The fact that water content remains steady in the primary even though water is removed continuously suggests that the same volume of hydrogen is generated in the primary. The permeability decreases as shown by red line of Fig.7-23. Since the oxidized layer can reduce the permeability, the red line implies the oxidized layer was well formed on the surface of heat transfer tubes of the IHX.

We are planning R&D for establishing oxidized layer control during reactor operations. The results will be utilized for the purification system design of the HTTR-IS hydrogen production system.

Reference

Sakaba, N. et al., Hydrogen Permeation Through Heat Transfer Pipes made of Hastelloy XR during the Initial 950℃ Operation of the HTTR, Journal of Nuclear Materials, vol.353, 2006, p.42-51.

7-10 Progress in Nuclear Production of Hydrogen

—Successful Production of Ceramic Sulfuric Acid Decomposer Prototype—

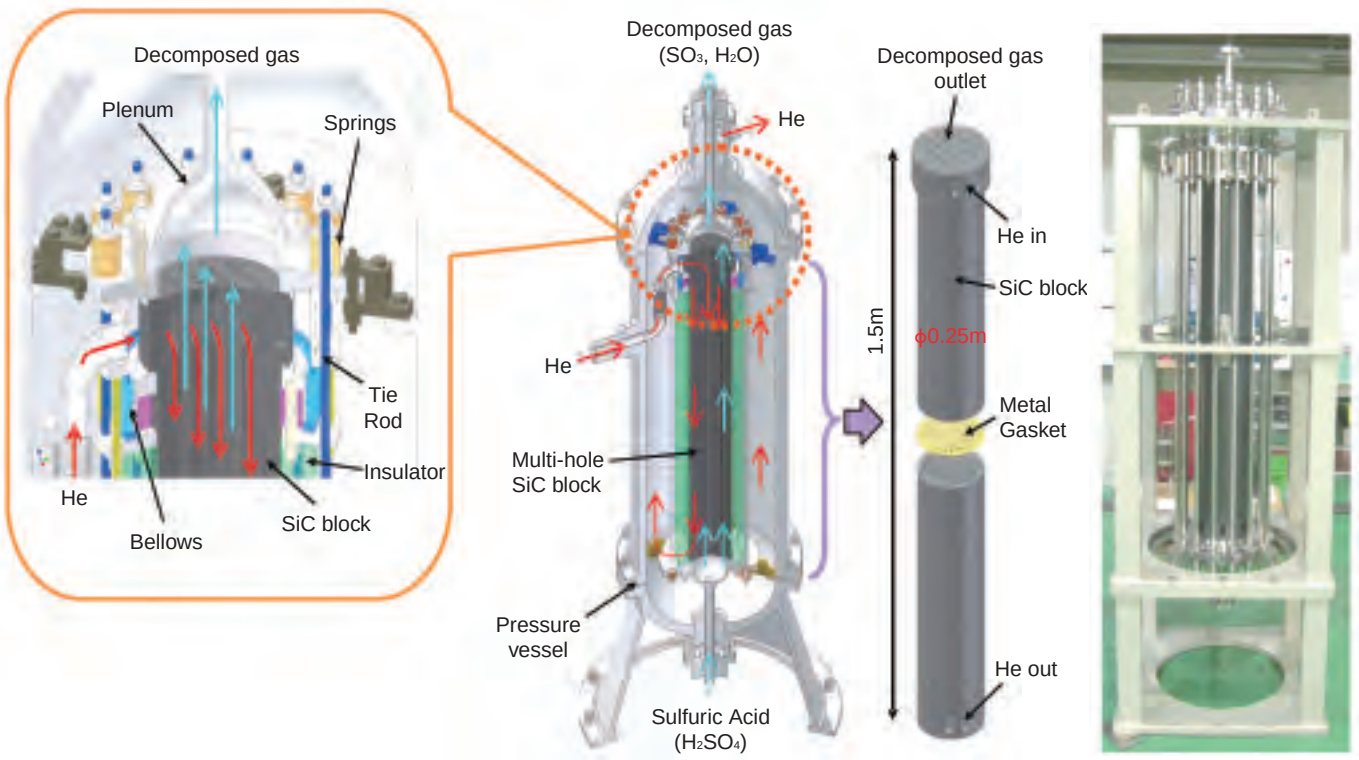

Fig.7-24 Concept of sulfuric acid decomposer ($30m^3$-H_2/hr class)
Sulfuric acid decomposer vaporizes concentrated sulfuric acid and decomposes it into sulfur trioxide (SO_3) and water (H_2O). A concept of the sulfuric acid decomposer has been developed that features heat exchanger made of silicone carbide (SiC) that exhibits excellent corrosion resistance in this environment.

Fig.7-25 Prototype
Prototypes of SiC blocks and the main parts of the decomposer have manufacturing feasibility.

We have been conducting R&D on both the HTGR and the IS process for CO_2-emission free production of hydrogen, two key technologies of future potential energy systems that are expected to contribute to national energy security as well as to global environmental protection. The IS process decomposes water to produce hydrogen via thermo-chemical reactions of sulfur and iodine using heat supplied by HTGR.

Development of the chemical processing reactors presents challenges, the most difficult of which is material resistance against the extremely corrosive process chemicals such as sulfuric acid. In the case of the sulfuric acid decomposer, an essential chemical reactor used to vaporize sulfuric acid concentrate and decompose it into sulfur trioxide and water, not only material corrosion resistance but also efficient heat transfer from HTGR-heated helium gas to the sulfuric acid fluid must be considered. This has led to the selection of silicon carbide (SiC) to be the structural material of core heat exchanging unit, since it has superior corrosion resistance and high thermal conductivity. The concept developed for the decomposer (Fig.7-24) consists of a column of stacked multi-hole cylindrical SiC blocks, the structural unit of heat exchanger where sulfuric acid and helium gas flow in separate, adjacent holes. The blocks are secured and connected to metallic components of the decomposer using gaskets, springs, bellows and tie rods. The structure of SiC ceramic block is made simple to facilitate fabrication. The mechanism of a combination of springs, bellows and gaskets secures gas tightness in spite of the large differential thermal expansion between the ceramic and metallic structural elements. The decomposer can be scaled up simply by stacking of more blocks in the column. A prototype of the SiC blocks and of the main components of the decomposer was made as shown in Fig.7-25 and manufacturing feasibility of the structure was confirmed.

This achievement will accelerate the R&D on nuclear hydrogen production underway in the world. This technology may also be utilized in chemical industries which handle corrosive chemicals.

The prototype production was entrusted by MEXT to JAEA.

Reference

Terada, A. et al., Development of Sulfuric Acid Decomposer for Thermochemical Hydrogen Production IS Process, Nippon Genshiryoku Gakkai Wabun Ronbunshi, vol.5, no.1, 2006, p.68-75 (in Japanese).


HTTR
JRR-1

8 Nuclear Fuel Cycle Technological Development

8-1 To Establish the Nuclear Fuel Cycle

—Promoting Light Water Reactor (LWR) Nuclear Fuel Cycle Technological Development and Technical Co-Operation with Private Industry—

Tokai Reprocessing Plant (TRP)

We execute research and development of spent nuclear fuel reprocessing, mixed oxide (MOX) fuel fabrication, etc., with various approaches including joint research to promote development of nuclear fuel cycle technology in Japan.

Moreover, we execute technology transfer, technical co-operation, entrusted research, consulting, etc. for the Rokkasho Reprocessing Plant (RRP) in Aomori prefecture operated by private industry, to support private industrialization of nuclear fuel cycle business based on current results of our research and development.

(1) Spent Fuel Reprocessing Technology

JAEA's Tokai Reprocessing Plant (TRP) was changed from a commercial reprocessing plant to a R&D facility, the reprocessing operation under contract with electric power companies being ended. TRP will execute the reprocessing experiments with MOX spent fuel of the Advanced Thermal Reactor (ATR) "FUGEN" and with high burnup uranium dioxide (UO_2) spent fuel of LWRs, and development the glass solidification processing technology of high-level radioactive waste (HLW).

1) Reprocessing Experiments with MOX Spent Fuel of "FUGEN"

TRP has the reprocessed about 20 tons of MOX spent fuel of "FUGEN".

Reprocessing experiments MOX spent fuel of "FUGEN" in TRP starting in FY2006 are planned to gather systematic data concerning the dissolution characteristics and the solvent deterioration, etc. using about 100 tons of spent fuel whose plutonium (Pu) content and burnup are higher than the MOX spent fuel that has been previously reprocessed.

In TRP, it is planned to examine it also through this reprocessing examination to contribute to the upgrade of the LWR reprocessing technologies for low environmental burden, nuclear proliferation resistance, economical operation, etc.

2) Reprocessing Experiments with High Burn-up UO_2 Spent Fuel of LWRs

We are planning reprocessing verification experiments using an LWR's high burn-up spent fuel to strengthen the technical base of the reprocessing technology.

In these reprocessing experiments with high burn-up spent fuel, a glass solidification processing method using HLW generated during reprocessing, properties of undissolved residue, and the corrosion behavior of various materials shall be investigated.

3) Glass Solidification Processing Technology of HLW

We are continuing operation of the Tokai Vitrification Facility (TVF) with an improved type glass melter started up in FY2004, gathering and storing data for stable operating of the new glass melter.

Glass Melter

Moreover, we are carrying out research on high volume reducing glass solidification and technology for glass melter dismantlement. In addition, we are pursuing technological development of a long-lived glass solidification melter which will be a business offered to the public by the Ministry of Economy, Trade and Industry (METI).

(2) Technical Co-operation

Nuclear fuel cycle operation by private industry is reaching an important stage of development in Japan.

Active examination of the reprocessing operation of the cycle is beginning at RRP.

For the uranium enrichment, technologies developed by JAEA will be collected, and to develop a new centrifuge, data, personnel, and research work will be shared.

To advance the LWR MOX fuel fabrication business, the grant of license to build a MOX fuel fabrication facility is being promoted.

These projects are based on technological results in fields that we developed and promoted.

In the future, we will positively promote technical co-operation with private industry based on the results of our R&D so that each business may progress surely, as requested by Japan Nuclear Fuel Co. Ltd. (JNFL).

1) Technical Co-operation with Reprocessing Businesses

Most of the main process technologies of the JNFL's RRP were introduced from France.

However, the technologies that we developed concerning uranium denitrating processing, the uranium-plutonium mixture conversion, and the HLW glass solidification were adopted by JNFL.

We are actively cooperating with private industry, sharing its experience in construction, operating, and maintenance of the TRP etc. by dispatch of its engineers, providing technical know-how, receiving JNFL engineers, joint research with JNFL, conducting experiments upon request, consulting etc., aiming at actual operation of RRP beginning in FY2007.

2) Technical Co-operation to Enrichment Business

The uranium enrichment technologies that we developed were consolidated in JNFL to develop a uranium enrichment centrifuge with global economic competitiveness.

And, to contribute to the development of this super-efficient new-material centrifuge (new model) that JNFL plans to be the replacement for their uranium enrichment factory, we shall provide technical co-operation through dispatch of its engineers, provision of technical know-how for the latest machines of us experiments performed on request, etc., to JNFL.

3) Technical Co-operation to MOX Fuel Fabrication Business

JNFL decided to enter the MOX fuel fabrication business for LWR in November 2000, and is promoting the grant of a license for the construction of the Rokkasho MOX fuel fabrication plant in Aomori Prefecture.

We have the technical expertise and experience in the design, construction, and operating of the MOX fuel fabrication facility for the ATR and FBR.

To incorporate this technical know-how in the Rokkasho MOX fuel fabrication facility, we are giving technical co-operation through the dispatch of its engineers, reception of JNFL engineers, provision of technical know-how, joint research, experiments performed on request, consulting, etc.

Especially, because the Rokkasho MOX fuel fabrication plant incorporates the technologies from France, we are conducting actual scale confirmatory testing of the mixture conversion powder technology, which uses a 1:1 mixture powder of nitric acid plutonium and nitric acid Uranil, to which heating desalination is done by micro wave (a JAEA-developed method), to confirm adaptability to the Rokkasho MOX fuel fabrication plant funded by JNFL.

8-2 Characteristics of HLW Generated from Future Cycles

—Perspectives on Application and Flexibility of Current Vitrification Technology for High Level Wastes (HLW) Generated from Future Fuel Cycles—

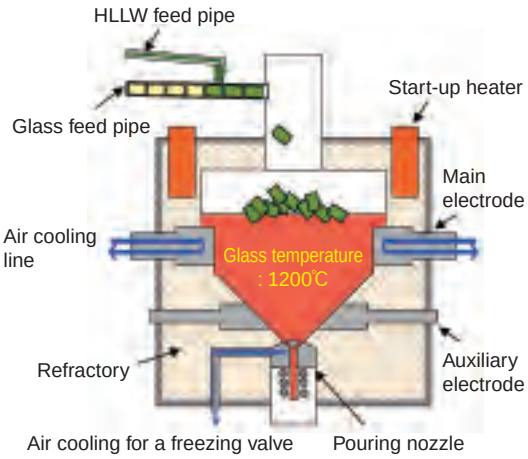

Fig.8-1 Configuration of the TVF melter
Glass is melted by its own Joule-heating generated by passing an electric current. High level radioactive waste fluid is supplied to the melter by a special glass fiber cartridge soaked with the fluid.

Table 8-1 Changes of compositions of noble metals and molybdenum, and heat generation of HLWs generated from future fuel cycles

Fuel Cycle (Burnup)	Composition at vitrification, kg/canister					Heat, kW/canister		
	Noble Metals				Mo	at Vitrification		
	Ru	Rh	Pd	Sub-total		Actinide	FP	Total
①Reference LWR (45GWD/t)	2.38	0.45	1.46	4.29	3.64	0.12	2.19	2.31
②High-burnup LWR (55GWD/t)	2.44	1.41	1.59	4.44	3.62	0.19	2.19	2.38
②/①	*1.03*	*0.91*	*1.09*	*1.04*	*0.99*	*1.53*	*1.00*	*1.03*
③Pu-thermal (55GWD/t)	2.95	0.80	2.98	6.73	3.30	2.15	1.89	4.04
③/①	*1.24*	*1.77*	*2.04*	*1.57*	*0.91*	*17.6*	*0.86*	*1.75*
④FBR core (153GWD/t)	3.18	0.94	2.62	6.74	3.36	—	1.68	1.68
④/①	*1.34*	*2.07*	*1.80*	*1.57*	*0.92*	—	*0.77*	*0.73*

In these evaluations, a reference HLW canister of 45 GWD/t burnup (1.25 canisters/tU) was considered and numbers of other evaluated canisters were converted to the equivalent for that burnup.

High level radioactive liquid waste (HLLW) generated from the Tokai reprocessing plant has been converted to stable glass in the TVF (Fig.8-1). The hot operation started in 1995. A total of 218 vitrified waste canisters were produced by the end of March, 2006. Aiming to prevent accumulation of noble metals at the bottom of the melter which affects heating efficiency etc., a low-temperature operation mode has been developed and applied to the operation.

It is recognized that vitrification is one of the key technologies for establishing future fuel cycles. Thus, continuous effort for further improvement and increased reliability is strongly required. We are now developing improvements focusing on the melter; a new bottom structure radically reducing accumulation of noble metals, extending the melter's life-time, and a simulation technique considering coupled physical phenomena.

High volume reduction technology is also being developed to decrease the number of HLW canisters by increasing the waste loading ratio. The most important research issues concern generation of a soluble molybdenum salt in the HLW. Basic experiments and melter tests for cold vitrification are now being carried out.

Applicability and flexibility of the current HLW vitrification technology in the LWR fuel cycle to the future fuel cycles were reviewed by examining characteristics of the HLWs; compositions of noble metals and molybdenum, and heat generation influencing storage and/or disposal facility designs of HLW. The present PUREX process was considered in both high-burnup LWR and Pu-thermal fuel cycles. For the FBR cycle, a flow sheet of the NEXT system which was studied as an advanced reprocessing system in the feasibility study on commercialized FBR cycle systems (FS-Ⅱ) (detail description is in Chap.1, Sec.16).

Table 8-1 indicates the evaluation results. Increase of burnup in LWR uranium fuel has negligible effect on fractions of noble metals and molybdenum and on heat generation. The close to 60% increase of noble metal content in Pu-thermal and FBR cycles suggests importance of development of measures preventing noble metal accumulation in the melter. Heat of HLW generated from the Pu-thermal cycle is increased remarkably due to higher heat generation by actinide. Such results make application of an MA recovery process in the NEXT system desirable. Since change of molybdenum concentrations in each cycle is small, this high volume reduction technology is expected to be applicable for these future cycles.

Reference

Shiotsuki, M. et al., Perspectives on Application and Flexibility of LWR Vitrification Technology for High Level Waste Generated from Future Fuel Cycle System, Proceedings of Waste Management 2006(WM'06), February 26 - March 2, 2006, Tucson, AZ, USA, 10p. in CD-ROM.

8-3 Study on the Denitration Process of Uranyl Nitrate Solution by Microwave Heating
—Uranium Powder Production Process from Uranium Nitrate Solution—

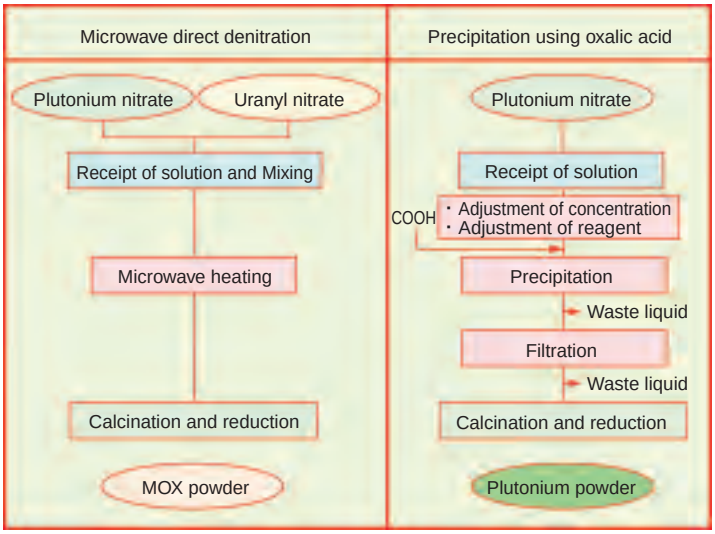

Fig.8-2 Comparison of conversion methods
Microwave denitration method was developed in Japan to directly produce MOX powder. There are three major merits compared to the conventional methods such as precipitation: 1) the process is simple and compact, 2) the produced powder has high homogeneity because plutonium and uranium are mixed in solution state and 3) volume of waste solution is extremely small because no reagent is used.

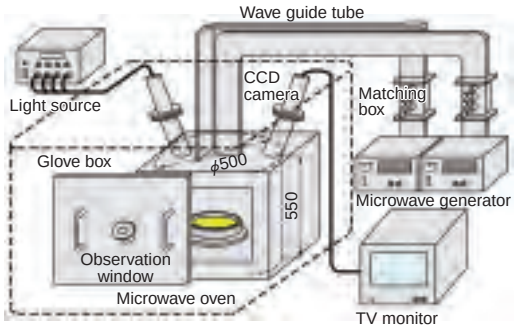

Fig.8-3 Schematic view of denitration testing apparatus
Microwave power is 3 kW.

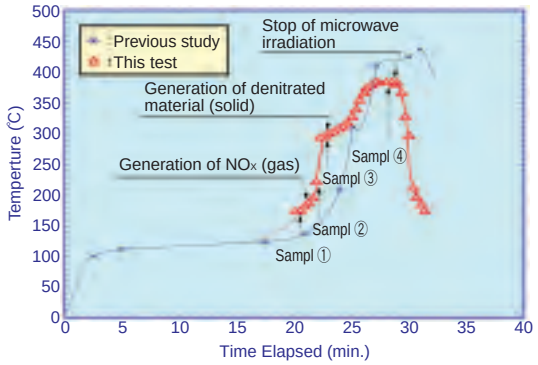

Fig.8-4 Temperature of uranium compounds during microwave irradiation
Crystallization water and nitrate start to be decomposed about 20 minutes after the start of irradiation, and finally only uranium oxide remains.

Spent fuel from nuclear power reactor is chemically treated in reprocessing plants, and then plutonium and uranium are recovered as reusable sources. In Europe, recovered plutonium is converted to the oxide powder by precipitation using oxalic acid and mixed with uranium oxide powder, followed by the mixed oxide (MOX) fuel fabrication. A new co–conversion method where plutonium and uranium are converted directly to MOX powder after mixing them in solution state was developed and adopted in Japan (Fig.8-2). This process has the feature of nuclear weapons proliferation resistance because there is no pure plutonium oxide powder in the process. This feature is exactly consistent with the policy of Japan that nuclear power should be used only for peaceful purposes. The microwave denitration method excites molecules by microwaves just like a household microwave oven, and nitrate is decomposed more rapidly by internal heating than by external heating. As a result, the produced powder is made up of fine particles which are suitable for sintering into high density pellets.

When mixed plutonium nitrate and uranium nitrate solution is heated, water and nitric acid evaporates at the first stage, then crystallization water of nitrates and nitrate itself are decomposed, and MOX remains at the end. In this study, we developed a special device to measure non-invasively and selectively the temperature of uranium material regardless of the moisture or NOx gas in the oven (Fig.8-3). The purpose of the development was that the conventional infrared thermometer could not measure temperature correctly because infrared rays were absorbed by moisture or NOx gas between the measured substance and the thermometer. The device was attached to the oven and temperature transition of the material was accurately measured. Then, samples were taken from each stage of reactions and thermometric analysis and X–ray analysis were carried out (Fig.8-4). As a result, we could confirm the chemical reactions formulae shown below :

$UO_2(NO_3)_2 \cdot 6H_2O \rightarrow UO_2(NO_3)_2 \cdot 3H_2O + 3H_2O$

$UO_2(NO_3)_2 \cdot 3H_2O \rightarrow UO_2(OH)NO_3 + HNO_3 + H_2O$

$UO_2(OH)NO_3 \rightarrow \beta\text{-}UO_3 + 0.5H_2O + NO_2 + 0.25O_2$

And/or $UO_2(OH)NO_3 \rightarrow \beta\text{-}UO_3 + HNO_3$

Reference

Kato, Y. et al., Reaction Mechanism of De-nitration of $UO_2(NO_3)_2$ by Microwave Heating, Nippon Genshiryoku Gakkai Wabun Ronbunshi, vol.4, no.1, 2005, p.77-83 (in Japanese).

8-4 Approach towards an Explication of the Corrosion Mechanism for Reprocessing Plant Instruments —Investigation of Causes of a Failed Steam Jet and Improving the Jet Design—

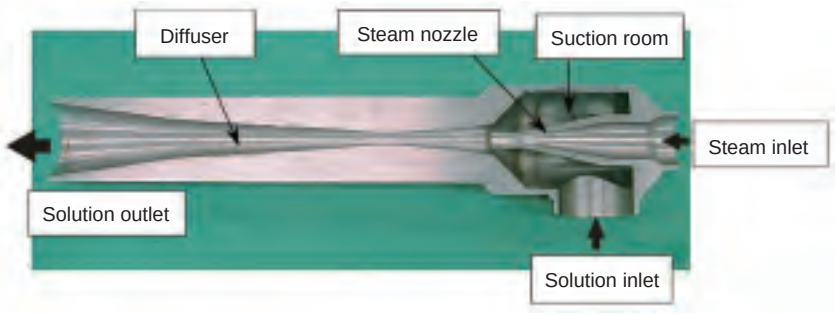

Fig.8-5 The configuration of a steam jet (SJ)
SJ is an instrument which transports solution by making steam blow out from a steam nozzle. Material of a failed SJ is equivalent to JIS-SUS304L, and operating time up to the accident was about 60,000 hours. Operating conditions:
(1) Steam temperature : About 170℃
(2) Temperature of the waste fluid : About 40℃
(3) Nitric-acid concentration in waste fluid : 2～3 mol/L
(4) Designed flow : 4m^3/h

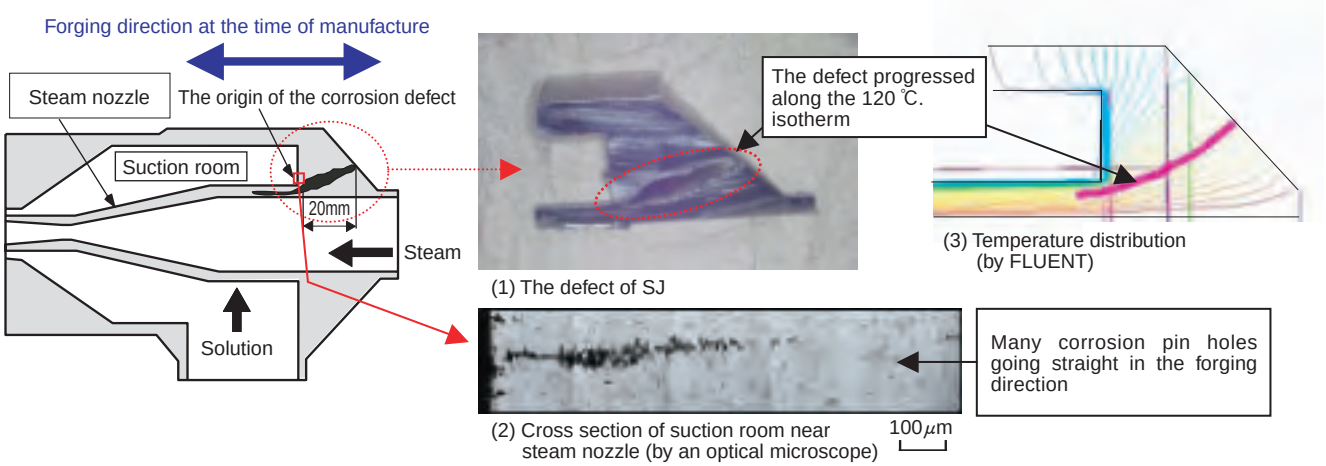

Fig.8-6 Defect and temperatures evaluation of a steam jet (SJ)

A corrosion accident occurred in the steam jet (SJ) during acid recovery processing at the Tokai reprocessing plant. About 400 SJ are used to transfer solution in cells where radiation doses are relatively high in the plant (Fig.8-5). Such a corrosion event in an SJ had never occurred in the 30 years of the plant's operation, so we investigated it from many aspects and determined the cause.

First of all, we retrieved the SJ from the cell and observed the inside by a high precision CCD camera and X-rays. As a result, it was revealed that corrosion had created cavities inside of the structure which extended to the outside surface (Fig.8-6).

Next, we made the following investigations to ascertain why such a failure occurred.

(1) Observation of constitution by a scanning electron microscope (SEM) and componential analysis by an X-ray micro analyzer (EPMA).
(2) Analysis of the temperature distribution of the structure and verification by experiment using a mock-up system.
(3) Investigation of the correlation between the processing direction of the structure and corrosion progress by corrosion test.

Consequently, it was revealed that the corrosion defect started with pin holes at the steam nozzle base connecting with the inlet portion, at the surface where nitric acid fluid had been in contact, and the defect progressed from the nozzle base along the 120 ℃ isotherm.

Moreover, we proved the following points regarding improvement of SJ design.

(1) R-SUS304 ULC-SA material has high corrosion resistance, so it is effective as the material for an SJ which is used for a long time.
(2) Smoothing the surfaces at the nozzle base which is the starting point of corrosion makes fluid flow smooth and lessens the temperature rise.

Reference

Shimizu, R., Takaya, A., Shirozu, H. et al., Investigation of Causes a Failed Steam Jet and Devising an Improved Jet Design, Nippon Genshiryoku Gakkai Wabun Ronbunshi, vol.4, no.3, 2005, p.203-212 (in Japanese).

8-5 Development of Acidity Analysis without Reagents
—Determination of Acidity in Nitric Acid Solutions Containing Pu and U at High Concentration by Electric Conductivity Measurement—

Table 8-2 Equivalent conductivity λ for cations at infinite dilution

Cation	λ (S•cm²) at 25℃
H^+	349.8
Li^+	38.6
K^+	73.5
$1/2Fe^{2+}$	54

Photo 8-1 Electric conductivity meter
This meter consists of a control device and a measurement cell, the cell being installed in a glove-box. Signals of electric conductivity and temperature of a sample in the cell pass through a signal cable and are displayed on the digital display of the control device.

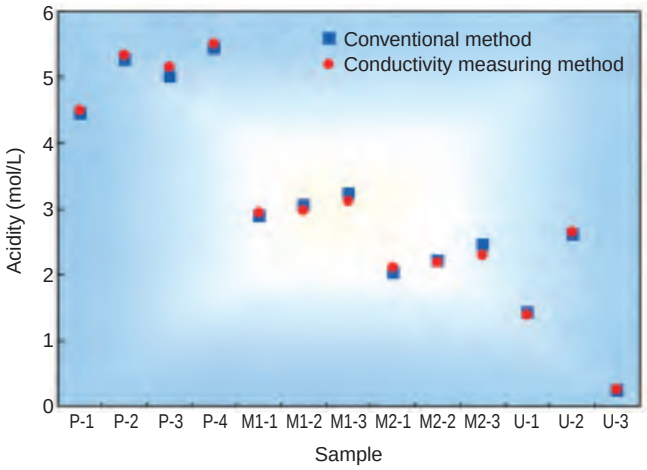

Fig.8-7 Comparison of results of electric conductivity measuring method and conventional method
This figure shows comparison of analysis results of acidity of nitrate acid solutions containing Pu and/or U by electric conductivity measuring method and conventional method. P means Pu nitrate solution(Pu:200g/L). M1 means Pu-U mixed nitrate solution(Pu:120g/L,U:120g/L). M2 means Pu-U mixed nitrate solution(Pu:85g/L,U:200g/L). U means uranyl nitrate solution (U:50～360g/L).

Acidity (hydrogen ion:H^+) in nitric acid solutions containing plutonium(Pu) and uranium(U) at high concentration handled in reprocessing plant is an important parameter for control of the reprocessing processes, specifically to prevent the hydrolysis of Pu in the processes.

Potentiometric titration method has been applied to determine the acidity in these solutions as conventional method. In this method, it is necessary to add reagents such as sodium hydroxide (NaOH), including fluoride ion (F^-), and they become waste liquid. Particularly, as it is known that F^- accelerates corrosion of stainless steel at room temperature, the corrosion of tanks and pipes for treatment of the waste liquid has been feared. Thus, we have searched for an analytical method that measures the acidity without using reagents including F^- and is rapid.

We focused on the electric conductivity of these solutions. Electric conductivity shows ease of current flow, and depends on the temperature of the solution, and on the variety and the concentration of ions (electrolytes) contained in the solution. Particularly, equivalent conductivity of H^+ is very high in comparison with that of other cations shown in Table 8-2, and so can be measured with high sensitivity. Furthermore, electric conductivity can be easily measured by a commercial electric conductivity meter without any improvements, as shown in Photo 8-1. However, when various ions exist in the solution, electric conductivity of the solution represents sum of electric conductivities from all the ions. Consequently, it is impossible to measure only electric conductivity of H^+, when Pu and U exist in solutions like Pu-U mixed nitrate solution at high concentration. Therefore, using the correlation between electric conductivity and concentration of H^+ in the solutions, we have investigated an analytical method that is able to determine H^+ in the solutions containing Pu and U by measuring electric conductivity of a sample diluted with distilled water at constant temperature (25℃), and correlating the electric conductivity and acidity using a multivariate analysis method. As a result, we obtained good results as follows,

(1) Acidity in the nitric acid solutions containing Pu and/or U obtained by this method was in good agreement with that of the conventional method, within 10%, as shown in Fig.8-7.
(2) For Pu nitrate solution and Pu-U mixed nitrate solution, the repeatability of the measurement of electric conductivity at 25.0℃ was within 1.5%.
(3) It takes about 5 min to analyze by this method, 1/6 the time of the conventional method.

From the results described above, an electric conductivity measuring method can be applied to analysis of acidity in the nitric acid solutions containing Pu and U at the high concentration handled in the Plutonium Conversion Development Facility. Furthermore, this method should be applicable to analysis of acidity in the nitric acid solutions containing Pu and U use in reprocessing process.

Reference

Kitagawa, O. et al., Determination of Acidity in Nitric Acid Solutions Containing Plutonium and/or Uranium at High Concentration by Electric Conductivity Measurement, 2006, JAEA-Technology 2006-031, 29p. (in Japanese).

9 Development of Technology on Nuclear Cycle Backend

9-1 Nuclear Facility Decommissioning and Radioactive Waste Management

1. Introduction

JAEA is the only organization established by the government for comprehensive R&D on atomic energy, and it now owns more than 200 nuclear facilities: Research Reactors, Reprocessing Plants, Accelerators, etc. In the future, these facilities will be decommissioned after completing their missions. In the 1st Midterm Plan, more than 30 facilities which should be decommissioned now or in the near future are identified.

In addition, low level radioactive wastes have been generated through a variety of JAEA's research activities, and approximately 340 thousand in 200 litter drum are stored in JAEA's site (FY2005).

Nuclear facility decommissioning and radioactive waste management are collectively known as "Nuclear Cycle Backend". It is considered to be a duty of nuclear institution installer or the radioactive waste generator to carry out the tasks of Nuclear Cycle Backend.

Long-term operations and large amounts of fund are needed to carry out Nuclear Cycle Backend. We have estimated that the total cost will be 2 trillion yen over the next 80 years. Therefore, we are carrying out the following R&D aimed at reducing the cost.

2. Development of Decommissioning Technology (Fig.9-1)

The fundamental decommissioning technology has been established based on the experience in dismantling gained during the JPDR decommissioning project etc. When applying the technology to other facilities, it is necessary to improve the technology in consideration of their specific features. Specifically, we are developing dismantling technologies for the "FUGEN" Nuclear Power Station (advanced thermal reactor that is heavy water moderated, light water cooled, and of the pressure tube type), the Uranium Enrichment Plant and the Conversion Facility in Ningyotoge, and the JAERI Reprocessing Test Facility which are suited to the features of these facilities, based on the existing technologies.

A lot of data on dismantling technology and related information have been accumulated through the dismantling activities of the facilities. In order to efficiently carry out the

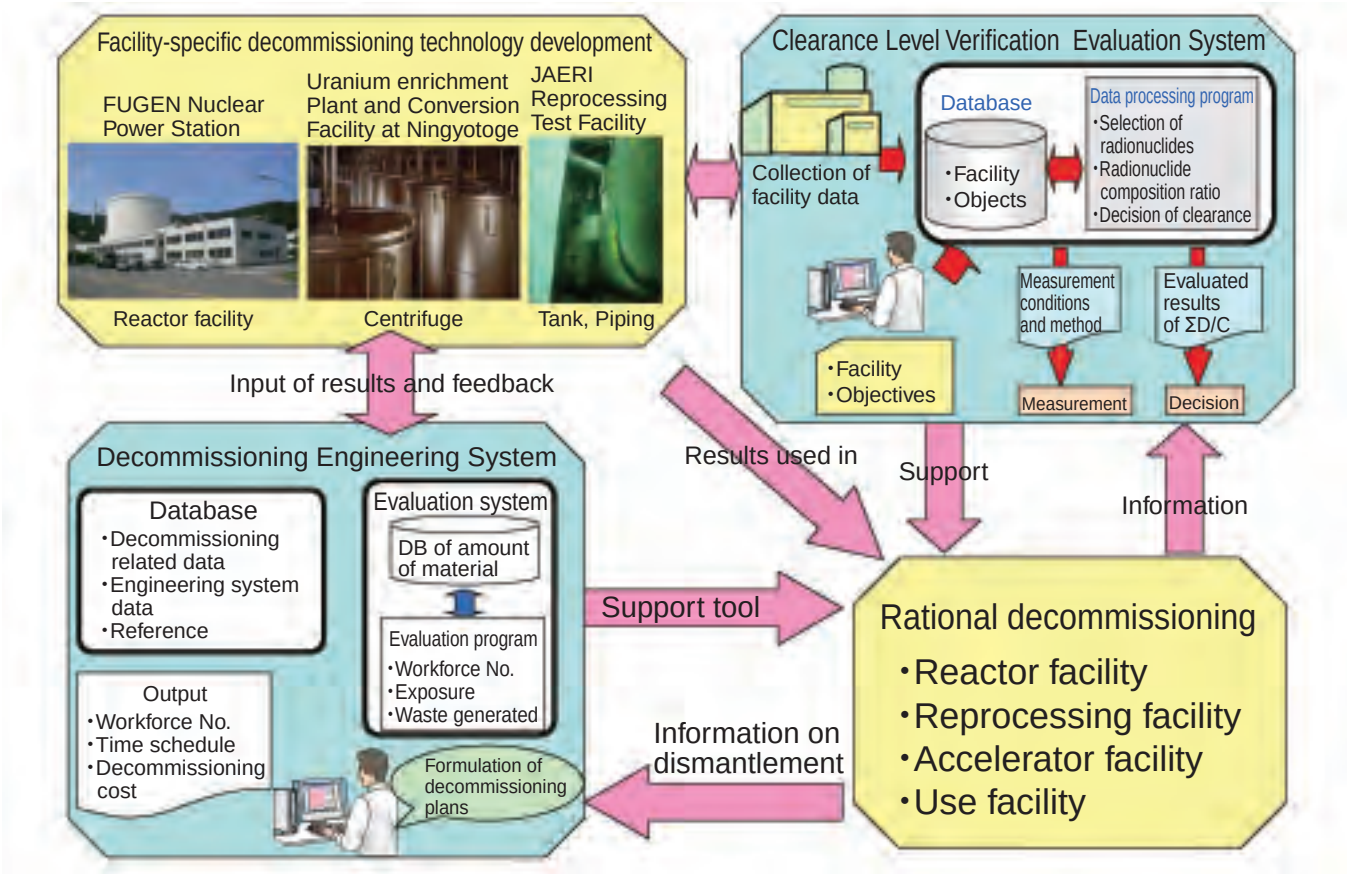

Fig.9-1 Development of Nuclear Facilities Decommissioning Technology

decommissioning of JAEA's facilities in the future, we are developing a computerized decommissioning engineering system which consists of databases including the above decommissioning-related data and evaluation systems such as a system for calculating residual radioactive contamination in the facility.

On the other hand, the Law on nuclear reactor regulations was amended in December 2005, and a clearance system was introduced in the Law. The clearance system is useful for reducing the amount of radioactive waste as well as waste disposal cost. We are developing a computerized clearance level verification evaluation system to easily and efficiently implement clearance.

The above mentioned technologies have been developed or are under development, and will be used for the future decommissioning activities in JAEA.

3. Development of Radioactive Waste Treatment and Disposal Technology (Fig.9-2)

Radioactive Waste is to be treated using a technology appropriate to the radioactivity level and waste characteristics. We are developing the following treatment technologies aiming to reduce the waste management cost: a calcination pre-treatment prior to volume reduction treatment and a decontamination process for waste contaminated with uranium and TRU nuclides.

The waste package, which is prepared by solidification by cement, melting, etc. for final disposal, has to be measured for radioactivity under the regulatory rules for waste disposal. We are developing an easy and rapid radioactivity measurement method to reduce measurement time and cost.

Waste packages are finally disposed of in a near surface repository (with or without engineered barriers), in a sub-surface disposal or in a deep geological repository, depending on its radioactivity. As safety of disposal is judged based on exposure dose assessment, we have been examining factors affecting migration of radionuclides, creating a database and method for the assessment of disposal of radioactive wastes arising from non-nuclear fuel cycle facilities, TRU bearing wastes and uranium bearing wastes.

And we are developing a waste records management system which manages an integrated set of information on radioactive waste in all phases of management from generation to disposal with good traceability of records.

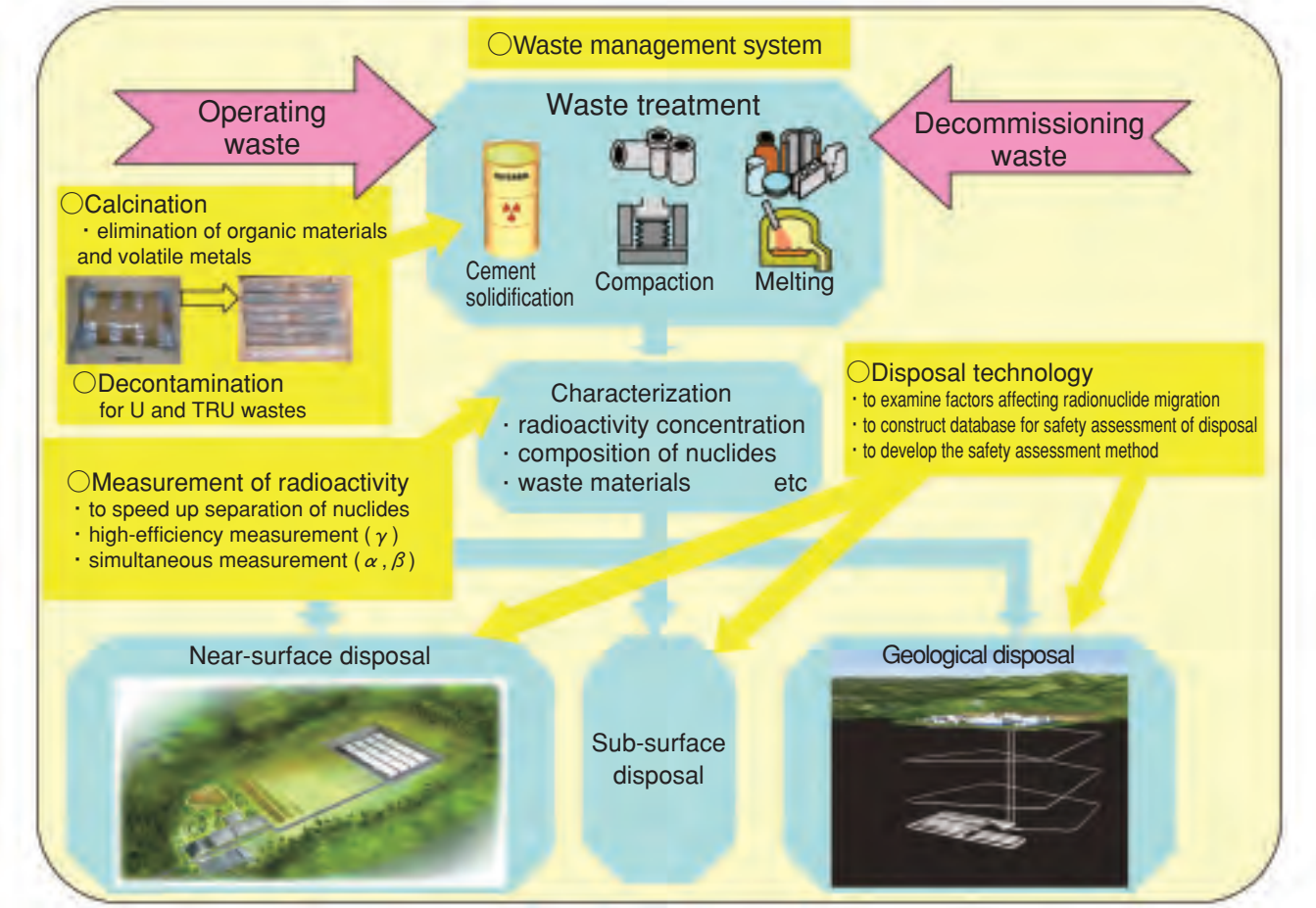

Fig.9-2 Development of Radioactive Waste Management Technology

9-2 Simplification of Radiochemical Analysis Method for Safe Disposal of Radioactive Wastes

— Effective Pretreatment for Radiochemical Analysis of Solidified Products with Microwave Heating Devices —

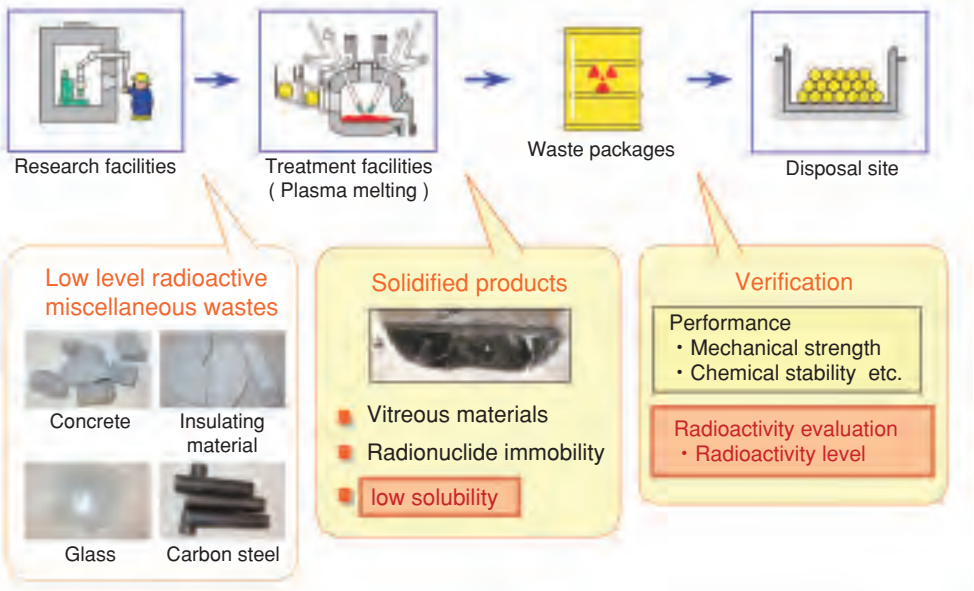

Fig.9-3 Disposal of low-level radioactive wastes
The disposal of low-level radioactive miscellaneous wastes generated from research facilities in packages solidified by plasma melting is planned. In order to dispose of radioactive wastes safely, it is indispensable to verify that each waste package is prepared in accordance with requirements for disposal.

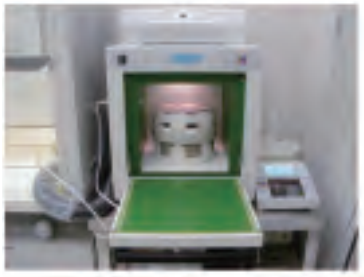

a) External view of the device

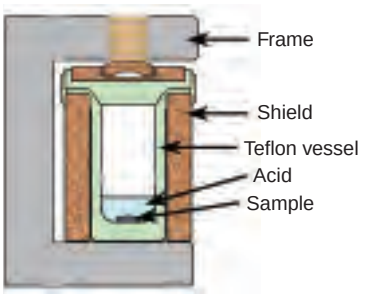

b) Cross-sectional view of a vessel

Fig.9-4 Microwave heating device
The mixture of sample and acids in a Teflon vessel is heated by microwave. a) External view of the device, b) Cross-sectional view of a vessel

Low-level radioactive miscellaneous wastes have been generated from various research facilities. The disposal of solidified packages of the wastes is planned. The solidification of miscellaneous wastes by plasma melting yields high chemical stability and immobilizes radionuclides effectively. For the safe disposal of radioactive wastes, it is indispensable to verify that each waste package is prepared in accordance with requirements for disposal, e.g. mechanical strength, radioactivity concentration, etc. (Fig.9-3). In order to establish a rational and reliable verification method for radioactivity in waste packages, radioanalytical data collected from both the original wastes and the solidified products are required, such as composition, concentration and distribution of radionuclides.

For the radiochemical analysis of radioactive wastes from research facilities, a larger quantity of sample solutions has to be prepared than in chemical composition analysis, because there are various kinds of radionuclides to analyze in the wastes and their radioactivities range widely in concentration. In addition, the solidified products yielded by plasma melting are difficult to dissolve.

In order to dissolve a sample of solidified products rapidly, a dissolution method using microwave heating devices was applied (Fig.9-4). In a conventional method involving only external heating with various mixtures of acids, a 0.1 g sample was dissolved with difficulty. However, upon applying the microwave - assisted dissolution method, a 1 g sample was completely dissolved in a shorter time. In this way the time for dissolution was shortened to less than one-tenth. In addition, the use of sealed vessels can prevent release of radionuclides. From the viewpoint of safety, the dissolution method with microwave heating devices is effective.

Reference

Haraga, T. et al., Rapid Dissolution Techniques with Microwave Heating Devices for Solidified Products Made from Non-Metallic Wastes by Plasma Melting, Bunseki Kagaku, vol.55, no.1, 2006, p.51-54 (in Japanese).

9-3 Development of Decommissioning Engineering Support System (DEXUS) —Database and Dismantling Work Simulation System (VRdose)—

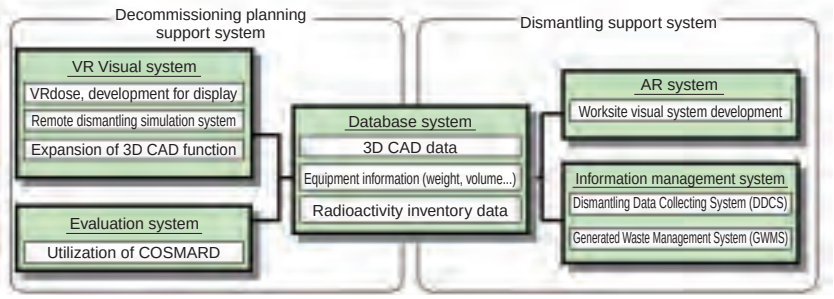

Fig.9-5 Structure of DEXUS

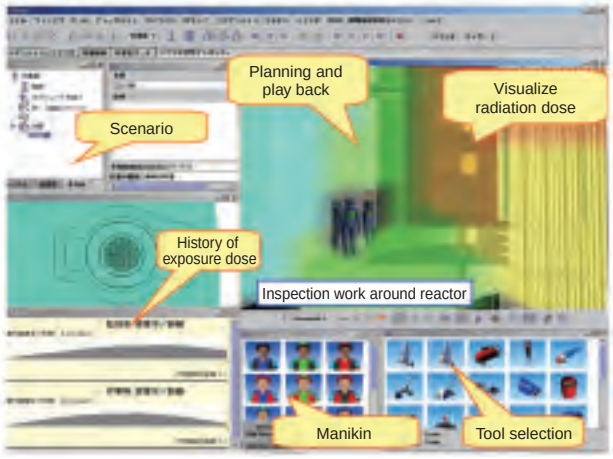

Fig.9-6 Userinterface of VRdose

In order to plan a rational decommissioning process with improved safety, reduced exposure dose and reduced waste generation, the Decommissioning Engineering Support System (DEXUS) has been developed in Fugen nuclear power station.

DEXUS consists of three subsystems; a Database System provides relevant data to a Decommissioning planning Support System and a Dismantling Support System.

Moreover, the Decommissioning Planning Support System consists of a VR Visual System and an Evaluation System. The Dismantling Support System also contains an AR Visual System and a Data Management System (Fig.9-5).

Here, the current status of the development of the Database System and the dismantling operation simulation system (VRdose) contained in VR Visual System in DEXUS are described.

(1) Database system

The Database System includes 3D-CAD data, equipment information, and radioactivity inventory data of Fugen. In particular, some 3D-CAD enhancing functions are added into for efficient planning, as follows.

1) A Coordination function between 3D-CAD and information such as specifications of equipment, pictures and diagrams for instruments and pipes (2D-CAD)
2) The function for cutting equipments in a 3D-CAD
3) The function for estimating amount of mass in a specified space in a 3D-CAD.

(2) VRdose

In the decommissioning of a nuclear power plant, many dismantling operations are executed by humans, excepting those for a reactor activated highly with radiation. Therefore, a prior determination of both the operation steps and the exposure dose is important to plan it appropriately, considering safety of the operation itself and reduction of exposure dose. VRdose has been developed in cooperation with the Institutt for energiteknikk (IFE) for this purpose (Fig.9-6). VRdose can evaluate the inside exposure and the outside exposure of the workers, simulating the behavior of the workers by a human model in VR space composed with 3D-CAD data and space dose data of Fugen. In addition, the system can be used for the education for workers before the work and PA for workers.

We are going to apply DEXUS to actual dismantling work in order to confirm and improve its performance.

Reference

Iguchi, Y. et al., Development of Decommissioning Engineering Support System(DEXUS) of the Fugen Nuclear Station, Journal of Nuclear Science and Technology, vol.41, no.3, 2004, p.367-375.

10 Computational Science and E-Systems Research

10-1 Promoting Innovation in Nuclear Energy with Computational Science

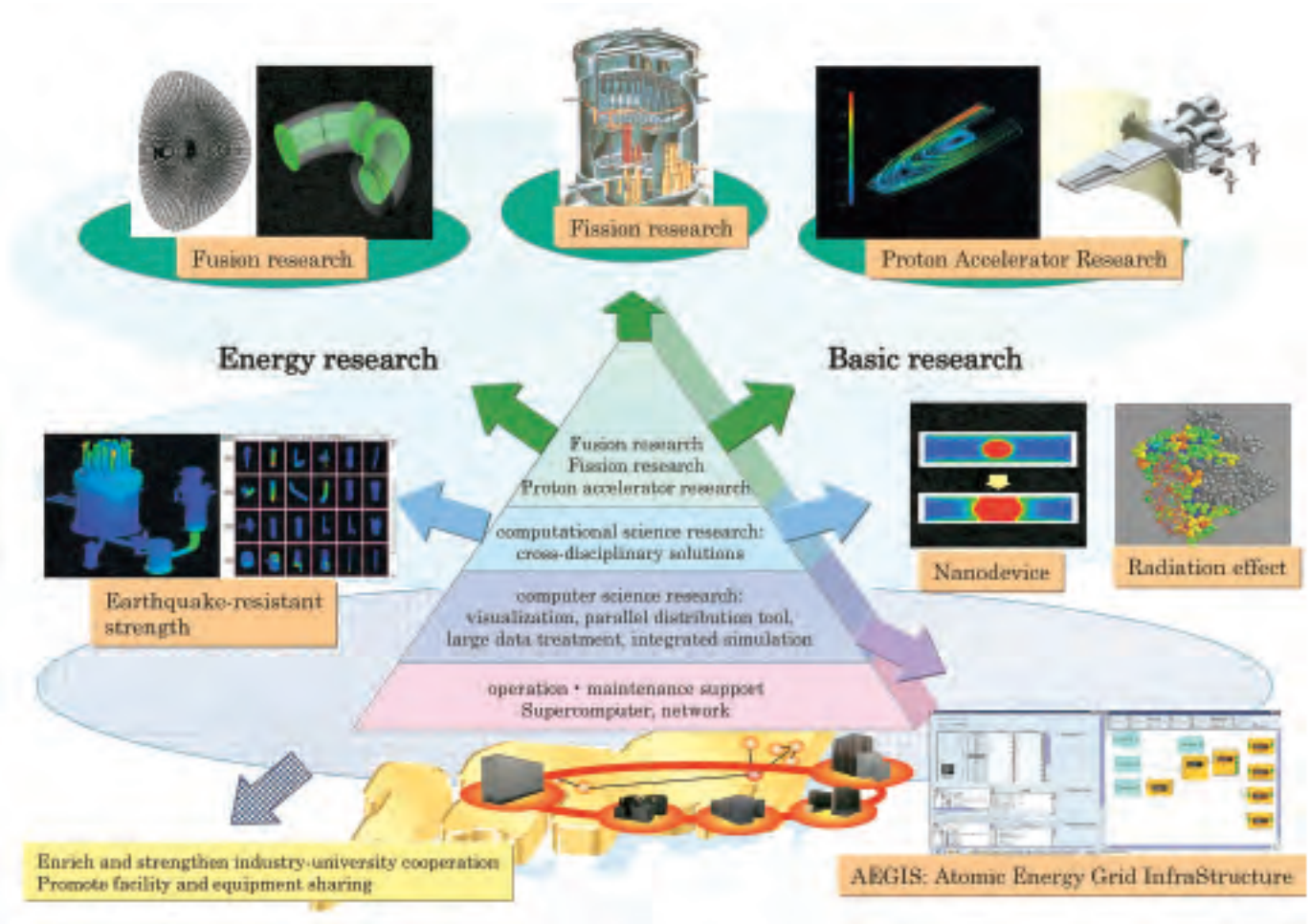

Fig.10-1 Roles of computational science in atomic energy field
Center for Computational Science and E-systems promotes leadership of experiments and creation of new ways in atomic energy field with research of computational science, research of computer science and operation and maintenance of computer and network systems.

Computational science has an important roles in atomic energy research, since experiments in such a large scale facilities are difficult due to stretched budgets or danger to the environment. Computational study is widely known as the third way adding to theoretical and experimental studies, and has gone far beyond the role of tools for verifying. It can lead in establishing a new theory such as detecting embrittlement mechanisms due to metal impurity, or a new experimental method for nuclear fusion from the results of simulations.

To meet such demands, CCSE has been promoting two research policies as follows:

(1) Joint promotion of computational science, computer technology, and computer and network system operation and maintenance support.

CCSE is promoting R&D for computational infrastructure and its application. The former aims for a suitable computation environment for high-performance computing. So far, we have established a virtual research environment sharing 57TFLOPS computer capacity in the Information Technology Based Laboratory (ITBL) project. The latter promotes research in such areas as quake-resistance of nuclear facilities, nano-devices, and radiation in the human body. We made numerical simulations to determine safety of nuclear power plant against extra-large earthquakes, and to design a high accuracy super-conducting neutron detector. These two results were selected as an honorable mention and the Gordon Bell Finalist respectively, at SC2005, one of the world's largest international supercomputing conferences.

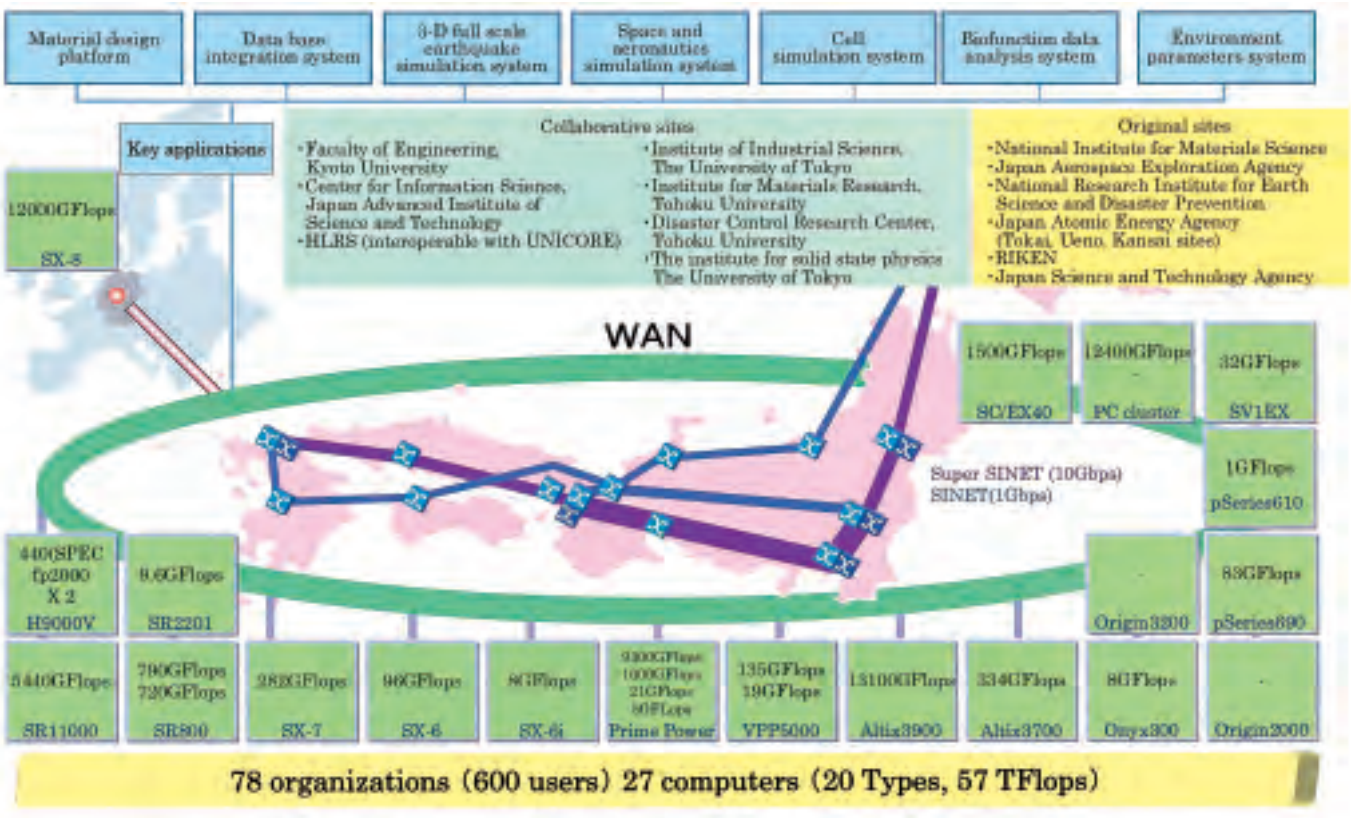

Fig.10-2 The environment established in ITBL project
Thanks to the collaborative works of ITBL member organizations, ITBL shares 27 supercomputers of 20 different types and offers 57TFLOPS using ITBL middleware. (as of Mar. 2005). SX-8 (12 TFLOPS) at HLRS, Germany is also available through the interoperability between UNICORE and ITBL middleware. This figure also shows key applications developed by ITBL research.

(2) Cross - disciplinary approach for theoretical and experimental studies in collaboration with other divisions

CCSE contributes a great deal to the sophistication and improvement of various studies with its cross- disciplinary approaches. Especially, CCSE promotes elucidation of phenomena with simulations, and analysis through interpolation of experimental data, digitalization of facilities in computer systems, and construction of a "Design by Analysis" system for fast-breeder reactors.

Next, we briefly describe the activity of CCSE in the ITBL project mentioned in (1) above.

CCSE has participated in ITBL (FY2001-FY2005), which is one of the e-Japan priority policy programs. The project has made a virtual research environment that allows its users to be able to execute complicated and advanced simulations and to do collaborative work with remote locations. This has been accomplished by R&D to gather computer resources, information, and know-how which lie scattered throughout the Internet. CCSE has taken important roles in developing and operating the ITBL middleware and researching and developing applications. ITBL shares its 57TFLOPS computer capacity with domestic and foreign institutions using ITBL middleware. The number of domestic and foreign universities, institutes and companies that have joined the ITBL totals 78, and the total number of users is over 600.

The ITBL project has expanded its environment by interoperating ITBL middleware and UNICORE, a middleware developed in Europe. This expansion and international collaboration has enabled ITBL users to use super computers at the High Performance Computing Center, Stuttgart (HLRS).

CCSE has been promoting new research on the Atomic Energy Grid Infrastructure System (AEGIS) to develop the computational infrastructure required in the atomic energy field. We conduct international collaborations with not only Germany but also France and the United States to offer a worldwide scale virtual research environment for large-scale experimental facilities of atomic energy research. In addition, we joined a national project called "Development and Applications of Advanced High - Performance Supercomputer" which has started in FY2006 to establish information infrastructure for sophisticated technology. In this project as well we are working on middleware for the infrastructure.

10-2 Exploration of Room Temperature Superconductivity through the Super Strong-Coupling Superfluid Quantized Vortex

— A World of the Room Temperature Superconductivity Revealed by Quantized Vortices in Atomic Fermi Gas —

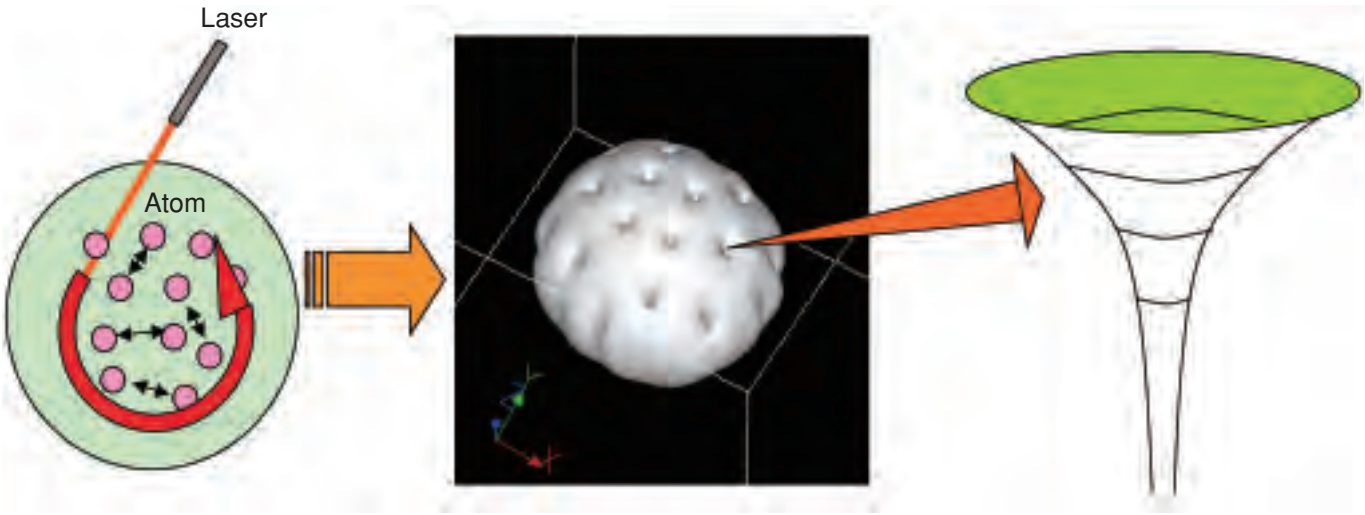

Fig.10-3 As seen in the central figure, vortices emerge everywhere inside an atomic gas when rotated using a laser (see the left-hand side figure). The vortices look like drilled holes in the atomic density profile. The vortex is quantized when the atomic gas enters the superfluid state. This study reveals structure of the quantized vortex by first principle calculation. Since the quantized vortex is a feature common to superfluidity and superconductivity, one can study the superconducting vortex through information for the superfluid vortex. Due to a strong attraction between atoms in the atomic gas, the vortex structure clarified by this study is considered to be equivalent to that of the superconducting vortex expected in the room temperature superconductivity.

It is said that "room temperature superconductivity may cause a revolution much beyond the Industrial Revolution". Zero electrical resistance at the room temperature would allow transfer of energy created by an electric power plant without any loss, a global electrical energy transport, a high-speed transportation network by linear motor car, a laptop parallel supercomputer without any coolers and so on. Due to such great possibilities, to raise the superconducting transition temperature up to the room temperature range is a dream of scientists today.

Very recently, study of the room temperature superconducting state is being attempted even though it has been not discovered yet. This is because the superfluidity in the atomic Fermi gas realized on 2004, is a very strong coupling superfluidity whose impact would be equal to room temperature superconductivity. In general, the superconductivity emerges when two electrons form a pair via an attractive interaction. The strength of this attraction is known to determine the superconductivity transition temperature. The attractive interaction in the atomic Fermi gas is so strong that the attraction causes the superconductivity in a 1000K range much beyond the room temperature. This fact raises a question of what features the strong superfluid state has, and especially, what structure the vortex seen in the superfluid flow exhibits. The vortex has a key role in both superfluid and superconductivity since its motion imposes a limitation on dissipation - free flow. Thus, one must inevitably study the vortex structure and its dynamics when considering the application of superconductivity.

In this study, we determined the vortex structure by a first-principle calculation, and succeeded in finding the structure from weak to strong attractive interaction beyond that of room temperature superconductivity. As a consequence, it is found that the strong attraction leads to drastically lowered atom-density inside the vortex core like the depression in the middle of water inside a bucket when rotated, whereas in contrast there is little density depression in the weak attraction. This result indicates that the electrical transport capacity of the room temperature superconductor will be great. We confirm through this study that the room temperature superconductivity may be quite fruitful if it is realized.

Reference

Machida, M. et al., Structure of a Quantized Vortex near the BCS-BEC Crossover in Atomic Fermi Gases, Physical Review Letters, vol.94, no.14, 2005, p.140401-1-140401-4.

10-3 Assembly Structure Analysis of Extra Large-Scale Nuclear Plants

—Grid-Based Extra Large-Scale Structural Analysis by a Part Oriented Approach—

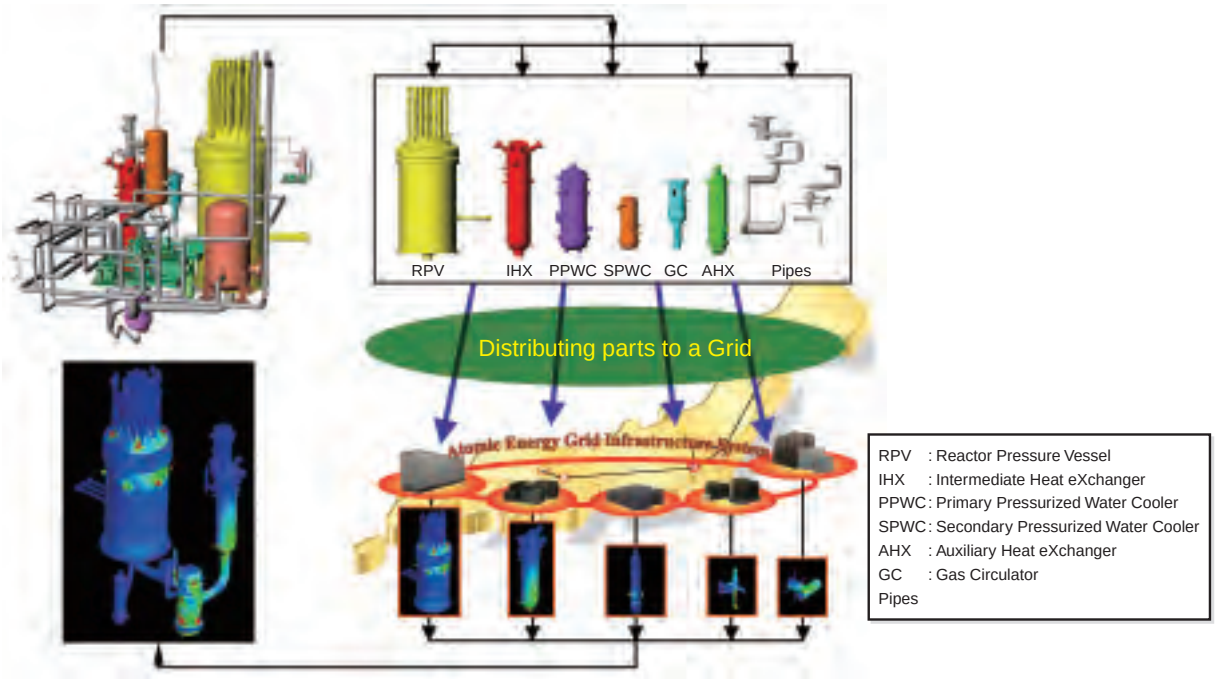

Towards a virtual plant vibration simulator: integrated simulation of over 10 million parts
- Distributed assembly structure analysis on Grid -

Fig.10-4 Summary of the proposed simulation framework
A framework for analyzing a whole nuclear plant consisting of over 10 million parts has been developed by preparing model data for each part, then distributing them to numerous supercomputers inter-connected by Grid, and finally simulate an entire by considering the connecting condition among the parts. Numerous supercomputers on the Grid are powerful enough to meet the demands on memory and disk capacities in visualization of gigantic analytics data. By distributing all the simulation processes such as the model data preparation, analysis execution, and the data visualization among multiple supercomputers located inside and outside of JAEA opens up the possibility of structural analysis of a whole extra large-scale nuclear plant.

The Center for Computational Science and E-systems of JAEA is conducting researches and developments for extra large-scale simulation technologies of whole nuclear plants using state-of-the-art computational and IT technologies. Specifically we focused on establishing a virtual plant vibration simulator on inter-connected supercomputers, for seismic response analysis of a whole nuclear plant. In order to achieve high accuracy simulation, we need to consider how connecting conditions affect the integrated behaviors (stresses and deformation etc.) of the parts of a plant. A nuclear plant is generally composed of a gigantic number of parts. The simulation of the whole plant becomes a very difficult task because an extremely large dataset must be processed which is too expensive to be carried out on a single supercomputer by the conventional simulation technique. To overcome this difficulty, we have established:

(1) a framework which allows model data preparation to be carried out in a part-wise manner, so that there is high scalability as the model size increases, and allows the connecting condition of the parts to be taken into consideration in the integrated simulation of the whole plant.

(2) a computing platform which enables extra large-scale whole nuclear plant simulation to be carried out on a Grid computing platform called Atomic Energy Grid InfraStructure(AEGIS) which is built by high-speed interconnection of dispersed heterogeneous supercomputers.

The simulation framework developed has been applied to an elasto-static analysis of the reactor pressure vessel and cooling systems of a nuclear research facility, the “High Temperature engineering Test Reactor (HTTR)” located at the Oarai R&D center of JAEA.

The simulation framework taking advantage of Grid distributed computing techniques showed early success in the extra large-scale simulation of the major parts of the nuclear plant, and opens a possibility of new simulation technologies for building a whole virtual nuclear plant in computers for virtual experiments. In SC05 held at Seattle, USA, one of the world largest international conferences on high performance computational technologies and sciences, our HPC Analytics Challenge contest entry giving these simulation results gained attention and was awarded “honorable mention” recognition.

Reference

Nishida, A., Wave Propagation Properties of Framed Structures based on the Timoshenko Beam Theory, Kozo Kogaku Ronbunshu, vol.52B, 2006, p.119-124 (in Japanese).

10-4 Attempt to Overcome Quantum Many-Body Problem Limits with the Earth Simulator
—Fast and Accurate Diagonalization of Enormous Matrix—

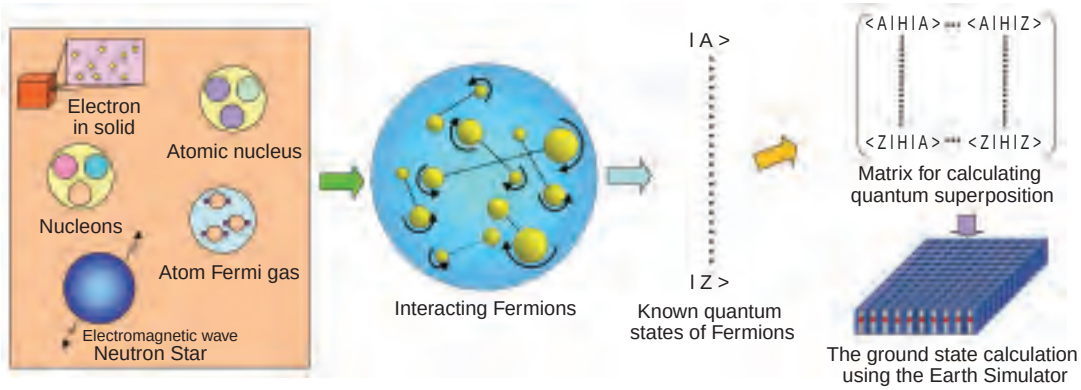

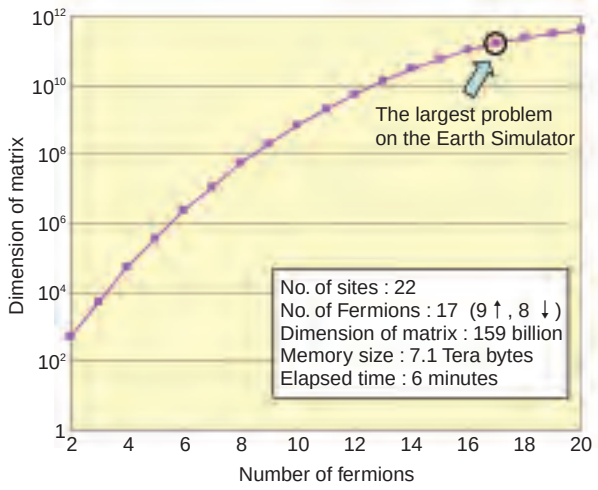

Fig.10-5 (upper) One can understand properties of electrons in a solid, nucleus, nucleon, atomic Fermi gas, neutron star etc. by calculating quantum states of interacting Fermi particles. The figure schematically demonstrates the calculation on the Earth Simulator. First, one sets up known (eg. non-interacting) quantum states and second, superpose their states via matrix diagonalization in order to contain their interaction. The huge memory size and the high operation speed of the Earth Simulator makes it possible to execute a huge matrix diagonalization.

Fig.10-6 (left) Relationship between the number of Fermi particles and the matrix size (dimension) in the lattice model. The full use of the Earth Simulator enables diagonalization of a 159 billion dimensional matrix for 9 up and 8 down-spin particles on 22 sites.

All matter in this universe is made by assemblies of the so-called Fermi particles, which obey Fermi statistics (Fig.10-5). Therefore, if one precisely identifies the dynamics of interacting Fermi-particles, the properties of that matter are in principle predictable from microscopic to macroscopic levels. Once Schröinger, a founder of quantum mechanics, succeeded in describing the quantum mechanics via the Schrödinger Equation, some physicists immediately jumped to a conclusion that physics will be completed soon. The reason is that they believed that the all matter would become understandable by a big computer solving Schrödinger Equations for quantum many-body systems. However, this understanding was not attained within the 20th century. Instead, physicists have made their efforts to create approximation techniques and tried to understand Fermi particles behaviors by using them.

On the other hand, the question, what is the largest number of quantum bodies whose system can be solved, has recently become an interesting issue since successively larger supercomputers have been developed. Thus, we attempted to solve a problem of atomic Fermi gas on the Earth Simulator, and succeeded in solving the ground state of 17 fermions loaded on 22 sites of an optical lattice (Fig.10-6). This problem is equivalent to a mathematical one calculating the eigenstate of a 159 billion dimensional matrix, which is one of the largest matrices ever solved to humankind. By adopting a new algorithm and taking advantage of specific architectures in the Earth Simulator, we were able to solve this problem within only 6 minutes. To our knowledge, there have been no studies of 20 fermion problems whose solutions were found on the order of minutes. Our calculation is the largest ever, and likely is the limit worldwide at present. In the future, further advancements of computers should enable to solve still larger matrices. Our new tasks will follow upon computer advancements.

References

Yamada, S. et al., 16.447 TFLOPS and 159-Billion-Dimensional Exact-Diagonalization for Trapped Fermion-Hubbard Model on the Earth Simulator, Proceedings of International Conference for High Performance Computing, Networking and Storage(SC'05), 2005, in CD-ROM.
Machida, M. et al., Novel Pairing in the Hubbard Model with Confinement Potential, Physica C, vol.445-448, 2006, p.90-93.

10-5 Why Water Can't Be Heated or Cooled Easily?
—A Molecular Theory for the Specific Heat of Water—

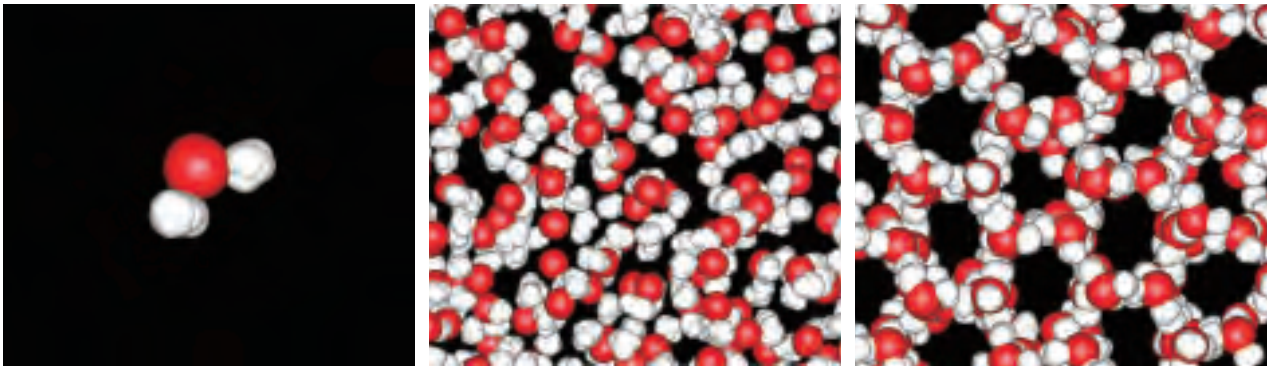

(a) Vapor (b) Liquid water (c) Ice (I_h phase)

Fig.10-7 Red and white spheres indicate oxygen and hydrogen atoms, respectively
By molecular dynamics simulation, the motion of molecules is analyzed in a computer.

Water is a ubiquitous chemical substance used in a vast range of research fields, from atomic energy to biology, but it possesses special characteristics that other substances do not have. For instance, as one of the 'anomalous' properties of water, it is known that the specific heat of water changes drastically according to the temperature and phase. At the melting point, the specific heat of liquid water becomes twice as large as that of the ice. Meanwhile, at the boiling point, the specific heat of vapor decreases to 1/3 that of liquid water. Liquid water has unusually large specific heat compared to other substances(about 4.19 J/gK, 1 cal/g℃) and it does not vary much by temperature. On the other hand, the specific heat of ice and vapor changes dramatically with temperature; It tends to increase with temperature both in the case of ice and vapor. It is known that heavy water has a larger specific heat than light water by about 10 % for a unit mol. How can these facts be understood from the view point of molecular theory?

As shown in Fig.10-7, water molecules, composed of hydrogen and oxygen atoms, form weak bonds (hydrogen bond) between each other. In liquid water, the creation and annihilation of these hydrogen bonds are perpetually repeated, causing complex motions. In addition, the light hydrogen atoms behave quantum mechanically. Although it can be expected that these factors affect the specific heat, this has never been actually confirmed by a theoretical simulation. Therefore, in this study, a molecular dynamics simulation has been performed for a quantitative analysis on the specific heat of the three states of water.

From this study, it has been found that there are two important factors in the specific heat of water. One is the 'strength' of hydrogen bonds. In the condensed phases, ice and liquid water, the molecular vibrations of individual molecules are induced and the hydrogen bonds are weakened as temperature is increased. The specific heat is determined by how much of the energy given by an external heat source the molecules can absorb. In the case of ice, the hydrogen bond is so firm that the whole molecule pair will be vibrated without absorbing much heat. However, liquid water can absorb more heat through the transforming or breaking of hydrogen bonds. In other words, it is because the hydrogen bonds play a role of large 'heat bath' that makes the specific heat of liquid water large and constant. In the vapor phase, since water exists as isolated molecules without hydrogen bonds, the specific heat is small since the 'heat bath' is small.

Another factor is that the mechanics of hydrogen bonds changes from classical mechanics to quantum mechanics as temperature is decreased. The bond with 'quantum nature' has a tendency to absorb less heat, because the vibrational energy levels become discrete and thus the molecular excitation is rather limited. This is why the specific heat tends to decrease with temperature.

The specific heat of water is realized by two factors: the 'strength' and 'quantum nature' of hydrogen bonds. Incidentally, the difference of specific heat between light and heavy water can also be explained by these two factors.

Reference

Shiga, M. et al., Calculation of Heat Capacity of Light and Heavy Water by Path Integral Molecular Dynamics, Journal of Chemical Physics, vol.123, no.13, 2005, p.134502-1-134502-8.

10-6 Phase Property and Interaction Force of Pulsating Multiple Bubbles
—Existence of an Unknown Characteristic Frequency Is Confirmed—

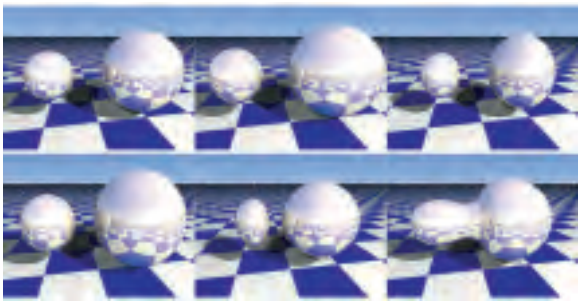

Fig.10-8 Numerical simulation of pulsating, interacting bubbles
When sound is applied, a bubble begins to pulsate. If several bubbles exist, an interaction force which can be either attractive or repulsive acts between the bubbles. In this simulation, an attractive force appears. Two pulsating bubbles gradually approach each other and finally collide to merge (temporal sequence from the upper left to the lower right).

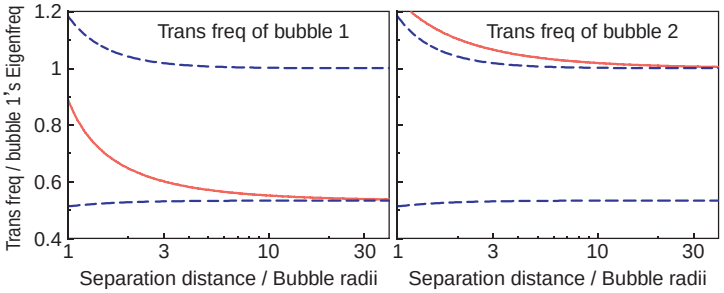

Fig.10-9 Transition frequencies of two interacting bubbles as functions of the distance between the bubbles
The blue lines denote the resonance frequencies and the red lines correspond to the transition frequencies that we have discovered. Though in a frequently cited explanation the direction reversal of the interaction force occurs at the resonance frequencies, in our theory it occurs around the characteristic frequencies we found.

Bubbles in a liquid are familiar objects to us. One can easily produce and observe many bubbles by shaking a water-filled bottle. Bubbles are significant in diverse fields including engineering and medicine. Microbubbles injected into blood vessels are used as ultrasound contrast agents; cavitation bubbles emerging in a depressurized liquid have a strong impact force that damages fluid machinery in nuclear plants; sonoluminescencing bubbles which emit light in a strong sound field are utilized as a chemical reactor. Also, the innumerable bubbles forming whitecaps on the ocean are assumed to have an effect on climate.

Despite their familiarity, bubbles still have many unsolved problems. Recently, by examining theoretically and numerically the pulsation phases of bubbles pulsating and interacting with each other in a sound field (Fig.10-8), we have found an unknown characteristic frequency (Fig.10-9). The characteristic frequency, which we call "transition frequency," inverts a bubble's pulsation phase (e.g., from in phase to out of phase with the driving sound) without resonance, and is thus essentially different from the resonance frequency.

We have also found that several unsolved problems of bubbles are resolved by our discovery. One of them is the mechanism of an interaction force acting between pulsating bubbles. It had already been known that the force changes its direction depending on whether phase differs between the bubbles and can thus be either attractive or repulsive. However, there has not yet been an established theory on the underlying mechanism of the direction reversal. We have found out that the transition frequency is precisely the factor determining this direction; that is, when one changes the frequency of the driving sound, the interaction force inverts its direction when the frequency passes through the transition frequency. This discovery questions the frequently cited explanation that the direction reversal occurs at the resonance frequency.

We are now performing additional investigations to fully confirm the existence of the transition frequency. The results given in this study will be useful tools for understanding phenomena observed in systems involving many bubbles, such as the collapse of cavitation bubble clusters and stable structure formation through bubbles. This work was partly supported by MEXT through a Grant-in-Aid for Young Scientists (B) (No. 17760151).

Reference

Ida, M., Phase Properties and Interaction Force of Acoustically Interacting Bubbles: A Complementary Study of the Transition Frequency, Physics of Fluids, vol.17, no.9, 2005, p.097107-1-097107-13.

10-7 Various Uses of Metal Ions by Living Organisms
—Prediction of Copper-Binding Proteins from Genome Sequences—

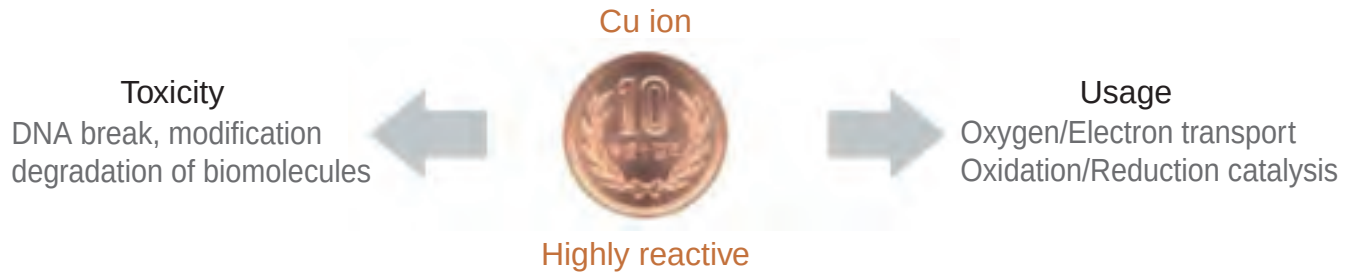

Fig.10-10 Functions of copper ion in living organisms

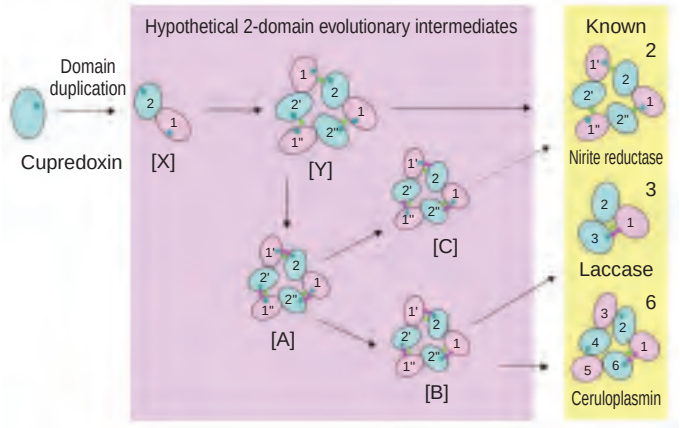

Fig.10-11 Proposed pathway of the evolution of Multi-Copper Blue Proteins

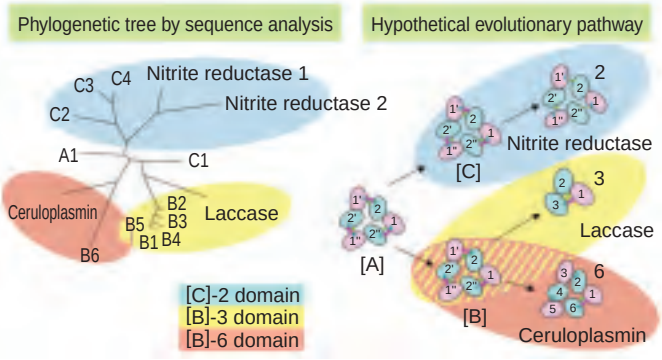

Fig.10-12 Phylogenetic tree and the inferred evolutionary pathway

It has been known that putting 10-yen coin made of copper in shoes prevents foot odor by deterring the growth of bacteria. Copper ion is highly reactive and mediates the formation of active oxygen, which destroys important bio-molecules such as DNA, and therefore is very harmful to simple organisms such as bacteria. However, through the long history of evolution, higher organisms have developed resistance against copper ions, developing a mechanism to excrete the heavy metal and to repair the damaged DNA. Furthermore, some organisms have even acquired a mechanism to exploit the high reactivity of copper ions, for transportation of electron or oxygen, and for the catalysis of the synthesis of useful molecules. (Fig.10-10)

Among those proteins, we focused on a group of proteins called multi-copper blue proteins and carried out analysis. Multi-copper blue protein is a group of proteins which exploits the unique redox ability of copper ions, produced by a wide variety of organisms and having important and versatile functions. It consists of three major groups. 1) Nitrite reductase which is responsible for denitrification, an important process in the circulation of nitrogen in nature. 2) Laccase, responsible for formation/degradation of cell walls of plants/fungi, and ascorbate oxidase which prevents oxidative stress that damages DNA. 3) Ceruloplasmin, responsible for the formation of hemoglobin that carries oxygen in blood stream of vertebrates.

As seen with the completion of human genome project, the amount of nucleotide sequence information is explosively increasing. We used this information efficiently to clarify the evolutionary history of multi-copper blue proteins, (Fig.10-11, Fig.10-12) and discovered new types of multi-copper blue proteins ([A], [B], [C]) from genome sequences.

Furthermore, by carefully comparing those newly identified sequences, we could gain insight into the "molecular evolution" process, through which the proteins have developed new functions.

With more careful analysis of metal-binding proteins and genome sequences, we are aiming to discover new proteins that are related to radiation resistance, such as DNA-repairing enzymes.

Reference

Nakamura, K. et al., Function and Molecular Evolution of Multicopper Blue Proteins, Cellular and Molecular Life Science, vol.62, 2005, p.2050-2066.

10-8 A Computational Method to Predict RNA Interface Sites on Protein
—Research in Structural Bioinformatics—

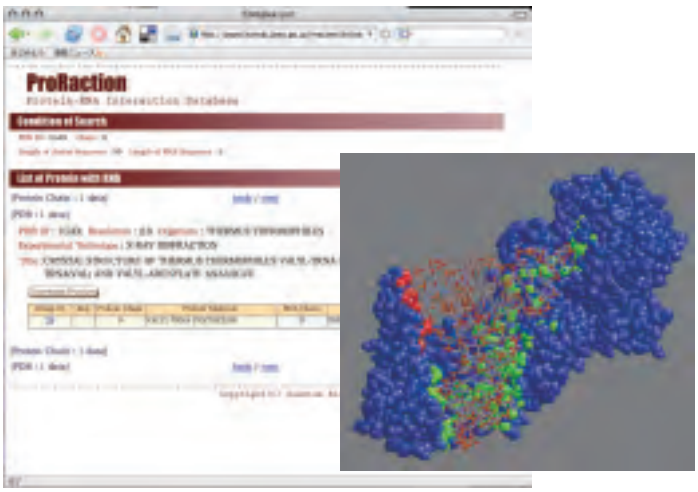

Fig.10-13 Database for RNA-protein complex structures
To understand how proteins interact with RNA, structure data of RNA-protein complexes were gathered and stored in a database. This database stores the 3D atomic structure of specific proteins bound with RNA. Here, the blue, red and green balls represent a protein and the wires represent an RNA molecule. Protein surfaces in red and green are the interfaces.

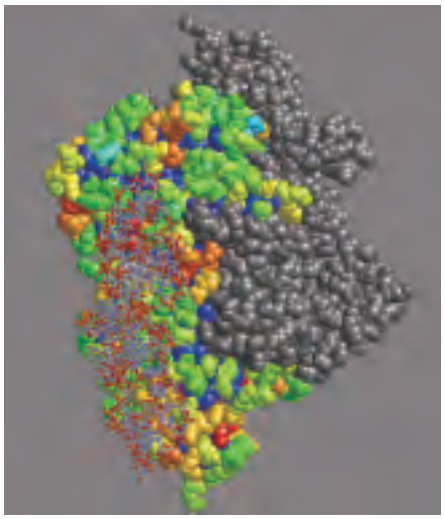

Fig.10-14 A result of RNA interface prediction
RNA interfaces on a protein are predicted from statistics of protein surfaces derived from the database. Prediction ability is tested on a protein in the database other than those used in the statistics. The balls (protein) in orange to red are the predicted RNA interface and the set of wires is an RNA molecule.

Organisms are under constant exposure to radiation including ultraviolet light. Irradiation of organisms is known to damage their DNA. High-energy light as well as oxygen is a known cause of damage to DNA and RNA. The damage is considered to be a cause many biological phenomena including aging. Organisms have evolved mechanisms to repair this damage and maintained the species. Molecules and mechanisms for DNA/RNA repair are the interest of a number of researchers, and extensive studies have been carried out. The studies have shown that protein molecules are the basic molecules for DNA/RNA repair.

DNA sequences of the human genome were all determined at the beginning of the 21st century, and we now have a blueprint for a human. However, the question we face now is how to read the blueprint. DNA sequences of human genome are equivalent to a string of three billion letters written with only four types of characters, and we need to 'decipher' the string. The process of deciphering is a collaboration of biological and computational science, and this new field is called bioinformatics. The bioinformatics research explained here is specifically a study to discover a DNA/RNA repair related protein by deciphering DNA sequences.

DNA/RNA repair proteins first need to bind to DNA/RNA. Finding out locations on the proteins for DNA/RNA interactions is one of the first steps for studying DNA/RNA repair. Many researchers have elucidated a lot of structures of protein that bind to a target RNA. We have gathered structural data of proteins and built a database (Fig.10-13). Using this database, we can carry out statistical analysis to find characteristics of RNA interfaces on proteins, such as size of RNA interfaces and characteristic atoms that appear in RNA interfaces. With these statistically derived characteristics, one can perform prediction of RNA interfaces on a protein not yet observed to bind RNA. We are developing new statistical methods and are trying to predict the interfaces with high quality (Fig.10-14).

By predicting RNA interfaces on proteins with high quality, we can design biochemical experiments to determine RNA interfaces. A collaboration of biological and computational sciences is now getting to elucidate mechanisms of molecules that sustain life.

Reference

Kim, T.P.O., Yura, K. et al., Newly Sequenced eRF1s from Ciliates: the Diversity of Stop Codon Usage and the Molecular Surfaces That Are Important for Stop Codon Interactions, Gene, 346, 2005, p.277-286.

10-9 Bubbles' Hidden Complexity

— An Anomalous Phenomenon "Avoided Crossing" Has Been Found in Bubbles Interacting through Sound —

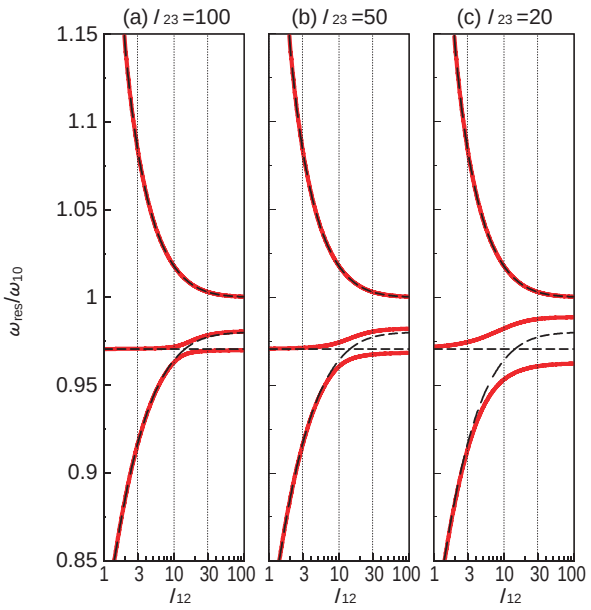

Fig.10-15 Avoided crossing in resonance frequencies
Shown are the resonance frequencies of three bubbles positioned on a line, as functions of the distances (l_{12}, l_{23}) between them. The dashed lines are when bubble 3 is isolated and the red lines are when all bubbles are coupled. Two resonance frequencies of different origin which crossed when bubble 3 is isolated blend together when all bubbles are coupled. This is the avoided crossing. As bubble 3 comes closer to the others (i.e., l_{23} decreases), this connection becomes stronger.

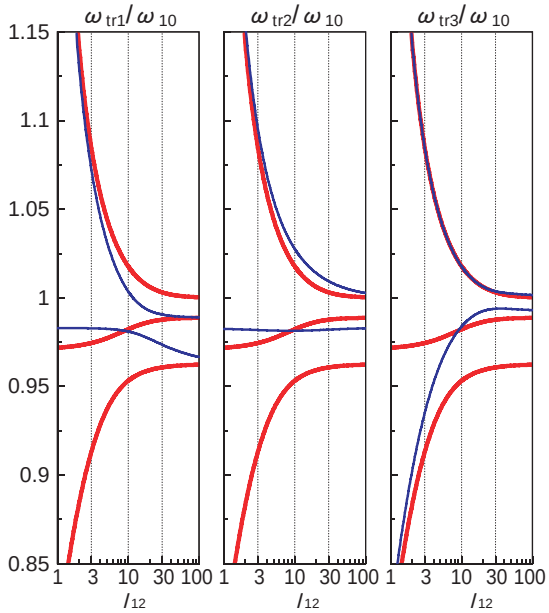

Fig.10-16 Transition frequencies in the avoided crossing region
Each panel shows the transition frequencies of one bubble in the triple-bubble system. The red lines correspond to the resonance frequencies shown in Fig.10-15(c). The blue lines denote the transition frequencies determined by the world's first transition-frequency analysis, and one of them crosses with a resonance frequency. Such a crossing was not observed in double-bubble systems. In this region, the bubbles appear to exchange their oscillation states with each other.

Bubbles are ubiquitous presences, appearing in many places around us. In nuclear engineering, bubbles emerge through, for example, boiling in an atomic reactor and cavitation in nuclear plants and accelerators. Bubbles that emerge through cavitation will pulsate violently and sometimes damage piping by emitting a high-speed liquid jet. In a cavitating liquid, a huge number of such bubbles interact with each other through sound, and hence the bubbles constitute a kind of system of interacting oscillators, that is, a "coupled oscillator system."

We have recently been studying the dynamics of multiple bubbles as a coupled oscillator system and have discovered a strange phenomenon "avoided crossing." Avoided crossings have been studied in many research fields including quantum chemistry and chaos dynamics, and have been found in several physical systems involving multiple eigenvalues (e.g., eigenfrequencies or Lyapunov exponents). In the parameter regions where an avoided crossing appears, two eigenvalues first approaching each other as a system parameter varies change their paths abruptly and swerve away from each other. In that region, an abrupt state change of the system also takes place.

In the case of bubbles we have considered, avoided crossings appear in their resonance frequencies. The red lines in Fig.10-15 denote the avoided crossing resonance frequencies. We, carefully examining this result, have found that in the avoided crossing region, the transition frequencies, at which the pulsation phase of a bubble inverts, cross (Fig. 10-16) and the bubbles act as if they exchange their oscillation states with each other. Our paper is the first to report such behavior of bubbles. We think that this finding uncovers a hidden complexity of bubbles, and that this is useful for understanding the very complicated dynamics of cavitation bubble clusters. This work was partly supported by MEXT through a Grant-in-Aid for Young Scientists (B) (No. 17760151).

Reference

Ida, M., Avoided Crossings in Three Coupled Oscillators as a Model System of Acoustic Bubbles, Physical Review E, vol.72, no.3, 2005, p.036306-1-036306-7.

11 Scientific & Technical Development for Nuclear Nonproliferation

11-1 Direction of Scientific & Technical Development for Nuclear Nonproliferation

Past and Present View of Nonproliferation

The Treaty on the Non-Proliferation of Nuclear Weapons (NPT) entered into force in 1970 as a mechanism to prevent further proliferation of nuclear weapons while simultaneously promoting the peaceful use of nuclear technology. Under the NPT, nuclear-weapon holding states are prohibited from transferring nuclear-weapon technology to other countries and are obliged to continue nuclear disarmament efforts. Non-nuclear-weapon states are obliged to accept safeguards by the International Atomic Energy Agency (IAEA) to assure that there is no diversion of nuclear materials to weapons, thus obtaining the right to use nuclear energy for peaceful purposes.

The NPT has functioned as the base for nuclear nonproliferation activities and the peaceful use of nuclear energy for more than 35 years. However, weak points in its regime recently have surfaced, such as the clandestine Iraqi weapons program, North Korea's nuclear weapon development and withdrawal from the NPT, and Iran's undeclared uranium enrichment activities. As a result of Iraq's program, the safeguards were strengthened to monitor and assess other undeclared activities. In addition, other unique problems exist, such as India and Pakistan who became nuclear weapon countries without ratifying the NPT.

New ideas have been proposed to support the NPT in this changing global situation. One idea is to apply limits to technology that could lead to proliferation upon holders of nuclear reprocessing and enrichment equipment, and/or control these parties under international cooperation. In the new nuclear energy policy of the US, the Global Nuclear Energy Partnership (GNEP) is proposed as an international fuel-services consortium where only "fuel supply nations" possess sensitive technologies. These countries then supply fuels to "user nations" who choose only to operate nuclear power plants.

Early on, Japan realized and pursued advanced peaceful nuclear applications and achieved favorable international nuclear nonproliferation status. At the same time that Japan has been complying with the international rules, it has been continually making efforts to improve transparency and confidence. Now, Japan is recognized to hold one of the highest standards in the international community for peaceful nuclear use. As such, Japan is also expected to contribute to the world's peaceful use of nuclear energy by proposing new nonproliferation systems and developing new Safeguards technologies.

JAEA Missions for Nuclear Nonproliferation

We have two primary missions regarding nuclear nonproliferation. One mission is to support the government in developing nonproliferation related policies through research and study.

The other mission is to support government and international organizations by performing nuclear nonproliferation technology development. Other important missions of JAEA are to support denuclearization, nuclear material control of its own facilities, and human resource development.

When JAEA was established in 2005, the "Nuclear Nonproliferation Science and Technology Center" was created to carry out JAEA's nuclear nonproliferation activities and obligations. This center works closely with other parties within JAEA and with the international nonproliferation community.

Policy Research and Study

We support the government by performing nonproliferation related policy research, utilizing in-house technical knowledge. At present, We are performing two major policy studies in cooperation with other domestic and international organizations and specialists. The first study is the "Evaluation of the Safeguards Achievements in Japan". This study evaluates safeguards achievements in Japan, extracting and highlighting "best practices" to develop an improved global standard.

The second project is the "Study of Peaceful Nuclear Use In Asia and Improvement of Its Transparency and Confidence." The study evaluates procedures to improve the transparency of the rapidly expanding nuclear use in Asia. To promote the better understanding of nonproliferation and to support peaceful nuclear use, We release result of their studies and other information through the Internet, and holds international conferences and forums.

Technical Development relating to nuclear nonproliferation

Technical development to support nuclear nonproliferation includes the reprocessing plants and the plutonium fuel fabrication plants, and development of Non-Destructive Analysis equipment and Remote Monitoring Systems. Also, development of the Advanced Safeguards System which will

Fig.11-1 The International Nonproliferation Science and Technology Forum held in Tokyo on 2006.05.18-19. Invited world specialists exchanged views about various nonproliferation issues

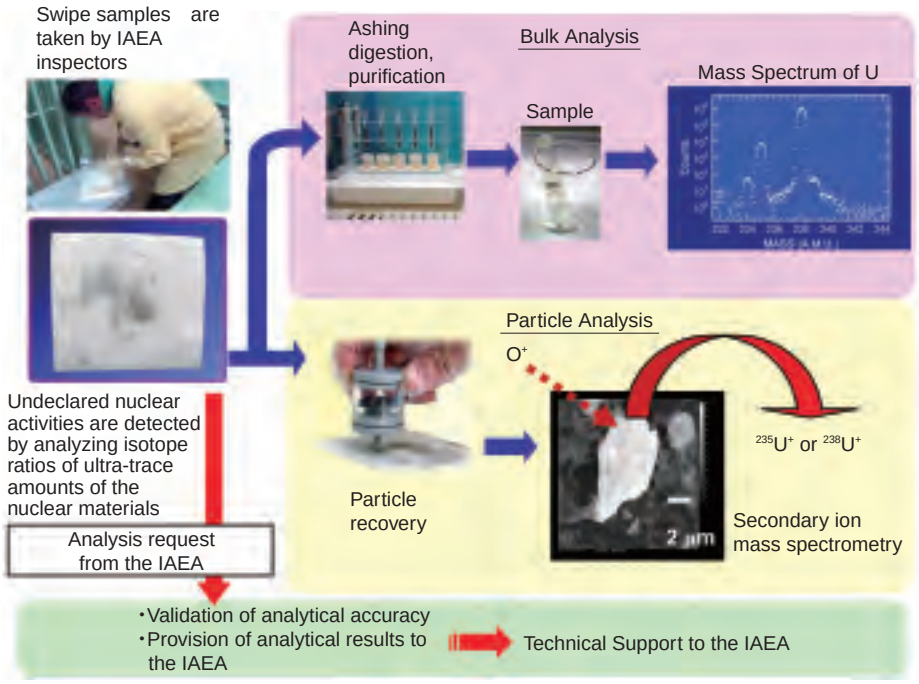

Fig.11-2 Schematic diagram of safeguards environmental sample analysis

be applied to the future Fast Breeder Reactor fuel cycle is underway. This should be considered from an early design stage to realize efficient and effective safeguards.

The IAEA established Safeguards Environmental Sample Analysis as a strong tool to detect undeclared nuclear activities. We are performing world-class research and development in this field, at a clean room facility (CLEAR). Safeguards Environmental Sample Analysis includes techniques to analyze isotope ratios etc. of ultra-trace amounts of nuclear material collected on cotton samples by swiping the surface of the floor, etc. inside nuclear facilities.

Other technical projects are also underway at the JAEA to improve the transparency of nuclear activities and thereby improve the reliability of, and confidence in, these peaceful activities. Remote monitoring techniques are being developed and perfected at the Fast Breeder Test Reactor "JOYO" in cooperation with the USDOE and Sandia National Laboratories. In addition, JAEA is participating in the Generation IV International Forum and International Project on Innovative Nuclear Reactors and Fuel Cycles. We are currently performing a study for quantification of the proliferation resistant features of various nuclear activities. Results of the study will be used to develop a more proliferation resistant FBR fuel cycle system.

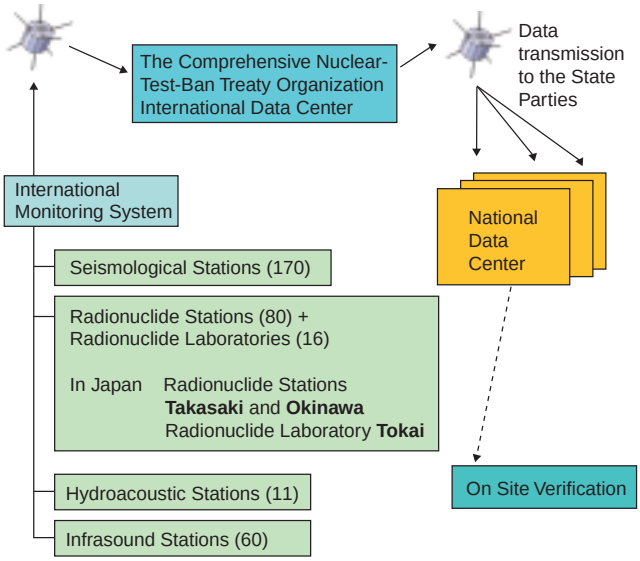

Fig.11-3 International verification system for the CTBT

Support of Denuclearization

We are performing technical development to contribute to nuclear disarmament and denuclearization efforts in the world. Currently, collaborative programs are underway for disposal of Russian surplus weapons plutonium, and for technical contributions to the international verification system for the Comprehensive Nuclear Test Ban Treaty (CTBT).

We also contribute to nuclear test ban monitoring using seismic and radioactive nuclide monitoring stations. For the atmospheric testing, very small particles are collected on a filter and measured every day. The results on the radionuclides are transferred to the International Data Center at the CTBT office in Vienna.

Nuclear Material Management

Strict nuclear material management is the underlying basis of the nonproliferation regime. Nuclear material management includes nuclear material accountancy, support of safeguards activities, physical protection, and nuclear material transportation. We perform research and development to improve the reliability and effectiveness for accountancy and the safeguards. Research and development are also underway to support and enhance physical protection of facilities, and to develop more efficient and safer transportation.

11-2 Exchange of Remote Monitoring Information for Transparent Nuclear Materials Utilization

— Development of Remote Monitoring Technology for Nuclear Nonproliferation and Transparency —

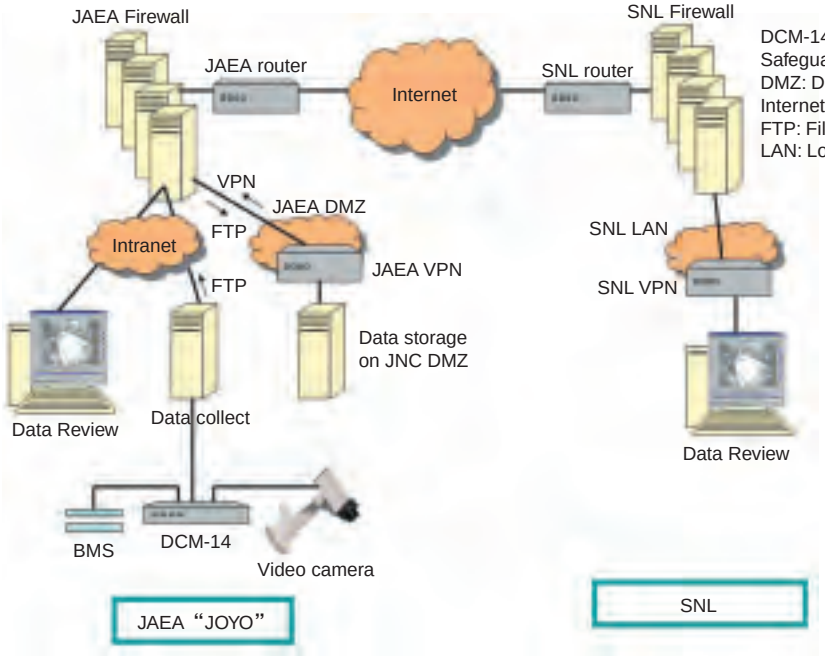

Fig.11-4 Configuration of Joyo Remote Monitoring System
A video camera in the Fresh Fuel Storage room takes pictures at intervals if the Balanced Magnetic Sensor (BMS) detects the door opening. Also, when the camera detects image changes, it takes pictures. Image data stored in the Data Collection Computer are transferred to the Data Storage Computer over the local Intranet, then to the Data Server at the remote site via a VPN (Virtual Private Network) over the Internet. Data are reviewed by the Data Review Stations.

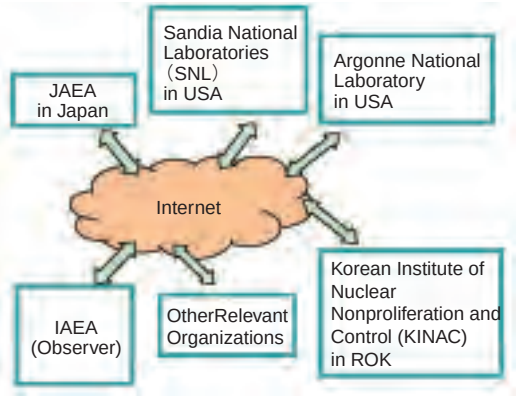

Fig.11-5 Remote Monitoring Network Plan
JAEA continues discussions with related laboratories utilizing the remote monitoring technology for information exchange among nuclear facilities to develop transparency and confidence building.

Recent concerns in nuclear nonproliferation include nuclear weapon development in India and Pakistan, and nuclear programs in North Korea and Iran. Nonproliferation discussion and negotiation are continuing among relevant countries. Therefore, improvement of transparency and confidence building concerning nuclear activities are more important than ever for developing the peaceful use of nuclear energy, and nuclear R&D activities. In addition, these improvements will help maintain compliance with domestic regulations and the international nonproliferation regime.

In 1995, we started a study for a prototype remote monitoring system, which consists of motion sensors (microwave, optical), neutron/γ-ray detectors, surveillance cameras, and data collection computers in the fresh fuel storage area and the spent fuel pond of the Fast Experimental Rector "JOYO". Since then, development and testing a remote monitoring system to monitor the transfer and storage of nuclear materials, human activities, etc. has been conducted

In the software development area, we developed a decision support system which has the capability to properly analyze and evaluate data, and make proper responses, such as giving an alarm upon unexpected events.

To utilize these technologies for improvement of regional transparency and confidence building, we are studying bilateral and multi-lateral exchange of information on nuclear facilities.

At present, we are promoting technical cooperation for transparency and confidence building with relevant organizations of the USA and Republic of Korea (ROK), and is considering future regional information exchange on a lab-to-lab basis among these countries.

Reference

Olsen, J., Hori, M., Hashimoto, Y. et al., Regional Cooperation in Remote Monitoring for Nuclear Nonproliferation and Transparency, Proceedings of the 46th Annual Meeting of the Institute of Nuclear Materials Management (INMM), Phoenix, USA, 2005.

11-3 How Can Weapons Plutonium Be Disposed of Safely and Effectively?
—Research into Russian Surplus Weapons Plutonium Disposition—

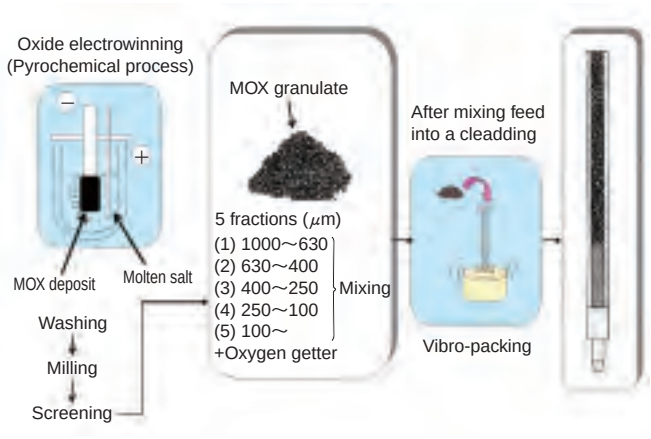

Fig.11-6 Outline of MOX vipac fuel production in RIAR
After melting Plutonium (Pu) and Uranium (U) chloride in high temperature crucible, Pu and U are oxidized and precipitated on electrodes by electrowinning into MOX granulate. A "Vipac fuel pin" is filled with high density fuel by vibro-packing. This method is cheaper than existing pellet fuel methods because of the compact facility and simple fuel fabrication process. Additionally it is more practical because the easy operation can be done remotely, for less radiation exposure during fuel fabrication.

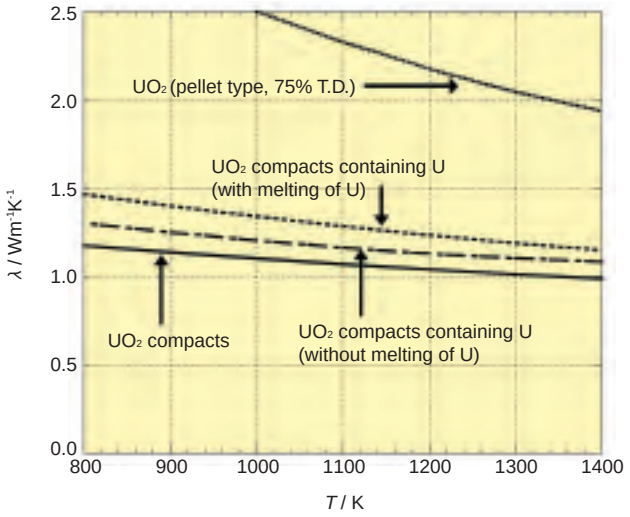

Fig.11-7 Improvement of thermal conductivity by U particles
In vipac fuels for FBR, a fuel restructuring phenomena similar to the ones seen in pellet type fuels occurs in high temperature regions during irradiation. However, in the low temperature regions below 1300K, such as the peripheral area of the fuel, no effective restructuring would occur, and granular fuel compact morphology remains as fabricated. The thermal conductivities of those regions are lower than pellet type fuels due to the morphology. However, adding some U particles to granular fuel compacts improves thermal conductivity of the vipac fuel, thus moderating the temperature of the vipac fuel.

There is weapons plutonium (W-Pu) remaining in dismantled nuclear weapons on the scale of several tens of tons through disarmament process in the US and Russia. In order to dispose of W-Pu, burning in reactors and immobilization, specifically in deep geologic repositories covered with high-level vitrified waste, are feasible; burning appears promising at the present.

Burning W-Pu in a light water reactor as MOX fuel is a proven technology. However, since Russia has no industrial scale MOX pellet fuel fabrication facility and no burning experience in LWR, a huge cost is necessary to introduce related technology from western countries.

Through several collaborative studies with Russian institutes, we have established the technical feasibility of a BN600 vipac fuel option, in which MOX fuel fabricated using Russian vipac fuel technology (Fig.11-6) is burned in a Russian fast reactor (BN600). Although this method has no solid past results and was held in doubt at first, thanks to the above studies it is one of the methods for disposition in the scenario adopted by G8 at present. It has lower disposition cost because of the compact facility and simple fuel fabrication process, and requires less troublesome technology transfer due to use of domestic technology.

In order to confirm the technology to convert BN600 into a hybrid core (23% is replaced by MOX fuel), the following studies were carried out in collaboration with Russia on essential technology; (1) Criticality test of simulated hybrid core, (2) 3LTAs (Leading Test Assemblies) irradiation test, (3) Core and fuel design, (4) Safety analysis, (5) Modernization of vipac fuel fabrication facility. All of above studies except (5) have been finished, and the technical preparation for conversion to hybrid core is completed.

In the 3LTAs irradiation test, MOX fuels were fabricated with W-Pu dismantled from nuclear weapons and burned in BN600, and given a post irradiation test in a hot laboratory. The test revealed that the Vipac fuel has similarity to pellet fuel in irradiation characteristics, fuel irradiation stability, and FCCI/FCMI (fuel-cladding chemical/mechanical interaction) feature. Additionally, examinations of thermal characteristics of vipac fuel pin were carried out by out-of-core experiments. It was confirmed that the addition of oxygen getter, which is metallic U in a granulate form unique to vipac fuel, causes a 10% improvement in thermal conductivity (Fig.11-7). These results will be adopted to make a calculation model to evaluate irradiation behavior of vipac fuel.

The disposition plan for the 34 tons of Russian surplus W-Pu, which is being conducted by G8 with international assistance, faces several problems and cannot move forward now. However, there is movement to proceed with the BN600 vipac fuel option as the leading disposition method at the initiative of US and Russia. Attention should be paid to future trends.

Reference

Ishii, T. et al., Thermal Conductivities of Granular UO_2 Compacts with/without Uranium Particles, Journal of Nuclear Science and Technology, vol.41, no.12, 2004, p.1204-1210.

11-4 Development of Analysis Method for Burnup and Generated Amount of Plutonium by Measurement of Dissolver Off-Gas at Reprocessing Facility

— Evaluation Technology for Burnup and Generated Amount of Plutonium by Measurement of Xenon Isotopic Ratio —

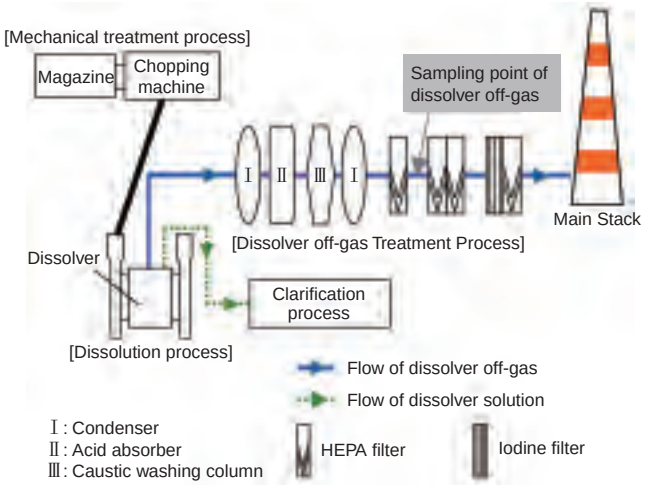

Fig.11-8 Outline of dissolver off-gas treatment process
Off-gas from three dissolvers passes through a condenser, acid absorber, caustic washing column and HEPA filter at Tokai Reprocessing Plant.

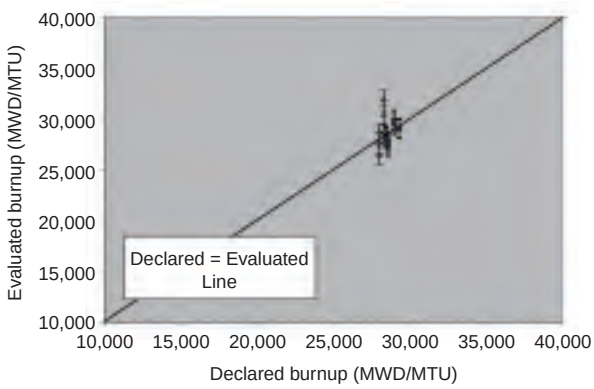

Fig.11-9 Evaluated burnup (based on $^{130}Xe/^{134}Xe$, $^{131}Xe/^{134}Xe$, and $^{132}Xe/^{134}Xe$ isotopic ratios) versus declared burnup

Table11-1 Plutonium amount derived from xenon isotopic ratios and concentration in dissolver off-gas

Sample	Plutonium concentration (kg/MTU)		Percent defference (%)
	Declared	Evaluated	
A	8.20	8.22	0.2
B	8.07	8.00	-0.9
C	8.13	8.31	2.2
D	7.70	8.01	4.0
E	8.15	8.10	-0.7
F	8.03	8.41	4.7

It is well-known that xenon (Xe) isotopic ratio is correlated with spent fuel characteristics (such as fuel type and burnup) and generated amount of plutonium (Pu). Since dissolver off-gas, which is released with dissolution of spent fuel in reprocessing facility, contains most of the gaseous fission products, Xe isotopic ratios in the dissolver off-gas sampled from the stack would be expected to provide a new measurement method applicable to safeguards inspection.

In this work, the amount of Pu related to burnup in the spent fuel was evaluated from Xe isotopic ratio in dissolver off-gas at reprocessing facility.

Six batches of dissolver off-gas at spent fuel dissolution process were sampled from the main stack in Tokai Reprocessing Plant during BWR fuel reprocessing campaign (Fig.11-8). Xenon isotopic ratio was determined with gas chromatography/mass spectrometry.

Burnup and generated amount of Pu were evaluated with Noble Gas Environmental Monitoring Application code (NOVA), developed by Los Alamos National Laboratory.

Using $^{130}Xe/^{134}Xe$, $^{131}Xe/^{134}Xe$ and $^{132}Xe/^{134}Xe$ isotopic ratios, fuel type was specified to be BWR fuel for all samples.

The burnup evaluated by Xe isotopic ratios and NOVA were in good agreement with those of declared burnup in the range from -3.8% to 7.1% (Fig.11-9). Also, the evaluated amount of Pu in spent fuel was found to agree with those of the declared amount of Pu calculated by ORIGEN code (Table11-1).

The evaluation technique is applicable for both burnup credit to achieve efficient criticality control and a new measurement method for safeguards inspection.

Reference

Okano, M. et al., Development of Analysis Method for Plutonium Amount and Burn up by Measurement of Xenon Isotopic Ratio in Dissolver Off-Gas at Reprocessing Facility, Proceedings of the 46th Annual Meeting of the Institute of Nuclear Materials Management(INMM), Phoenix, USA, 2005.

11-5 Determination of Small Amounts of Plutonium in Highly Radioactive Liquid Waste
—Development of a Simple Inspection Technique Using Spectrophotometry—

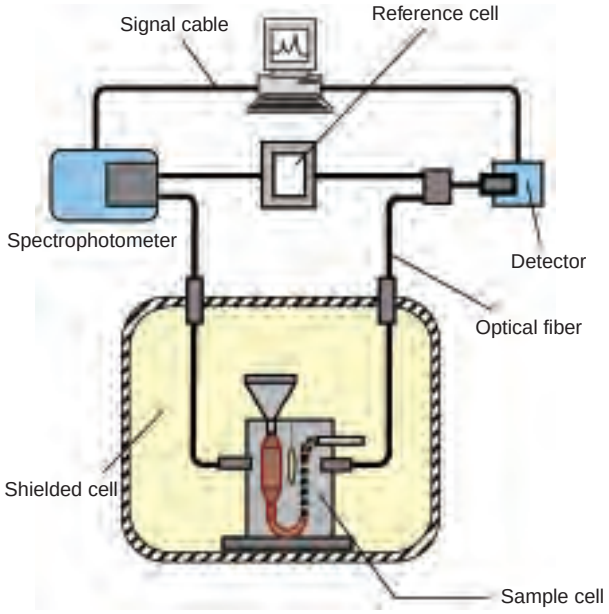

Fig.11-10 Schematic diagram of spectrophotometer using optical fiber
The sample preparation is carried out by remote control in a shielded cell because HALW sample, which contains fission products, is highly radioactive. The sample cell was designed to be easily remote controlled. The sample cell was made of materials which are highly radiation resistant. The sample cell installed in a shielded cell was connected to a spectrophotometer by a set of optical fibers.

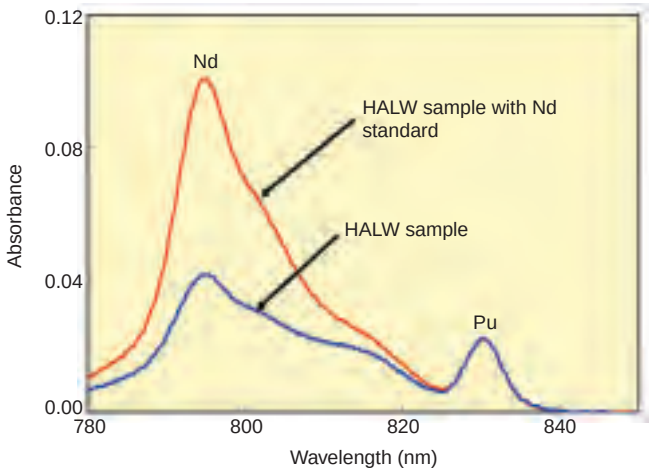

Fig.11-11 Absorption spectra of HALW and HALW with neodymium standard
A known amount of non-radioactive neodymium was added to the sample aliquot. From the absorbance ratio of the neodymium standard and plutonium, the plutonium concentration was calculated. The neodymium initially contained in HALW as one of the fission products was corrected for by measuring the absorbance ratio of plutonium and neodymium.

Spent nuclear fuel from a nuclear power plant is reprocessed to recover residual uranium and newly produced plutonium. Highly radioactive liquid waste (HALW) is produced in this process. It contains small amounts of plutonium at low concentration, but it is necessary to be controlled because it is the material which must be most safeguarded. The HALW samples are transported to IAEA's Safeguards Analytical Laboratory (IAEA-SAL) for independent measurement. Therefore, it takes a few months for IAEA to obtain analytical results. Isotope dilution mass spectrometry (IDMS) has been applied to safeguards analysis to determine the plutonium in the HALW. IDMS involves a complicated procedure and requires highly skilled operators. A rapid safeguards analysis of plutonium in HALW using conventional spectrophotometry is proposed to achieve on-site safeguard measurements and overcome these disadvantages.

A schematic diagram of UV-VIS spectrophotometry system used in this work is shown in Fig.11-10. A known amount of neodymium standard was added to the sample aliquot as an internal standard. Fig.11-11 shows the absorption spectra for HALW as well as HALW with the neodymium standard. Plutonium concentration is calculated from the absorbance ratio of the neodymium and plutonium.

Validation of the proposed method was carried out with an actual HALW sample, comparing results with IDMS. The plutonium concentration ratio of values of this method and IDMS was 0.91 to 1.10. The analytical results using this method agreed well with those obtained using IDMS. The time required for an analysis was about 4 hours.

This method offers easy and rapid determination of plutonium in HALW, requiring neither complicated analytical procedures nor skilled operators. The method greatly simplifies the process of inspection, eliminating the necessity for transport of nuclear materials for off-site analyses. After a performance test carried out with inspectors from the Ministry of Education, Culture, Sports, Science and Technology (MEXT) and IAEA, the proposed method was successfully applied for rapid and independent safeguards analysis of plutonium in HALW at Tokai Reprocessing Plant, achieving the timely attainment of inspection goal.

This work was performed as a part of a support program for IAEA.

Reference

Taguchi, S. et al., Determination of Plutonium in Highly Radioactive Liquid Waste by Spectrophotometry Using Neodymium as an Internal Standard for Safeguards Analysis, 2006, JAEA-Technology 2006-041, 58p.

12 Developent of Experimental Techniques/Facilities at JAEA R&D Centers

JAEA has been promoting a wide range of R&D activities systematically by coordinating between R&D sectors, including the R&D Directorates whose activities have been described in previous chapters and 11 R&D Centers located in various places in Japan.

The R&D Directorates of JAEA have been promoting R&D for their own purposes with the experimental equipment/facilities at each R&D Center. The R&D Centers have not only been operating and managing various types of equipment/facilities but have also been working on innovations and improvements for them, and in addition have themselves been developing experimental techniques, management techniques and equipment/facilities necessary for various R&D projects of JAEA.

In this chapter, those developments which have been made over recent years at each R&D center are introduced.

12-1 "Representative Point Calibration Method" for Efficiency Calibration of Radioactivity Measuring Instrument

— Development of a Method for Determining Radioactivity in Samples of Various Shapes —

Fig.12-1 Standard volume sources of various shapes
Manufacture of these sources requires a skilful technique. The source after use must be treated as a radwaste.

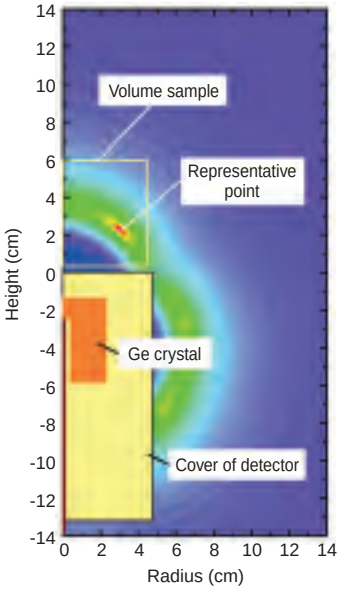

Fig.12-2 Positional relationship among a volume sample, a detector, and the representative point
We found out that there exists a "representative point (RP)" around the detector where the efficiency of a volume sample is transposed to a single point. The peak-efficiency curve at the point coincides with that of the volume sample measured. One of the significant advantages of the RP method is that even if there is ambiguous information about the sensitive region of the crystal and so on, the position of the RP does not change so much.

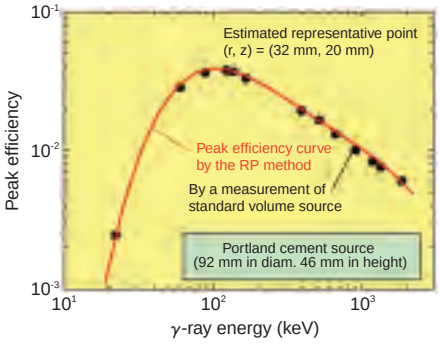

Fig.12-3 Comparison of the peak-efficiency curves obtained by the RP method and by the actual measurement of the standard volume source
The RP method gives reliable peak-efficiency curves in the γ-ray energy range between 20 keV and 2 MeV. The curve obtained by the RP method agrees well with the existing method.

It is one of the most important tasks in radiation control to measure radioactivity in the environmental samples precisely and promptly. Additionally, with the rapid and widespread use of accelerators in these days, there arises an urgent need to estimate the induced radioactivity in activated samples of various shapes and materials (Fig.12-1). The radioactivity measurements for this purpose are usually performed by the γ-ray spectrometry method. In order to quantify the radioactivity, the efficiency calibration, viz. determination of the peak-efficiency curves (PECs), must be achieved for various combinations of sample and detector.

We have developed a novel method, we call the Representative Point calibration method (RP method) for quantifying radioactivity in volume samples based on both the experimental measurement and the calculations. The RP method is made up of the following two steps; (1) calculations to find the position of the RP which is intrinsic to each shape of volume sample, and (2) single point calibration at the RP using a standard point radiation source. In (1), PECs at multiple points around a detector are calculated by means of a Monte Carlo γ-ray transport code and a data interpolation algorithm giving the spatial relation among the efficiency values. Among the multiple PECs, the optimal position (the RP, Fig.12-2) is selected. The single point calibration at the RP gives a comparable efficiency curve with that of the volume sample measured. However, the measured PEC at the RP does not reflect the effect of self-absorption by the sample material and a sample container. In the procedure (2), this effect is corrected by multiplying the measured efficiency curve at the RP by the self-absorption correction factors calculated with the Monte Carlo code, and consequently the desired PEC can be obtained.

Fig.12-3 shows a comparison of two PECs for a cylindrical standard volume source made of Portland cement. One was obtained by the RP method and the other by direct measurement of the standard volume source. In addition to this example, effectiveness of the RP method was verified for various volume samples, and it was found that the method can give reliable PECs in the γ-ray energy range between 20 keV and 2 MeV, with the accuracy required for practical radiation control.

One of the significant merits of the RP method is that both the position of the RP and the self-absorption correction factor remain nearly unaffected by detailed parameters inside a detector. This enables us to conduct reliable efficiency calibration even if there are ambiguities in geometrical conditions, in particular regarding the dead layer of the crystal, and the distribution of charge collection efficiency inside the detector, both of which are usually hard to determine.

Because this method does not need the standard volume sources, it contributes to reduce radioactive wastes, as well as the costs for the efficiency calibrations. It should be useful in establishing a system to measure radioactivity promptly, precisely and nondestructively for a broad range of volume samples.

Reference

Saegusa, J. et al., Determination of Detection Efficiency Curves of HPGe Detectors on Radioactivity Measurement of Volume Samples, Applied Radiation and Isotopes, vol.61, 2004, p.1383-1390.

12-2 Development of Human Dosimetry Technique in Criticality Accidents by Combined Use of Small Dosimeters

—Speedy and Accurate Notification of Dose Information for Radiation Emergency Medicine—

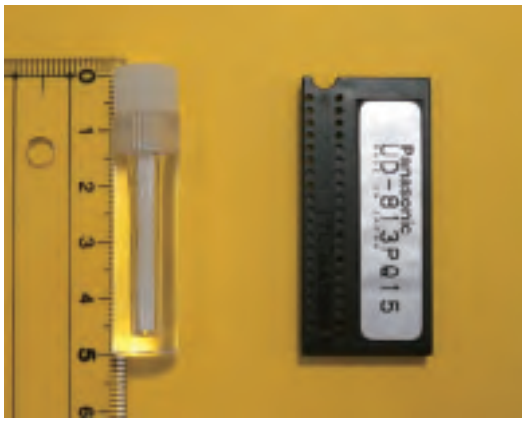

Photo 12-1 Alanine dosimeter (left) and lithium tetra borate dosimeter (right)
The neutron and γ-ray absorbed doses in muscle can be separately estimated by the combined use of two dosimeters: the alanine dosimeter whose sensitivity to both neutrons and γ-rays is equivalent to that of muscle, and the lithium tetra borate dosimeter whose sensitivity to γ-rays is equivalent to that of muscle. Both of these small and lightweight dosimeters can be used as personal dosimeters.

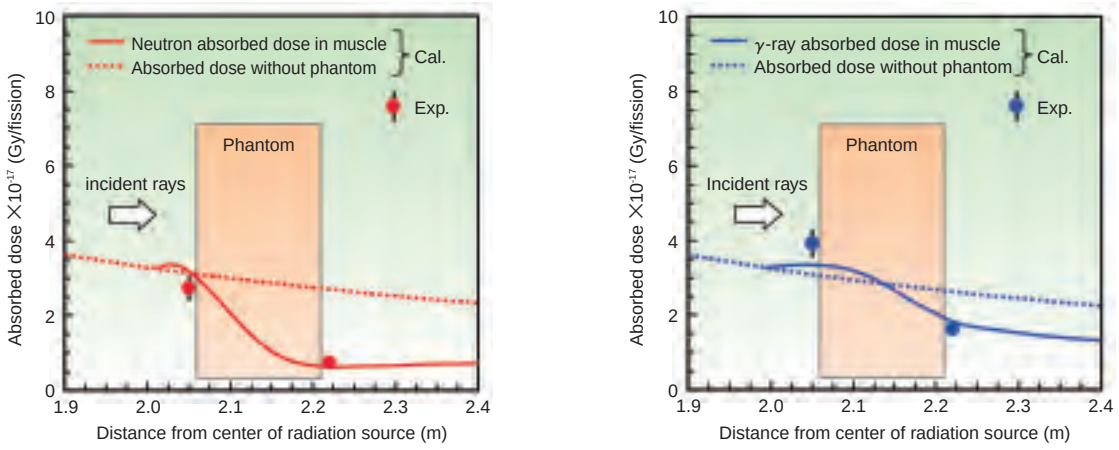

Fig.12-4 Comparison of neutron and γ-ray absorbed doses in muscle between measurement and calculation
The neutron and γ-ray absorbed doses measured with the above two dosimeters on the surface of a phantom approximately agreed with the calculated distribution of the absorbed doses in muscle in and out of the phantom. This result demonstrated that this simple dosimetry technique could give an accurate estimation of the absorbed doses in muscle. This result also showed the quantitative correlation between the body-surface doses and the body-internal doses.

When personnel receive significant exposures (e.g., at the JCO criticality accident in 1999), radiation emergency treatment is conducted immediately. Speedy and accurate notification of absorbed doses is required for determining the treatment strategy.

A study on human dosimetry in criticality accidents has been conducted using an alanine dosimeter and a lithium tetra borate dosimeter (Photo12-1). For the application of the combined use of these two dosimeters to personal dosimetry, a dosimetry experiment for a criticality accident situation created at the Transient Experiment Critical Facility (TRACY) and its computational simulation were constructed. In the experiment, the neutron and γ-ray absorbed doses in muscle were separately estimated with the two dosimeters attached on a phantom of the human body. In the simulation, a Monte Carlo calculation was made taking account of the dose components of neutrons and γ-rays emitted in the criticality accident situation. It was demonstrated by comparison between the measurements and the calculations that this simple dosimetry technique could provide medical staffs with dose information accurate enough to perform proper radiation emergency treatment (Fig.12-4).

This dosimetry technique can also be applied to radiation control in high dose-rate areas and dosimetry of non-critical radiation accidents.

Reference

Sono, H. et al., Assessment of Human Body Surface and Internal Dose Estimations in Criticality Accidents Based on Experimental and Computational Simulations, Journal of Nuclear Science and Technology, vol.43, no.3, 2006, p.276-284.

12-3 Contribution to Leading-Edge Medical Technology

—Development of a Supporting System for Boron Neutron Capture Therapy—

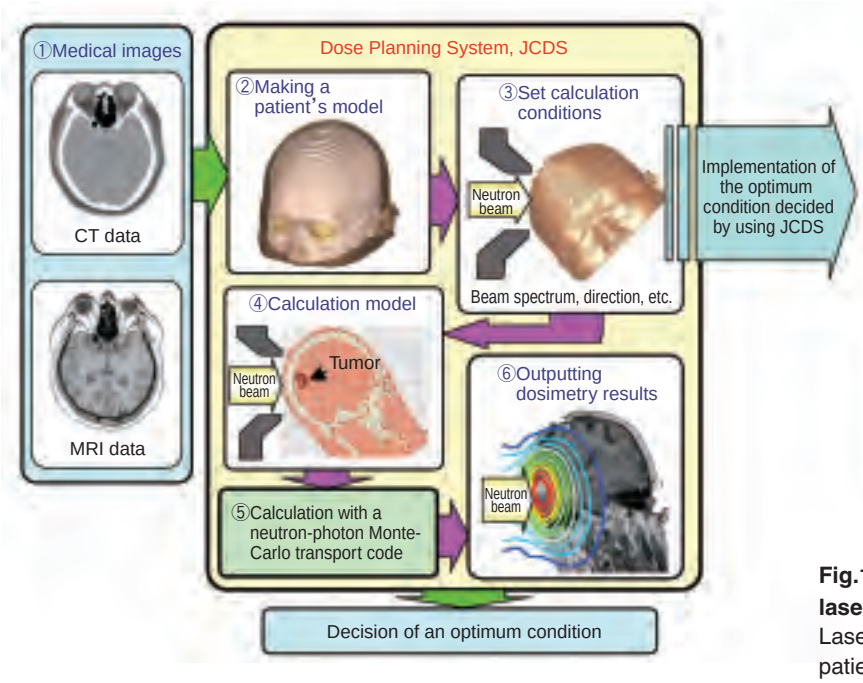

Fig.12-5 The Process flow of dosimetry by JCDS
JCDS creates a patient's 3D model using patient's medical images. Doses are determined by calculation with Monte-Carlo transport code. Optimum conditions for irradiation are identified based on the calculation results.

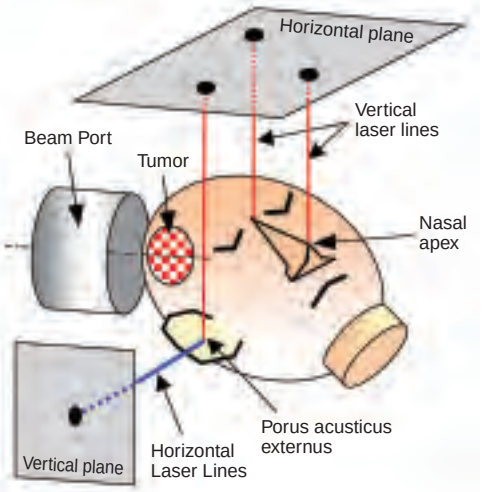

Fig.12-6 Patient immobilization method using laser beams
Laser beams are directed at where points on the patient's face such as nasal apex, eyes, and ears should be. By aligning the actual patient's head with these beams, it is fixed accurately to the irradiation position.

Boron neutron capture therapy (BNCT) is a sort radiation therapy for an obstinate cancer like a malignant brain tumor. In the BNCT procedure, doctors first inject a boron compound that builds up selectively in the cancer cells of a patient, and subsequently the patient is irradiated by a neutron beam. Alpha particles and lithium atoms, which are generated by interaction between neutrons and boron-10 atoms in the cells, destroy the cancer cells. Now it is expected that a malignant tumor located in the deeper part of the brain can be also treated by using an epithermal neutron beam.

The supporting system consisting of a dose planning code and a patient immobilization device was developed to perform the BNCT irradiation with high accuracy. The former, called the JAEA Computational Dosimetry System (JCDS), can estimate doses around the diseased part precisely. JCDS employs the Monte-Carlo transport method to determine doses based on patient's medical images. Fig.12-5 shows the process flow of dosimetry by JCDS.

The development of JCDS enables determination of the optimum conditions for irradiation. Next, in the actual BNCT, the implementation of irradiation according to these conditions is required. In particular, the patient's position greatly affects the accuracy of the irradiation. Thus, the patient setting system, which can immobilize the patient to the precise irradiation position by using laser beams, was developed. Fig.12-6 shows the positioning method using laser lines.

To improve the irradiation accuracy, JCDS and the patient setting system were integrated in one support system. Technologies which can support BNCT comprehensively including treatment planning, patient's positioning and retrospective evaluation of an irradiation have been established.

These support technologies have been developed for practical use, and BNCT clinical trials with epithermal neutron beam have been performed at Japan Research Reactor No.4 (JRR-4) since 2003. Clinical trials for head-&-neck cancer and lung tumor began in 2004.

Technological development to apply reactor functions to the medical field is continuing, and thus support is being given to advanced medical research aimed at overcoming intractable cancers.

Reference

Kumada, H. et al., Verification of the Computational Dosimetry System in JAERI for Boron Neutron Capture Therapy, Physics in Medicine and Biology, vol.49, 2004, p.3353-3365.

12-4 More Precise Measurement of Fuel Temperature Distribution in HTTR
—Development of HTTR Fuel Temperature Estimation Model—

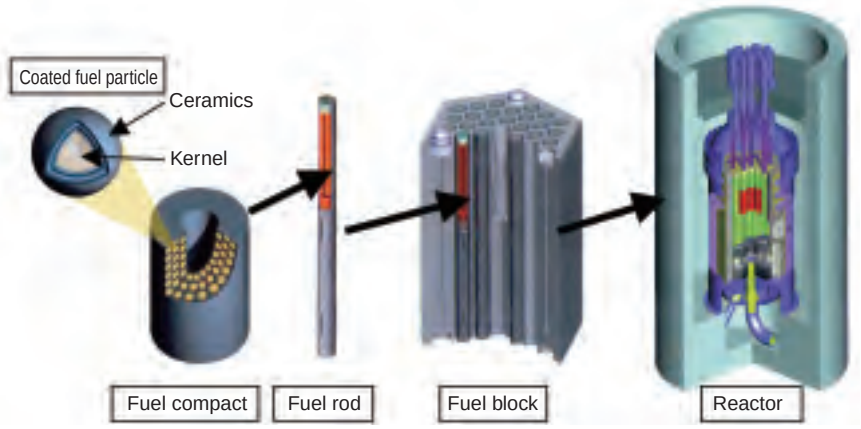

Fig.12-7 HTTR fuels
Coated fuel particle (CFP) composed of fuel kernel and 4-coated layers is used in HTTR. The coated layer protects the fuel kernel and confines fission products (FP) to within the particle. CFPs are dispersed in the graphite matrix and sintered to form a fuel compact. The fuel compacts are contained in a fuel rod. Fuel rods are inserted into the fuel block. The reactor core is formed by piling-up the fuel blocks. To ensure the fuel integrity, it is determined that the maximum fuel temperature should be kept below 1495℃ in normal operations.

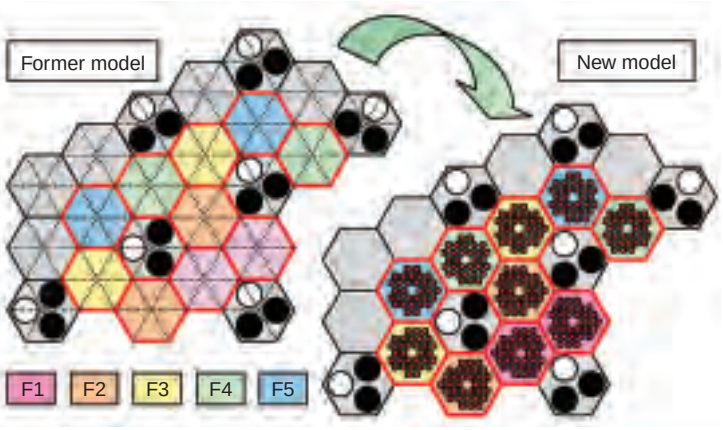

Fig.12-8 HTTR fuel temperature estimation model
The 6-divided fuel block model is used in the former HTTR fuel temperature estimation. To obtain a more detailed fuel temperature distribution, the each fuel rod representation model (detailed model) is newly constructed. The temperature of each fuel rod can be obtained.

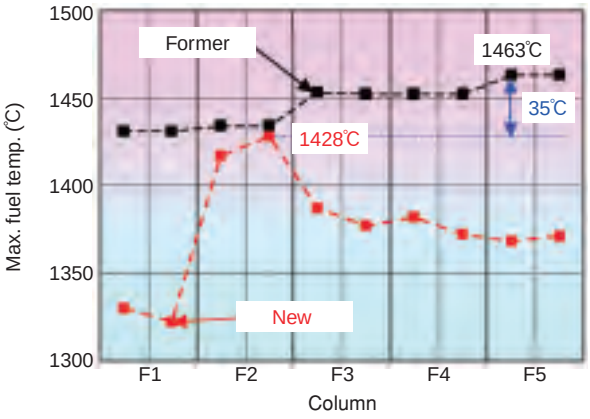

Fig.12-9 Estimation result of fuel temperature
The maximum fuel temperature is estimated to be about 1463 ℃ in the former model. With the detailed model, the maximum fuel temperature is estimated to be about 1428 ℃.

The High Temperature Gas-cooled Reactor (HTGR) is one of the next-generation reactors. It has inherent safety features, and enables multi-purpose heat utilization and high-efficiency power generation. The High Temperature Engineering Test Reactor ("HTTR") is the first HTGR in Japan constructed by us. In "HTTR", the reactor outlet coolant temperature of 950 ℃ was achieved on April 2004. Coated fuel particle (CFP) composed of a fuel kernel coated with 4 layers is used in "HTTR". To ensure the fuel integrity, the maximum fuel temperature should be kept below 1495℃ in normal operation (Fig.12-7).

The maximum fuel temperature is estimated as about 1463 ℃ in the current fuel temperature estimation. The various hot spot factors are considered to obtain conservative maximum fuel temperature in the former model. Realistic fuel temperature cannot be obtained. Also, a detailed fuel temperature distribution cannot be obtained.

Here, a representation model of each fuel rod (detailed model) is newly constructed to obtain a more realistic and detailed fuel temperature (Fig.12-8). In the former model, a fuel block is divided into 6 regions and the highest fuel temperature is estimated considering hot spot factors. In the new detailed model, each fuel pin is represented and its temperature can be estimated. All of the hot spot factors need not be considered in the new model because of representation of each fuel rod. The maximum fuel temperature is estimated as about 1428℃ with the new model, which is about 35℃ lower than the former model (Fig.12-9).

A realistic and detailed fuel temperature distribution can be estimated with the new model. It is expected that this model can contribute to improve the economy of HTGR, that is, the high-powered HTGR can be designed. In the future, more improvement of the model will be sought to obtain fuel temperature with high-accuracy.

Reference

Tochio, D. et al., Evaluation of Fuel Temperature on High Temperature Test Operation at High Temperature Gas-Cooled Reactor 'HTTR', Nippon Genshiryoku Gakkai Wabun Ronbunshi, vol.5, no.1, 2006, p.57-67 (in Japanese).

12-5 Remote Handling Techniques for Irradiation Assisted Stress Corrosion Cracking (IASCC) Study
—Assembling of Irradiated Specimens in Capsule—

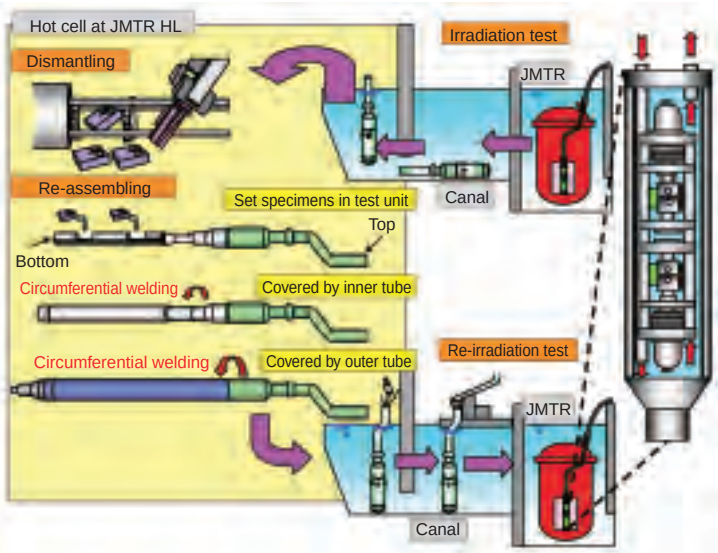

Fig.12-10 Flow image of re-irradiation test
The irradiated capsule is transported from JMTR to a concrete cell of JMTR HL, and is dismantled to take specimens out. They are re-installed in the in-pile IASCC test capsule for the re-irradiation test after several kinds of inspections.

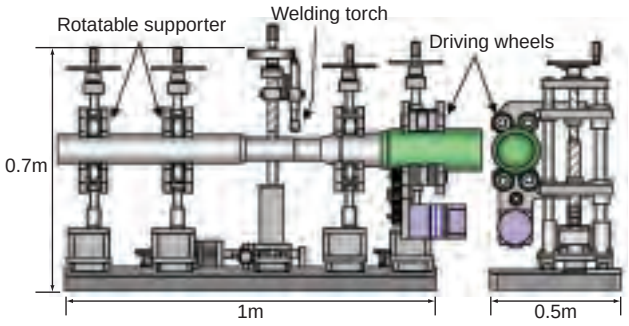

Fig.12-11 Schematic drawing of welding apparatus
A capsule tube from 40 to 65 mm in diameter can be welded by this apparatus.

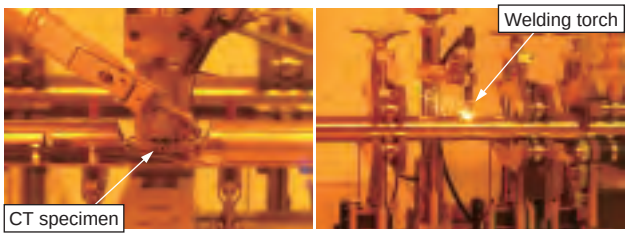

Fig.12-12 Photographs of assembling work of the IASCC test capsule in hot cell
Irradiated specimens are set in the test unit by remote manipulation in the hot cell.

Since the Hot Laboratory of Japan Materials Testing Reactor (JMTR HL) has an advantage that its No.1 concrete cell is connected with "JMTR" by a canal pool, it is easy to transport a re-assembled capsule containing previously irradiated specimens from the hot cell to "JMTR" through the canal for re-irradiation tests (Fig.12-10). This advantageous feature was used to investigate the behavior of irradiation assisted stress corrosion cracking (IASCC) caused by the simultaneous effects of neutron irradiation and high temperature water environment in Light Water Reactors (LWRs). Crack growth tests and unified constant load tests of irradiated specimens were performed using in-pile IASCC test capsules in "JMTR". The development of techniques for remotely installing irradiated specimens in this capsule and then welding capsule tubes in the hot cell is essential for these tests.

The in-pile IASCC test capsule is 3 m in length and is bent at its upper part. It also consists of inner and outer tubes made of stainless steel. The inner tube is 3 mm in thickness for strength against pressure.

The remote welding technique that the welding torch moves along the capsule tube's surface circumferentially had been developed in JMTR HL for assembling the coupling capsules. When this technique was applied to the welding for a butt joint of the inner and outer tubes of the in-pile IASCC test capsule, flaws like craters were observed in the weld beads on the outside surface of the tube. Therefore, a new remote-welding technique had to be developed for assembling the long and bent in-pile IASCC test capsule. We manufactured a new remote-controlled welding apparatus whose torch was fixed right over the tube and which rotates the capsule tube. The apparatus has the welding torch, the driving wheels, and rotatable supporters (Fig.12-11).

The techniques to perform a pressure test, helium leak test and liquid penetrant test remotely in the hot cell were also established to evaluate the integrity of the assembled capsule and were applied in the final inspection before the re-irradiation test in "JMTR". Eight in-pile IASCC test capsules containing irradiated specimens were remotely assembled in the hot cell (Fig.12-12) and their re-irradiation tests were done successfully. The data obtained by re-irradiation tests using in-pile IASCC test capsules is essential to investigate the mechanism of initiation and progress of IASCC in structural materials.

Reference

Ugachi, H. et al., Development of Test Techniques for In-Pile SCC Initiation and Growth Tests and the Current Status of In-Pile Testing at JMTR, Proceedings of 12th International Conference on Environmental Degradation of Materials in Nuclear Systems-Water Reactors, Salt Lake City, USA, 2005, p.319-326.

12-6 Neutronic Evaluation for Irradiation Tests of JMTR
—Accurate Evaluation of Tritium Production—

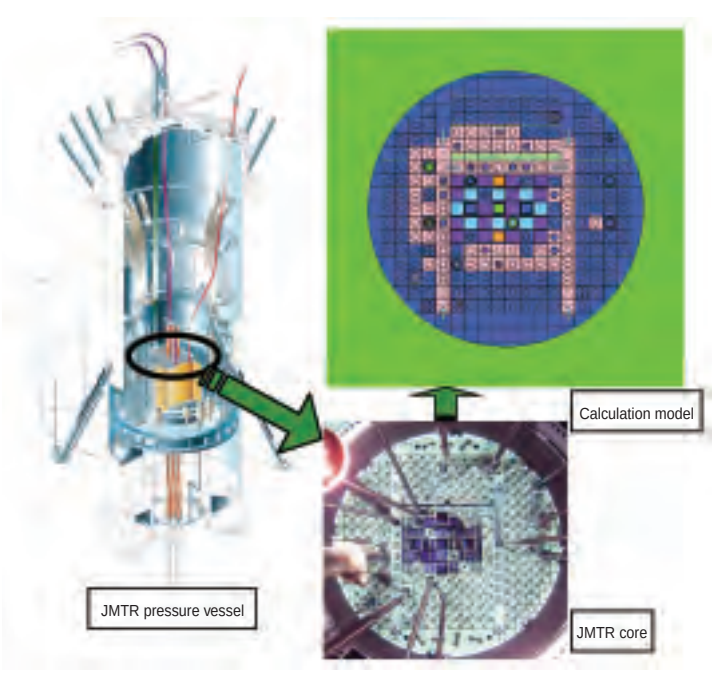

Fig.12-13 Calculation model of JMTR
The JMTR is a tank-in-pool type reactor with thermal power of 50MW and maximum neutron fluxes of $4\times10^{18}m^{-2}s^{-1}$. Test pieces were installed in the JMTR core and were irradiated. Neutronic analyses are conducted using MCNP. The whole 3-D JMTR core was modeled in detail. Irradiation parameters of neutron flux/spectrum, γ dose, etc. are predicted, controlled and evaluated by the calculation model.

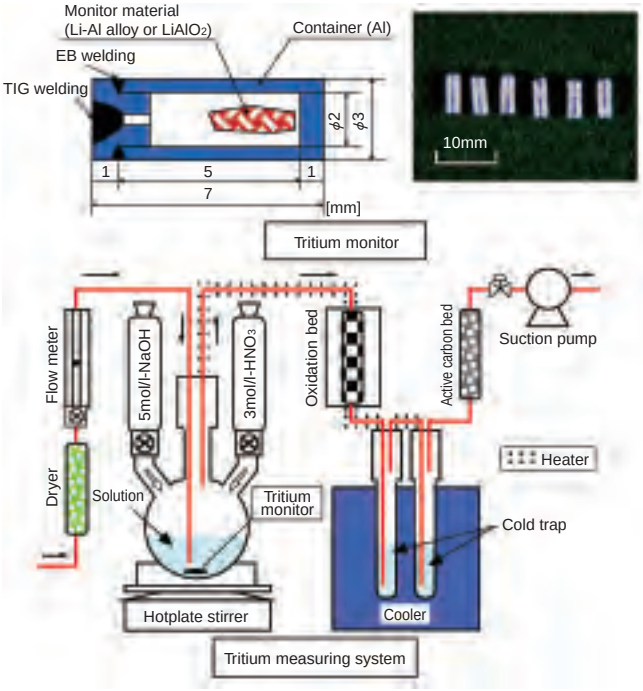

Fig.12-14 Tritium monitor and its measuring system
A tritium monitor consists of monitor material (Li-Al alloy or $LiAlO_2$) and its container. Tritium monitors are installed in irradiation capsules and irradiated in the JMTR. Irradiated tritium monitors are dissolved in tritium measuring system. Almost all the tritium produced in the tritium monitor is trapped in the flask and cold trap. Trapped tritium is measured by a liquid scintillation counter.

Current irradiation research on aging of Light Water Reactor core internal materials, specifically Irradiation Assisted Stress Corrosion Cracking, tritium release of fusion blankets under neutron irradiation, etc. generally needs more accurate prediction, control, and evaluation of irradiation parameters such as neutron fluence, γ dose, and production of nuclear transformation products (Helium, Hydrogen, etc.).

An evaluation procedure using continuous energy Monte Carlo code MCNP with a calculation model of the whole 3-D JMTR core (Fig.12-13) has been therefore introduced to evaluate irradiation parameters. Detail analyses of irradiation parameters are conducted before irradiation using this procedure and there results are verified by comparing with the measured values.

Calculated neutron fluence was verified against measurements of irradiated fluence monitors (Iron and Aluminum-Cobalt wires). With regard to γ dose, calculated γ heating rates were verified against measurements of the nuclear heating evaluation capsule which was developed in order to measure nuclear heating rate (generated from interaction between materials and neutrons or γ -rays). As a result, it was confirmed that the calculated fast and thermal neutron fluence agreed with measurements within ±10%, ±30%, respectively, and the calculated γ dose agreed within -3 to +14%.

Amounts of different products of nuclear transmutation, caused by interaction between neutron and nuclide, must be verified individually because they vary depending on the neutron energy spectrum. In the present study, a tritium monitor and a specialized tritium measuring system (Fig.12-14) were developed for verification of tritium production. Tritium measurement experiments to verify the calculated amount of tritium were conducted using the tritium monitors irradiated in the "JMTR". As the result, it was confirmed that the calculated tritium matched the measurement within an error of -1% to +8%. This method is contributing to research and development of the fusion blanket materials.

Development of evaluation techniques of irradiation parameters will be conducted to aid in advanced irradiation research.

Reference

Nagao, Y. et al., Development of Tritium Production Measurement Method for In-Pile Tests of Fusion Blanket in the JMTR, Fusion Engineering and Design, vol.81, 2006, p.619-623.

12-7 Cyclotron Beam Stabilization Technique
—Improvement of Beam Quality for Microscopic Irradiation—

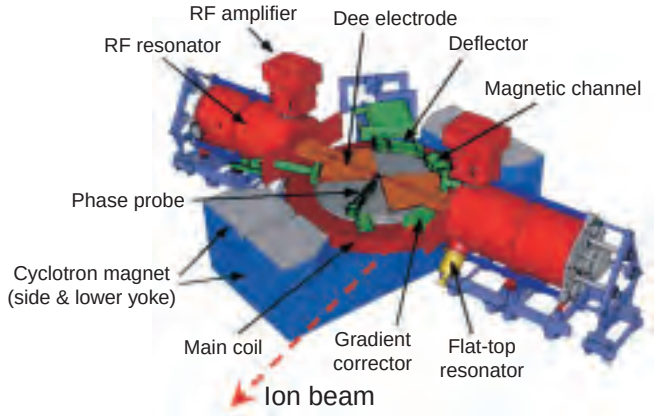

Fig.12-15 TIARA cyclotron
The magnet upper half is cut away to show the interior. Ions are accelerated by 2 dee-electrodes along a spiral path up to the maximum energy and extracted to the beam transport system by the deflector and other components.

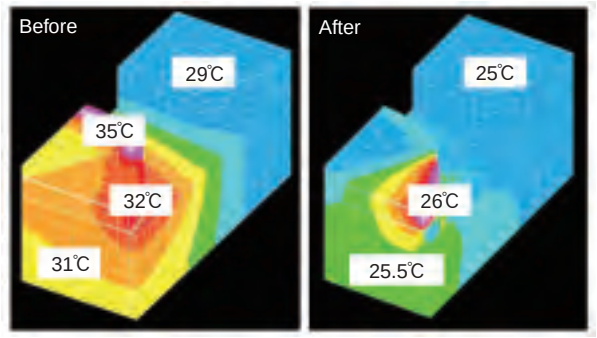

Fig.12-16 Temperature distributions
In one eighth of the cyclotron magnet; before installing (left side) and after installing (right side). Those were derived from calculation based on measured data. The initial temperature of 25°C is maintained after installing the control system.

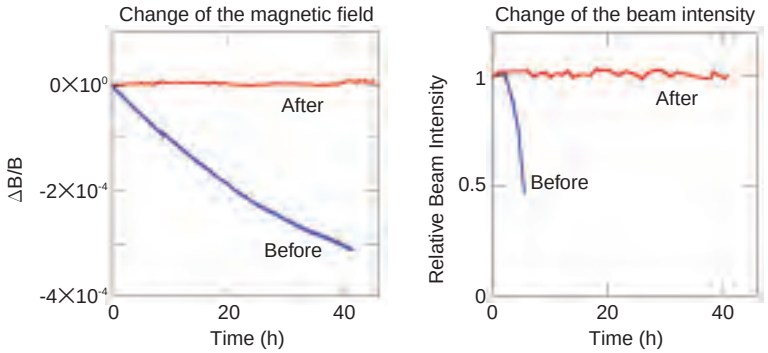

Fig.12-17 Magnetic field change (left side) and beam intensity change (right side)
The difference before and after installing is shown. After installing the control system, beam intensity became remarkably steady along with the stabilized magnetic field.

The cyclotron at the ion-irradiation research facility, "TIARA" (Takasaki Ion Accelerators for Advanced Radiation Application), (Fig.12-15) provides ion beams for wide ranging research in biotechnology and materials science. A microbeam with a beam size on the order of μm or less is expected to be very useful in these fields because of its micro- or nano-scale irradiation ability. However, cyclotrons generally have a problem with beam instability; specifically, beam intensity rapidly decreases shortly after start-up of the machine if there is no readjustment. Therefore, it has been difficult to tune the cyclotron precisely enough to obtain a high quality beam with a small energy spread, which is indispensable to micro-beam production.

Development of technology for cyclotron beam stabilization was started at "TIARA". Research for precise measurement of the magnetic field of the cyclotron even in an electrically noisy environment revealed that the cause of the beam instability was the change of the magnetic field due to temperature increase of the iron of the cyclotron magnet. It was also shown that the heat source was the coils of the magnet. A temperature control system, suppressing the heat flow from the coils and maintaining the yoke temperature, was developed. Fig.12-16 shows the temperature distribution of the magnet, confirming the system's performance. While the previous change of the magnetic field was more than 0.01 %, the temperature control system achieves the stability of the magnetic field within 0.001 %, the lowest value in the world, thus realizing constant beam intensity without readjustment (Fig.12-17).

Reference

Okumura, S. et al., Magnetic Field Stabilization by Temperature Control of an Azimuthally Varying Field Cyclotron Magnet, Review of Scientific Instruments, vol.76, no.3, 2005, p.033301-1-033301-6.

12-8 Construction of an Underground Research Laboratory Fully Underway
—Research and Development of Geological Disposal Technology—

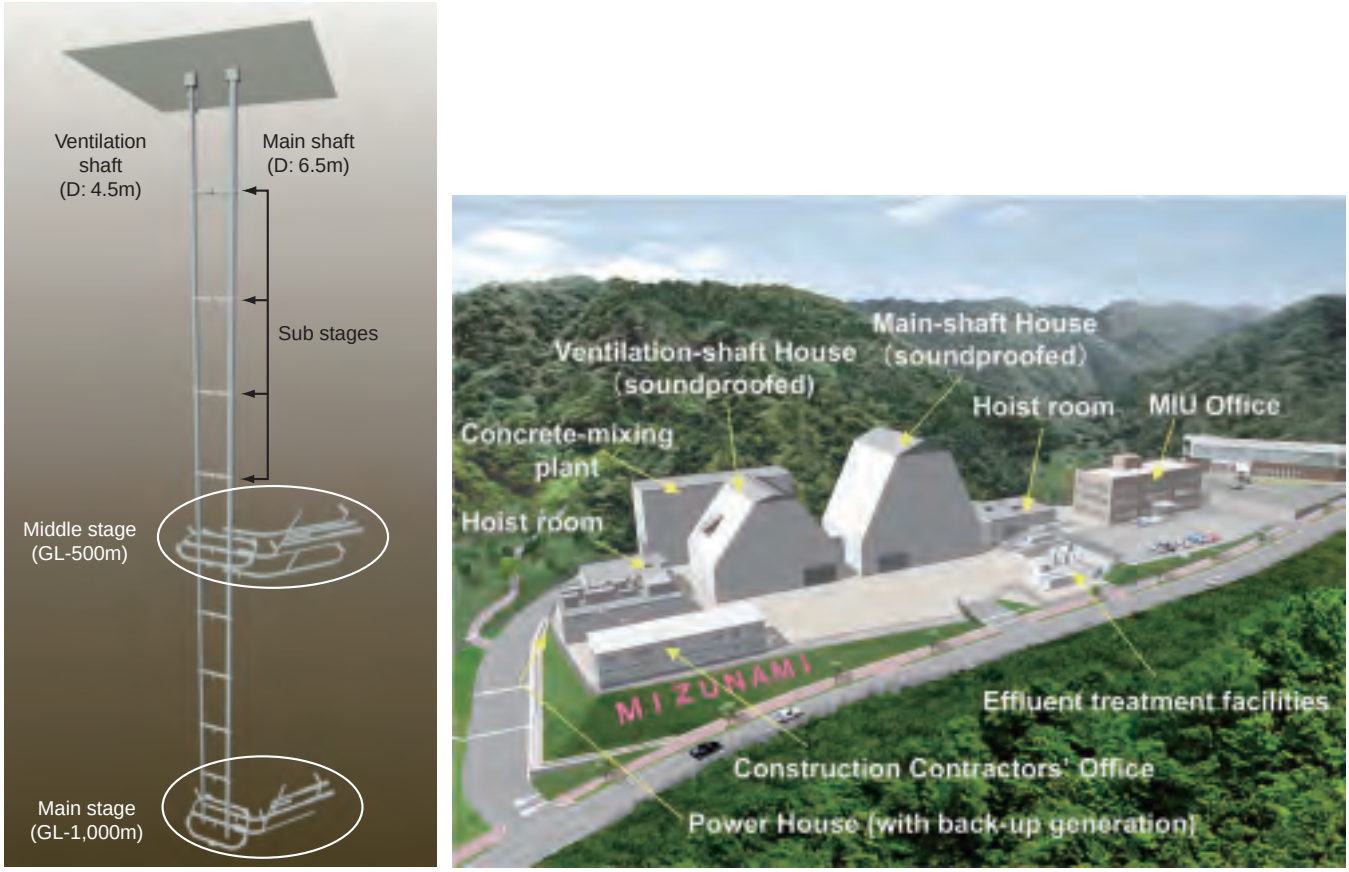

(a) Basic layout of research shafts

(b) Layout of surface facilities

Fig.12-18 Outline of the Mizunami Underground Research Laboratory
The Mizunami Underground Research Laboratory consists of underground facilities (research shafts) and surface facilities. The conceptual design includes two 1,000 m deep shafts, the Main Shaft (6.5m ϕ) and the Ventilation Shaft (4.5m ϕ), and two research stages, the Middle Stage at 500 m depth and the Main Stage at 1,000 m (a). Surface facilities include excavation equipment, head frame, hoists, water-treatment facility, and electrical plant (b).

The Mizunami Underground Research Laboratory, one of the main facilities in Japan for research and development of the technology for high-level radioactive waste disposal, is being constructed in Mizunami City. This facility consists of two shafts to be excavated to a depth of 1,000 m below ground level and horizontal research tunnels at different depths (Fig.12-18). This facility will be used not only as a research laboratory to establish techniques for the investigation, analysis and assessment of deep geological environments and engineering technologies, but will also enable visitors to learn about the deep geological environment. Based on pre-excavation studies, layouts of shafts and research tunnels were designed, and the mechanical stability of openings, earthquake-resistance of shafts and ventilation requirements were analyzed. Construction procedures are planned to reduce shaft excavation cycle time as well as for safety. A double blasting system with two consecutive drill, blast and mucking cycles followed by a shaft-lining step has been adopted.

In February 2005, shaft excavation started using scaffold-mounted drilling and mucking equipment and deep capacity hoists needed for excavation of the shafts at depth. By October 2005, the excavation of the Main and Ventilation Shafts had reached depths of 172m and 191m, respectively. However, shaft sinking was then suspended for about 6 months due to high concentrations of boron and fluorine in the inflow water in the shafts, which exceeded the environmental discharge limits. To resolve this problem, an additional effluent treatment system was adopted, and shaft sinking resumed in April 2006. Scientific investigations during shaft sinking will be performed during the excavation of the Main and Ventilation Shafts down to a planned depth of approximately 1,000 m below ground level.

Reference

Sato, T. et al., Status of Japanese Underground Research Laboratory —Design and Construction of 1000 m-deep Shafts and Research Tunnels—, In Underground Space Use: Analysis of the Past and Lessons for the Future, Erdem & Solak (eds), 2005, p.335-341.

12-9 High Sensitivity Measurement of Iodine-129 by Accelerator Mass Spectrometry (AMS) —New Technique Has Shorter Processing Time, Higher Precision and Higher Sensitivity than Neutron Activation Analysis (NAA)—

Fig.12-19 AMS at the Mutsu Establishment
This AMS consists of two ion injection lines (left), a tandem accelerator (center) and two mass analyzing lines (right). The measurement of ^{129}I uses the outer beam line. This beam line has a high-resolution magnet, a high-energy resolution electrostatic analyzer and a time of flight detector.

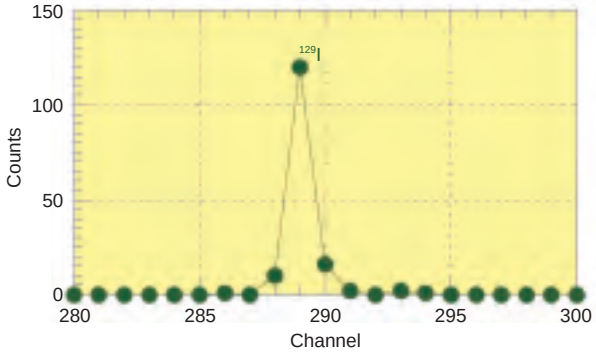

Fig.12-20 ^{129}I spectrum detected by time of flight detector
There is no interfering peak around the ^{129}I peak, showing that interfering ions were removed by the analyzing magnet and electrostatic deflector.

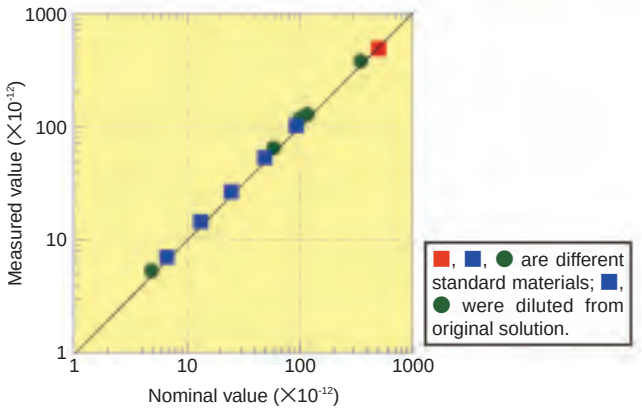

Fig.12-21 Linearity experiment
This experiment demonstrated that this AMS has excellent linearity with nominal value between 10^{-10}-10^{-12} iodine isotopic ratio.

Iodine-129 (^{129}I) is a long-lived radioactive isotope with a half-life of 15.7 million years which is released from spent nuclear fuel reprocessing plants. ^{129}I is an important nuclide for monitoring around nuclear facilities and also useful for tracing in hydrogeologic and oceanographic research. NAA is recommended as a measurement technique for ^{129}I in the "Analytical method of radioactive iodine-129" published by the Ministry of Education, Culture, Sports, Science and Technology of Japan. Because NAA has a high detection limit (^{129}I/^{127}I = 10^{-9}-10^{-10}), it takes much time for analysis, has low precision, and would cause radiation exposure during analysis, it is not suitable for environmental samples (^{129}I/^{127}I = 10^{-10}-10^{-12}) except for the monitoring around nuclear facilities. Therefore, a measurement technique for ^{129}I with short processing time, high precision and high-sensitivity was developed using accelerator mass spectroscopy (AMS) (Fig. 12-19) set up at Mutsu establishment.

In mass analyzing for $^{129}I^{5+}$ (m/e=25.8), $^{103}Rhodium^{4+}$ (m/e=25.75) and $^{52}Chromium^{2+}$ (m/e= 26.0) interfere with analysis because the mass to charge ratio is close. We succeeded in removing the interfering ions by the improvement of the mass resolution using a high mass resolution magnet, high energy resolution electrostatic deflector and time of flight detector (Fig.12-20). Also, a stable beam from the target is obtained by mixing sufficient Niobium in the target to increase conductivity, resulting in reliable measurement.

Standard samples which had a variety of iodine isotopic ratios between 10^{-10} and 10^{-12} were measured for about 60 min and the excellent linearity of the plot of nominal and measured values (Fig.12-21) shows that this AMS has good precision. Evaluating the detection limit of this method using commercial silver iodide, it was possible to measure as low as a 10^{-14} iodine isotopic ratio.

This measurement technique enables not only the simplification of the monitoring around the nuclear facilities but also breakthrough use of ^{129}I in environmental migration research.

Reference

Suzuki, T. et al., Performance of Iodine Beam Line for Accelerator Mass Spectrometry, 2006, JAEA-Technology 2006-018, 40p. (in Japanese).

R&D Centers of JAEA

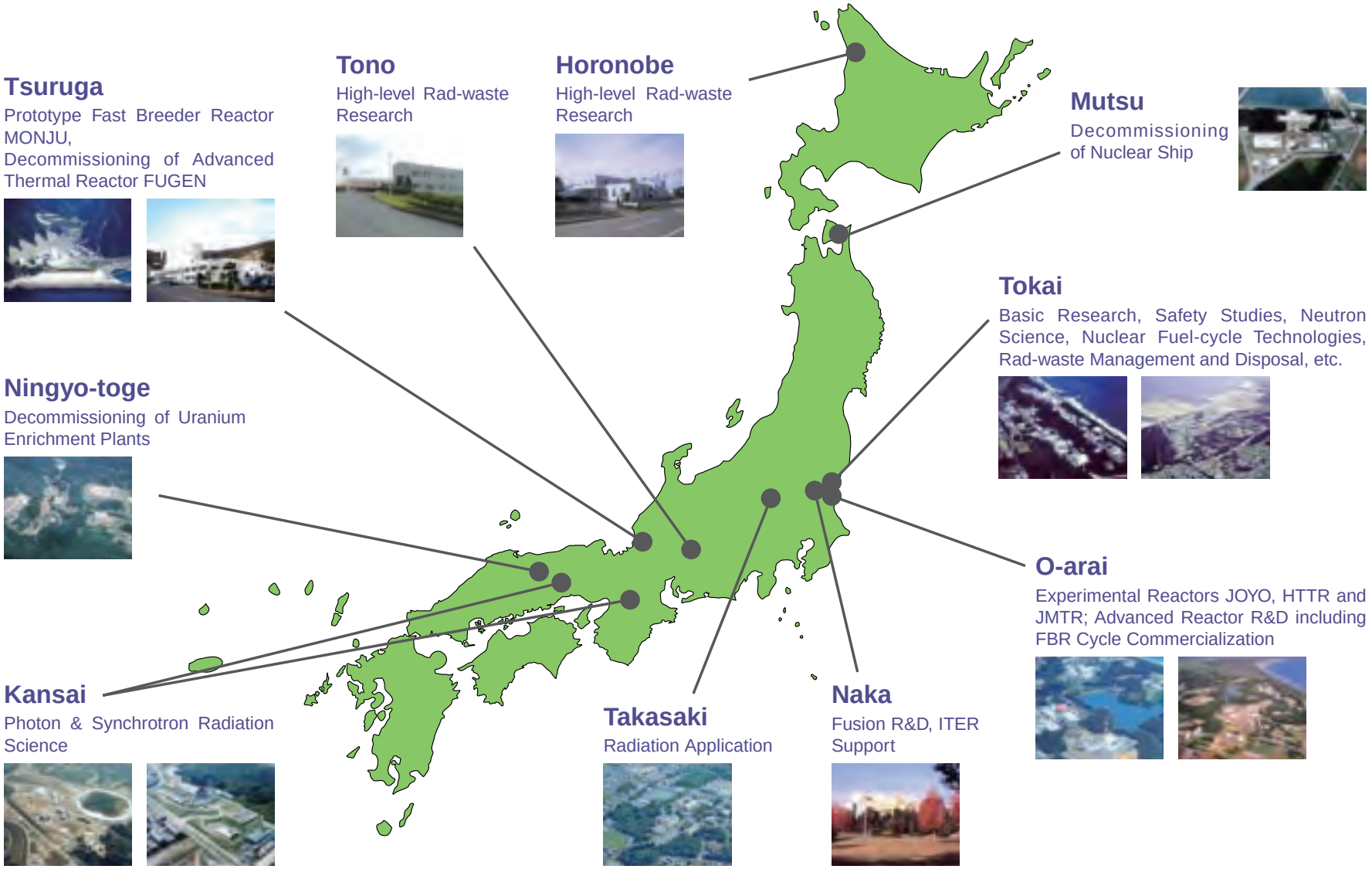

Tsuruga
Prototype Fast Breeder Reactor MONJU,
Decommissioning of Advanced Thermal Reactor FUGEN

Tono
High-level Rad-waste Research

Horonobe
High-level Rad-waste Research

Mutsu
Decommissioning of Nuclear Ship

Tokai
Basic Research, Safety Studies, Neutron Science, Nuclear Fuel-cycle Technologies, Rad-waste Management and Disposal, etc.

Ningyo-toge
Decommissioning of Uranium Enrichment Plants

O-arai
Experimental Reactors JOYO, HTTR and JMTR; Advanced Reactor R&D including FBR Cycle Commercialization

Kansai
Photon & Synchrotron Radiation Science

Takasaki
Radiation Application

Naka
Fusion R&D, ITER Support

Japan Atomic Energy Agency —Outline of Organization—

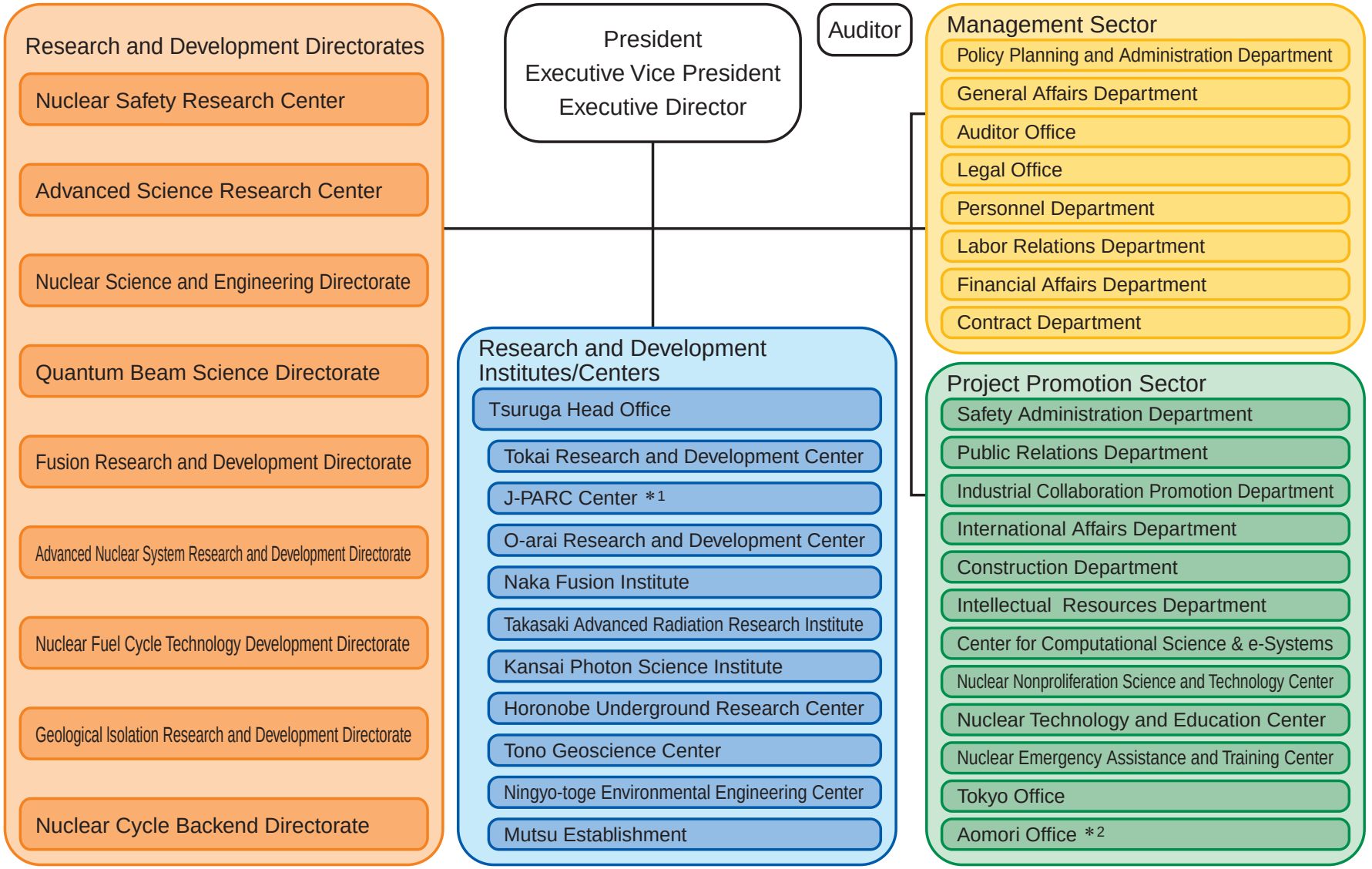

*1: since Feb. 2006, *2: since Apr. 2006

About the Design of the Cover:

The cover is designed envisage a hopeful future shining in the sky with a blue color derived from the color of the JAEA logo. This is accompanied with white colored hexagons similar to the pattern in a tortoise shell symbolizing the wish of people for longer lives since ancient times in Japan. Coincidentally, this shape is the same as that of the core fuel assemblies both of the prototype Fast Breeder Reactor, "MONJU", and the High Temperature Test Reactor, "HTTR".

The two ellipses are bird's-eye views of "MONJU" (at Tsuruga Site) and the Japan Proton Accelerator Research Complex, "J-PARC" (at Tokai Site, under construction), both of which are major facilities of JAEA. They are expected to make great scientific breakthroughs as well as technological innovations in the near future.

JAEA R&D Review 2006

Editorial Board
Chief editor: Hideo Matsuzuru
Vice editor: Shunichi Miyakawa
Editors: Toru Nakatsuka, Hideo Kaburaki, Masaki Ichihashi, Ken Muramatsu, Satoshi Chiba, Takemasa Shibata, Takakazu Takizuka, Kenji Kikuchi, Takuji Kojima, Mitsuru Yamagiwa, Yoshitaka Ikeda, Tetsuo Ikegami, Munetaka Myochin, Kiyoshi Tamayama, Yoshihiko Nagasato, Yoshifumi Yamaguchi, Hiromichi Ogawa, Koichi Shirahashi, Isao Usami, Keiji Chatani, Tomihiro Kamiya, Keiichi Setoguchi

Published by Japan Atomic Energy Agency (JAEA)

Editorial Office: Intellectual Resources Section, Intellectual Resources Department

2-4 Shirakatashirane, Tokai-mura, Naka-gun, Ibaraki-ken 319-1195, Japan

Phone: +81-29-282-6387 Facsimile: +81-29-282-5920

e-mail: ird-seika_shi@jaea.go.jp

All Rights Reserved by JAEA ©2006